

**AIR-CONDITIONING
PLANT COMPONENT TAXONOMY
BY PRIMITIVE PARTS**

Tin-tai Chow B.Sc. M.Sc. M.B.A.

A thesis submitted for the
Degree of Doctor of Philosophy

Department of Mechanical Engineering
Energy Systems Division
University of Strathclyde, Glasgow, U.K.

May 1995

ABSTRACT

This thesis is concerned with the development of a plant component taxonomy for system simulation.

An analysis of the energy and mass flow paths in air conditioning systems is described. From the engineering viewpoints, many of the heat and mass transfer processes found within air conditioning systems can be unimportant to the simulation tasks or have insignificant impact on the results. Therefore, these flow paths are generally ignored in the plant component modelling process for the reasons of code simplification and simulation time-saving. At the same time these component models are often rigid and difficult to debug or modify. As a result, contemporary simulation software is often seen as being monolithic and lacking the flexibility to deal with the range of problems encountered in practice. This current work is therefore concerned with the development of a generalised plant database at a level allowing the component modeller to 'mix and match' models at the flow path level to produce component models tailored to their problem.

A literature review of plant component models, in particular the heat transfer coils and fluid flow conduits, is presented and used to define and justify the new approach. Subsequently, a range of air conditioning equipment is explicitly modelled by the finite difference control volume conservation method and based on the fundamental physical laws. By a process of generalisation, twenty seven 'primitive parts' are identified by which any air conditioning component may be represented. The method is explained and several illustrative examples are given. Matrix templates of the plant components obtained in this way are generally shown to be identical to those derived from other ESP-r component models previously developed.

The validity of the new approach is then demonstrated making use of the ESP-r system as the testing platform. The 27 primitive parts, as well as a number of new plant components synthesised from them, have been added to the ESP-r's plant component database. Three different validation approaches, analytical, inter-model, and empirical comparisons have been performed. The results have verified that the primitive parts modelling technique can improve on the accuracy (and of course flexibility) of the other modelling techniques.

Several application examples, relating to air conditioning and other thermal systems, are presented to demonstrate the applicability and flexibility of the primitive part approach. Also elaborated are the advantages and disadvantages of the approach based on the needs of the next generation simulation programs and the limitations imposed by our present knowledge in thermofluid theory, numerical

techniques and software engineering. Finally, possible future work is discussed, especially in relation to concepts such as neutral model formats and product models.

Acknowledgements

I would like to thank Professor J.A. Clarke, my supervisor at the University of Strathclyde, who have given me full support in all aspects of the research work throughout these years. His precious visions and precise advices have been the key factors leading to the success of this study.

I could never forget the hospitality of the members of the Energy Systems Research Unit, and in particular J. Hand, P. Strachan, and D. Tang (in nothing more than the alphabetical order), since my first visit to the University of Strathclyde in 1990 in the Department of Architecture and Building Science and later on after the move of the ESRU to the Department of Mechanical Engineering. Their guidance had been always timely and diversifying - from the essence of simulation research to the introduction about the exciting city of Glasgow and the beautiful landscape of Scotland. My gratitude is also expressed to E. Aasem, J. Hensen, K. James, N. Kelly, M. Lindsay, J. MacQueen, A. Nakhi, C. Negrao, and many others, for their helps in an unselfish way. The sharing of their academic expertise was happened to be the most meaningful.

I must also thank my local supervisor Dr. A. Dunn of the University of Hong Kong who have patiently shared with me his valuable experience about the modelling of air conditioning equipment and system simulation. Also it has been the laboratory work of his research team on piped fluid flow that has made possible the empirical validation of my numerical transport delay model.

The acknowledgement would not be complete without mentioning my employer, the City University of Hong Kong, that had partially funded this study, and those colleagues who had shared my duties during my periods of stay in Glasgow.

Finally, I must thank for the spiritual supports and endurance of my parent, my wife Fung-chi, and my children Chit-yau and Chit-sze in the past five years. It was from them that I have stolen the time to complete this study, and to them I dedicate this thesis.

Table of Contents

Page		
1.	INTRODUCTION	1
1.1	Air-conditioning and the Built Environment	1
1.1.1	The needs	1
1.1.2	The complexity	2
1.2	Building & Plant Simulation	3
1.2.1	System simulation	3
1.2.2	Evolutions in HVAC simulation	4
1.3	Elements in System Simulation	6
1.3.1	Component models	6
1.3.2	Networking	8
1.3.3	Solution methods	9
1.4	New Developments in Modelling Techniques	10
1.5	Objectives and Outline of the Present Work	14
	References	16
2.	AIR-CONDITIONING HEAT & MASS TRANSFER	21
2.1	Air-conditioning Systems	21
2.2	Heat-transfer coils	23
2.2.1	Common features	23
2.2.2	Air side heat transfer	25
2.2.3	Thermal conduction in tubings	33
2.2.4	Single-phase flow inside tube	33
2.2.5	Two-phase flow inside tube	34
2.3	Electric Heaters	36
2.4	Humidifiers	39
2.5	Flow Conduits	39
2.6	Flow Inducers & Restrictors	43
2.7	Direct Contact Equipment	45
2.8	Overall Review	47
	References	49
3.	PLANT COMPONENT MODELLING BY A FINITE DIFFERENCE METHOD	51
3.1	Finite Difference Control Volume Conservation Approach	51
3.2	Flow Conduit Models	56
3.2.1	Review of modelling theory	56
3.2.2	A numerical model of flow conduit	58
3.3	Heat-transfer Coil Models	67
3.3.1	Review of modelling theory	67
3.3.2	Mathematical model by constant volume conservation formulation	72
3.4	Extension of Work to Other Plant Components	85
3.4.1	Electrically heated pan humidifier	85
3.4.2	Flow restrictors	91
3.4.3	Duct heaters	93
3.4.4	Flow inducers	94
3.4.5	Air washers	95
	References	97

4.	THEORETICAL FRAMEWORK OF PRIMITIVE PART MODELLING	100
4.1	The Concept of Primitive Parts	100
4.2	The Principle of Superposition	103
4.3	Examples of Application	108
4.3.1	Insulated water pipe	108
4.3.2	Heat transfer tube	110
4.3.3	Electrically heated pan humidifier	112
4.3.4	Fan with submerged motor	116
	References	118
5.	SIMULATION ENVIRONMENTS & PRIMITIVE PARTS	120
5.1	TRNSYS	120
5.2	HVACSIM ⁺	123
5.3	ESP-r	125
5.4	Primitive Parts Added to ESP-r	128
5.5	Primitive Parts in TRNSYS & HVACSIM ⁺	130
5.6	Primitive Parts in Neutral Model Format	131
5.7	Product Modelling	133
	Reference	138
6.	VALIDATION	140
6.1	Model Validation Techniques	140
6.2	Validation of Flow Conduit Model	142
6.2.1	Comparison with analytical solution	142
6.2.2	Inter-model comparison	145
6.2.3	Experimental validation	147
6.3	Validation of Cooling Coil Model	151
6.3.1	Inter-model comparison	151
6.3.2	Sensible Cooling	151
6.3.3	Latent Cooling	155
6.4	Validation of Fan-duct Components	159
6.5	Validation of Air-conditioning System	162
	References	166
7.	APPLICATIONS	168
7.1	Study of Effect of Radiant Energy in Duct Electric Heater	168
7.2	Microscopic Analysis of Cooling Coil Performance	172
7.3	Study of Varying Heat Flux Distribution on a Boiling Tube	175
7.4	Steam Heating System Simulation	182
7.5	Barriers & Future Work	187
7.5.1	Uncertainties in input data	187
7.5.2	Cost effectiveness	188
7.5.3	Automatic model construction	189
	References	191
8.	SUMMARY & CONCLUSIONS	192
8.1	Summary of Work Achieved	192
8.2	The Significance	194
8.3	Conclusions	196

APPENDIX A	List of Symbols	198
APPENDIX B	List of Primitive Parts	200
APPENDIX C	The Concept of Cascade Time Constants	250

CHAPTER ONE

INTRODUCTION

"Since the advent of the digital computer the potential to predict future reality has taken a quantum jump. ... the availability of increasing computing power has allowed a large number of possibilities to be examined and assessed in the context of some underlying model, established in software form, which embodies the causal relationships observed in reality. In almost every field the potential is considerable and such computer-based modelling systems, if properly integrated within the decision-making process, hold much promise for the improvement in efficiency and quality of the related process or product." (Clarke 1985)

1.1 Air-Conditioning and the Built Environment

1.1.1 The needs

Air conditioning is the control of temperature, moisture content, cleanliness, air quality, and air circulation, as required by occupants, a process, or a product in the space. Hence it is often referred as environmental control. Human beings have a long history of struggling to make their lives more comfortable through the control of the immediate environment. But it was not until the end of the nineteenth century that the concept of central heating was fairly well developed, and early in the twentieth century cooling for comfort got its start. Since then developments have been rapid. (McQuiston & Parker 1988; Sauer & Howell 1990; Thorton 1995) Detailed analytical methods and systems have evolved to meet the needs of increasing complexity in building structures, high construction costs, and energy shortages.

The Energy Crisis of 1973 marked the beginning of consciousness about energy conservation in buildings. The International Energy Agency (IEA) was established in 1974 within the framework of the Organisation for Economic Cooperation and Development (OECD) and since then had implemented a number of international energy programmes (IEA 1990). Excessive use of fossil fuels for the purpose of seeking comfort eventually brings about global problems such as acid rain, greenhouse effect, thermal pollution as well as the shortage of non-renewable fuels. (CBI 1989; Masters 1991) There is an ever-increasing need for the architectural scientists and air conditioning engineers to understand the quality and behaviour of

building thermal performance to avoid making detrimental disturbances to our planet. Engineers nowadays are fighting for 'green' alternatives to replace the energy-intensive mechanical cooling techniques. A strategy known as nocturnal ventilation is perhaps one typical example by which cool air from the outdoors is circulated through the building at night to flush out the heat absorbed at day time and cool the interior thermal mass to a lower temperature. As the outdoor air temperature rises the following day, the cool mass absorbs heat and stabilizes the indoor temperature. (Abrams 1986)

The rapid growth of the use of building energy management systems have made a substantial impact on the control of environmental plants and on their energy efficiency (Levermore 1992). As microprocessors have become more powerful and cheaper, the buildings and plants are becoming intelligent. Equipment scheduling methods such as night setback (which changes room temperatures for energy saving during nonbusiness hours) and duty cycling (in which the system is temporarily turned off when it is not needed) are introduced together with a variety of compensator and optimiser control techniques (Patrick et al. 1993).

1.1.2 The complexity

Design comfort conditions of an air conditioned space vary with the servicing considerations such as the type of space occupied, the climatic conditions, and the occupant activities. These diverse environmental conditions require entirely different types and sizes of equipment to create and maintain the controlled environment. Moreover, in real buildings the layout of air-conditioning systems varies dramatically owing to the difference in conceptual design and the relationship between building and plant topologies. The number of heating, ventilation and air-conditioning (HVAC) system combinations can exceed 1,000,000, which indicates the problems of trying to limit the number of system types modelled in a particular computer program (Dallinger 1984). Improperly sized equipment or incorrect installations often exist as a result of tight project programme or less than thoughtful selection by the designers or the contractors. An oversized equipment not only wastes both initial and running costs, but also degrades the environmental control performance for instance, leading to heat spots in the indoor space, ineffective humidity control, and severe wear on the moving parts because of the more intermittent operation (Abrams 1986).

1.2 Building and Plant Simulation

1.2.1 System simulation

System simulation refers to the observations on a synthetic system that imitates the performance of a real system. For numerical simulation, the model equations are converted into a computer program by means of a numerical algorithm. Through the use of computer, this is one of the most powerful and economical tools currently available for the analysis and design of complex systems. There is a vast amount of literature describing computer simulation in detail, for instance, Gordon (1978), Ingels (1985) and Payne (1988).

The approach proposed by Gaz de France (Jeandel & Palero 1990) uses the following breakdown of stages to describe a simulation process:

- the experimenter takes us from "reality" to the "measured" world,
- the modeller from the "measured" to the "modelled" world via his "imaginary" world,
- the numerical analyst from the "modelled" to the "numerical" world,
- the computer specialist from the "numerical" to the "computer" world,
- the model user reaches the "simulated world".

Much of the early work in HVAC system simulation was sponsored by the American Society of Heating, Refrigerating, and Air-conditioning Engineers Inc. (ASHRAE) in the USA. A notable landmark was the publication by the Task Group on Energy Requirements for Heating and Cooling of Buildings (Stoecker 1975); in which a one-sentence definition of system simulation for HVAC plant was suggested:

"... predicting operating quantities within a system (pressure, temperature, energy and fluid flow rates) at the condition where all energy and material balances, all equations of state of working substances and all performance characteristics of individual components are satisfied."

From an application point of view system simulation of air conditioning provides a means of effective evaluation of the system or plant performance so that a desirable comfort level can be achieved with a minimum consumption of energy and through optimising design and operation of the air conditioning system. Besides its obvious usefulness in the design stage, it can be applied to an existing system to explore retrofit opportunities.

Figure 1.1 gives a general picture of the elements involved in building and plant simulation. (Clarke & Irving 1988) The effectiveness of heat supply or removal from an interior space by an air-conditioning system depends very much on the nature of the thermal energy that flows across the building envelope, the

room air flow, as well as the system response to the deviations from the controlled environment. Here the mathematical representations of the heat and mass transfer mechanism in the underlying processes are often highly non-linear, interacting and depending on time varying design parameters. The scientific bases of building and air conditioning plant simulation have been well explained in a number of literatures for instance, Kimura (1977), Clarke (1985). New concepts are continuously evolving through the endeavour and wisdom of the researchers in these years.

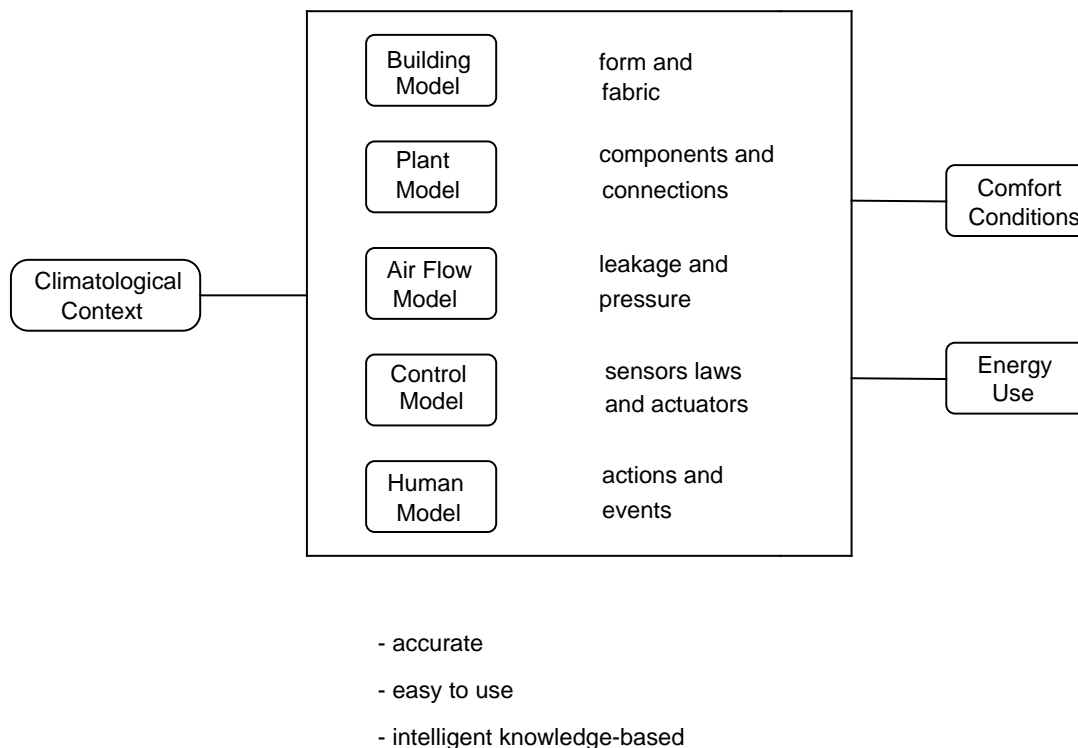


Figure 1.1 The Elements of Advanced Building Energy Simulation

1.2.2 Evolutions in HVAC simulation

Computer simulation programs for building performance evaluations emerged in the late 1960s. From then onwards the development process has been evolutionary and influenced by three main driving forces (Judkoff 1988):

- i) the improved understanding of the underlying physical processes,
- ii) the developments in computer hardware and software, and
- iii) the knowledge gained from constructing the previous generation of models.

The interaction of these three driving forces helped to solve possible areas of limitations and uncertainty. The growth in cooling coil model has been one typical example. The better understanding of the wet surface heat transfer mechanism has brought about improved accuracy in the prediction of coil performance; the tedious calculations involved in the dynamic response with combined heat and mass transfer has been made practical by the sharp increase in computer speed and memory storage; and the flexibility in model applications has been supported by the modular simulation environment and the use of graphical user-interface.

Hanby (1987) identified the two main lines of evolution in the developments of HVAC system simulation. The earliest published work in the field was found to concern with the dynamics of closed loop control of specific subsystems. The modelling techniques were generally derived from classical control theory. In this direction system simulation allowed the examination of partial load operating conditions and also has been helpful in the design optimization and equipment selection process (Stoecker 1989). As this line of investigation progressed the area of interest expanded and eventually a stage was reached at which a model of the building, or a room at least, had to be incorporated. Building or room components were then modelled as if they were plant components so that the set of equations could be solved consistently. In this way building energy and fluid flow paths were unavoidably over-simplified. As a consequence, the mathematical models of the plant components limited the complexity of the building model.

The second line of evolution originated from the emerge of dynamic thermal models of buildings in the 1970s as a response to the global demand of energy-efficient building designs. As a start, ideal and static plant behaviour was assumed. Reseachers gradually realised that not only was this assumption unrealistic, but also that a 'piecemeal' representation of the plant was totally inconsistent with the level of modelling complexity applied to the buildings at that time. Since the late 1980's, dynamic plant simulation has been incorporated in most whole-building energy simulation software. Readers can refer to Clarke & Maver (1991), Wright, Bloomfield & Wilshire (1992) for more systematic descriptions about the changes in this area.

Depending upon the focus of interest, HVAC simulation programs can be broadly categorised as performance simulation basis, which seek to reproduce all the operational characteristics of the plant, or as energy simulations basis, which are generally restricted to thermal analysis (ASHRAE 1990). With the advancements in computer technology it is more than natural that in the 1990s efforts are spent to merge the two categories in the same simulation program to satisfy the more challenging analytical tasks and diversifying needs of the users.

1.3 Elements in System Simulation

There are three elements common to all system simulation environments:

- i) component models,
- ii) their connections (networking), and
- iii) solution methods.

Structured around these three elements an overview of the approaches adopted to the problem of HVAC dynamic system simulation is given below.

1.3.1 Component models

Component modelling is the choice of physical laws and formulation of mathematical equations which are solved to provide information on the phenomena dominating an equipment (or component) under study. This choice depends totally on the technical objectives defined at the outset and is of vital importance in ensuring the success of the study.

Many component models in use originate from simplifications adopted for various reasons (Augenbroe 1986), such as:

- reduction of computational effort, e.g. reduction of required computer power and run-time;
- reduction of modelling complexity;
- utilization of model parameters from experimental results.

Often the choice of a model is purely coincidental - so far as it is strongly connected to the scientific background of the individual researchers and availability of resources. Depending on the level of sophistication in the background theories from which the models are based upon, component models can be grouped as 'fundamental', 'semi-empirical', and 'empirical' (Hanby 1987).

Fundamental component models are those which are adequately described by established theoretical principles of thermodynamics, heat transfer, mass transfer, and momentum transfer to predict pressure, temperature, energy flow rates and fluid flow rates to, from, and within each component; numerical data requirements are limited to such quantities as thermophysical constants which are usually reliable. Little or no performance test data are used. Fundamental relationships feature strongly in internal component representations. In many cases, the numerical algorithm or nodal representation is sufficiently detailed to permit studies of equipment dynamics or of retrofits of components. However, for complex devices this amount of detail requires numerous inputs, and programs that implement these algorithms or models tend to consume considerable amounts of computer time.

Empirical component models use a simple 'black box' concept that ignores physical laws. The whole component is treated as a single entity. The major descriptive elements are empirical in that they predict the response of the component to perturbations in the operating variables but lack any internal description of the component. No information is required about the physical dimensions, properties, and processes that determine the component behaviour. These are used in many system simulations to model complex mechanical plant such as chillers and fans, generally by regression analysis or polynomial curve fitting of manufacturer data. This level of representation may be satisfactory for many simulation purposes but considerable care is required in the formulation and use of empirical models, particularly where they are obtained through curve fitting. An obvious pitfall where component models are written in the form of curve fits is that the simulation may look for an operating point outside the limits of the original data (extrapolation). On the other hand, opportunities of seeking improvement on the model based on more up-to-date theory are almost impossible.

Semi-empirical models are widely available and popularly used today. Component behaviour is modelled as far as possible from first principles, but empiricism is resorted to where theoretical treatments are unavailable or would be inappropriate. Information is required about the physical dimensions, properties, and processes that determine the behavior of the equipment. A semi-empirical model can be used to predict the performance of other similar types of components operating in similar configurations. This approach would be used, for example, in modelling an air-water heat exchange coil where specific physical configurations are assumed and empirical correlations are used to calculate film heat transfer coefficients and air and water pressure drops.

With regard to the form in which the component model equations are written the following two classifications can be made:

i) algorithmic

This is based on input/output relations. The equations will give a solution representing the component behaviour for a given set of inputs. Most of the earlier documented component models are of this type. They can be further subdivided as steady state or dynamic type, depending on whether or not time transient response has been considered.

ii) numerical

This is based on finite volume conservation equations. The model generates matrix coefficients which are then passed on to an external matrix equation solver by which the solution at each time step is obtained. One earliest well-known simulation program that has adopted this methodology is perhaps the ESP program (currently known as ESP-r), where discrete nodal schemes for the plant

components are written in a form compatible with the building model, thus permitting the application of a unified solution process. (Clarke 1985)

Comparing with the algorithmic approach, the numerical approach in these days can be regarded as notably superior from the following viewpoints:

- i) modelling sophistication and flexibility;
- ii) mathematical rigour, especially in presence of non-linearity and time variance;
- iii) applicability of conceptual component modelling.

These advantages will be well observed as we move along the following Chapters.

1.3.2 Networking

Practical design of an HVAC system is frequently described by a schematic diagram. A switch of mind from a practical schematic diagram to a conceptual 'network' in system simulation is straight forward. The concept borrows the descriptive terminology of network theory where systems are represented by 'nodes' and 'arcs'. (Sowell 1984) Nodes are regions of physical space described by conservation and performance equation sets. Arcs are information flow lines or vectors which link the nodes together. In these terms a node may be seen as an equipment component or a portion of an equipment component (sub-part), depending upon the modelling complexity. The node relationships are augmented by control relationships.

There are two types of linking methods in a network: those where the node/arc relationships are fixed within the code (menu-based simulations) and those where the network topology is established by the user by linking models chosen from a library of components (component-based simulation).

Menu-based simulation

Most of the early work in this field simulated a single fixed system. Along this road the logical step is to combine many systems within one single program. This has been the approach adopted in some whole building simulation programs - the building energy analysis program DOE-2 (Hirsch 1982) is perhaps the best known example. By incorporating a comprehensive menu of systems and also options such as economy cycle control and thermal wheel regenerator, the possibilities can be quite numerous. This approach has two limitations. Firstly the programs are inefficient in that they contain large amounts of code which is unused; the programs are thus large and slow in execution. Secondly, even the most

extensive menu does not mirror the flexibility in system configuration which is faced by the designers in real situations.

Component-based simulation

Component-based simulation allows the user to choose components from a library file and specify their inter-connections and control schemes. The constraints on the user are the availability and the accuracy of the component models in the library, though options are generally offered to adopt user created component models. This methodology is widely used in building and plant performance appraisal softwares, for instance, HVACSIM+ (Clark 1985), TRNSYS (Klein et al. 1990) and ESP-r (ESRU 1995). These programs are compact, execute faster, and provide better representation of the real systems than the menu-based approach.

1.3.3 Solution methods

The end result of the above processes of specifying component models and their connections is the assembly of a set of coupled algebraic and/or differential equations which must be solved to find the time-variant operating conditions of the system. In the case of differential equations the usual treatment is to establish instantaneous values for the time derivatives and to integrate these to obtain the system response at each time step. Strategically, one of the following three solution methods is used:

- i) sequential method,
- ii) simultaneous method,
- iii) optimised method.

Sequential method

A sequential pattern is evident in all systems as defined by the fluid flows through the plant components. The solution process is the computation sequence where the output variables of one component model become the input variables for the next. The calculation proceeds from a suitable well-defined starting point such as the outside air inlet and proceeds around the system in the prescribed manner. The process may come to a point where a value for an input variable is required which itself is the output of some future calculation (e.g. the state of the return air from a room in an air conditioning system or the temperature and mass flow rate of water supplied to a coil). Techniques for overcoming this problem are to give assumptions to the unknown value or use an iterative procedure such as Newton-Raphson to converge on a

solution. There can be problems of accuracy with the first approach and stability and convergence with the latter.

A typical example of a sequential method applies to dynamic simulation is the TRNSYS program.

Simultaneous method

In a simultaneous method, the calculation is either performed by solving simultaneous equations or by some iterative process of assuming a trial value of an unknown variable at one point and calculating through the loop several times until the value stabilizes to within a specified tolerance. This is normally more complex than a sequential method. Experience with programs which obtain simultaneous solutions for large equation sets has shown that numerical difficulties can prevent a solution being reached in some cases. The solution time increases with the cube of the size of the equation set. So the simulation of a complete HVAC system can be time consuming.

An typical example of a simultaneous method applied to dynamic simulation is the energy analysis program ESP-r (Clarke 1985). A fast matrix solving technique has been developed in the program recently, through which the solution time can be shorten tremendously. (Aasem 1993)

Optimised methods

Simulation languages have been available for some years. The development has been to allow a generalised problem specification and solution. Most simulation languages can organise the equation sets so that a more efficient solution process is obtained. In its simplest form this involves identifying those equations which can be solved sequentially and therefore treating them separately, leaving a smaller 'cut set' to be solved simultaneously. Recent developments based on an application of graph theory suggest that a more effective reduction in the size of simultaneous equation sets is feasible. (Buhl et al. 1990)

1.4 New Developments in Modelling Techniques

The trend of developments in this field was summarized by Clarke (1986), Sowell (1991), and Wright et al. (1992).

Efforts were launched in 1985 to improve modelling tools for building energy systems. In this connection, the "Energy Kernel System" (EKS) projects in both the United Kingdom (UK) and the United States (US) grew out of earlier collaborative efforts to identify weaknesses in the current softwares, and to establish directions for new research and development. The projects in both countries identified problems such as lack of modelling flexibility for the building services engineering (BSE) practitioner, and the difficulty of implementing improvements to the softwares themselves. Both of these deficiencies were seen to be related to the monolithic nature of the existing programs. The obvious solution to these was a software that provides a high degree of modularity. It was realized that the development of the simulation softwares, since their growing out of the programming languages and practices available in the early 1970s, could be limited. More recent developments in computer science and software engineering offered great opportunities for alternative software design and development. As these ideas coalesced, terminology was borrowed from the computer disciplines to describe them. The software modules became known as objects, conveying important ideas from the new field of Object Oriented Programming (OOP). Being somewhat analogous to a modern computer operating system in which the set of low-level functions needed by all higher-level software is called the kernel, the term "Energy Kernel System" was adopted, reflecting also the primary concern with simulation of building energy systems.

The EKS/UK and EKS/US were based on the same idea, i.e. to capitalize on the low-level commonality among BSE programs, and to introduce modern concepts from computer science and software engineering. An outgrowth of EKS/US was the Simulation Problem Analysis Kernel (SPANK), comprising methodology for describing and solving equation systems such as those that arise in simulation problems. However, from this common beginning the efforts of the US and UK projects diverged due to different goal emphases, technical approaches, and development time frames. The primary goal of the EKS/US became improvement of the modelling and solution processes, while that of the UK became improvement of the software development process. The EKS/UK defines objects to be modules of substantial size and complexity that may be extracted from existing softwares. The EKS/US implementation takes a lower level view, with individual equations as atomic objects that are interconnected to form larger entities (macro objects), which in turn are interconnected to form simulation problems.

In parallel with the EKS projects there are a number of research work which carry out new approaches of modelling and new capabilities of problem solving. Modern development work in the field are heading towards the following directions:

- i) input-output free,
- ii) modular,
- iii) hierarchical,

- iv) universal,
- v) powerful user interface,
- vi) extensive documentation,
- vii) integration.

These are explained below.

Input-output Free

The pre-selection of 'known' variables often leads to limitations in the actual use of the models. Frequently a 'system' modeller, when using the available components with pre-defined input/output relationships to set up a simulation network, would like to connect the inputs of one component with the inputs of another, and perhaps similarly for the outputs. Too often a 'system' modeller is forced to become a 'component' modeller and needs to re-write a component model (then re-compile the source code) in order to modify its input-output relationship. Leaving the input-output designation to the global simulation environment will substantially increase the versatility of the component models.

Modular

Under a modular structure, separate subprogram modules will be used to perform most of the computations. In this way, de-bugging a very large program as well as future modifications can be addressed in manageable stages. Most of the outcome of the extensive modelling efforts in the past can be re-used without hesitation by the modellers of to-day. In an object-oriented simulation environment, all objects exist in a modular manner. A module in its generalised form can be easily transported for use in other programs.

Hierarchical

A basic feature in the future component models is 'hierarchical sub-model decomposition', i.e. one sub-model within another in multiple levels. One major advantage of this method is that it enables incremental modelling and validation. A model developer can make sure that, for example, a tube model behaves properly through rigorous validation tests before it is used as part of a cooling coil model, which is then undergone another severe validation exercise before it is used as part of an air-handling unit, and so on. The work continues and incrementally approaches the whole system level. Another advantage is that good graphical interfaces can be constructed for a corresponding hierarchical presentation of a model, where a user first gets an overall view of the system and then can zoom down for successively increased levels of detail. (Sahlin & Sowell 1989)

Universal

Mechanism will be provided to allow all model developers to access to the developments of others whilst retaining the flexibility to tailor a simulation system to individual needs. There will be more task sharing and resource sharing through international efforts. The neutral model format (NMF) is a well-known example. The work is to overcome many of the obstacles encountered in these days such as the lack of a comprehensive component database, inaccessibility of manufacturer's data and inadequacy in model validation. A neutral component model can be described in which the equations describing the model are defined together with the parameters attached to it in a standard format. These neutral models could then be accessed by other simulation environments. In this sense, the NMF defines a formalism for precise description of component models that is independent of any particular programming environment. Additionally, translation software is proposed so that BSE software developers can automatically generate component models for their products directly from a NMF library.

Powerful User Interface

From a user point of view, the main barrier to the appraisal of environmental systems via simulation lies in problem description and data preparation in the face of uncertainty. The future development will be a marked shift towards intelligent knowledge based system in which simulation primitives are mixed with artificial intelligence techniques to create models with human-like characteristics. One approach to deal with such problems is the design of an intelligent knowledge based system which offers an intelligent front end (IFe). The IFe acts as an expert consultant, conducting a dialogue to gather information on the design, identifying the user's objectives and commissioning the required performance simulations. (Clarke, Rutherford & MacRandal 1989)

Extensive Documentation

In order to prevent the users from using a library component in a non-intended way, extensive textual documentation will be provided along with the library entry, including the background of the underlying mathematical model, their ranges of validity, together with the assumptions, nomenclature, and physical basis. Most of the French simulation work in the BSE area has concerned with this aspect, for instance the emphases on thorough model documentation (the Proforma project) and on advanced model base management system (the Modelotheque project). (Dubois 1990) Another objective of the approach is to provide a natural and standardised form of model expression, i.e. a form which makes it easy and fast to express new models for any environment and appeals to engineers as well as to well trained simulation experts.

Integration

There is a need for a joint effort between design researchers and simulation tool developers of various professions in the construction industry to formulate procedures and standards for integrating simulation into the building design process. The basic idea is the development of a central database of a building project as a whole, and through this a variety of simulation tools can exchange common data, eliminating the duplication of data when simulating a building in various design tools, and giving a single consistent model of the building at any one time. Such a model is called a 'product model' by the Computer Integrated Manufacturing (CIM) community. The pioneer of the work has been the COMBINE project which involves 15 partners from eight European countries. The first phase of the project officially commenced in August 1990 for a two years period. (Monaghan et al. 1991; Augenbroe et al. 1993) It is envisaged that the first generation intelligent integrated building design systems (IIBDS's) will provide complete building descriptions in the form of a conceptual schema (i.e. a building data model) along with a physical implementation (e.g. a database to hold the data of an actual building) and interface specifications (e.g. in some neutral format) which specify how the data is actually exchanged among a broad range of actors (i.e. architects, consulting engineers, quantity surveyors, contractors etc.) in the building design process.

1.5 Objectives and Outline of the Present Work

It was against the above background situations that this research work commenced in the early 1990s. The following visions on the future models were particularly observed:

- i) In the traditional plant modelling approach, it is usual to reduce the complexity of the real system in order to lessen the computational overhead and the input demands on the users. The advancement in computer technology will, sooner or later, allow a new plant simulation approach in which all heat and mass flow paths are assigned a counterpart mathematical equivalent in an attempt to emulate the reality. (Clarke 1989)
- ii) In the process of creating a plant component model to suit a particular analytical task, the decomposition of the component into its sub-parts is goal-oriented - it may be based upon the real objects or upon the thermal phenomena, depending on the software to be used or on the modeller's uses and needs. This is actually a very important part of the modelling task. (Laret 1989; Dubois 1990)

In real buildings, the layout of air-conditioning systems varies dramatically. Accurate representation of the system requires a simulation program to accommodate a large number of component modules within its code. Most of the component models in use to-day with simultaneous solution method are internally pre-defined rigid semi-empirical models. With the continuous changes in air-conditioning technology, the demands on inserting new component models into the standard library will be endless. It is desirable that in future the plant database can be composed of a finite number of 'process-based' sub-component models built upon fundamental physical laws. A variety of plant equipment models can then be represented through different combinations of these sub-components in a hierarchical manner. For instance, a 'fan' component can be represented by three physically coupled sub-components: the 'fan impeller', the 'driving motor' and the 'fan casing'. In turn, an 'air handling unit' meta-component can be viewed as a combined integral of the following six component types: 'air damper', 'air-mixing chamber', 'cooling coil', 'humidifier', 'heater', 'fan' and associated with these, the control laws. Even a sub-component like a 'fan casing', where desirable for a particular simulation task, can be further decomposed into its sub-parts of layers of metallic sheets and thermal insulation. The thermal process taking place in an internal solid layer, where existed, is limited to (1, 2 or 3-dimensional) thermal conduction which can be represented mathematically by some finite volume conservation equations. A component model developed in this way is a fundamental model at an appropriate level of complexity. At each sub-part, the state variables can be monitored closely during the course of simulation and the results obtained can serve to assist a wide range of decision making in plant performance evaluation.

When this 'plant component taxonomy' concept is fully established and implemented, most plant components for system simulation may not exist in the source code at all. Instead, each component is user-created by a selective linkage of the sub-parts from a plant component library, with a specific simulation task in the user's mind. The system model is finally defined by specifying the interconnections between these components. The approach is then close to the highly flexible building-side simulation methods that we are enjoying in these days.

Upto this point the objectives of this research work become relatively clear. Firstly, the goal of this research work is to facilitate the development of a taxonomy of plant components, by which air conditioning system in real life can be described and simulated to suit diversified purposes.

Air conditioning processes afterall are combined energy and mass transfer processes to the fluid(s) being handled. It has been well aware that the ESP-r software allows rigorous analysis of energy performance of building/plant systems. The program offers a modular simultaneous simulation environment as well as many other features which are indispensable for applying modern simulation techniques, for instance:

- i) component-based,
- ii) finite volume energy/mass flow conservation description of physical processes, and
- iii) a fluid flow solution process detachable from the energy simulation process.

It is worth notice that within the ESP-r system, a fluid flow simulation may be initiated independently of the main energy simulation or pursued in tandem. Based on the zonal method (Hensen & Clarke 1990), a nodal network of connecting fluid flow components/resistances is constructed. Nodes may represent connection points of plant components, ambient conditions, rooms, or parts of rooms etc. Fluid flow components refer to discrete fluid flow passages such as ducts, pipes, fans, pumps, doorways, construction cracks, etc. During each simulation time step, the computation is constrained to the steady flow of fluid along the connections when subjected to certain boundary conditions regarding pressure and/or flow. This is achieved by an iterative mass balance approach in which nodal pressures are adjusted until the mass residual of each internal node satisfies some user-specified criterion.

This research work has encompassed the following three objectives:

- i) To identify the energy and mass flow paths in existence in real-life air conditioning systems, by which the development of component models upon fundamental physical laws can be enhanced;
- ii) To recommend a structure of air conditioning plant component database in a generalized and flexible form of mathematical representation, by which the performance of real-life air conditioning equipment and systems can be analysed;
- iii) To implement and validate the above in the ESP-r program as the testing platform.

In this Chapter, the needs and developments of system simulation have been reviewed. Based on these, the objectives of this research work are presented. The following Chapter 2 will cover the investigation of the energy and mass flows in air conditioning systems. Chapters 3 and 4 will explain the ways of modelling plant components in detail by sets of finite volume conservation equations and how the mathematical concepts of the generalised plant component database were derived. Chapter 5 will explore the feasibility of applying the so called 'primitive part' concept in a variety of simulation environments. Chapter 6 will describe the validation tests of this new modelling approach, and the discussions about the applications and future developments will be covered in the last two Chapters.

References

- Aasem, E.O. 1993. Practical simulation of building and air-conditioning systems in the transient domain. PhD Thesis, Energy Systems Division, Department of Mechanical Engineering, University of Strathclyde, Glasgow, U.K.
- Abrams, D.W. 1986. Low-energy Cooling, a Guide to the Practical Application of Passive Cooling and Cooling Energy Conservation Measures. Van Nostrand Reinhold, New York.
- ASHRAE 1990. An Annotated Guide to Models and Algorithms for Energy Calculations Relating to HVAC Equipment. American Society of Heating, Refrigerating, and Air-Conditioning Engineers, Inc., Atlanta.
- Augenbroe, G.L.M. 1986. "Research-Oriented Tools for Temperature Calculations in Buildings." In Proceedings of the 2nd International Conference, System Simulation in Buildings, December, Liege, Belgium, pp.234-255.
- Augenbroe, G., Bijvoet, P., Nederlof, L., Rombouts, W. & Vries, P. 1993. "An Integrated Simulation Network." In Proceedings of Building Simulation '93, International Conference of the International Building Performance Simulation Association, August, Adelaide, Australia, pp.161-167.
- Buhl, F. et al. 1990. "The U.S. EKS: Advances in the SPANK-based Energy Kernel System." In Proceedings of the 3rd International Conference, System Simulation in Buildings, December, Liege, Belgium, pp.107-150.
- CBI. 1989. The Greenhouse Effect and Energy Efficiency. Confederation of British Industry, London.
- Clark, D.R. 1985. HVACSIM+ Building Systems and Equipment Simulation Program Reference Manual. U.S. Department of Commerce, NBSIR 84-2996.
- Clarke, J.A. 1985. Energy Simulation in Building Design. Adam Hilger, Bristol.
- Clarke, J.A. 1986. "The Energy Kernel System." In Proceedings of the 2nd International Conference, System Simulation in Buildings, December, Liege, Belgium, pp.455-470.

Clarke, J.A. & Irving, A.D. 1988. "Building Energy Simulation: An Introduction." *Energy and Building*, Vol.10., pp.157-159.

Clarke, J.A. 1989. "Building Energy Simulation: the State-of-the-Art. " *Solar & Wind Technology*, Vol.6, No.4, pp.345-355.

Clarke, J.A. & Maver, T.W. 1991. "Advanced Design Tools for Energy Conscious Building Design: Development and Dissemination." *Building and Environment*, Vol. 26, No. 1, pp.25-34.

Clarke, J.A., Rutherford, J. & MacRandal, D. 1989. "Building Performance Simulation: Delivering the Power to the Profession." In *Proceedings of Building Simulation '89, International Conference of the International Building Performance Simulation Association*, June, Vancouver, Canada, pp.305-311.

Dallinger, D.W. 1984. *Energy Conservation Applied to Environmental Plant Control*. PhD Thesis, The Hatfield Polytechnic, UK.

Dubois, A.M. 1990. "Component Model Documentation and Management: the Evolution of the PROFORMA and MODELOTHEQUE." In *Proceedings of the 3rd International Conference, System Simulation in Buildings*, December, Liege, Belgium, pp.17-39.

ESRU. 1995. *ESP-r : A Building Energy Simulation Environment. User Guide Version 8 series, Manual U95/1*, Energy Systems Research Unit, Department of Mechanical Engineering, University of Strathclyde, U.K.

Gordon, G. 1978. *System Simulation*. 2nd edit., Prentice-Hall.

Hanby, V.I. 1987. "Simulation of HVAC Components and Systems." *Building Services Engineering Research & Technology*, Vol.8, pp.5-8.

Hensen, J.L.M. & Clarke, J.A. 1990. "A Fluid Flow Network Solver for Integrated Building and Plant Energy Simulation." In *Proceedings of the 3rd International Conference, System Simulation in Buildings*, December, Liege, Belgium, pp.151-167.

Hensen, J.L.M., Clarke, J.A., Hand, J.W. & Strachan, P. 1993. "Joining Forces in Building Energy Simulation." In *Proceedings of Building Simulation '93, International Conference of the International Building Performance Simulation Association*, August, Adelaide, Australia, pp.17-23.

Hirsch, J.J. 1982. "Simulation of HVAC Equipment in the DOE-2 Program." In Proceedings of the 1st International Conference, System Simulation in Buildings, December, Liege, Belgium, pp.89-109.

IEA. 1990. R&D for the Future, a Strategy Plan for the Executive Committee. International Energy Agency, Energy Conservation in Buildings and Community Systems, Swedish Council for Building Research, Stockholm.

Ingels, D.M. 1985. What Every Engineer Should Know about Computer Modelling and Simulation. Marcel Dekker, New York.

Jeandel, A. & Palero, I. 1990. "Thermal Modelling and Simulation of Buildings at Gaz de France." In Proceedings of the 3rd International Conference, System Simulation in Buildings, December, Liege, Belgium, pp.41-62.

Judkoff, R.D. 1988. "Validation of Building Energy Analysis Simulation Programs at the Solar Energy Research Institute." Energy and Building, Vol.10, pp.221-239.

Kimura, K.I. 1977. Scientific Basis of Air Conditioning. Applied Science Publisher, London.

Klein, S.A. et al. 1990. TRNSYS, A Transient System Simulation Program. University of Wisconsin-Madison, Engineering Experiment Station Report 38-13, Version 13.1.

Laret, L. 1989. "Building & HVAC Simulation: the Need for Well-suited Models." In Proceedings of Building Simulation '89, International Conference of the International Building Performance Simulation Association, June, Vancouver, Canada, pp.199-204.

Levermore, G.J. 1992. Building Energy Management Systems, an Application to Heating and Control. E & FN Spon, London.

Masters, G.M. 1991. Introduction to Environmental Engineering and Science. Prentice Hall.

McQuiston, F.C. & Parker, J.D. 1988. Heating, Ventilating, and Air-Conditioning Analysis and Design. 3rd edit., John Wiley & Sons, New York.

Patrick, S.R., Patrick, D.R. & Fardo, S.W. 1993. Energy Conservation Guidebook. The Fairmont Press Inc., U.S.A.

Payne, J.A. 1988. Introduction to Simulation: Programming Techniques and Methods of Analysis. International edition, McGraw-Hill, New York.

Sahlin, P. & Sowell, E.F. 1989. "A Neutral Format for Building Simulation Models." In Proceedings of Building Simulation '89, International Conference of the International Building Performance Simulation Association, June, Vancouver, Canada, pp.147-154.

Sauer, H.J. & Howell, R.H. 1990. Principles of Heating, Ventilating and Air-conditioning. American Society of Heating, Refrigeration, and Air-conditioning Engineers Inc., Atlanta.

Sowell, E.F. et al. 1984. "Generation of Building Energy System Models." ASHRAE Transactions, Vol. 90, Part IB, pp.573-586.

Sowell, E.F. 1991, "Next Generation Building Services Engineering Software: Opportunities for the Practitioner." In Proceedings of Building Environmental Performance '91 Conference, BEPAC, April, Canterbury, U.K.

Stoecker, W.F. 1975. Procedures for Simulating the Performance of Components and Systems for Energy Calculations. 3rd edit., American Society of Heating, Refrigerating, and Air-Conditioning Engineers Inc., Atlanta.

Stoecker, W.F. 1989. Design of Thermal Systems. 3rd edit., McGraw-Hill, New York.

Thorton, R.C. 1995. "The History and Growth of HVAC&R Since the 1930s." ASHRAE Journal, Vol.37, No.1, January, pp.S68-80.

Wright, A.J., Bloomfield, D. & Wiltshire, T.J. 1992. "Building Simulation and Building Representation: Overview of Current Developments." Building Services Engineering Research & Technology, Vol. 13, Part 1, pp.1-11.

CHAPTER TWO

AIR-CONDITIONING HEAT & MASS TRANSFER

The main function of an air-conditioning system is to control the thermal environment of an indoor space. This can be achieved through a finite number of air-conditioning processes in relation to fluid heat and mass transfer. In these days a variety of air-conditioning systems exist to meet the requirements of different building types, occupant activities, load variations, and economic considerations. Nevertheless all air-conditioning systems have the same basic components or sub-components, though their physical appearance, sizes and arrangements may vary dramatically from case to case. The manner in which the systems are controlled and operated to satisfy individual needs can also be quite different.

A brief description about the features and functions of the common air conditioning systems and equipment in use to-day is given below. More detailed information can be found in standard references on the topic, for instance Stoecker & Jones (1982), Jones (1985), Martin & Oughton (1989), ASHRAE (1992), and McQuiston & Parker (1994). The purpose here is to explore the energy and mass flow paths which (may) exist in air conditioning components. In comprehensive dynamic system simulation these flow paths must be tackled accurately.

2.1 Air-Conditioning Systems

An air conditioning system can be simple as a package-type room air-conditioner, or complicated as a central station serving groups of decentralized sub-systems for multi-space applications. The system can be classified in different ways, viz equipment utilization, zoning, fluid distribution and flow rates.

Extent of equipment utilization (unitary or central)

Unitary systems are factory-assembled air-conditioning units located in or near to the conditioned space and are available as single packages containing all major components. A central system on the other hand is equipped with one or more air-handling units located in a number of air conditioning plant rooms, each of which supplies treated air to individual conditioned space.

Zoning (single or multi-zone)

A zone is an air conditioned space under the control of a group of thermal sensors, say in the simplest case, by a single thermostat. Multi-zone refers to a more complicated system with distributed equipment and control devices.

Cooling/heating fluid distribution (all-air, all-water or air-water)

In an all-air system, the capacity required for offsetting the space thermal load is provided by the supply of conditioned air to the space only. In an air-water system, space-conditioning is performed by the supply of both conditioned air and chilled/hot water which are distributed to the terminal units installed at the conditioned space (say within the ceiling void). In an all-water system, space-conditioning is entirely accomplished by supplying chilled/hot water to the terminal units.

Air-flow rate (CAV or VAV)

In a constant air volume (CAV) system, the supply air temperature is modulated to match the variations of space load during the part-load operation. In a variable air volume (VAV) system, the supply air volume flow rate is reduced during the part-load operation. Further sub-classifications are possible, for instance the VAV systems can be identified as single zone VAV system, VAV re-heat system, VAV dual-duct system, fan-powered VAV system etc.

Air conditioning systems with completely different design concepts or under different classification headings can co-exist in the same building. Such complication does not alter the fact that all systems generally have the same basic components responsible for the same thermofluids or psychrometric duties. Table 2.1 gives a list of basic components and their associated duties. Involved in these duties are the processes of energy and mass transfers to or from the working fluids like moist air, water, steam as well as refrigerants.

In this sense, the performance of an air conditioning system, including its transient response and power consumption, can be predicted accurately by a thorough analysis of the energy and mass flow paths interacting amongst the working fluids, the associated system components and their immediate surroundings.

Table 2.1 Duties of Air-Conditioning System Components

Components	Duties
Air cooling coil	cooling & dehumidification
Air heating coil	sensible heating
Flow converger	mixing of fluid streams
Flow diverger	division of a fluid stream
Flow inducer	creating fluid motion
Flow conduit	distributing fluid to desired destination
Flow restrictor	flow regulation
Humidifier	increasing air moisture content
Air washer	humidifying, cooling and cleaning of air

2.2 Heat-transfer Coil

2.2.1 Common features

Heat-transfer coil is a key element used to control the room temperature and humidity level through forced-convective cooling or heating of supply air. Cooling and dehumidifying is normally accomplished with chilled water or refrigerant circulating through the coil tubings, while heating is accomplished by circulating hot water or steam through the same. In air cooling coils, dehumidification occurs only when the external (extended) surface of the tubings is below the dew point temperature of the air stream in contact. If the surface temperature is below the freezing temperature of water vapour in the air stream, frost will deposit on the metallic surface and will grow with time.

Finned-tube coils are used extensively as the heat-transfer device in central-station air-handling units, room air terminals, and factory-assembled self-contained air conditioners. The extension of the heat transfer surface by fins gives significantly greater heat exchange rate than that without the fins. This results in a compact heat exchange surface which provides economy of materials and space. Aluminium and copper are the most popular materials for both the tubes and fins. Copper tubes with aluminium fins dominate the commercial equipment market as the most popular material combination. Because of the low mass capacitance of the tube material, conductive thermal resistance is low comparing with the convective thermal resistances with the fluids at both side of the tubings.

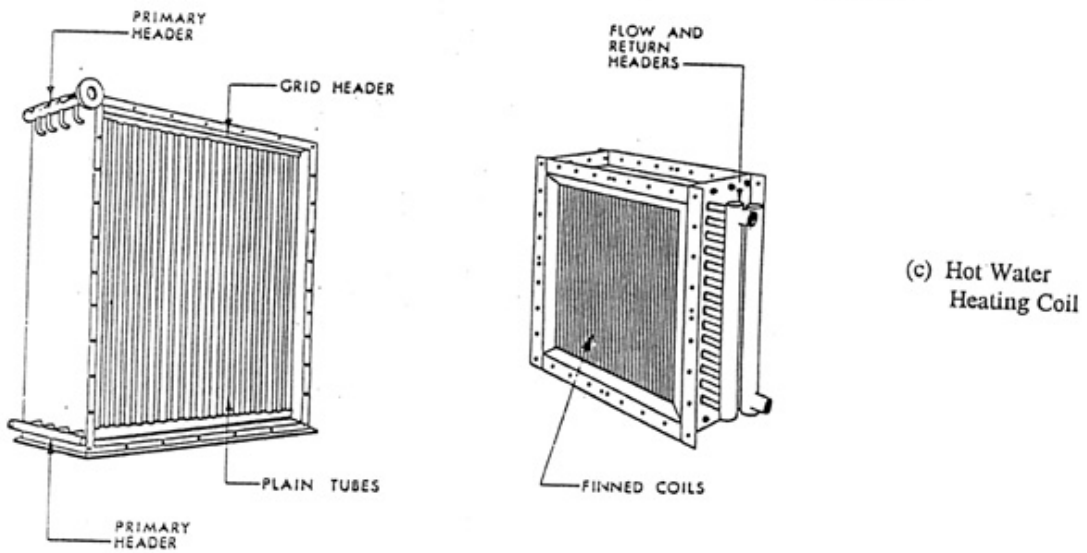
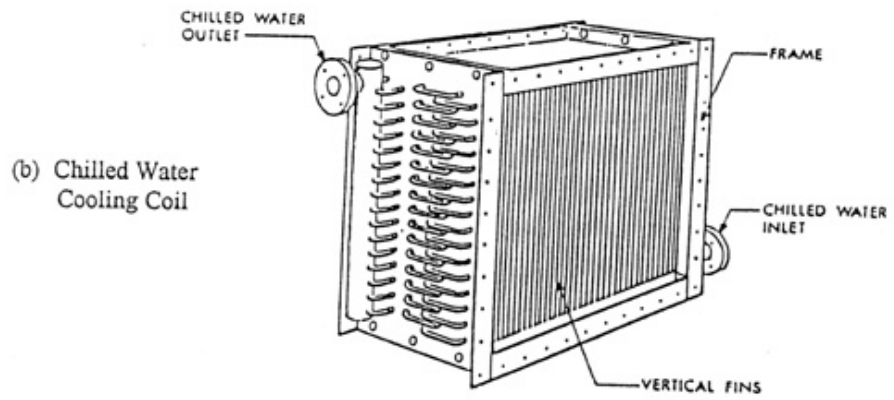
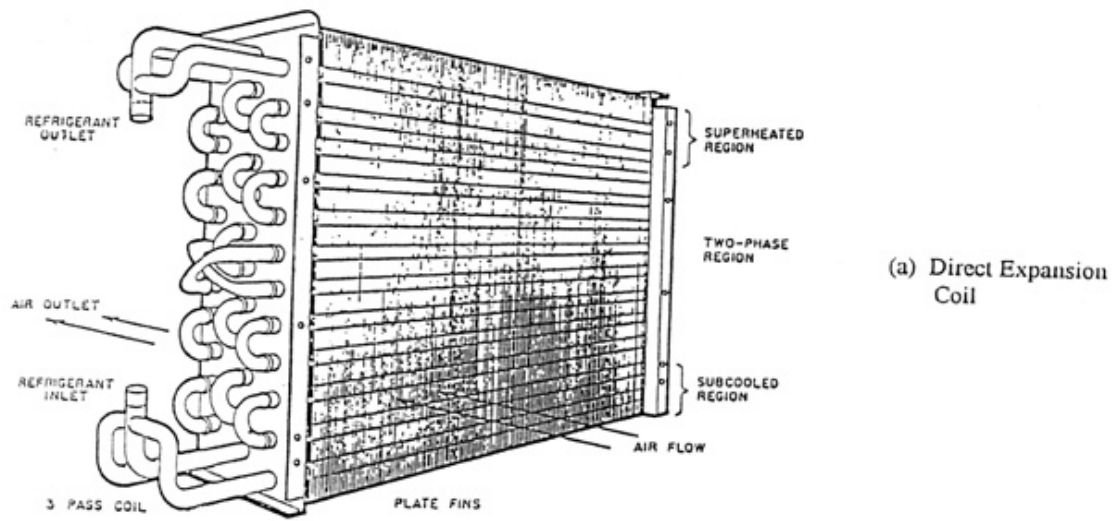


Figure 2.1 Heat Transfer Coils

Figures 2.1 (a) to (c) show the features of different common heat-transfer coils. The face area of a heat-transfer coil is defined as the area where finned tubing exists within the limits of the coil casing. The tubes of a coil are arranged in rows across which the air flows. For purposes of reference, the rows are usually numbered sequentially starting on the entering air side of the coil. The rows can be arranged in line or staggered. Chilled or hot water coils use a supply header for fluid entry to the coil circuits. A direct expansion (DX) coil, on the other hand, feeds refrigerant through a distributor which circulates an equal amount of refrigerant to each coil circuit via its feeder tubes. Fluid exits through a return header.

Chilled/hot water coils use either flow modulation or water temperature adjustment for capacity control. When water temperature adjustment is used, water flow is usually relatively constant. When water flow modulation is used, the water velocity within the tubes of the coil can vary through a broad range. Controllable capacity reduction with a DX air cooling coil is not as free of restrictions as is that for chilled water coils. Because of this, coil splits are provided which make partial deactivation of the evaporator possible.

2.2.2 Air side heat transfer

In the context of heat and mass transfer relating to moist air flow, the enthalpy potential theory has been developed to quantify the transfer of total heat (sensible plus latent) at the air side of the heat transfer coil. The theory is particularly important when the tube external surface is wet. (ASHRAE 1993)

Enthalpy potential theory

It is known from Fick's law that the rate of water vapour mass transfer from the water surface to the air is proportional to the partial pressure difference of water vapour at the moist air and at the tube surface temperatures. Since the moisture content of air is proportional to the vapour pressure, this implies that

$$\Delta m_v = K_d A (g_s - g_a) = -m_{cd} \quad (2.1)$$

where m_{cd} indicates the condensation rate, which is positive if $g_a > g_s$. K_d is the mass diffusion coefficient.

The rate of latent heat transfer due to moisture transfer to air is therefore

$$Q_l = \Delta m_v H_{fg} = K_d A (g_s - g_a) H_{fg} \quad (2.2)$$

where the latent heat of evaporation H_{fg} is evaluated at the wall temperature.

The rate of total heat transfer Q_t (from wetted surface to air) is given by the sum of sensible heat transfer rate Q_s and latent heat transfer rate Q_l . Hence,

$$Q_t = h_{ow} A (\theta_s - \theta_a) + K_d A (g_s - g_a) H_{fg} \quad (2.3)$$

where g_a is evaluated at the incoming condition; h_{ow} refers to the convective heat transfer coefficient at the outside tube surface when it is wet.

While the driving potential for heat transfer is 'temperature difference', the driving potential for mass transfer is 'mass concentration', or 'partial pressure'. Because the transport mechanism at a water surface that controls the rate of sensible heat transfer and the rate of mass transfer are the same, there exists a proportional relation between h_o and K_d such that (Stoecker & Jones 1982)

$$K_d = \frac{h_{ow}}{Cp_{ma}} \quad (2.4)$$

where Cp_{ma} is the specific heat of moist air.

This expression is the well-known Lewis relation. It is a good approximation for moist air at low mass transfer rates when the Lewis Number is close to unity (ASHRAE 1993). A derivation of the relationship can be found in McQuiston & Parker (1994). Modifying equation (2.3) by adding a negligible term $(g_s - g_a)H_f$ to the right hand side gives

$$Q_t = K_d A (H_s - H_{ma}) \quad (2.5)$$

The name 'enthalpy potential' originates from equation (2.5) because the potential for the transfer of the sum of sensible and latent heats is expressed as the difference between the enthalpy of saturated air at the wetted-surface temperature and the enthalpy of moist air in the free stream.

Making use of the link between the transports of momentum, heat and mass, an extension of the theory is

the Colburn analogy (or the j-factor analogy) from which the convective heat transfer coefficient can be determined (McQuiston 1978 and 1978a). The general form of the air side coefficient is best represented by the following relationship involving three dimensionless numbers: Stanton (St), Prandtl (Pr) and Reynolds (Re):

$$j = St Pr^{2/3} = f(Re) \quad (2.6)$$

Air-side heat transfer coefficient is then given by

$$h_o = j G_x C_{p_{ma}} Pr^{-2/3} \quad (2.7)$$

where Pr is expressed as $\mu_a C_{p_{ma}}/k_a$; μ_a is the dynamic viscosity of moist air in N.s/m² and k_a is the thermal conductivity of moist air in W/m².K. G_x is the mass velocity (i.e. mass flow rate per unit area) in kg/m².s based on the minimum exposed flow area A_x in the coil on the finned side, i.e.

$$G_x = \frac{m_a}{A_x} \quad (2.8)$$

Making use of a stepwise regression analysis to measured data, Elmahdy and Biggs (1979) deduced a relation of the j-factor in terms of four coil parameters: the hydraulic diameter D_h , the fin thickness y_f , the fin spacing x_f and the fin length L_f . The expression is as follows:

$$j = C_1 Re_{D_h}^{C_2} \quad (2.9)$$

where,

$$C_1 = 0.159 \left(\frac{y_f}{L_f} \right)^{0.141} \left(\frac{D_h}{y_f} \right)^{0.065} \quad (2.10)$$

$$C_2 = -0.323 \left(\frac{y_f}{L_f} \right)^{0.049} \left(\frac{x_f}{y_f} \right)^{0.077} \quad (2.11)$$

This is valid for the range $200 < Re_{D_h} < 2000$ and $Re_{D_h} = G_x D_h / \mu_a$.

If L_t is the flow length through the coil parallel to the air flow and A_o the total finned side surface area for heat transfer, then

$$D_h = \frac{4L_t A_x}{A_o} \quad (2.12)$$

In the frame of the International Energy Agency (IEA) Annex 10 project, Holmes (1988) summarized the different correlation expressions for different applications as follows:

i) for bare tubes

$$Nu = 0.33 Re_D^{0.6} Pr^{0.3} \quad (2.13)$$

where Nu is the Nusselt number.

ii) for circular fins

$$St Pr^{2/3} = 0.19 Re_D^{-0.37} \quad (2.14)$$

iii) for plate fins

$$St Pr^{2/3} = 0.0987 Re_D^{-0.35} \quad (2.15)$$

In the above expressions,

$$Nu = h_o \cdot D_o / k_a$$

$$St = h_o / G_x \cdot C_{pma}$$

$$Pr = \mu_a \cdot C_{pma} / k_a$$

$$Re_D = D_o \cdot G_x / \mu_a$$

where D_o is the external tube diameter in meters.

It is not difficult to see that Nu is equivalent to $(St \cdot Pr \cdot Re)$. Equation (2.15) is a typical relationship for a coil with not too many fins with 17 mm outside diameter tubes on a 38 mm pitch.

The experimental work of McQuiston in the 1970's pointed out the limitations of the j-factor approach in that the j-factors change with coil configurations and the nature of condensate on tube surface; their values decrease for each successive row in the coil and hence the value of h_o actually decreases from the inlet to the exit of the coil (Rich 1975; McQuiston & Parker 1994).

Simplified expressions for average value of h_o are quoted in different literatures in that it is simply related

to the air face velocity u_a (m/s). For a staggered tube arrangement, the usual disposition of fins (316 per metre) and standard air, the following expression is given in Jones (1985):

$$h_o = 27.42u_a^{0.8} \quad (2.16)$$

In the Specification of IEA Annex 10 the following is quoted:

$$h_o = 38u_a \quad (2.17)$$

It is known that when the tube external surface turns from dry to wet, the air side coefficient changes. h_{ow} can be related to h_o through a correction factor C_f such that

$$h_{ow} = h_o C_f \quad (2.18)$$

where C_f is a function of air flow Reynolds number (Elmahdy & Mitalas 1977).

One simplified expression relating h_{ow} to h_o is through the sensible heat ratio (SHR) such that (Jones 1985)

$$h_{ow} = h_o / SHR \quad (2.19)$$

Another approach to the enhancement is through a velocity correction term as suggested by Hiller and Glicksman (Goldstein 1983) as follows:

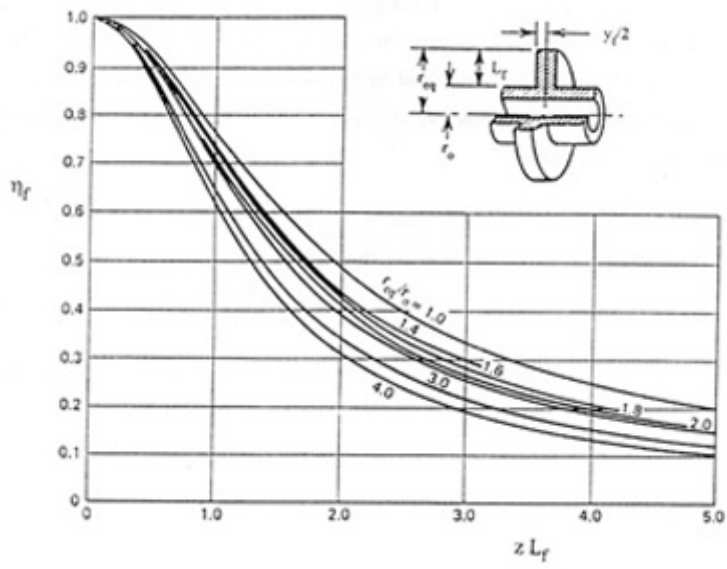
$$h_{ow} = h_o 0.626u_a^{0.101} \quad (2.20)$$

External surface area

The effective external surface area of the tube is given by

$$A_{oe} = A_p + \eta_f A_f = \eta_s A_o \quad (2.21)$$

where, A_p = prime area
 A_f = finned area
 A_o = total heat transfer area = $A_p + A_f$
 η_f = fin efficiency
 η_s = surface effectiveness



Figures 2.2 Performance of Circumferential Fins of Rectangular Cross-section

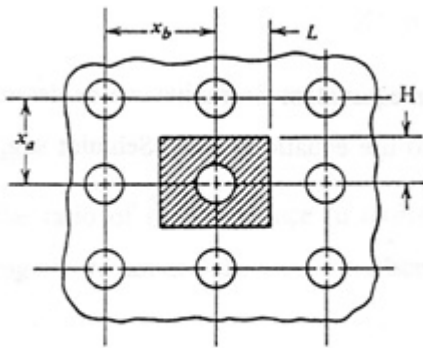


Figure 2.3 Rectangular Tube Array

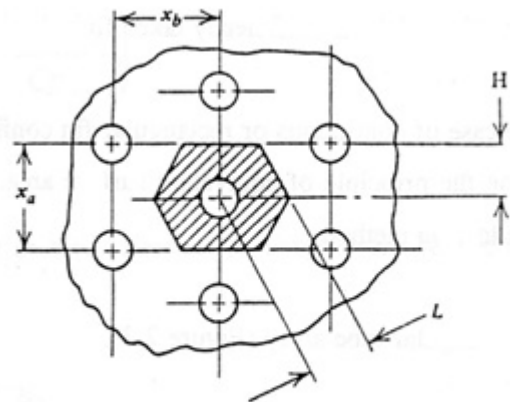


Figure 2.4 Hexangular Tube Array

Typically the fin will be very thin. In the case of the circular fin the solution for the fin efficiency is very complex (Elmahdy & Biggs 1983) and is not generally used for practical problems. Figure 2.2 shows a plot of the solution. An approximate but quite accurate method of predicting η_f for a circular fin with dry surface has been developed by Schmidt. The method is largely empirical but has many advantages when an analytical expression is required. The method is summarized as follows (McQuiston & Parker 1994):

$$\eta_f = \frac{\tanh(zr_o\phi)}{zr_o\phi} \quad (2.22)$$

In the above equation, r_o is the outside radius of the tube and z & ϕ are given by the following expressions:

$$z = \left(\frac{2h_o}{k_f y_f} \right)^{0.5} \quad (2.23)$$

and,

$$\phi = \left(\frac{r_{eq}}{r_o} - 1 \right) \left[1 + 0.35 \ln \left(\frac{r_{eq}}{r_o} \right) \right] \quad (2.24)$$

where k_f = thermal conductivity of the fin material, W/m.K
 y_f = fin thickness, m
 r_{eq} = equivalent fin radius, m

When r_{eq}/r_o is between 1.0 and 8 and η_f falls between 0.5 and 1.0, the error is less than one percent of the value of the fin efficiency taken from Figure 2.2.

In the case of continuous or rectangular fin configuration, an equivalent fin radius can be determined base on the principle of equivalent surface area. In order to use equation (2.24) Schmidt suggested the following method.

For rectangular tube array (Figure 2.3),

$$\frac{r_{eq}}{r_o} = 1.28 \psi(\beta - 0.2)^{0.5} \quad (2.25)$$

where,

$$\psi = \frac{H}{r_o} \quad (2.26)$$

and,

$$\beta = \frac{L}{H} \quad (2.27)$$

H and L are the row parameters defined in Figure 2.3 where L is always selected to be greater than or equal to H. In other words, $\beta \geq 1$.

For stagger (hexangular) tube array (Figure 2.4),

$$\frac{r_{eq}}{r_o} = 1.27 \psi (\beta - 0.3)^{0.5} \quad (2.28)$$

H and L are defined in Figure 2.4 where $L \geq H$.

For the case of wetted plate-fin-tube surface, the following approach to determine wetted fin efficiency η_{fw} is suggested by McQuiston (1975):

$$\eta_{fw} = \frac{\tanh(Zr_o\phi)}{Zr_o\phi} \quad (2.29)$$

where Z is given by the expression

$$Z^2 = \frac{2h_{ow}}{k_f y_f} \left(1 + \frac{C_r H_{fg}}{Cp_{ma}} \right) \quad (2.30)$$

C_r is the ratio of the difference in moisture content to the difference in temperature between the incoming air stream and the wetted surface, i.e.

$$C_r = \frac{g_a - g_s}{\theta_a - \theta_s} \quad (2.31)$$

This method is thought to be the most accurate available and is readily adapted to the use in computer.

2.2.3 Thermal conduction in tubings

Metallic Thermal Resistance

The thermal resistance of the finned tube R_m can be given by

$$R_m = R_f + R_t \quad (2.32)$$

where R_f & R_t are the thermal resistance of the fin and the tube respectively.

In the case of an imperfect mechanical bonding between the fins and the tube exists, an extra thermal resistance terms known as the thermal contact resistance has to be included. A brief discussion of the thermal contact resistance can be found in Holman (1989).

2.2.4 Single-phase flow inside tube

In piped flow, three different flow regions exist if the Reynolds number is large enough. Immediately adjacent to the wall is a laminar sublayer where heat transfer occurs by thermal conduction; outside the laminar sublayer is a transition region called the buffer layer, where both eddy mixing and conduction effects are significant; beyond the buffer layer and extending to the centre of the pipe is the turbulent region, where the dominant mechanism of transfer is eddy mixing. Flow in tubes are generally turbulent, except for very low flow velocity situation (for considerable reduction in system demand) where laminar flow may take place theoretically. However, Holmes (1988) pointed out that laminar flow is most unlikely to occur in cooling coils because in addition to the usual hysteresis in transition, vibration and entry effects may result in turbulent flow at much lower Reynolds numbers than is usual. The view was echoed by the work of Mirth, Ramadhyani & Hittle (1993) who found that a laminar developing flow correlation for water-side Reynolds numbers less than 2,300 underpredicted coil performance.

For fully developed turbulent flow in smooth tubes the following relation can be derived from the Colburn analogy (Ozisik 1985):

$$Nu = 0.023 Re^{0.8} Pr^{1/3} \quad (2.33)$$

Hence,

$$h_i = 0.023 \frac{k_w}{D_i} Re^{0.8} Pr^{1/3} \quad (2.34)$$

If water is the working fluid, the following expression from McAdams can be used (Clark 1985):

$$h_i = 1.429(1 + 0.0146\theta_w)u_w^{0.8}D_i^{-0.2} \quad (2.35)$$

where h_i relates to the bulk water temperature θ_w , water flow velocity u_w and tube inside diameter D_i .

For tubes with turbulence other correlations should be used .

2.2.5 Two-phase flow inside tube

Two phase flow occurs when steam condenses in an air heating coil or when refrigerant evaporates/boils in an air cooling coils. The following discussions refer to the refrigerant evaporation process but also fits well to the steam condensation process.

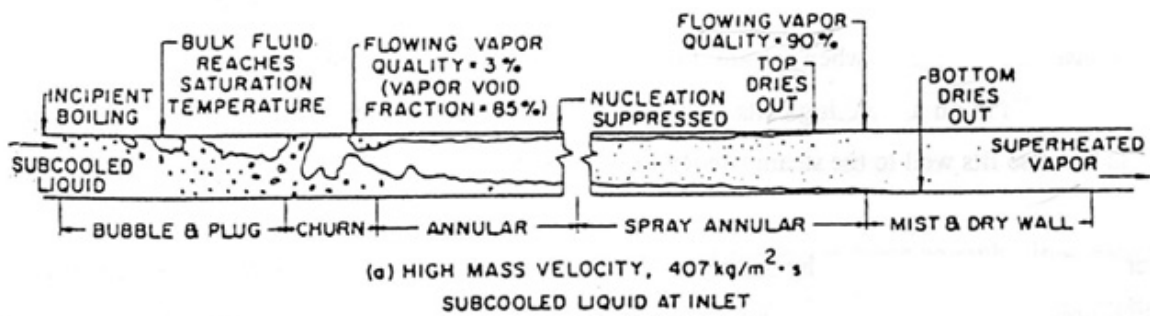
Different flow patterns exist in the boiling process in tubes. The flow patterns differ from a vertical to a horizontal tube arrangement. Figure 2.5 shows the flow patterns, which occur one after the other, in a horizontal evaporating tube as the flow velocity increases because of the fluid expansion. The flow is complicated by the fact that the flowing mass quality x' (which represents the ratio of the mass flow rate of vapour to the entire mass flow rate) can be different from the static quality x (which represents the fraction of liquid by mass) at a particular cross-section. The ratio of the vapour flow velocity to the liquid flow velocity can be different and is described by a factor known as 'slip'. However for general application, the slip can be taken as unity and this gives $x = x'$ (Stephan 1992). In this case for the fluid moved from section 1 to section 2 with a mass flow rate $m_1 (= m_2)$ and a heat transfer rate Q across the tube wall, the following heat balance equation can be used:

$$m_1 [x_1 H_{g1} + (1 - x_1) H_{f1}] + Q = m_2 [x_2 H_{g2} + (1 - x_2) H_{f2}] \quad (2.36)$$

In the above equation, the changes in kinetic and potential energy have been disregarded. It has been further assumed that the vapour and liquid are in thermodynamic equilibrium and that the specific enthalpies in the saturated state are to be taken at the corresponding fluid pressure. x' is therefore representing the thermodynamic quality. Stephan (1992) pointed out that the latter assumption is not accurate when the value of x' becomes very small or approaching unity. When x' is small, vapour bubble can already form on the hot wall while the core of the flow is still subcooled. Vapour and liquid thus have different temperatures. With high quality the flow pattern is the spray flow type. Heat is transferred mainly to the

vapour which becomes superheated, although in the core of the flow liquid drops are still swept along and evaporate only gradually. In the range of intermediate qualities however, the equation gives very good approximation.

Numerous efforts had been done to predict the heat transfer coefficients for refrigerants. The work of Stoneham, Saluja & Dunn (1979), Said & Azer (1983) and Goldstein (1983) are several out of hundreds examples.



Constant heat flux; tube diameter approximately 12 mm

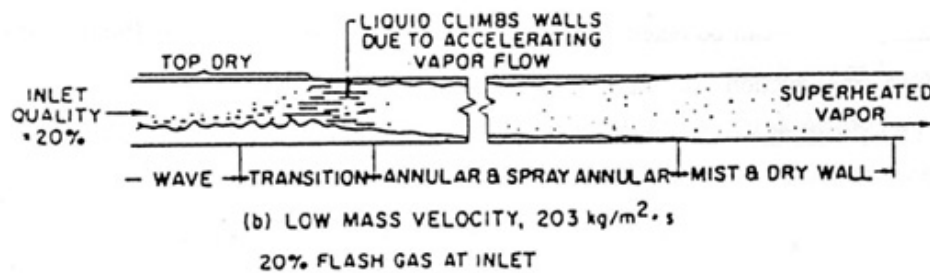


Figure 2.5 Flow Regimes in Horizontal Tube Evaporator

2.3 Electric Heaters

Electric heaters provide an easily installed, clean source of heat for warming of supply air or room air directly. They are also popularly used in boilers or water baths either to provide hot water or to generate steam for the use in terminal units or humidifiers. Frequently, they are used as auxiliary or backup heat sources in heat-pump systems and in solar heating systems.

The types of electric heaters suitable for comfort heating includes: open wire sheathed or finned tube, immersion elements, and infrared heaters. A finned tube type is shown in Figure 2.6 In sheathed pan humidifier, the heating elements are immersed in a water bath. Electric infra-red heaters use heat produced by electric current flowing in a high-resistance wire or ribbon. Figure 2.7 shows some common features.

Heat is generated within the heater element itself. The heat energy is conveyed to the fluid in contact through convective heat transfer and to the neighbouring solid surfaces through long wave radiation heat transfer. The amount and characteristics of radiant energy emitted depend on the nature of the heater surface, its microscopic arrangement and its absolute temperature. Net energy transfer rate Q_r depends on the temperatures and spatial relationships of the surface (denoted by 1) and its surroundings (denoted by 2), in that for black body radiation

$$Q_r = F_{12}A_1\sigma(\Theta_1^4 - \Theta_2^4) = F_{21}A_2\sigma(\Theta_2^4 - \Theta_1^4) \quad (2.37)$$

where σ is the Boltzman's constant; F stands for the view factor, A for the surface area, and Θ the absolute temperatures.

If the heater is totally surrounded by the neighbouring surface, the value of F_{12} can be taken as unity and the radiative heat transfer coefficient h_r can be expressed as

$$h_r = \sigma(\Theta_1^3 + \Theta_1^2\Theta_2 + \Theta_1\Theta_2^2 + \Theta_2^3) \quad (2.38)$$

Conductive heat transfer to the casing on which the filament is fixed is possible. The quantity is nevertheless negligible because of the good thermal insulation between the two.

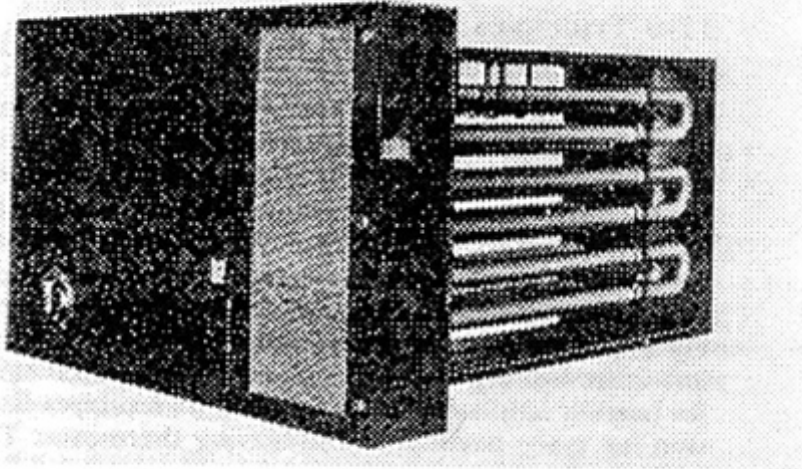


Figure 2.6 Finned-tube Duct Electric Heater

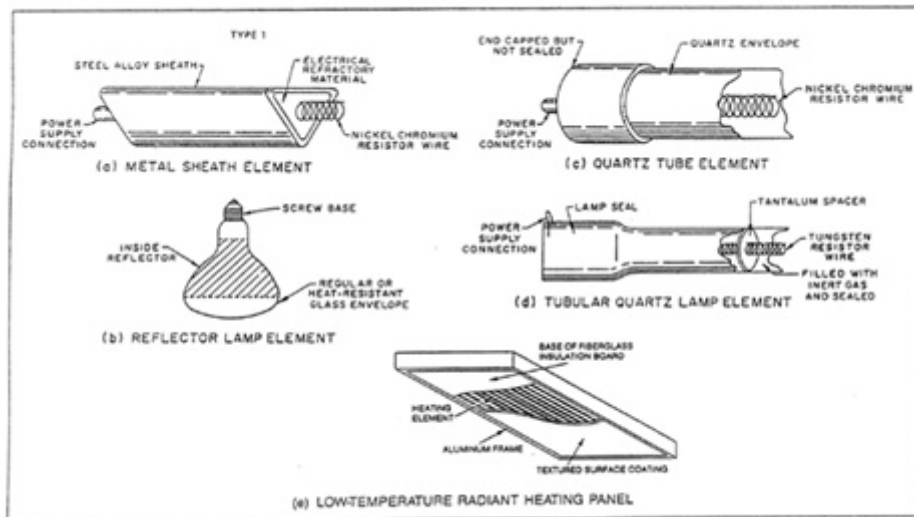


Figure 2.7 Common Electric Infrared Heaters

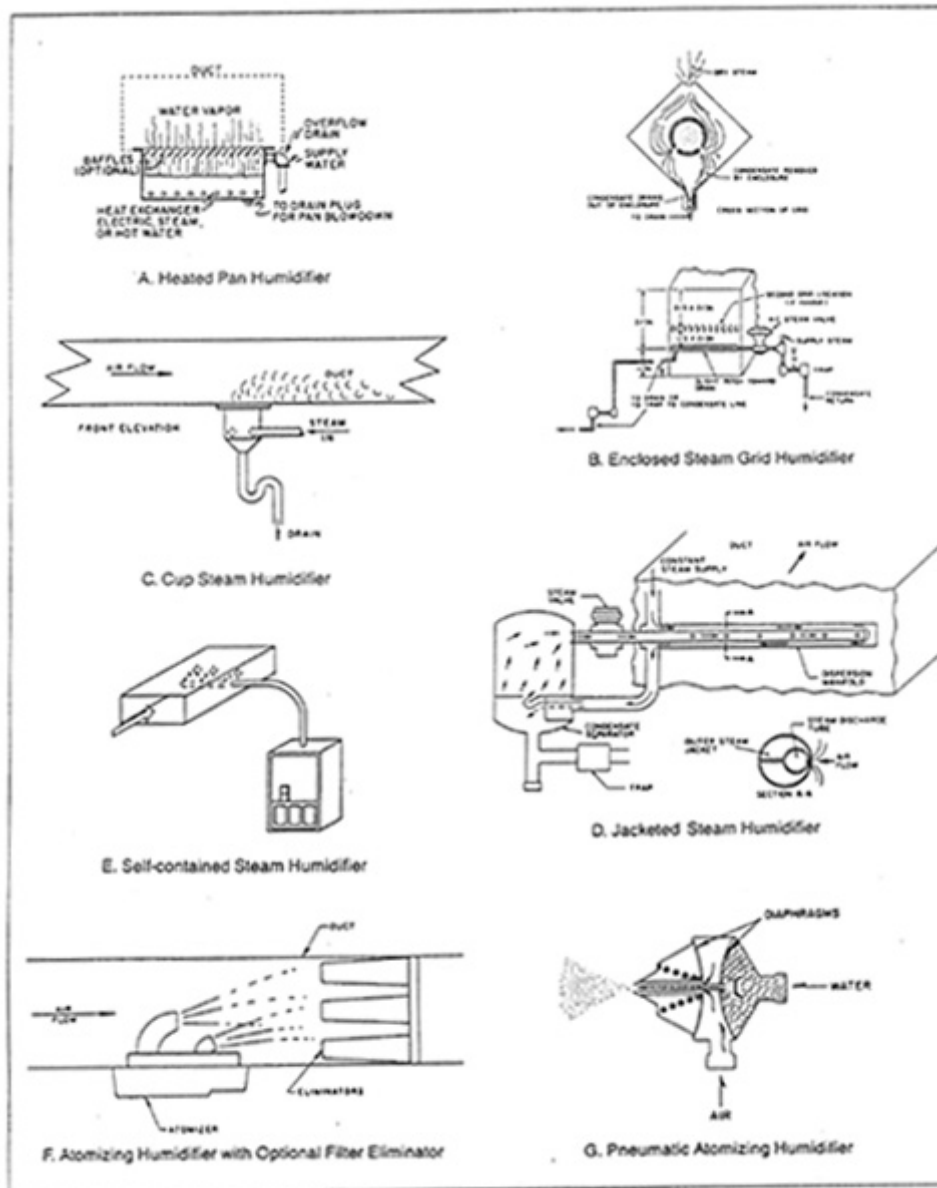


Figure 2.8 Typical Humidifiers

2.4 Humidifiers

A humidifier is a device that adds moisture to an air stream. The moisture can be added by evaporating or atomizing water, or by injecting steam. The types generally include:

- (i) pan types (heated or unheated),
- (ii) wetted element,
- (iii) atomizing types, and
- (iv) direct steam injection types.

Figure 2.8 shows some typical examples. While air washers and evaporative coolers may be used as humidifiers, they are usually selected for some additional functions such as air cooling or air cleaning. Evaporation of water is achieved in a process approximating adiabatic saturation for pan type and for wetted-element type water humidifiers. The process is explicable by the enthalpy potential theory that has been described earlier. In some cases, the pan type humidifier is heated by an electric resistance element, or by a steam or hot-water coil, in order to increase the evaporation rate. The humidification process, as described by the condition line on the psychrometric chart, is solely a function of the injected water/steam enthalpy.

In injection type humidifiers, the mixing of the injection stream and the air stream will come to a fluid (dry air and water vapour) mass balance and an enthalpy balance situation. If the air stream becomes over saturated, condensate will come out and deposit onto any solid surface in contact, though trace of water droplets may carry along the stream sometimes.

In the water bath of the direct steam injection type humidifier, steam is generated when the water inside the bath reaches the boiling point. Radiant heat loss from the heating element is negligible as the transmission of thermal radiation through a liquid is extremely low. A small amount of heat energy is finally lost through the container casing by thermal conduction and subsequently through free convection with ambient air.

2.5 Flow Conduits

The distribution of fluids by pipes, ducts and conduits is essential to all heating and cooling systems. Fluids encountered can be gases, vapours, liquids, and mixture of liquid and vapour (2-phase flow).

Ducts are channels for transporting and distributing moist air. A complete duct system includes supply and return ducts for recirculation, as well as fresh and exhaust air ducts for ventilation purpose. Ducts

within buildings generally are fabricated from sheet metal, sometimes added with fibrous glass which provides combined air barrier, thermal insulation, and sound absorption. Ducts embedded in or below floor slabs may be of compressed fiber, asbestos cement, ceramic tile, or other rigid materials. Figures 2.9 and 2.10 show some typical details of an air ductwork. Metallic duct sections are fastened together with special seams, slips, and locks. As the joints are not perfect, air leakage may occur. A supply duct under positive pressure will have the air leaks from inside to outside and vice versa for a return duct under negative pressure.

In air-conditioning applications, pipes convey heat transfer fluids like hot/chilled water, steam and refrigerants. Liquid flow in pipes is generally incompressible. Two-phase fluid flow is compressible; the rate and the direction of conversion between vapour and liquid in the fluid stream depend on the heat flux across the pipe wall.

Design fluid flow in conduits is turbulent in most applications. The expressions of convective heat transfer coefficients for piped flow quoted in Section 2.2.3 also apply well to here. Under partial load operation the flow can become laminar (for $0 < Re \leq 2300$) and the following empirical relation by Hausen can be used:

$$Nu = 3.66 + \frac{0.0668(D/L) Re Pr}{1 + 0.04[(D/L) Re Pr]^{2/3}} \quad (2.39)$$

This is for fully developed laminar flow at constant wall temperature and the heat transfer coefficient calculated is the average value over the entire length of tube. If the tube is sufficiently long the Nusselt number approaches a constant value of 3.66 and in this case

$$h = 3.66 \frac{k_a}{D} \quad (2.40)$$

Any disturbance of the incoming fluid condition at the conduit inlet will affect the fluid outlet condition some time later. The time lag of the response is caused by the time required for the fluid to travel from one end of the conduit to the other and the phenomenon is called 'transport delay'. Heat exchange rate between the fluid in conduit and the ambient air depends on the magnitude of the surface convective resistances at both sides of the conduit wall and also the thermal conductance of the conduit wall itself. Thermal insulations for exterior surface application may have attached vapor barriers to prevent moisture absorption. Imperfect insulation may lead to moisture condensation at an exposed metallic surface. When a conduit is located outdoors, the external surface is subject to solar radiation absorption and long-wave radiation exchange on a sunny day. In such circumstances non-uniform conduit wall temperature can occur at any cross-section.

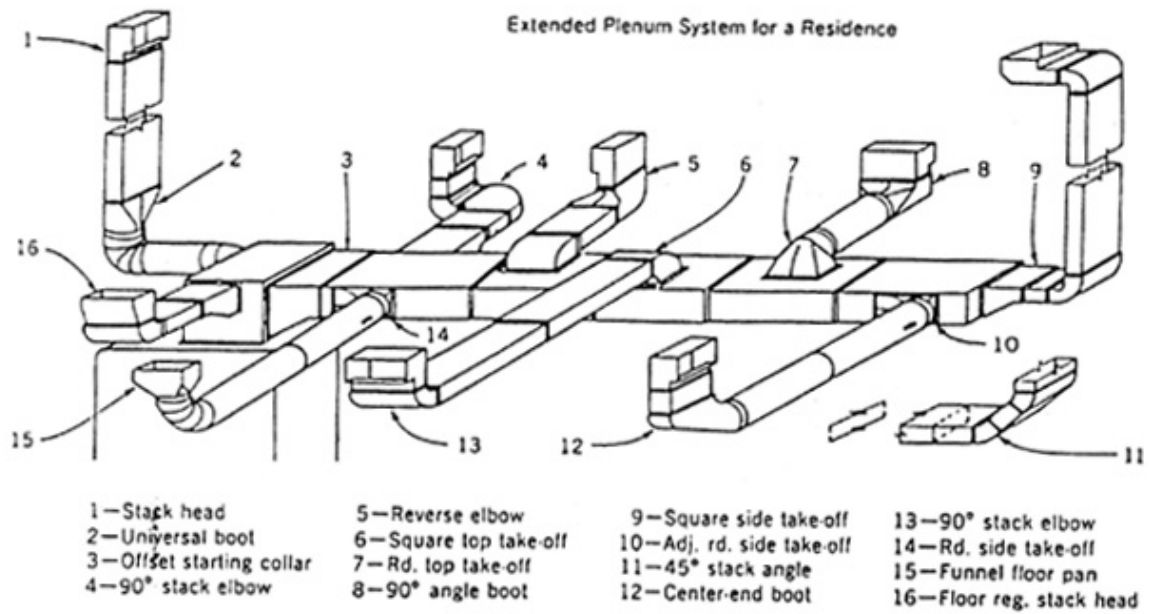


Figure 2.9 Diagram of An Air-duct System

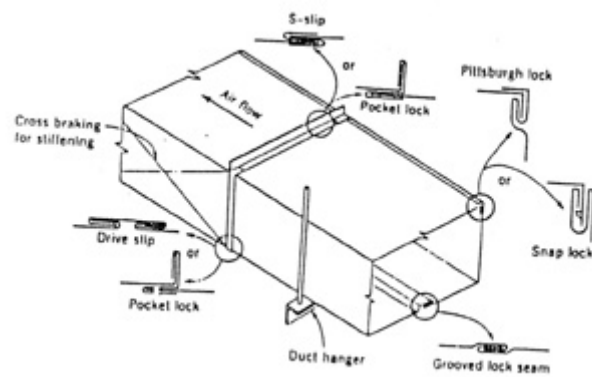


Figure 2.10 Methods of Fabricating and Assembling Ductwork

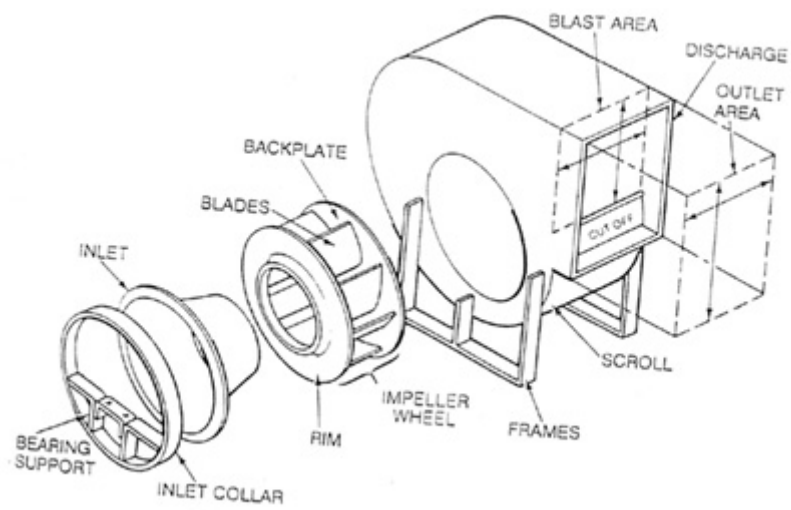


Figure 2.11 Centrifugal Fan Components

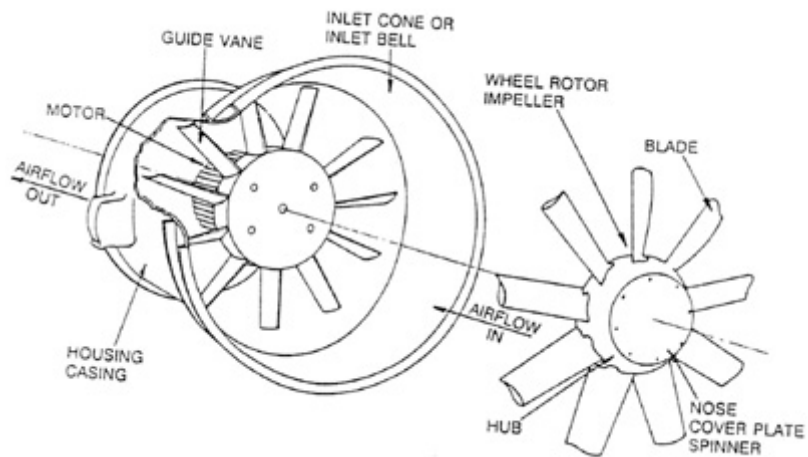


Figure 2.12 Axial Fan Components

2.6 Flow Inducers & Restrictors

Flow inducers

Flow inducers include fans and pumps. In air-conditioning systems the fan creates pressure difference and generates air flow. Electric motors are the usual prime mover. The fan impeller does work on the air, imparting to it both static and kinetic energy which vary in proportion depending on the fan type. Fans are generally classified as centrifugal type (Figure 2.11) or axial flow type (Figure 2.12) according to the direction of airflow through the impeller. Other flow types do exist.

All fans produce pressure by altering the velocity vector of the flow. The fans produce pressure and/or flow because the rotating blades of the impeller impart kinetic energy to the air by changing its velocity. Velocity change is the result of tangential and radial velocity components in the case of centrifugal fans, and of axial and tangential velocity components in the case of axial flow fans. Fluid pressure possessed by the air stream at the fan outlet will eventually dissipate as heat energy because of the friction losses in the duct system downstream. This rate of energy dissipation will contribute to a temperature rise in the air stream and is given by

$$Q_{\eta} = \eta W \tag{2.41}$$

where W is the instantaneous motor power and η is the instantaneous fan efficiency.

In-efficiency in motor power will be absorbed by the motor-impeller body as heat energy at a rate given by

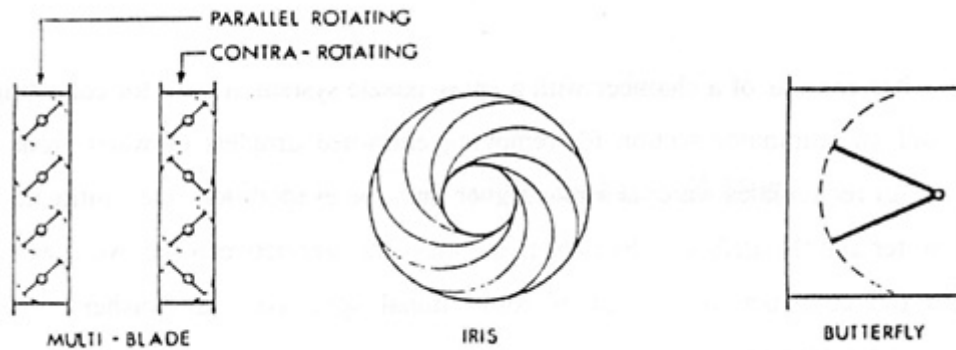
$$Q_{1-\eta} = (1 - \eta)W \tag{2.42}$$

In the case of submerged fan-motor, this energy will be released to the air stream later on as a result of the elevated temperature at the exposed motor surface. If the motor is not over-heated, the radiant energy released from the motor surface is negligible.

Flow restrictors

Examples of flow restrictors are volume control dampers, fire dampers, louvres, air filters, etc. Each of these components in the air stream serves a particular function. For instance, a volume control damper (Figure 2.13) is used for regulating the air volume flow rate; a fire damper (Figure 2.14) is used as an automatic shut-off device to stop the chance of fire spread through the air duct; a louver is employed as an

air-intake or air-exhaust device; an air filter is for eliminating air-borne particulates in the air stream. The presence of these components unavoidably incurs additional friction loss. Their masses can store heat energy and therefore heat transfer may actually take place through any of the three basic modes: thermal conduction, convection, or radiation. In most cases, the majority of the heat exchange will be through convective heat exchange with the air in contact. Free convection will take place if the air is stagnant for instance in a shut-off VAV box. Here the fluid flow remains local and is buoyance driven. Substantial radiative heat transfer may take place for an exposed component like a louver where absorption of solar radiation may occur. Moisture condensation may occur if the component surface temperature is for any reason lower than the dew point temperature of the air in contact.



Figures 2.13 Typical Balancing Dampers for Insertion in Ducting

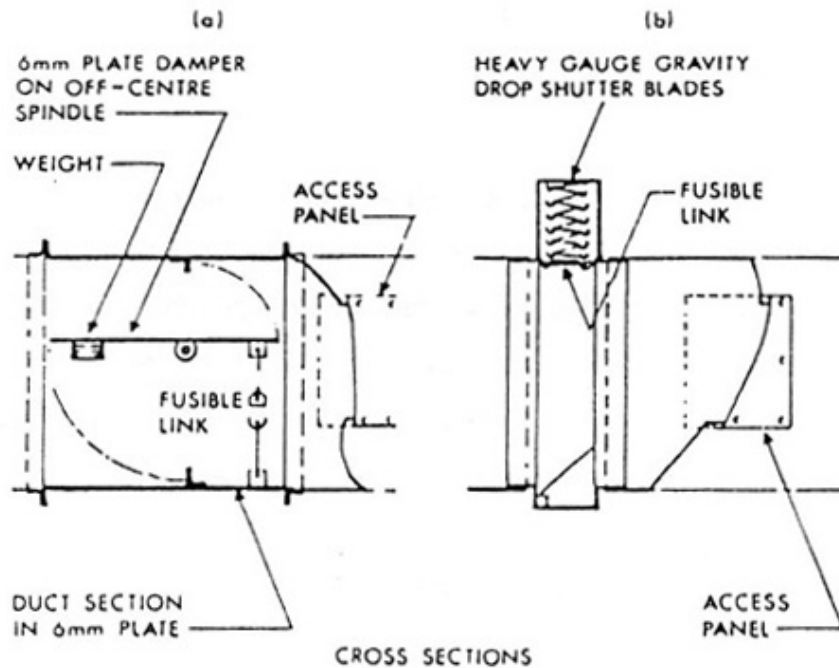


Figure 2.14 Typical Construction Methods for Fire Dampers

2.7 Direct Contact Equipment

Direct contact equipment includes air washers, spray dehumidifiers and cooling towers. In this equipment the quantity of water in contact with the air is much larger than the quantity added to or withdrawn from the air stream. The primary reason for treating direct contact equipment as a separate group arises from the difficulty in evaluating the effective heat and mass transfer areas. For an air washer or any spray-type device that does not have packing materials, the heat and mass transfer areas are approximately equal. For a cooling tower the difference may be considerable.

Direct-contact equipment is usually classified as spray-type and cell-type.

spray-type

A spray-type air washer consists of a chamber with a spray nozzle system, a tank for collecting spray water as it falls, and an eliminator section for removing entrained droplets of water from the air stream. A pump circuit recirculates water at a rate higher than the evaporation rate. Intimate contact between the spray water and the airflow induces heat and mass transfer between the two fluid streams. Figure 2.15 shows the construction features of conventional spray-type air washers. Essential requirements in the operations are:

- i) uniform distribution of the air across the air stream,
- ii) an adequate amount of spray water broken up into fine droplets,
- iii) good spray distribution across the airstream,
- iv) sufficient length of travel through the spray and wetted surfaces,
- v) elimination of free moisture from the outlet air.

Cell-type

These washers obtain intimate air-water contact by passing the air through cells packed with glass, metal, or fiber screens (Figure 2.16). Water passes over cells arranged in tiers. Behind the cells are blade-type or glass-mat eliminators. Most cell washers are arranged for concurrent air and water flow. Cell washers come in many sizes of insulated or uninsulated construction complete with fan, motor, pump, and external spray piping. Atomization of the spray water is not required in cell washers, but good water distribution over the face of the cell is essential.

Air can be humidified in any one of the following three ways:

- i) using recirculated spray water without prior treatment of the air,
- ii) pre-heating the air and washing it with recirculated spray water, and
- iii) using heated spray water.

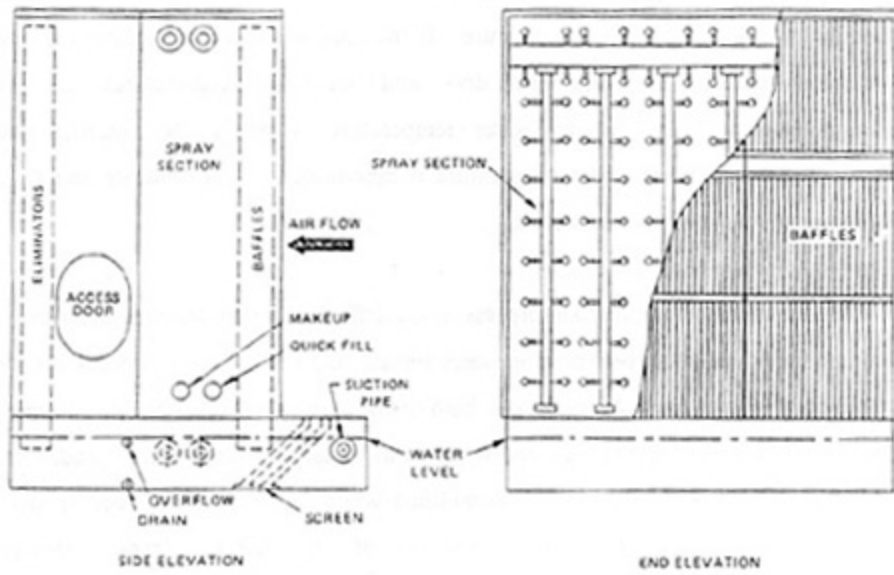


Figure 2.15 High Velocity Spray Washers

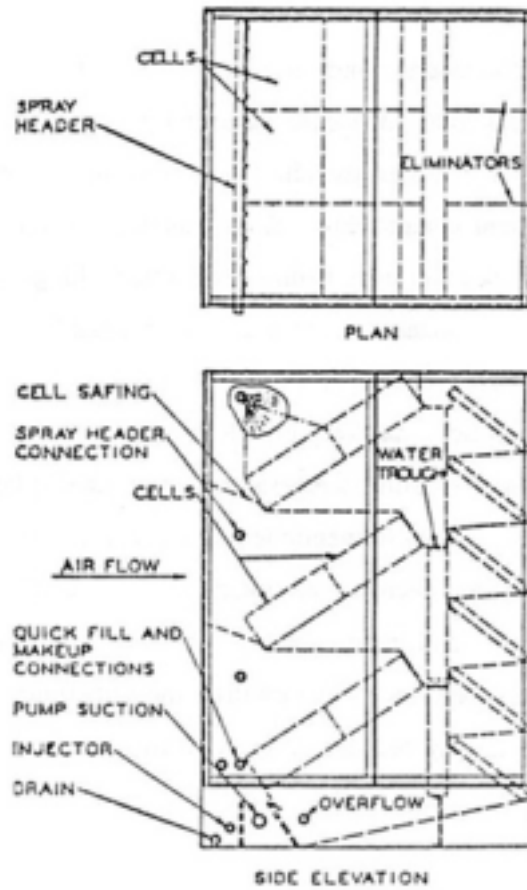


Figure 2.16 Typical Cell Air Washer

An alternative function of the equipment is to cool and dehumidify an air stream. Heat and moisture removed from the air raise the water temperature. If the entering water temperature is below the entering wet-bulb temperature, both the dry- and wet-bulb temperatures are lowered. Dehumidification results if the leaving water temperature is below the entering dew-point temperature. Moreover, the final water temperature is determined by the sensible and latent heat pickup and the quantity of water in circulation.

There are two driving forces in the thermal process: i) the difference in dry bulb temperatures, and ii) the difference in vapour pressures between the water surface and the air. The process can be again explained by the enthalpy potential theory, in that both the heat and mass transfer rates depend on the interface temperature between the moist air and water-spray streams. The interface condition during the process changes as the air is heated and humidified while the water is cooled, or vice versa. Accurate performance analysis requires the physical data of the actual heat transfer area per unit volume of the chamber. Moreover, additional water loss from the spraying stream is bound to occur for an imperfect eliminator.

2.8 An Overview

Figure 2.17 gives a pictorial view of the energy and mass flow paths possibly found in air conditioning systems. From the above discussions, one would admit that in the actual operation of an air conditioning system, many of these flow paths in existence may have no direct relation to the intended psychrometric duties of the system components. Solar radiation falling on an air duct casing, room air leaking into a negative-pressure air duct, natural convection taking place at a shut-off branch are some examples out of thousands actual occurrences. Occasionally relatively dry air passing across a wetted cooling coil may result in temporal humidification of the air stream rather than dehumidification. An electric heater element may keep on releasing heat energy after the cut-off of electricity supply because of its elevated metallic temperature. In most plant performance appraisal studies using computer simulation, the above mentioned flow paths may be unimportant, or totally irrelevant to the problem under study, and therefore are intentionally ignored in order to arrive at a practical solution in terms of costs, time, and manpower input. There are situations, however, some of the flow paths may result in a loss of accuracy when omitted and sometimes, they are in fact the key elements of a particular study. It is only because of the over-simplified component models being installed at a building/plant analysis software that make the study of a particular issue impossible.

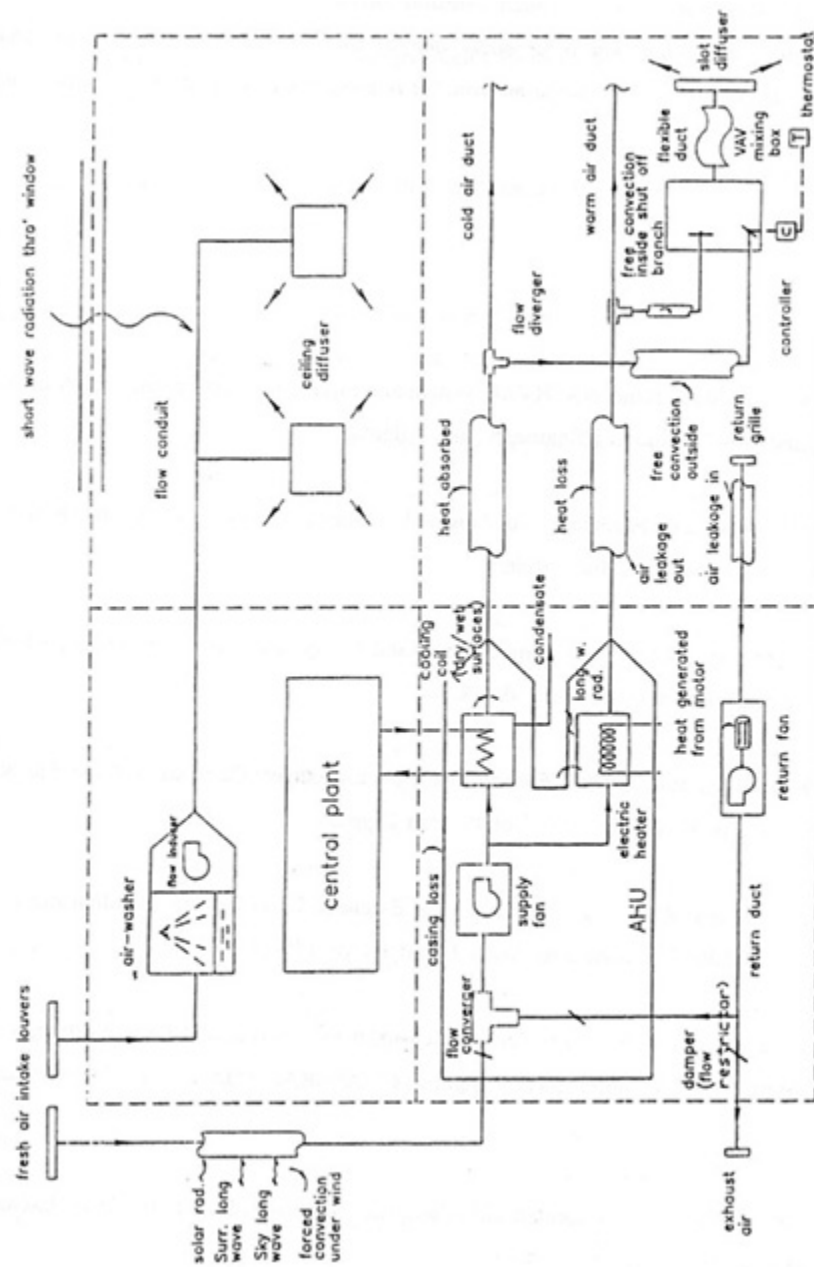


Figure 2.17 Basic Energy and Mass Flow Paths in Air-conditioning System

It will be desirable if there exists a flexible model-building environment that, during the plant component creation process, allows the inclusion or exclusion of any or all of the possible energy and mass flow paths taking place in reality. Such a flexible environment would strengthen and widen the plant simulation applicability and is probably one of the promising features of an advanced simulation software we are looking for to-morrow. It is from this point that the following Chapters are developed.

References

ASHRAE 1992. ASHRAE Handbook, HVAC System and Equipment. American Society of Heating, Refrigerating and Air-Conditioning Engineers, Inc., Atlanta.

ASHRAE 1993. ASHRAE Handbook, Fundamental. American Society of Heating, Refrigerating and Air-Conditioning Engineers, Inc., Atlanta.

Clark, D.R. 1985. HVACSIM+ Building Systems and Equipment Simulation Program Reference Manual. U.S. Department of Commerce, NBSIR 84-2996.

Elmahdy, A.H. & Biggs, R.C. 1979. "Finned Tube Heat Exchanger: Correlation of Dry Surface Heat Transfer Data." ASHRAE Transactions, Vol. 85, Part 2, pp.262-273.

Elmahdy, A.H. & Biggs, R.C. 1983. "Efficiency of Extended Surfaces with Simultaneous Heat and Mass Transfer." ASHRAE Transactions, Vol. 89, Part 1A, pp.135-143.

Elmahdy, A.H. & Mitalas, G.P. 1977. "A Simple Model for Cooling and Dehumidifying Coils for Use in Calculating Energy Requirements for Buildings." ASHRAE Transactions, Vol. 83, Part 2, pp. 103-117.

Goldstein, S.D. 1983. "A Mathematically Complete Analysis of Plate-fin Heat Exchangers." ASHRAE Transactions, Vol. 89, Part 2A, pp.447-470.

Holman, J.P. 1989. Heat Transfer. SI Metric edit., McGraw Hill, Singapore.

Holmes, M.J. 1988. "HVAC Component Specification: Heating And Cooling Coils." Energy Conservation in Building & Community Systems Programme, Annex X: system simulation (S6), International Energy Agency.

Jones, W.P. 1985. Air Conditioning Engineering. 3rd. edition, Edward Arnold, London.

Martin, P.L. & Oughton, D.R. 1989. Faber and Kell's Heating and Air-conditioning of Buildings. 7th edit., Butterworths, UK.

McQuiston, F.C. 1975. "Fin Efficiency with Combined Heat and Mass Transfer." ASHRAE Transactions, Vol. 81, Part 1, pp.350-355.

McQuiston, F.C. 1978. "Heat, Mass and Momentum Transfer Data for Five Plate-Fin-Tube Heat Transfer Surfaces." ASHRAE Transactions, Vol. 84, Part 1, pp.266-293.

McQuiston, F.C. 1978a. "Correlation of Heat, Mass and Momentum Transport Coefficients for Plate-Fin-Tube Heat Transfer Surfaces with Staggered Tubes." ASHRAE Transactions, Vol. 84, Part 1, pp.294-309.

McQuiston, F.C. & Parker, J.D. 1994. Heating, Ventilating, and Air Conditioning Analysis and Design. 4th edit., John Wiley & Son, New York.

Mirth, D.R., Ramadhyani, S. & Hittle, D.C. 1993. "Thermal Performance of Chilled-water Cooling Coils Operating at Low Water Velocities." ASHRAE Transactions, Vol. 99, Part 1, pp.43-53.

Ozisik, N.M. 1985. Heat Transfer, a Basic Approach. McGraw-Hill, USA.

Rich, D.G. 1975. "The Effect of the Number of Tube Rows on Heat Transfer Performance of Smooth Plate-Fin-Tube Heat Exchangers." ASHRAE Transactions, Vol. 81, Part 1, pp.307-319.

Said, S.A. & Azer, N.Z. 1983. "Heat Transfer and Pressure Drop during Condensation inside Horizontal Finned Tubes". ASHRAE Transactions, Vol. 89, Part 1A, pp.114-134.

Stephan, K. 1992. Heat Transfer in Condensation and Boiling. Springer-Verlag, New York.

Stoecker, W.F. & Jones, J.W. 1982. Refrigeration and Air Conditioning. 2nd edit., McGraw Hill, Singapore.

Stoneham, H.G., Saluja, S.N. & Dunn, A. 1979. "Prediction of Heat Transfer Coefficients for Refrigerants Evaporating inside Horizontal Tubes." Technical Memorandum No. 70, Institute of Environmental Science and Technology, Polytechnic of South Bank, U.K.

CHAPTER THREE

PLANT COMPONENT MODELLING BY A FINITE DIFFERENCE METHOD

Numerical methods play an important role in engineering analysis, both static and dynamic. These must be regarded as approximate-solution procedures only, though the accuracy through cautious design can be made to satisfy even the most demanding criteria. In this Chapter a variety of air conditioning plant components are modelled by one particular numerical method - the finite difference control volume conservation method. It will be shown that the matrix templates of the component models developed in this way share lots of similarities. Extension of the method is required when it comes to the modelling of fluid flow transport delay and phase change phenomena. The structures of the models derived give hinds to the development of a more generalized plant database.

3.1 Finite Difference Control Volume Conservation Approach

The finite difference control volume conservation approach to dynamic plant simulation was developed in the 1980s, for instance the work of McLean (1982) on solar energy system and Tang (1985) on hot-water central heating system. It has been proved to be very useful and powerful in developing building or plant component models in that it offers a model infrastructure which conserves integrity by numerically processing all elements of the problem as a single system, fully connected in space and time, and under the influence of dynamic influences and constraints (Clarke 1985). It does provide a promising future for the advanced building and plant simulation software of the next generation. It follows that a series of the plant components to be introduced here are modelled through this methodology.

Control volume conservation method

A plant component is firstly physically decomposed into a finite number of sub-parts, each of which is represented by a control volume in space. Each control volume is an arbitrarily defined physical space enclosed by a boundary surface. The volume can be uniform in material and therefore possesses "homogeneous" properties, or spatially heterogeneous in that different materials may co-exist. In the

latter case suppose that there are N numbers of different materials (constituents) in the volume, any material property of the control volume will be determined by the mass weighted average of the N constituents. For example, in a control volume with a mixture of N numbers of fluids, the specific heat at constant pressure is given by

$$Cp = \frac{\sum_{i=1}^N (Cp_i M_i)}{\sum_{i=1}^N (M_i)} \quad (3.1)$$

This is often referred as the "lumped" parameter approach. It should be noted that any parameter in the numerical scheme can be time-variant; also the use of a small control volume for heterogeneous materials should be cautious since this sometimes could lead to modelling/solution problems.

Then, for each of these finite volumes in turn, and in terms of all nearby volumes in thermal or flow contact, conservation equations are developed in relation to the transport properties of interest, here in particular heat energy and fluid mass exchange.

By virtue of the basic conservation laws in physics, for any control volume,

$$\sum(\text{Energy flow in}) - \sum(\text{Energy flow out}) + \sum(\text{Energy generated}) = \text{Energy stored} \quad (3.2)$$

and for any fluid type in the volume,

$$\sum(\text{Mass flow in}) - \sum(\text{Mass flow out}) + \sum(\text{Mass generated}) = \text{Mass stored} \quad (3.3)$$

The arbitrariness of the control volume discretization scheme makes these equations possible to apply to any object with irregular shape, non-unified structure, or multi-dimensional energy or mass flows. The time derivatives of these equations can be in the forms of algebraic, ordinary differential or partial differential.

For the control volume 'i' of a single-phase pure fluid flow shown in Figure 3.1 where Q is the rate of thermal energy added to the control volume, the energy and fluid flow balance equations can be respectively written as

$$m_{i-1}Cp_{i-1}\theta_{i-1} - m_iCp_i\theta_i + Q = \frac{\partial}{\partial t}(M_iCp_i\theta_i) \quad (3.4)$$

$$m_{i-1} - m_i = \frac{\partial}{\partial t}(M_i) \quad (3.5)$$

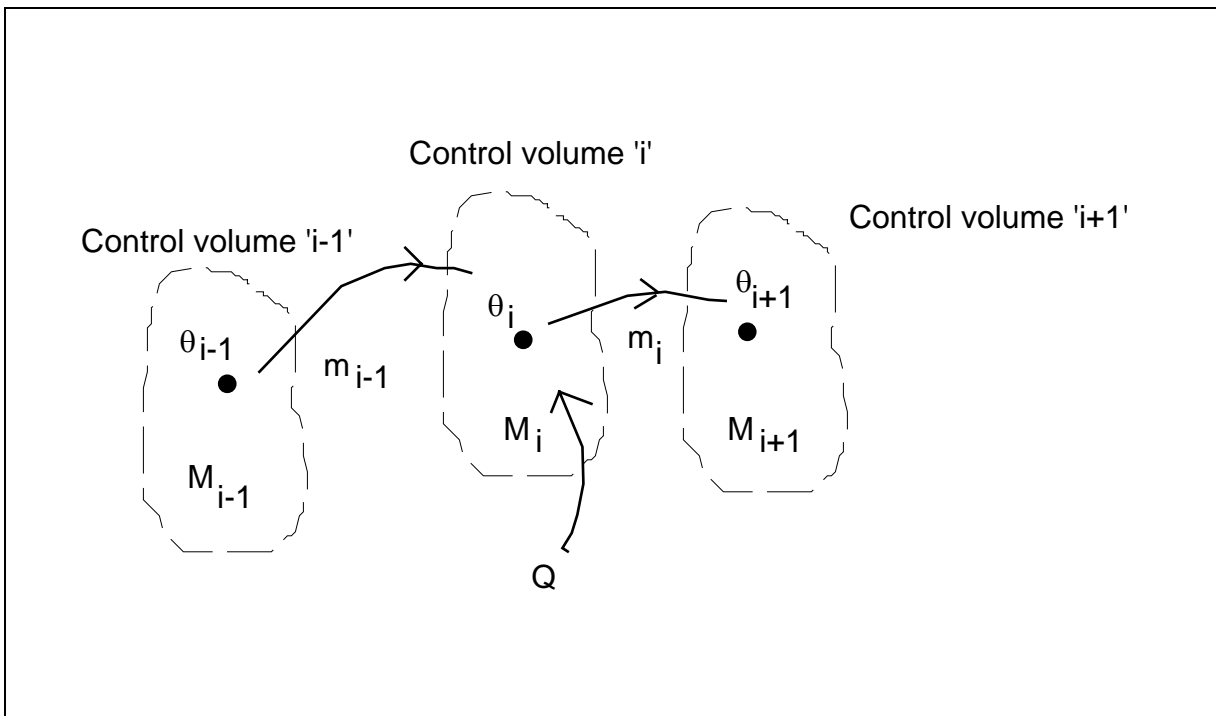


Figure 3.1 Control Volume Energy and Fluid Flow

If the material in a control volume is a solid, then the fluid flow balance equation will be absent. Or if the volume contains moist air or a two-phase fluid, then two mass flow balance equations (first phase and second phase) can be derived. In moist air, the first phase refers to dry air and second phase refers to water vapour. In a two-phase fluid, the first phase refers to liquid and second phase refers to vapour.

For the sake of computer simulation, all equations derived are eventually converted into the algebraic form by numerical methods, for instance, the finite difference methods.

Finite difference methods

Finite difference methods are concerned with approximating the derivatives of the equation either directly by a truncated Taylor series expansion, or as in this case, indirectly by application of the principle of conservation of energy to small control volumes. Alternative mixes of the approximation schemes are possible and this leads to different formulations, namely explicit, implicit and Crank-Nicolson. (Chapra & Canale 1988; Minkowycz et al. 1988)

For a small time interval δt , equation (3.4) can be expressed in the finite difference forms as follows, assuming incompressible flow (i.e. for a constant value of M_i):

i) explicit formulation,

$$m_{i-1}^* Cp_{i-1}^* \theta_{i-1}^* - m_i^* Cp_i^* \theta_i^* + Q^* = M_i Cp_i^* \left(\frac{\theta_i - \theta_i^*}{\delta t} \right) \quad (3.6a)$$

ii) implicit formulation,

$$m_{i-1} Cp_{i-1} \theta_{i-1} - m_i Cp_i \theta_i + Q = M_i Cp_i \left(\frac{\theta_i - \theta_i^*}{\delta t} \right) \quad (3.6b)$$

iii) Crank-Nicolson formulation,

$$\left(\frac{m_{i-1} Cp_{i-1} \theta_{i-1} + m_{i-1}^* Cp_{i-1}^* \theta_{i-1}^*}{2} \right) - \left(\frac{m_i Cp_i \theta_i + m_i^* Cp_i^* \theta_i^*}{2} \right) + \left(\frac{Q + Q^*}{2} \right) = M_i (Cp_i + Cp_i^*) \left(\frac{\theta_i - \theta_i^*}{\delta t} \right) \quad (3.6c)$$

Using the terminology of computer simulation, δt is the length of a simulation time step; those symbols with the superscript * are present time step values and those without are either future time step values or constant parameters.

The above finite difference formulations can be generalized using a weighting factor α in that the value of α equals 0, 1 and 0.5 respectively gives the explicit, implicit and Crank-Nicolson expressions. This generalised equation, re-arranged with the future time step values at the left hand side and the present time step values as well as the excitations (e.g. heat addition) at the right hand side, is as follows:

$$\left[-\alpha m_i - \frac{M_i}{\delta t} \right] C p_i \theta_i + \alpha m_{i-1} C p_{i-1} \theta_{i-1} = \left[(1-\alpha) m_i^* - \frac{M_i}{\delta t} \right] C p_i^* \theta_i^* + (1-\alpha) m_{i-1}^* C p_{i-1}^* + \alpha Q + (1-\alpha) Q^* \quad (3.7)$$

Care has to be taken in choosing a finite difference scheme for a specific simulation problem, since some schemes do have higher order of accuracy but cannot pass the condition of stability or can only be used in relative limited time and space steps. The explicit scheme is known to be convergent and stable only for a finite time step; here convergence means that as δt approaches zero, the results approach the true solution, and stability means that errors at any stage of the computation are not amplified but are attenuated as the computation progresses. The implicit scheme is unconditionally stable and therefore allows a longer time step to be used; but it has the limitations that the temporal difference approximation is first-order accurate and the solution scheme always involves the solving of an equation set. The Crank-Nicolson scheme is an alternative implicit scheme which is second-order accurate.

plant component model

In the concept of simulation as introduced in Chapter 1, the discretized and interconnecting control volumes can be seen as a network of "nodes" interconnected through the "arcs". Since each control volume in maximum can be described by three number of equations, a "multi-node" plant component model can be represented by 3 sets of characteristic equations, each for energy flow, first phase mass flow, and second phase mass flow. A generalized form of these 3 sets of equations with the same pattern of matrix coefficients become the matrix template of the plant component. This concept will be more clear when the actual component models are discussed in the following sections.

For a network of plant components as in the case of system simulation, the above steps up to this point give rise to an overall system of equations with 3 sub-matrix sets, where each equation describes how a state variable of one node varies together with the other interconnecting nodes over some small interval of time. Control laws are then added to this equation-set to prescribe, limit or impose conditions on the system behaviour. Once established for a time step by finding out the numerical values of all matrix coefficients, the equation-set is solved by a solution method before being re-established for the next time step. The solution method used in ESP-r is described in Chapter 5.

The following are the general review of the air conditioning component models and then the derivation of their matrix templates using the finite difference control volume conservation method.

3.2 Flow Conduit Models

3.2.1. Review of modelling theory_

In a flow conduit, the change of fluid temperature originates from heat transfer at the conduit surface and the influx of fluid mass at a different temperature. With the assumption that the temperature of the air surrounding a conduit is uniform and steady, Gartner & Harrison (1963) derived the following two partial differential equations for the temperature of fluid flowing through it at any distance:

$$\rho A_x C_p \frac{\partial \theta'_f}{\partial t} + m C_p \frac{\partial \theta'_f}{\partial y} + \frac{h_i A_i}{Y} (\theta'_f - \theta'_c) = 0 \quad (3.8)$$

$$M_c C_c \frac{\partial \theta'_c}{\partial t} + (h_i A_i + h_o A_o) \theta'_c - h_i A_i \theta'_f = 0 \quad (3.9)$$

where A_x is the cross-sectional area; y the distance from inlet; Y the pipe length; and M_c the mass of conduit wall. θ'_f and θ'_c are respectively the fluid and conduit temperatures above the surrounding air temperature.

Taking the Laplace transform and solving the first order differential equations for θ'_f , the following transfer function was derived which describes the response of temperature at any place in the conduit to temperature changes at the inlet:

$$\frac{\theta'_f(y,s)}{\theta'_f(0,s)} = e^{-\frac{y}{u}s} e^{-\frac{(1-K)y}{L}} e^{-\frac{Ky}{L} \left(\frac{\tau s}{\tau s + 1} \right)} = H(y,s) \quad (3.10)$$

In view of the difficulty in finding the inverse Laplace transform of the last expression $e^{-Ky\tau s/L(\tau s+1)}$, Tobias (1973) suggested a simplified transfer function as follows:

$$\frac{\theta_f'(y,s)}{\theta_f'(0,s)} = e^{-\frac{y}{u}s} e^{\left[\frac{(1-K)y}{L}\right]} \left(\frac{\tau_1 s + 1}{\tau_2 s + 1}\right)$$

(3.11)

With the advancement in digital computer technology, simulation models of flow conduits were gradually developed. In HVACSIM+ (Clark 1985) a fifth-order time-dependent polynomial is used to model the axial temperature distribution in a pipe or duct. At each time step, the DELAY subroutine evaluates the fluid temperatures at five points and a new set of coefficients for the polynomial is found by Gaussian elimination. The validity of the models were supported by comparisons with experimental data. It was pointed out that the accuracy of the model diminishes when the outside heat transfer coefficient becomes relatively large, and hence the model is not suitable for ducts exposed to wind (Clark et al. 1985). Accuracy also decreases when temperature oscillations are much faster than the transport time.

TRNSYS employs the "plug-flow" concept by which the fluid in the conduit is considered as variable size segments and the mass of each is equal to the flow rate times the simulation time step (Klein et al. 1990). Fluid at the conduit outlet is a collection of the fluid segments that are pushed out by the inlet flow. The average outlet temperature is computed as the mass weighted average of the leaving segments. The total energy loss to the environment is the summation of the individual losses from each segment using a user-defined thermal resistance value which remains unchanged throughout the simulation period. Also the maximum number of segments has been limited to 25.

In the fluid flow simulation program Bristol, the pipe model readjusts the number of sections and temperatures at each time step, as the water velocity or time step size changes (Ip et al. 1989). New conduit sections are formed by either repeated combination of two adjacent sections or by repeated division of each section into halves using the following rule:

$$1 < \frac{Y}{u \Delta t N} < 2 \quad \text{where } N = 2^k$$

(3.12)

The rationale behind the rule was not fully explained in the paper.

All the above models take into account dynamic radial heat transfer through the conduit wall and thermal

energy brought by incoming fluid assuming plug flow. The TRNSYS pipe model nevertheless ignores the thermal storage effect of the pipe wall. Based on a similar approach a new flow conduit model is developed below, which as demonstrated later, is theoretically robust and more accurate.

3.2.2 A numerical model of flow conduit

Numerical model of transport delay

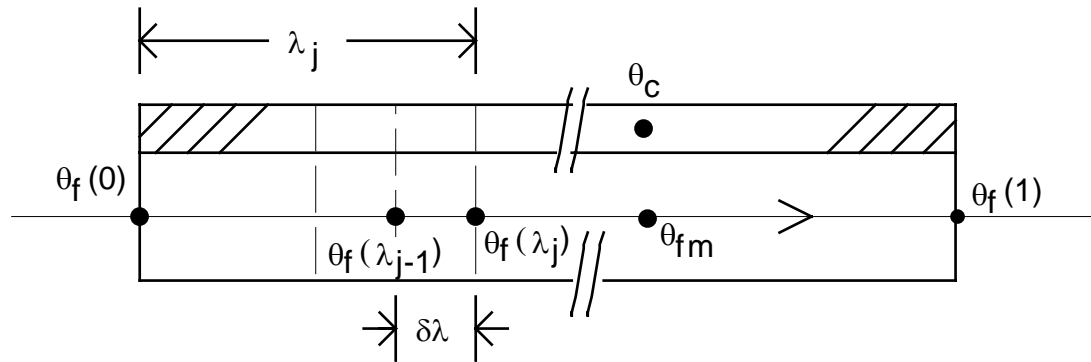


Figure 3.2 Numerical Model of Fluid Conduit Flow

Figure 3.2 shows a conduit model in which the temperature at the conduit wall is taken as uniform throughout the length. Within one finite time increment δt , a fluid element in the conduit advances by a distance δy which is equal to $u\delta t$. For the simplicity of discussions the entire conduit is considered to be evenly divided into N number of sections such that

$$N = \frac{Y}{\delta y} = \frac{1}{\delta \lambda} \quad (3.13)$$

It can be seen that $\delta \lambda$ is the normalized length of a fluid element. The fluid element which moves from section "j-1" to section "j" will have travelled a distance of $(\lambda_j - \lambda_{j-1})$ where λ is the normalized distance from the conduit entrance and has a value in the range of 0 to 1. This fluid element will experience a thermal change according to the following equation if a thermal equilibrium between the fluid and the surface in contact is assumed

$$mC_p[\theta_f(\lambda_j) - \theta_f^*(\lambda_{j-1})] = h_i A_i \delta \lambda [\theta_c^* - \theta_f(\lambda_j)] \quad (3.14)$$

θ_f^* and θ_c^* in the equation denote the present time step values. Rearranging the equation gives

$$\theta_f(\lambda_j) = \frac{mCp\theta_f^*(\lambda_{j-1}) + h_iA_i\delta\lambda\theta_c^*}{mCp + h_iA_i\delta\lambda} \quad (3.15)$$

Within the section j, as in all other sections, the fluid temperature at any position λ can be determined by linear interpolation such that

$$\theta_f(\lambda) = \theta_f(\lambda_{j-1}) + [\theta_f(\lambda_j) - \theta_f(\lambda_{j-1})] \frac{\lambda - \lambda_{j-1}}{\lambda_j - \lambda_{j-1}} \quad (3.16)$$

The average fluid temperature θ_{fm} in the conduit is given by the weighted mean of the array of the axial temperature values along the conduit such that

$$\theta_{fm} = \frac{1}{N} \left[\frac{\theta_f(0) + \theta_f(1)}{2} + \sum_{j=1}^{N-1} \theta_f\left(\frac{j}{N}\right) \right] \quad (3.17)$$

Constant volume conservation formulation

Two examples are given below: an insulated water pipe and a ventilating air duct.

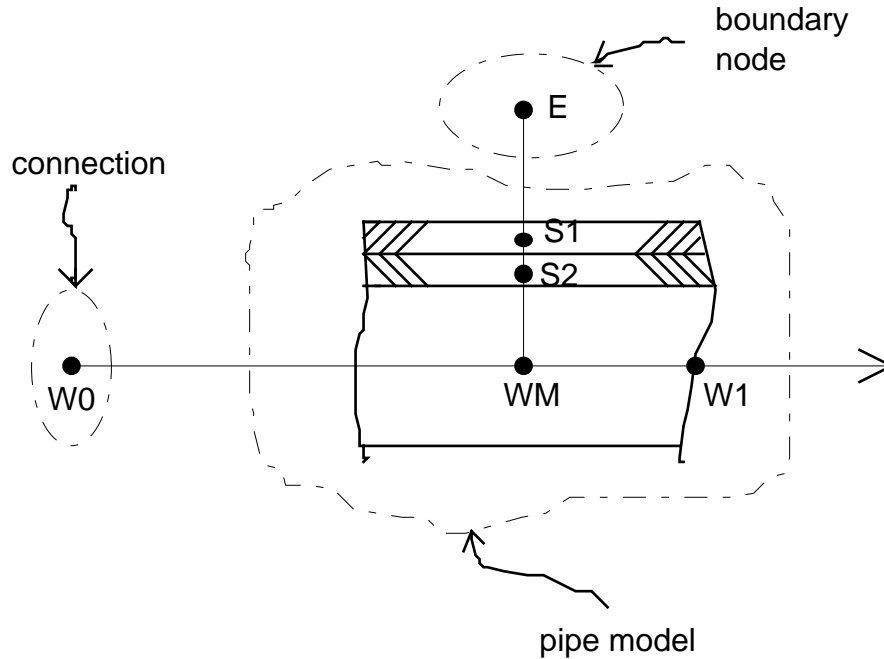


Figure 3.3 4-node Insulated Water Pipe

a) Insulated water pipe

An insulated water pipe model with 4 nodes is shown in Figure 3.3. Two solid nodes S1 and S2 are used to represent the thermal insulation and the metallic pipe body respectively. Two other nodes in the water stream are required. The water in contact node WM represents the control volume of water in the tube. The leaving water node W1 actually occupies no physical space in that it does not represent any physical fluid mass in the water flow, but instead, represents the state of the interconnecting variables for passing the information to the downstream component. The ambient air temperature is taken as an external excitation. The energy balance equations for the four nodes are given as follows:

for thermal insulation,

$$h_o A_o (\theta_e - \theta_{s1}) + k_{12} A_{12} (\theta_{s2} - \theta_{s1}) = M_{s1} C_{s1} \frac{d\theta_{s1}}{dt} \quad (3.18)$$

$$k_{12}A_{12}(\theta_{s1} - \theta_{s2}) + h_i A_i (\theta_{wm} - \theta_{s2}) = M_{s2} C_{s2} \frac{d\theta_{s2}}{dt}$$

for metallic pipe,

(3.19)

for water in contact,

$$m_{w0} C_{p_{w0}} \theta_{w0} - m_{w1} C_{p_{w1}} \theta_{w1} + h_i A_i (\theta_{s2} - \theta_{wm}) = M_{wm} C_{p_{wm}} \frac{d\theta_{wm}}{dt}$$

(3.20)

for leaving water (in the case of no transport delay):

$$\theta_{w1} = \theta_{wm}$$

(3.21)

The fully-implicit and fully-explicit finite difference expressions of equation (3.18) are respectively:

$$C_{es} (\theta_e - \theta_{s1}) + C_{12} (\theta_{s2} - \theta_{s1}) = M_{s1} C_{s1} \frac{\theta_{s1} - \theta_{s1}^*}{\delta t}$$

(3.22)

$$C_{es}^* (\theta_e^* - \theta_{s1}^*) + C_{12}^* (\theta_{s2}^* - \theta_{s1}^*) = M_{s1} C_{s1}^* \frac{\theta_{s1} - \theta_{s1}^*}{\delta t}$$

(3.23)

where,

$$C_{es} = h_o A_o$$

$$C_{12} = k_{12} A_{12}$$

Weighted-summation of the above fully-implicit and fully-explicit formulations with a ratio α to $(1-\alpha)$ gives

$$\begin{aligned} & -[\alpha(C_{12} + C_{es}) + \frac{M_{s1} C_{s1}}{\delta t}] \theta_{s1} + \alpha C_{12} \theta_{s2} \\ & = [(1-\alpha)(C_{12}^* + C_{es}^*) - \frac{M_{s1} C_{s1}^*}{\delta t}] \theta_{s1}^* - (1-\alpha) C_{12}^* \theta_{s2}^* - [\alpha C_{es} + (1-\alpha) C_{es}^*] \theta_e^* \end{aligned}$$

(3.24)

Repeating the same for the metallic-tube side and water side energy balance equations (3.19) and (3.20) gives respectively

$$\begin{aligned}
& \alpha C_{12} \theta_{s1} - \left[\alpha (C_{12} + C_{sw}) + \frac{M_{s2} C_{s2}}{\delta t} \right] \theta_{s2} + \alpha C_{sw} \theta_{wm} \\
& = -(1-\alpha) C_{12}^* \theta_{s1}^* + [(1-\alpha)(C_{12}^* + C_{sw}^*) - \frac{M_{s2} C_{s2}^*}{\delta t}] \theta_{s2}^* - (1-\alpha) C_{sw}^* \theta_{wm}^*
\end{aligned} \tag{3.25}$$

and,

$$\begin{aligned}
& \alpha C_{sw} \theta_{s2} - \left(\alpha C_{sw} + \frac{M_{wm} C_{pwm}}{\delta t} \right) \theta_{wm} - \alpha C_{w1} \theta_{w1} + \alpha C_{w0} \theta_{w0} \\
& = -(1-\alpha) C_{sw}^* \theta_{s2}^* + [(1-\alpha) C_{sw}^* - \frac{M_{wm} C_{pwm}^*}{\delta t}] \theta_{wm}^* + (1-\alpha) C_{w1}^* \theta_{w1}^* - (1-\alpha) C_{w0}^* \theta_{w0}^*
\end{aligned} \tag{3.26}$$

where,

$$\begin{aligned}
C_{sw} &= h_i A_i \\
C_{w1} &= m_{w1} C_{pw1} \\
C_{w0} &= m_{w0} C_{pw0}
\end{aligned}$$

The energy balance matrix equation is therefore in the form of

$$\begin{bmatrix} C(1) & C(2) & 0 & 0 & 0 \\ C(3) & C(4) & C(5) & 0 & 0 \\ 0 & C(6) & C(7) & C(8) & C(11) \\ 0 & 0 & C(9) & C(10) & 0 \end{bmatrix} * \begin{bmatrix} \theta_{s1} \\ \theta_{s2} \\ \theta_{wm} \\ \theta_{w1} \\ \theta_{w0} \end{bmatrix} = \begin{bmatrix} C(12) \\ C(13) \\ C(14) \\ C(15) \end{bmatrix} \tag{3.27}$$

where,

$$\begin{aligned}
C(1) &= -\alpha (C_{12} + C_{es}) - M_{s1} C_{s1} / \delta t \\
C(2) &= \alpha C_{12} \\
C(3) &= \alpha C_{12} \\
C(4) &= -\alpha (C_{12} + C_{sw}) - M_{s2} C_{s2} / \delta t \\
C(5) &= \alpha C_{sw} \\
C(6) &= \alpha C_{sw} \\
C(7) &= -\alpha C_{sw} - M_{wm} C_{pwm} / \delta t \\
C(8) &= -\alpha C_{w1} \\
C(9) &= -1
\end{aligned}$$

$$\begin{aligned}
C(10) &= 1 \\
C(11) &= \alpha C_{w0} \\
C(12) &= [(1-\alpha)(C_{12}^* + C_{es}^*) - M_{s1}^* C_{s1}^* / \delta t] \theta_{s1}^* - (1-\alpha) C_{12}^* \theta_{s2}^* - [\alpha C_{es} \theta_e + (1-\alpha) C_{es}^* \theta_e^*] \\
C(13) &= -(1-\alpha) C_{12}^* \theta_{s1}^* - [(1-\alpha)(C_{12}^* + C_{sw}^*) - M_{s2}^* C_{s2}^* / \delta t] \theta_{s2}^* - (1-\alpha) C_{sw}^* \theta_{wm}^* \\
C(14) &= -(1-\alpha) C_{sw}^* \theta_{s2}^* + [(1-\alpha) C_{sw}^* - M_{wm}^* C_{pwm}^* / \delta t] \theta_{wm}^* + (1-\alpha) C_{w1}^* \theta_{w1}^* \\
&\quad - (1-\alpha) C_{w0}^* \theta_{w0}^* \\
C(15) &= 0
\end{aligned}$$

and of which C(1) to C(10) are the component self-coupled coefficients; C(11) is the cross-coupled coefficient, and C(12) to C(15) are the present-time & excitation coefficients.

If the water velocity is low such that at a particular time step the distance travelled by the water is less than the pipe length, the error of assuming the leaving water temperature equal to the average water temperature in the pipe can be significant. In this case both the water temperatures in pipe and at the outlet should be determined separately and then substitute back into the above matrix format.

In other words, the values of θ_{wm} and θ_{w1} will be determined by a DELAY subprogramme.

Accordingly, the expressions for the following six coefficient in equation (3.27) will be revised to

$$\begin{aligned}
C(6) &= 0 \\
C(7) &= 1 \\
C(8) &= 0 \\
C(9) &= 0 \\
C(11) &= 0 \\
C(14) &= \text{DELAY}(\theta_{wm}) \\
C(15) &= \text{DELAY}(\theta_{w1})
\end{aligned}$$

In actual simulation, the conduit length is not evenly divided by δy . N by equation (3.13) is therefore rounded-off to the nearest integer. To determine the array of temperature distribution at a future time step, the present step values of $\theta_f^*(\lambda_j - \delta\lambda)$ are firstly computed by equation (3.16) and then substituted into equation (3.15) to get

$$\theta_f(\lambda_j) = \frac{mCp\theta_f^*(\lambda_j - \delta\lambda) + h_i A_i \delta\lambda \theta_c^*}{mCp + h_i A_i \delta\lambda} \tag{3.28}$$

In the case of a change in flow velocity during the simulation, the value of N will be revised and again equation (3.16) gives the new array of temperature distribution at the present time step before equation (3.15) is applied to give the future time values. If N is equal to one at a time step, the transport delay will not be applied at that particular time step and instead the equation (3.21) will be used.

In the case of mass balance, the concept of continuity of incompressible flow can be applied to the water flow in that

$$m_{w1} = m_{wm} = m_{w0} \quad (3.29)$$

Fluid mass flow is irrelevant for the solid nodes S1 and S2. The mass flow matrix of the pipe model can be described by the same coefficient pattern as in the case of energy matrix, i.e.

$$\begin{bmatrix} C(1) & C(2) & 0 & 0 & 0 \\ C(3) & C(4) & C(5) & 0 & 0 \\ 0 & C(6) & C(7) & C(8) & C(11) \\ 0 & 0 & C(9) & C(10) & 0 \end{bmatrix} * \begin{bmatrix} m_{s1} \\ m_{s2} \\ m_{wm} \\ m_{w1} \\ m_{w0} \end{bmatrix} = \begin{bmatrix} C(12) \\ C(13) \\ C(14) \\ C(15) \end{bmatrix} \quad (3.30)$$

and here,

$$\begin{aligned} C(1) &= 1 \\ C(2) &= 0 \\ C(3) &= 0 \\ C(4) &= 1 \\ C(5) &= 0 \\ C(6) &= 0 \\ C(7) &= 1 \\ C(8) &= 0 \\ C(9) &= -1 \\ C(10) &= 1 \\ C(11) &= -1 \\ C(12) &= 0 \\ C(13) &= 0 \\ C(14) &= 0 \\ C(15) &= 0 \end{aligned}$$

b) ventilating air duct

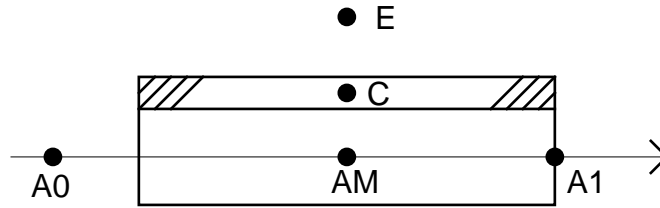


Figure 3.4 3-node Ventilating Duct

An energy balance at the duct wall (Figure 3.4) gives

$$h_o A_o (\theta_e - \theta_c) + h_i A_i (\theta_{am} - \theta_c) = M_c C_c \frac{d\theta_c}{dt}$$

(3.31)

An energy balance at the air flow inside duct gives

$$(m_{a0} C_{p_{a0}} + m_{v0} C_{p_{v0}}) \theta_{a0} - (m_{a1} C_{p_{a1}} + m_{v1} C_{p_{v1}}) \theta_{a1} - h_i A_i (\theta_{am} - \theta_c) = M_{am} C_{p_{ma}} \frac{d\theta_{am}}{dt}$$

(3.32)

Using the same procedures as described in the pipe model, the following form of energy matrix equation can be derived:

$$\begin{bmatrix} X & X & 0 & 0 \\ 0 & X & X & X \\ X & X & X & X \end{bmatrix} * \begin{bmatrix} \theta_c \\ \theta_{am} \\ \theta_{a1} \\ \theta_{a0} \end{bmatrix} = \begin{bmatrix} X \\ X \\ X \end{bmatrix}$$

(3.33)

where the "X" are "non-empty" matrix coefficients.

Condensation

Moisture condensation may occur when the inside duct surface temperature is below the dew point temperature of the duct air in contact. In this case the energy balance equation of the inside air will be similar to the case of a wetted surface of a heat transfer coil. This will be elaborated in the next section.

The mass flow matrices are then

for the first phase (dry air),

$$\begin{bmatrix} 1 & 0 & 0 & 0 \\ 0 & 1 & 0 & -1 \\ 0 & -1 & 1 & 0 \end{bmatrix} * \begin{bmatrix} m_c \\ m_{am} \\ m_{a1} \\ m_{a0} \end{bmatrix} = \begin{bmatrix} 0 \\ 0 \\ 0 \end{bmatrix}$$

(3.34)

for the second phase (water vapour),

$$\begin{bmatrix} 1 & 0 & 0 & 0 \\ 0 & 1 & 0 & -1 \\ 0 & -1 & 1 & 0 \end{bmatrix} * \begin{bmatrix} m_c \\ m_{vm} \\ m_{v1} \\ m_{v0} \end{bmatrix} = \begin{bmatrix} 0 \\ m_{cd} \\ 0 \end{bmatrix}$$

(3.35)

where m_{cd} is the rate of moisture condensation if any.

In this situation however the transport delay calculation will not be proceeded because of the complexity of the latent heat transfer involved in each individual duct section. Instead, the value of N will be arbitrarily taken as one. This if happened will affect the accuracy in the transient response for small time step simulation. The problem, however, can be readily improved by a better discretization scheme, for example, by using two or more consecutive duct sections in the simulation run so that the first section deals with the condensation problem and the later sections the transport delay phenomenon.

3.3 Heat-transfer Coil Models

3.3.1 Review of modelling theory

Studies of Heat Exchanger Dynamics

Many modern methods and empirical formulae for evaluating heat transfer coil performance are based on the fundamental work done at least half a century ago. The boom in modelling and investigation of heat exchanger (one-dimensional flow) dynamics came in the 1950s. In the 1960s, the emphasis was gradually switched to the more practical and more complex problem of flow-forced dynamics, or the dynamics of cross-flow heat exchangers. There are two types of cross-flow heat exchangers: a "tube" cross-flow heat exchanger and a "plate" cross-flow heat exchanger. In the analysis of the former type, the primary fluid is assumed to be mixed, that is, it is at a uniform temperature across its flow passage which contains the entire flow. Both fluids are considered to be unmixed in the plate cross-flow heat exchanger.

Gartner and Harrison (1965) developed an analytical model of a tube cross-flow heat exchanger suitable for control engineering purpose. The following 3 partial differential equations were derived which describe the energy flow in each of the primary fluid (say water), conduit and secondary fluid (say air) as follows:

$$\frac{\partial \theta_w}{\partial t} + u_w \frac{\partial \theta_w}{\partial y} + \frac{4h_o}{\rho_w C p_w D_i} (\theta_w - \theta_c) = 0 \quad (3.36)$$

$$\frac{\partial \theta_c}{\partial y} + \frac{D_o h_o}{\rho_c C_c \bar{D} b} (\theta_c - \bar{\theta}_a) - \frac{D_i h_i}{\rho_c C_c \bar{D} x} (\theta_w - \theta_c) = 0 \quad (3.37)$$

$$\theta_{a1} - \theta_{a0} + \frac{\pi D_o h_o}{\rho_a u_a x C p_a} (\theta_c - \bar{\theta}_a) = 0 \quad (3.38)$$

where x is the thickness of tube; y is the distance from tube inlet; and,

$$\bar{\theta}_a = \frac{\theta_{a1} + \theta_{a0}}{2} \quad (3.39)$$

i.e. the average of the incoming and leaving air temperatures.

From these, transfer functions were obtained to relate the ratios of the outlet air to inlet water and outlet water to inlet water temperature variations. The results obtained from the experimental portion of this study favourably indicated the validity of the assumed model.

Gartner and Daane (1969) developed a mathematical model for the serpentine cross-flow heat exchanger with fluid velocity change. Their experimental results obtained by employing a periodic binary perturbation method correlated well with their model computations. The findings are as follows:

- i) The transfer function ratio relating outlet air temperature response to an inlet water temperature disturbance may be suitably described by a first-order model representation.
- ii) The transfer function ratio relating outlet air temperature response to an inlet water velocity disturbance may be suitably described by a first-order model representation.
- iii) The main variable affecting the speed of response of the heat exchanger is the water velocity.

Tamm (1969) applied the same equations from Gartner and Daane to study the dynamic response for multi-row crossflow heat exchangers. They concluded that the theory worked for both parallel and counterflow arrangements. However, the algebra of this method quickly becomes tedious as the number of rows increases.

The above models followed the "distributed parameter" approach. A lumped parameter approach was proposed by McNamara and Harrison (1967). They found that as the number of axial segments is increased, the results tend to approach the axially distributed analysis results. But so far the above models did not involve latent heat exchange.

McCullagh, Green & Chandrasekar (1969) developed an analytical model of chilled water cooling dehumidifying coils. Based on a two dump approximation of the tubes and fin (one lump for the tube and the other for the fin), a series of 5 basic equations were used to represent each row of coil as one section:

$$\frac{\partial \theta_a}{\partial \tau} + u_a \frac{\partial \theta_a}{\partial y_a} = - \frac{(\theta_a - \theta_f)}{R_a C_a} \quad (3.40)$$

$$\frac{\partial g_a}{\partial \tau} + u_a \frac{\partial g_a}{\partial y_a} = - \frac{(g_a - g_f)}{L_e R_a C_a} \quad (3.41)$$

$$\frac{\partial \theta_f}{\partial \tau} = \frac{(\theta_a - \theta_f)}{R_a C_f} + \frac{H_g - H_{ft}}{L_e C p_a} (g_a - g_f) - \frac{(\theta_f - \theta_c)}{R_f C_f} \quad (3.42)$$

$$\frac{\partial \theta_t}{\partial t} = -\frac{(\theta_f - \theta_t)}{R_f C_t} - \frac{(\theta_t - \theta_w)}{R_w C_t}$$

(3.43)

$$\frac{\partial \theta_w}{\partial t} + u_w \frac{\partial \theta_w}{\partial y_w} = R_w C_w (\theta_t - \theta_w)$$

(3.44)

where L is the tube length and R is the thermal resistance.

The equations were solved with a computer to find the steady state performance of cooling coils. The results compared well with experimental data, except for two row coils, where the assumption of complete mixing between rows is not valid.

Shekar and Green (1970) extended the work of McCullagh to include dynamic responses. The frequency response to describe the transfer function in moisture content and temperature of air and water by small perturbation in inlet temperature showed a second order system.

Generally speaking, the following assumptions were made in the formulation of the above models:

- i) The tube is distributed in the direction of primary fluid flow, but lumped in the radial directions.
- ii) The densities of the tube material, the primary fluid, and the secondary fluid are considered to be constant.
- iii) The outside film coefficient is assumed to be constant throughout the temperature ranges encountered. The inside film coefficient is assumed to be a function only of the primary fluid velocity.
- iv) Axial mixing of the primary fluid is neglected and the primary fluid temperature is assumed to be constant across a given cross section.
- v) The tube material has a uniform temperature at a given cross section at a given time.
- vi) All heat conduction in the axial direction is neglected.
- vii) The secondary fluid has a uniform temperature and velocity throughout the entrance section.
- viii) The effective secondary fluid temperature to be considered for heat transfer purposes is the average of the incoming temperature and the outgoing temperature at any cross section. The average temperature is a function of time and distance along the tube.

These assumptions were generally used in the developments of the coil models for plant simulation in the later years.

Simulation Models

Exact transfer functions of heat exchangers have, in general, complex transcendental forms and are inconvenient to treat with. The most popular method of approximating the transfer functions is the replacement of them with a dead time and first- or second-order lag, the parameters of which are determined by the curve-fitting in the frequency response diagram. Although a number of papers used this method, this approach suffers from no relationship between the parameters determined by fitting and the original ones; each application will require a separate fitting of the parameters.

In most HVAC simulations in the 1970s, the coil is usually treated as a "black box" and assumptions of some kind are made for moist air conditions off the coil (during cooling and dehumidification). In other applications, performance curves from manufacturers catalogs are used. Coil models recommended by the Task Group on Energy Requirements for Heating and Cooling of Buildings (Stoecker 1975) were products mixing basic heat exchanger theories (like the concepts of effectiveness and log mean temperature difference) and polynomial fittings with specific coefficients deduced from manufacturer data. For system simulation purposes, Stoecker (1975) presents an empirical model for cooling coils which requires the determination of 15 empirical constants from performance data. Based on this model the cooling coil type 32 had been developed in the TRNSYS simulation program (Klein et al. 1990).

The Lewis relation has been a standard practice in designing air cooling and dehumidifying coils under wet conditions - where both heat and mass are transferred simultaneously (El-Mahdy and Mitalas 1977; McQuiston & Parker 1994). Heat transfer and friction data are used together with the Colburn analogy to obtain the mass transfer coefficient needed to make the design process possible. In the HVACSIM+ program (Clark 1985), the cooling or dehumidifying coil model Type 12 has been based on the work of Elmahdy and Mitalas on steady state model and dynamic have been added to it in a very simple and somewhat artificial manner - in which the same time constant of

$$\tau = \frac{Cm}{UA_o} \tag{3.45}$$

is used for the changes of both air and water temperatures. Both dry and wet surfaces were analyzed and a method to identify the dry/wet interface was presented. Transport delay has been included as in the HVACSIM+ flow conduit model. The subprogram uses equations for log mean temperature difference (LMTD) and log mean enthalpy difference (LMHD) which are strictly correct only for counterflow heat exchangers. Use of the model to represent coils with fewer than four rows is thus not recommended

(Clark et al. 1985).

Goldstein (1983) developed a mathematical model for the analysis of heat transfer in plate fin heat exchangers with boiling or condensing refrigerant through tubes. He did not consider single phase tube fluids in his analysis since the heat transfer relations that he used did not account for variations in tube fluid temperature. He subdivided his analysis into three main regions: subcooled, two phase and superheated. In the superheated region he assumed that there is minimum moisture removal which can be neglected. This enabled him to use the dry surface relations in the superheated region. Physically, this is not very accurate if there is condensation on the surface. The effects of heat exchanger geometry were not included in the determination of the outside film heat transfer coefficient and details regarding the computation of the fin effectiveness were omitted.

Holmes (1982) showed that the dynamic performance of water coils can be represented by a pair of simultaneous equations modelling the bulk storage of heat in the water and coil metal, with a correction for the coil geometry. This correction allows for delays in the water circuitry, in particular,

- i) the overall time taken for the water to pass through the coil;
- ii) the time differences for water entering each tube where there are a number of parallel tubes served by the same header;
- iii) the change in water temperature along a tube.

The model presented by Holmes is regarded as adequate for the determination of time constants and analysis in the frequency domain.

In his later work, Holmes summarized the techniques in heating and cooling coil simulation in the IEA Annex 10 exercise (Holmes 1988). He pointed out that whilst there is an accepted approach to the calculation of the former (heating coil) there is yet no general consensus as to how the latter (cooling coil) can be determined. He put the coil models under two general headings: single zone and two zone models. The single zone models are appropriate to all types of coil and is normally all that need be considered. The concept of effectiveness as presented by Kays and London is applicable for heating application. For cooling and dehumidifying coil, two approaches namely bypass factor and effectiveness can be used for the single zone model. In the bypass factor model, a fraction of the entering air is assumed to bypass the coil and mix with air that is saturated at the coil surface temperature. To calculate the total heat transfer it is assumed that the air side heat transfer coefficient is enhanced by the sensible heat ratio, so that only dry bulb temperatures are involved in the calculation. The effectiveness model uses enthalpy as the driving forces for heat transfer, very good results are claimed. In both cases however the leaving air dry bulb is determined by similar equations. The bypass factor model is good for most realistic operating conditions.

Cooling coil component 400 in the ESP-r program had been developed based on this bypass factor approach (Hanby & Clarke 1988). The effectiveness model may be more appropriate for cases where the entering air is saturated which is unlikely in most typical air conditioning situations.

The paper of Braun, Klein and Mitchell (1989) presents a simple, yet mechanistic method for modelling the performance of cooling towers and cooling coils. Through the introduction of an air saturation specific heat, effectiveness relationships are developed. The advantages of the approach as claimed are its simplicity, accuracy, and consistency with the methods for analyzing sensible heat exchangers. It is based on this that the cooling coil type 52 has been developed in the TRNSYS program.

All the simulation models described above are basically algorithmic type assuming counter-flow approximation. The models become less accurate when the coil arrangement deviates from the counter-flow arrangement (for instance those coils with a few passes), and they are over-simplified and too rigid for the studies of intra-coil behaviour (as required by the coil designers and manufacturers) and mis-handling cases experienced in real projects (for instance an incorrect field installation made the coil a parallel flow heat-exchanger). A new simulation model developed from the finite volume constant volume conservation approach is given below which, as can be seen, overcomes these limitations.

3.3.2 Mathematical Model by Constant Volume Conservation Formulation

Chilled/Hot Water Coils

It appears that the structure of the analytical models introduced by Gartner (1965) on dry coil and by McCullagh (1969) on wet coil can be readily transformed into the control volume conservation formulation. A combination of the two form a very good starting point for deriving a numerical model in detail.

Consider a single pass of a heat transfer coil (assuming chilled water cooling for the time being) as shown in Figure 3.5. The tube can be represented by a 4 node model: one for the encapsulated moist air, one the metal tube-plus-fins, one for the water in contact, and one for the leaving water. Two nodes WM and W1 at the water side are required for the inclusion of the transport delay model introduced in Section 3.1. One node S for the metal is deemed adequate since the temperature variation across the metal is negligible. The thermal resistance of the tube body is very small and when included, can be absorbed by the surface convective coefficients at both the air and the water sides.

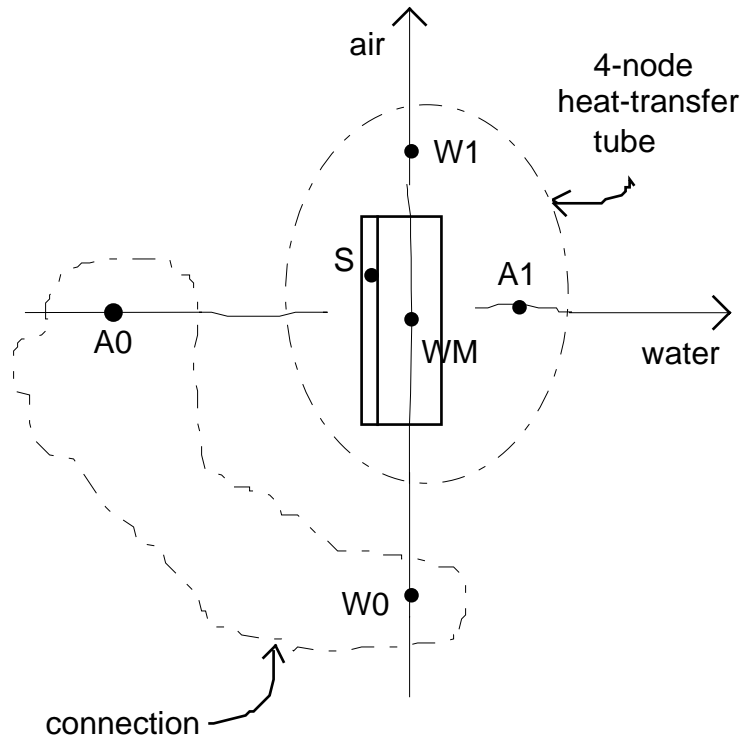


Figure 3.5 Heat-transfer Tube Model

The external surface of a tube is firstly considered as wet. This occurs when the dew point temperature of the incoming air is lower than the external surface temperature of the tube, i.e. when $(\theta_{a0})_{dew} < \theta_s$. By enthalpy potential theory, the heat exchange rate from air to tube is given by

$$Q = K_d A_{oe} (H_{ma1} - H_s) \quad (2.5)$$

where,

- K_d - mass diffusion coefficient
- H_{ma1} - specific enthalpy of humid air over coil
- H_s - specific enthalpy of saturated air at surface temperature θ_s
- A_{oe} - effective external surface area of tube

i) air-side (secondary fluid) energy balance gives

$$\begin{aligned} & (m_{a0}Cp_{a0} + m_{v0}Cp_{v0})\theta_{a0} - (m_{a1}Cp_{a1} + m_{v1}Cp_{v1})\theta_{a1} - (h_o)_{wet} A_{oe} (\theta_{a1} - \theta_s) + H_{fg} (m_{v0} - m_{v1}) \\ & = M_{a1}Cp_{a1} \frac{d\theta_{a1}}{dt} \end{aligned} \quad (3.46a)$$

or,

$$C_{as}\theta_s - (C_{a1} + C_{as})\theta_{a1} - C_{ao}\theta_{a0} - C_{av} = M_{a1}Cp_{a1} \frac{d\theta_{a1}}{dt} \quad (3.46b)$$

where,

$$C_{a0} = m_{a0}Cp_{a0} + m_{v0}Cp_{v0}$$

$$C_{a1} = m_{a1}Cp_{a1} + m_{v1}Cp_{v1}$$

$$C_{as} = (h_o)_{wet} A_{oe}$$

$$C_{av} = H_{fg} (m_{v1} - m_{v0})$$

ii) tube-side energy balance gives

$$(h_o)_{wet} A_{oe} (\theta_{a1} - \theta_s) - h_i A_i (\theta_s - \theta_{wm}) = M_s C_s \frac{d\theta_s}{dt} \quad (3.47a)$$

or,

$$-(C_{as} + C_{sw})\theta_s + C_{as}\theta_{a1} + C_{sw}\theta_{wm} = M_s C_s \frac{d\theta_s}{dt} \quad (3.47b)$$

where $C_{sw} = h_i A_i$

iii) water-side (primary fluid) energy balance gives

$$m_{w0}Cp_{w0}\theta_{w0} - m_{w1}Cp_{w1}\theta_{w1} + h_i A_i (\theta_s - \theta_{wm}) = M_{wm} Cp_{wm} \frac{d\theta_{wm}}{dt} \quad (3.48a)$$

or,

$$C_{sw}\theta_s - C_{sw}\theta_{wm} - C_{w1}\theta_{w1} + C_{w0}\theta_{w0} = M_{wm} Cp_{wm} \frac{d\theta_{wm}}{dt} \quad (3.48b)$$

and in the case of no transport delay,

$$\theta_{w1} = \theta_{wm} \quad (3.49)$$

As discussed in Section 3.1 in relatively slow water flow such that the distance travelled by the water in unit time step is less than the tube length, the temperature of the water leaving the tube will not be the same as the average water temperature in the tube. θ_{wm} and θ_{w1} in this case have to be calculated separately before the equation-set is solved simultaneously.

For the case of dry tube surface the same equations derived above can be used except that the outside heat transfer coefficient is given by $(h_o)_{dry} = h_o$ and there will be no condensation i.e. $m_{v0} = m_{v1}$.

By weighted-summation of the fully-implicit and fully-explicit formulation with the ratio α to $(1-\alpha)$, the tube-side, air-side and water side energy balance equations give respectively

$$\begin{aligned} & \left[-\alpha(C_{as} + C_{sw}) - \frac{M_s C_s}{\delta t} \right] \theta_s + \alpha C_{as} \theta_{a1} + \alpha C_{sw} \theta_{wm} \\ & = \left[-(1-\alpha)(C_{as}^* + C_{sw}^*) - \frac{M_s C_s^*}{\delta t} \right] \theta_s^* - (1-\alpha)C_{as}^* \theta_{a1}^* - (1-\alpha)C_{sw}^* \theta_{wm}^* \end{aligned} \quad (3.50a)$$

$$\begin{aligned} & \alpha C_{as} \theta_s + \left[-\alpha(C_{a1} + C_{as}) - \frac{M_{a1} C_{p_{a1}}}{\delta t} \right] \theta_{a1} + \alpha C_{a0} \theta_{a0} \\ & = -(1-\alpha)C_{as}^* \theta_s^* + \left[(1-\alpha)(C_{a1}^* + C_{as}^*) - \frac{M_{a1} C_{p_{a1}}^*}{\delta t} \right] \theta_{a1}^* - (1-\alpha)C_{a0}^* \theta_{a0}^* + \alpha C_{av} + (1-\alpha)C_{av}^* \end{aligned} \quad (3.50b)$$

$$\begin{aligned} & \alpha C_{sw} \theta_s + \left[-\alpha C_{sw} - \frac{M_{wm} C_{p_{wm}}}{\delta t} \right] \theta_{wm} - \alpha C_{w1} \theta_{w1} + \alpha C_{w0} \theta_{w0} \\ & = -(1-\alpha)C_{sw}^* \theta_s^* + \left[(1-\alpha)C_{sw}^* - \frac{M_{wm}^* C_{p_{wm}}^*}{\delta t} \right] \theta_{wm}^* + (1-\alpha)C_{w1}^* \theta_{w1}^* - (1-\alpha)C_{w0}^* \theta_{w0}^* \end{aligned} \quad (3.50c)$$

where the superscript * denotes the present time step variables.

Hence the energy balance matrix can be written as

$$\begin{bmatrix} C(1) & C(2) & C(3) & 0 & 0 & 0 \\ C(4) & C(5) & 0 & 0 & C(11) & 0 \\ C(6) & 0 & C(7) & C(8) & 0 & C(12) \\ 0 & 0 & C(9) & C(10) & 0 & 0 \end{bmatrix} * \begin{bmatrix} \theta_s \\ \theta_{a1} \\ \theta_{wm} \\ \theta_{w1} \\ \theta_{a0} \\ \theta_{w0} \end{bmatrix} = \begin{bmatrix} C(13) \\ C(14) \\ C(15) \\ C(16) \end{bmatrix}$$

(3.51a)

where,

$$C(1) = -\alpha(C_{as} + C_{sw}) - M_s C_s / \delta t$$

$$C(2) = \alpha C_{as}$$

$$C(3) = \alpha C_{sw}$$

$$C(4) = \alpha C_{as}$$

$$C(5) = -\alpha(C_{a1} + C_{as}) - M_{a1} C_{pa1} / \delta t$$

$$C(6) = \alpha C_{sw}$$

$$C(7) = -\alpha C_{sw} - M_{wm} C_{pwm} / \delta t$$

$$C(8) = \alpha C_{w1}$$

$$C(9) = -1$$

$$C(10) = 1$$

$$C(11) = \alpha C_{w0}$$

$$C(12) = \alpha C_{as}$$

$$C(13) = -(1-\alpha)C_{as}^* \theta_s^* + [(1-\alpha)(C_{a1}^* + C_{as}^*) - M_{a1}^* C_{pa1}^* / \delta t] \theta_{a1}^* - (1-\alpha)C_{a0}^* \theta_{a0}^* + \alpha C_{av} + (1-\alpha)C_{av}^*$$

$$C(14) = [- (1-\alpha)(C_{as}^* + C_{sw}^*) - M_s C_s^* / \delta t] \theta_s^* - (1-\alpha)C_{as}^* \theta_{a1}^* - (1-\alpha)C_{sw}^* \theta_{wm}^*$$

$$C(15) = -(1-\alpha)C_{sw}^* \theta_s^* + [(1-\alpha)C_{sw}^* - M_{wm}^* C_{pwm}^* / \delta t] \theta_{wm}^* + (1-\alpha)C_{w1}^* \theta_{w1}^* - (1-\alpha)C_{w0}^* \theta_{w0}^*$$

$$C(16) = 0$$

If the transport delay is active, then

$$C(6) = 0$$

$$C(7) = 1$$

$$C(8) = 0$$

$$C(9) = 0$$

$$C(12) = 0$$

$$C(15) = \theta_{wm}(\text{DELAY})$$

$$C(16) = \theta_{w1}(\text{DELAY})$$

So, the energy matrix template is in the generalised form of

$$\begin{bmatrix} X & X & X & 0 & 0 & 0 \\ X & X & 0 & 0 & X & 0 \\ X & 0 & X & X & 0 & X \\ 0 & 0 & X & X & 0 & 0 \end{bmatrix} * \begin{bmatrix} \theta_s \\ \theta_{a1} \\ \theta_{wm} \\ \theta_{w1} \\ \theta_{a0} \\ \theta_{w0} \end{bmatrix} = \begin{bmatrix} X \\ X \\ X \\ X \end{bmatrix}$$

(3.51b)

Mass flow balance

In the case of first phase mass balance, the concept of continuity of incompressible flow can be applied to the dry air and the water flow in that

$$m_{a1} = m_{a0}$$

(3.52)

$$m_{w1} = m_{wm} = m_{w0}$$

(3.53)

In the case of second phase mass balance, this has no effect on the chilled water flow circuit but affects the rate of water vapour flow in the moist air stream, in that

$$m_{v1} - m_{v0} = -m_{cd}$$

(3.54)

where m_{cd} is the condensation rate of water vapour onto the tube and fin surfaces.

Fluid mass flow is irrelevant for the solid node S. The mass flow matrix of the tube model can be described by the same coefficient pattern as in the case of energy matrix, i.e.

$$\begin{bmatrix} C(1) & C(2) & C(3) & 0 & 0 & 0 \\ C(4) & C(5) & 0 & 0 & C(11) & 0 \\ C(6) & 0 & C(7) & C(8) & 0 & C(12) \\ 0 & 0 & C(9) & C(10) & 0 & 0 \end{bmatrix} * \begin{bmatrix} m_s \\ m_{a1} \\ m_{wm} \\ m_{w1} \\ m_{a0} \\ m_{w0} \end{bmatrix} = \begin{bmatrix} C(13) \\ C(14) \\ C(15) \\ C(16) \end{bmatrix}$$

(3.55)

where for,	first phase	&	second phase	respectively,
C(1)	= 1,		1	
C(2)	= 0,		0	
C(3)	= 0,		0	
C(4)	= 0,		0	
C(5)	= 1,		1	
C(6)	= 0,		0	
C(7)	= 1,		1	
C(8)	= 0,		0	
C(9)	= -1,		0	
C(10)	= 1,		1	
C(11)	= -1,		-1	
C(12)	= -1,		0	
C(13)	= 0,		0	
C(14)	= 0,		-m _{cd}	
C(15)	= 0,		0	
C(16)	= 0,		0.	

3.3.3.2 Two-phase flow inside tube

If two-phase fluid flow occurs inside the tubings, for instance, refrigerant evaporates in a direct-expansion cooling coil or steam condenses in a heating coil, modification of the above state equations of the primary fluid is required. Different mathematical treatments are incurred depending on the thermal states of the fluid at the ends of the tube.

Air-side and tube-side state equations are the same as before as described by equations (3.46) and (3.47). For the sake of discussions let us take the primary fluid under consideration to be heating steam for the time being. By conversation of mass,

$$m_r = m_{w0} + m_{v0} = m_{w1} + m_{v1} \quad (3.56)$$

Two cases of inlet steam conditions are considered: wet vapour at tube inlet and superheated steam at inlet.

wet vapour at inlet

This refers to the case of $m_{w0} > 0$, $m_{v0} > 0$ and $\theta_{r0} = \theta_{sat}$ at the tube inlet. By taking $\theta_{rm} = \theta_{sat}$ the cooling rate ($-Q_c$) at the tube surface is given by

$$Q_c = h_i A_i (\theta_s - \theta_{rm}) = h_i A_i (\theta_s - \theta_{sat}) \quad (3.57)$$

Q_c is then positive in value. The latent heat content of the steam at inlet is

$$Q_l = m_{v0} H_{fg} \quad (3.58)$$

If $Q_l > Q_c$, then the exit fluid is still at wet steam condition and this gives

$$m_{w1} = m_{w0} + \frac{Q_c}{H_{fg}} \quad (3.59a)$$

$$m_{v1} = m_{v0} - \frac{Q_c}{H_{fg}} \quad (3.59b)$$

$$\theta_{r1} = \theta_{sat} \quad (3.59c)$$

If $Q_l \leq Q_c$, then

$$m_{w1} = m_r \quad (3.60a)$$

$$m_{v1} = 0 \quad (3.60b)$$

$$\theta_{r1} = \theta_{sat} - \frac{Q_c - Q_l}{m_r C_{p_w}} \quad (3.60c)$$

superheated steam at inlet

This refers to the case of $m_{w0} = 0$, $m_{v0} = m_r$ and $\theta_{r0} > \theta_{sat}$ at the tube inlet.

The superheat content of the steam at inlet is

$$Q_{sp} = m_{v0} C_{p_{v0}} (\theta_{r0} - \theta_{sat}) \quad (3.61)$$

If $Q_{sp} > Q_c$, then the exit steam is still at superheated condition and this gives

$$m_{w1} = 0 \quad (3.62a)$$

$$m_{v1} = m_{v0} \quad (3.62b)$$

$$\theta_{r1} = \theta_{r0} - \frac{Q_c}{m_{v0} C p_v} \quad (3.62c)$$

$$\theta_{rm} = \frac{\theta_{r0} + \theta_{r1}}{2} \quad (3.62d)$$

If $Q_c > Q_{sp}$ but $Q_c < (Q_{sp} + Q_l)$, then the exit fluid is at wet steam condition, so

$$m_{w1} = m_{v0} + \frac{Q_c - Q_{sp}}{H_{fg}} \quad (3.63a)$$

$$m_{v1} = m_{v0} - \frac{Q_c - Q_{sp}}{H_{fg}} \quad (3.63b)$$

$$\theta_{r1} = \theta_{sat} \quad (3.63c)$$

If $Q_c > (Q_{sp} + Q_l)$, then the exit fluid is at liquid water condition, and

$$m_{w1} = m_r \quad (3.64a)$$

$$m_{v1} = 0 \quad (3.64b)$$

$$\theta_{r1} = \theta_{sat} - \frac{Q_c - Q_{sp} - Q_l}{m_r C p_w} \quad (3.64c)$$

The above check-then-calculate procedure avoids unnecessary iterations before arriving at the correct solution and enhance computational stability. Iteration however is unavoidable if the steam in tube remains at superheated state throughout. In all these cases the component matrix template remains the same as in equation (3.51b) for single phase fluid flow. What needed to be changed are the expressions of several matrix coefficients. A similar approach can be used to analyse evaporating refrigerant flow in tube.

3.3.3.3 Coils with surface deposits and poor mechanical bonding

Coil's capacity will be reduced in the presence of additional thermal resistance on tube which can be caused by:

- i) poor mechanical bonding between the fins and the tubes;
- ii) deposit formed on either the external or internal surfaces of the tube, or both.

In order to model such degradation in coil performance, individual nodes to represent the fins, the tube body, or the desposit layers respectively are required. A heat transfer tube thus becomes a component with five nodes or more.

poor bonds

If poor bonding between the fins and the tubings is to be modelled, one node can be used to represent the fins and the other node the tube. Heat transfer between the two solid nodes is described by the additional thermal resistance in between. The energy balance matrix equation is then of the form

$$\begin{bmatrix} X & X & X & 0 & 0 & 0 & 0 \\ X & X & 0 & X & 0 & 0 & 0 \\ X & 0 & X & 0 & 0 & X & 0 \\ 0 & X & 0 & X & X & 0 & X \\ 0 & 0 & 0 & X & X & 0 & 0 \end{bmatrix} * \begin{bmatrix} \theta_{sf} \\ \theta_{st} \\ \theta_{a1} \\ \theta_{wm} \\ \theta_{w1} \\ \theta_{a0} \\ \theta_{w0} \end{bmatrix} = \begin{bmatrix} X \\ X \\ X \\ X \end{bmatrix}$$

(3.65)

frost formation

Frost will occur on the exterior tube surface of a DX coil when the tube surface temperature is below the freezing temperature of the water vapour in the incoming moist air stream. Frost will grow with time and this continuously changes the heat transfer rate. Within the modelling framework here introduced, this can be modelled by adding an extra node to represent the frost layer. Before the formation of the frost layer the mass M_f of the node is zero; and as time in progress, the law of conservation of mass applying to moist air stream gives

$$m_{v1} - m_{v0} = \frac{dM_f}{dt} = \frac{M_f - M_f^*}{\delta t}$$

(3.66)

This is coupled to the energy balance equations in that

for moist air,

$$\begin{aligned} & (m_{a0}Cp_{a0} + m_{v0}Cp_{v0})\theta_{a0} - (m_{a1}Cp_{a1} + m_{v1}Cp_{v1})\theta_{a1} - (h_o)_{frost} A_{oe} (\theta_{a1} - \theta_f) + H_{frost} (m_{v0} - m_{v1}) \\ & = M_{a1}Cp_{a1} \frac{d\theta_{a1}}{dt} \end{aligned} \quad (3.67)$$

where H_{frost} is the sum of the latent energy required to convert water vapour to frost and the sensible heat for the corresponding temperature changes, all measured at the surface temperature of the frost layer;

and for the frost layer,

$$h_{af} A_{af} (\theta_{a1} - \theta_f) + k_{fs} A_{fs} (\theta_s - \theta_f) = \frac{d}{dt} (M_f C_f \theta_f) \quad (3.68)$$

The matrix template of the component can then be established through the same procedures as before; for instance the state equation for the frost layer is

$$\begin{aligned} & \alpha C_{af} \theta_{a1} - \alpha (C_{af} + C_{fs} + \frac{M_f C_f}{\delta t}) \theta_f + \alpha C_{fs} \theta_s \\ & = -(1 - \alpha) C_{af}^* \theta_{a1}^* + (1 - \alpha) (C_{af}^* + C_{fs}^* + \frac{M_f^* C_f^*}{\delta t}) \theta_f^* - (1 - \alpha) C_{fs}^* \theta_s^* \end{aligned} \quad (3.69)$$

with the notations follow the same convention. And it can be shown that the same matrix pattern as described by equation (3.65) results.

Growth of the frost layer will change the air velocity and also the values of A_{af} , h_{af} , and k_{fs} . These must be calculated at each time step during the simulation run.

3.3.3.4 Multi-row and multi-circuit coils

In a heat transfer coil with multi-rows and more than one circuit (tube per row), the coil model can be represented in detail by interconnecting all the heat transfer tubings together. In this case for a coil with M rows and N circuits and if each heat transfer tube is a 4-node model, the entire coil is then represented by $4 \times M \times N$ number of nodes. The extensive discretization scheme enables the provision of thorough information about all energy and mass flow paths inside the coil, for instance the surface temperature of a particular tube or row, the condensation rate at different parts of the coil, etc. Usually the coil can be modelled using fewer number of nodes by taking advantage of the coil symmetry. This is demonstrated below.

Consider a 4-row chilled water coil with 36 parallel circuits and in counter-flow arrangement. The fluid flow rates and the energy balance at all parallel circuits can be taken as the same, the coil can then be represented by just one 4-row circuit (Figure 3.6) with both the air and water flow rates reduce to the flow rates passing through that particular circuit only, i.e. $1/36$ of the original flows.

The overall energy balance matrix template is in the form of equation (3.70) shown in Figure 3.7. The same template applies to the mass flow matrix.

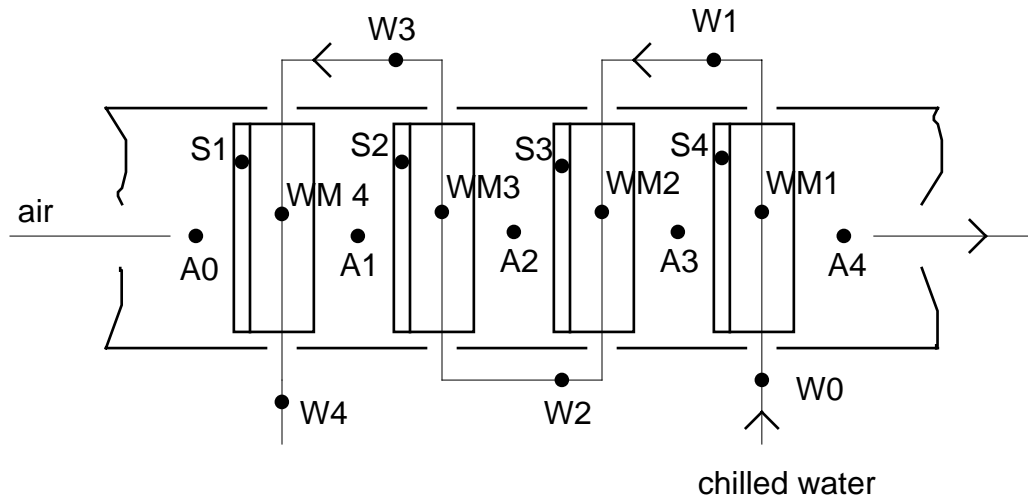


Figure 3.6 Cooling Coil Represented by a 4-row Circuit

$$\begin{bmatrix}
X & X & 0 & 0 & 0 & 0 & 0 & 0 & 0 & 0 & 0 & 0 & 0 & 0 & 0 & X & 0 \\
X & X & X & 0 & 0 & 0 & 0 & 0 & 0 & 0 & 0 & 0 & 0 & 0 & 0 & 0 & 0 \\
X & 0 & X & X & 0 & 0 & 0 & X & 0 & 0 & 0 & 0 & 0 & 0 & 0 & 0 & 0 \\
0 & 0 & X & X & 0 & 0 & 0 & 0 & 0 & 0 & 0 & 0 & 0 & 0 & 0 & 0 & 0 \\
0 & X & 0 & 0 & X & X & 0 & 0 & 0 & 0 & 0 & 0 & 0 & 0 & 0 & 0 & 0 \\
0 & 0 & 0 & 0 & X & X & X & 0 & 0 & 0 & 0 & 0 & 0 & 0 & 0 & 0 & 0 \\
0 & 0 & 0 & 0 & X & 0 & X & X & 0 & 0 & 0 & X & 0 & 0 & 0 & 0 & 0 \\
0 & 0 & 0 & 0 & 0 & 0 & X & X & 0 & 0 & 0 & 0 & 0 & 0 & 0 & 0 & 0 \\
0 & 0 & 0 & 0 & 0 & X & 0 & 0 & X & X & 0 & 0 & 0 & 0 & 0 & 0 & 0 \\
0 & 0 & 0 & 0 & 0 & 0 & 0 & 0 & X & X & X & 0 & 0 & 0 & 0 & 0 & 0 \\
0 & 0 & 0 & 0 & 0 & 0 & 0 & 0 & X & 0 & X & X & 0 & 0 & 0 & 0 & 0 \\
0 & 0 & 0 & 0 & 0 & 0 & 0 & 0 & 0 & 0 & 0 & X & X & X & 0 & 0 & 0 \\
0 & 0 & 0 & 0 & 0 & 0 & 0 & 0 & 0 & 0 & 0 & X & 0 & X & X & 0 & X \\
0 & 0 & 0 & 0 & 0 & 0 & 0 & 0 & 0 & 0 & 0 & 0 & 0 & X & X & 0 & 0
\end{bmatrix}
\begin{bmatrix}
\theta_{s1} \\
\theta_{a1} \\
\theta_{wm4} \\
\theta_{w4} \\
\theta_{s2} \\
\theta_{a2} \\
\theta_{wm3} \\
\theta_{w3} \\
\theta_{s3} \\
\theta_{a3} \\
\theta_{wm2} \\
\theta_{w2} \\
\theta_{s4} \\
\theta_{a4} \\
\theta_{wm1} \\
\theta_{w1} \\
\theta_{a0} \\
\theta_{w0}
\end{bmatrix}
=
\begin{bmatrix}
X \\
X
\end{bmatrix}$$

Figure 3.7 Energy Matrix Template of a 4-row Cooling Coil

3.4. Extension of Work to Other Plant Components

In the past, the modelling approach to plant components other than flow conduits and heat transfer coils are much less rigorous. It is deemed, for the advantages of the next generation softwares, the use of a similar comprehensive fundamental modelling approach is appropriate. Demonstration of the work to some representative plant components are given below.

3.4.1 Electrically heated pan humidifier

For a heated pan humidifier as shown in Figure 3.8(a) the electrical element is totally submerged in the water bath. The heater increases the water temperature in the pan, thus increasing the rate of evaporation. Humidification rate is positive. Because of the relatively low thermal capacitance of the electrical element, the supply of thermal energy (as a conversion from the electrical energy) into the water bath can be considered as immediate. Water vapour generated is carried away by the moist air stream located directly above the pan. The supply (make-up) water rate is controlled in a way to maintain a constant water level in the pan.

Suppose, for the time being, the thermal insulation of the pan outside surface is perfect so that the heat loss to the environment can be neglected. A model of the humidifier can be formed making use 4 nodes (A1, V2, W3, S4) as shown in Figure 3.8(b). In this humidifier model the nodes A0 and W0 are the connections from the incoming air and water streams respectively. It can be shown from the first principle that the actual energy and mass balance equations for the 4 nodes are as follows:

Energy balance

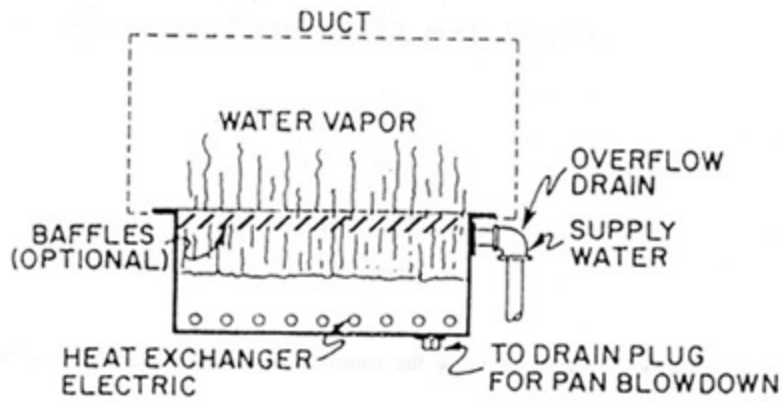
for A1,

$$(m_{a1}Cp_{a1} + m_{v1}Cp_{v1})\theta_{a1} - m_{v2}Cp_{v2}\theta_{v2} - (m_{a0}Cp_{a0} + m_{v0}Cp_{v0})\theta_{a0} = -Hfg_1m_{c1} \quad (3.71)$$

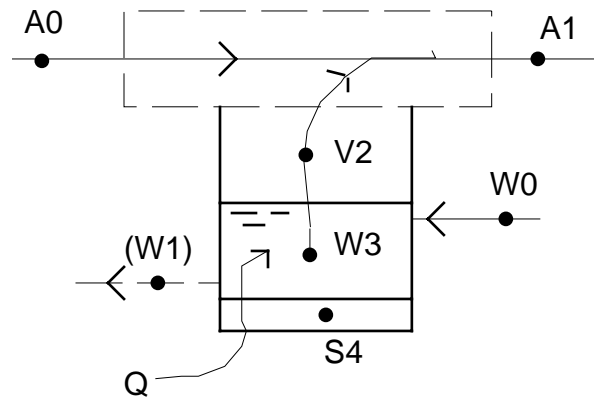
where m_{c1} is the condensate forming rate at A1 in case the moist air stream is over saturated.

for V2,

$$\theta_{v2} = \theta_{w3} \quad (3.72)$$



(a) physical arrangement



(b) component model

Figure 3.8 Heated Pan Humidifier

for W3,

$$h_{sw}A_{sw}(\theta_{s4} - \theta_{w3}) + m_{w0}Cp_{w0}\theta_{w0} - m_{w3}H_{fgw3} + Q = \frac{d\theta_{w3}}{dt} \quad (3.73)$$

for S4,

$$h_{sw}A_{sw}(\theta_{w3} - \theta_{s4}) = \frac{d\theta_{s4}}{dt} \quad (3.74)$$

Re-arranging the above equations using the numerical approach as before gives the following equations:

For A1,

$$C_{a1}\theta_{a1} - C_{v2}\theta_{v2} - C_{a0}\theta_{a0} = C_{c1} \quad (3.75)$$

where $C_{v2} = m_{v2}Cp_{v2}$; $C_{c1} = H_{fg1} m_{c1}$

For V2,

$$-\theta_{v2} + \theta_{w3} = 0 \quad (3.76)$$

For W3,

$$\begin{aligned} & -[\alpha C_{sw} + \frac{M_{w3}Cp_{w3}}{\delta t}]\theta_{w3} + \alpha C_{sw}\theta_{s4} + \alpha C_{w0}\theta_{w0} \\ & = [(1-\alpha)C_{sw}^* - \frac{M_{w3}^*Cp_{w3}^*}{\delta t}]\theta_{w3}^* - (1-\alpha)C_{sw}^*\theta_{s4}^* - (1-\alpha)C_{w0}^*\theta_{w0}^* - [\alpha M_{w3} + (1-\alpha)M_{w3}^*]H_{fg2} - [\alpha Q + (1-\alpha)Q^*] \end{aligned} \quad (3.77)$$

For S4,

$$-[\alpha C_{sw} + \frac{M_{s4}C_{s4}}{\delta t}]\theta_{s4} + \alpha C_{sw}\theta_{w3} = [(1-\alpha)C_{sw}^* - \frac{M_{s4}C_{s4}^*}{\delta t}]\theta_{s4}^* - (1-\alpha)C_{sw}^*\theta_{w3}^* \quad (3.78)$$

Mass balance

i) first-phase (dry air or liquid water) mass balance

For A1,

$$m_{a1} = m_{a0} \quad (3.79)$$

liquid flow not applicable and therefore,

For V2,
$$m_{w2} = 0 \quad (3.80)$$

For W3,
$$m_{w3} - m_{w0} = -C_{vw} \quad (3.81)$$

and the built-in control loop set that $m_{w0} = C_{vw}$ in order to make $m_{w3} = 0$ (constant water level)

For S4,
$$m_{s4} = 0 \quad (3.82)$$

ii) second-phase (water vapour) mass balance

For A1,
$$m_{v1} = C_v \quad (3.83)$$

where the value of C_v depends on the saturation stage of A1;

$$\begin{aligned} C_v &= m_{a0}g_{a1} && \text{if A1 is not saturated} \\ &= m_{a0}g_{a1sat} && \text{if A1 is saturated} \end{aligned}$$

For V2,
$$m_{v2} = C_{vw} \quad (3.84)$$

vapour flow not applicable and therefore,

$$\text{For W3,} \quad m_{v3} = 0 \quad (3.85)$$

$$\text{For S4,} \quad m_{s4} = 0 \quad (3.86)$$

component matrix template

As from the above derivation, the matrix template of this humidifier model is of the following form:

$$\begin{bmatrix} C(1) & C(2) & 0 & 0 & 0 & C(9) \\ 0 & C(3) & C(4) & 0 & 0 & 0 \\ 0 & 0 & C(5) & C(6) & C(10) & 0 \\ 0 & 0 & C(7) & C(8) & 0 & 0 \end{bmatrix} * \begin{bmatrix} A1 \\ V2 \\ W3 \\ S4 \\ W5 \\ A0 \end{bmatrix} = \begin{bmatrix} C(11) \\ C(12) \\ C(13) \\ C(14) \end{bmatrix}$$

(3.87)

of which,

$$\begin{aligned} C(1) &= m_{a1}C_{pa1} + m_{v1}C_{pv1} \\ C(2) &= -m_{v2}C_{pv2} \\ C(3) &= 1 \\ C(4) &= -1 \\ C(5) &= -\alpha h_{sw} A_{sw} - M_{w3}C_{pw3}/\delta t \\ C(6) &= \alpha h_{sw}A_{sw} \\ C(7) &= \alpha h_{sw}A_{sw} \\ C(8) &= -\alpha h_{sw}A_{sw} - M_{s4}C_{s4}/\delta t \\ C(9) &= \alpha m_{w0}C_{pw0} \\ C(10) &= -(m_{a0}C_{pa0} + m_{v0}C_{pv0}) \\ C(11) &= -Hfg_1 m_{c1} \\ C(12) &= 0 \end{aligned}$$

$$C(13) = [(1-\alpha)h_{sw}A_{sw} - (M_{w3} *C_{pw3} */\delta t)] \theta_{w3}^* - (1-\alpha)m_{w0} *C_{pw0} *\theta_{w0}^* - (1-\alpha)h_{sw}A_{sw}\theta_{s4}^* - [\alpha m_{w3} Hfg3 + (1-\alpha)m_{w3} *Hfg3^*] - [\alpha Q + (1-\alpha)Q^*]$$

$$C(14) = [(1-\alpha)h_{sw}A_{sw} - (M_{s4} C_{s4} */\delta t)] \theta_{s4}^* - (1-\alpha)h_{sw}A_{sw}\theta_{w3}^*$$

For the first phase mass flow (dry air or liquid water),

$$\begin{aligned} C(1) &= 1 \\ C(2) &= 0 \\ C(3) &= 1 \\ C(4) &= 0 \\ C(5) &= 1 \\ C(6) &= 0 \\ C(7) &= 0 \\ C(8) &= 1 \\ C(9) &= -1 \\ C(10) &= -1 \\ C(11) &= 0 \\ C(12) &= 0 \\ C(13) &= -C_{vw} \\ C(14) &= 0 \end{aligned}$$

For the second phase mass flow (water vapour),

$$\begin{aligned} C(1) &= 1 \\ C(2) &= -C_{sx} \\ C(3) &= 1 \\ C(4) &= 0 \\ C(5) &= 1 \\ C(6) &= 0 \\ C(7) &= 0 \\ C(8) &= 1 \\ C(9) &= 0 \\ C(10) &= -1 \\ C(11) &= 0 \\ C(12) &= C_{vw} \\ C(13) &= 0 \\ C(14) &= 0 \end{aligned}$$

3.4.2 Flow restrictors

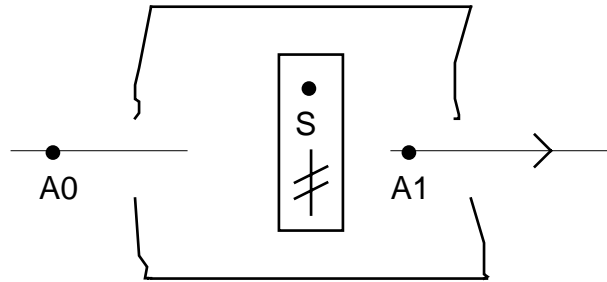


Figure 3.9 2-node Model of Damper in Duct

Consider one particular flow restrictor (Figure 3.9), for instance a damper inside an air duct. In its simplest case the entire damper is assumed to be under uniform temperature condition and therefore can be represented by one single node (or otherwise a multi-node model, which may be necessary for dealing with some specific problem definition). Radiative and conductive heat exchange with the surrounding surfaces or masses are considered negligible. This allows the flow restrictor be represented by a 2-node model: one node for the encapsulated air and the other the submerged solid material of the restrictor.

energy balance

i) Air side:

$$(m_{a0}Cp_{a0} + m_{v0}Cp_{v0})\theta_{a0} + h_{as}A_{as}(\theta_s - \theta_{a1}) - (m_{a1}Cp_{a1} + m_{v1}Cp_{v1})\theta_{a1} = M_{a1}Cp_{a1} \frac{d\theta_{a1}}{dt} \quad (3.88)$$

ii) Solid side:

$$h_{as}A_{as}(\theta_{a1} - \theta_s) = M_s C_s \frac{d\theta_s}{dt} \quad (3.89)$$

mass balance

i) First phase (dry air):

$$m_{a1} - m_{a0} = 0 \quad (3.90)$$

ii) Second phase (water vapour):

In the case of dry surface,

$$m_{v1} - m_{v0} = 0 \quad (3.91)$$

and for wet surface (solid surface temperature < air in contact temperature),

$$m_{v1} - m_{v0} = K_d A_{as} (g_s - g_{a1}) \quad (3.92)$$

By these the following matrix patterns is formed:

energy matrix,

$$\begin{bmatrix} X & X & 0 \\ X & X & X \end{bmatrix} * \begin{bmatrix} \theta_s \\ \theta_{a1} \\ \theta_{a0} \end{bmatrix} = \begin{bmatrix} X \\ X \end{bmatrix} \quad (3.93)$$

first-phase mass matrix,

$$\begin{bmatrix} 1 & 0 & 0 \\ 0 & 1 & -1 \end{bmatrix} * \begin{bmatrix} m_s \\ m_{a1} \\ m_{a0} \end{bmatrix} = \begin{bmatrix} 0 \\ 0 \end{bmatrix} \quad (3.94)$$

second phase mass matrix,

$$\begin{bmatrix} 1 & 0 & 0 \\ 0 & 1 & -1 \end{bmatrix} * \begin{bmatrix} m_s \\ m_{v1} \\ m_{v0} \end{bmatrix} = \begin{bmatrix} 0 \\ X \end{bmatrix} \quad (3.95)$$

Component matrix template is thus of the following format:

$$\begin{bmatrix} X & X & 0 \\ X & X & X \end{bmatrix} * \begin{bmatrix} S \\ A1 \\ A0 \end{bmatrix} = \begin{bmatrix} X \\ X \end{bmatrix}$$

(3.96)

If the restrictor is composed of different materials or is too large to be considered as uniform, the restrictor has to be decomposed into sub-parts for more accurate computation. The above matrix template can be interconnected in parallel or in series and perhaps to be expanded to include 3-dimensional thermal conduction within the solid materials. This is easily achievable within the context of the control volume conservation equations.

3.4.3 Duct heater

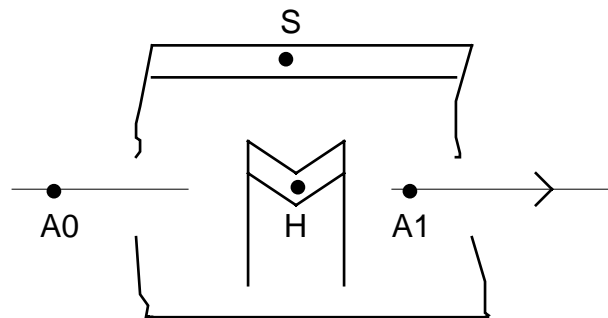


Figure 3.10 3-node Model of Duct Heater

Figure 3.10 shows a 3-node model of a duct heater, of which the nodes represent the heating element, the encapsulated air, and the casing material respectively. Since the heating element operates at an elevated temperature, a considerable portion of the released energy will be in the form of long-wave radiation in addition to the convective heat transfer to the air stream in contact.

Energy balance

For air,

$$(m_{a0}Cp_{a0} + m_{v0}Cp_{v0})\theta_{a0} + h_{ah}A_{ah}(\theta_h - \theta_{a1}) + h_{as}A_{as}(\theta_s - \theta_{a1}) - (m_{a1}Cp_{a1} + m_{v1}Cp_{v1})\theta_{a1} = M_{a1}Cp_{a1} \frac{d\theta_{a1}}{dt} \quad (3.97)$$

For heating element,

$$h_{ah}A_{ah}(\theta_{a1} - \theta_h) + h_{hs}A_{hs}(\theta_s - \theta_h) + Q_h = M_h C_h \frac{d\theta_h}{dt} \quad (3.98)$$

For casing,

$$h_{as}A_{as}(\theta_{a1} - \theta_s) + h_{hs}A_{hs}(\theta_h - \theta_s) = M_s C_s \frac{d\theta_s}{dt} \quad (3.99)$$

The following matrix template can then be derived:

$$\begin{bmatrix} X & X & X & 0 \\ X & X & X & 0 \\ X & X & X & X \end{bmatrix} * \begin{bmatrix} H \\ S \\ A1 \\ A0 \end{bmatrix} = \begin{bmatrix} X \\ X \\ X \end{bmatrix} \quad (3.100)$$

3.4.4 Flow inducers

Unlike all other plant components, flow inducer (an axial flow fan connected with a submerged electric motor for example) provides the flow momentum instead of introducing flow resistance to the handling fluid. Nevertheless from a heat- and mass- transfer point of view, a flow inducer has lots of similarity to a duct heater model or a flow restrictor model. A fan can be described by a component model of 3 nodes, each represents respectively the encapsulated air, the submerged motor body (resemblance to an electric heater), and the casing solid (resemblance to a flow restrictor). Further simplification can be made in that the radiative heat exchange between the motor body and the casing interior surface can be ignored because the temperature of the motor surface is much lower than the heater element surface.

3.4.5 Air washer

The vital part in the performance of an air washer is the intimate contact between the spray water and the air flow which causes heat and mass transfer between the air and the water. The interior space of the air washer chamber in fact can be considered as building up from a number of cells and each cell occupies a fixed control volume in space, thus forming a 3-dimensional grid.

Consider one particular control volume as in Figure 3.11(a) where moist air simply passes from the left to the right and the spray water passing down from the top to the bottom. This is therefore a two dimensional problem.

Energy balance

For air side,

$$(m_{a0}Cp_{a0} + m_{v0}Cp_{v0})\theta_{a0} + h_{aw}A_{aw}(\theta_{w1} - \theta_{a1}) - (m_{a1}Cp_{a1} + m_{v1}Cp_{v1})\theta_{a1} - Hf_8(m_{v0} - m_{v1}) = M_{a1}Cp_{a1} \frac{d\theta_{a1}}{dt} \quad (3.101)$$

For water side,

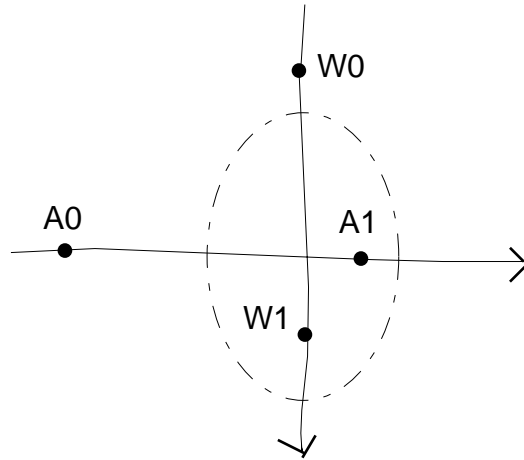
$$m_{w0}Cp_{w0}\theta_{w0} + h_{aw}A_{aw}(\theta_{a1} - \theta_{w1}) - m_{w1}Cp_{w1}\theta_{w1} = M_{w1}Cp_{w1} \frac{d\theta_{w1}}{dt} \quad (3.102)$$

Mass balance

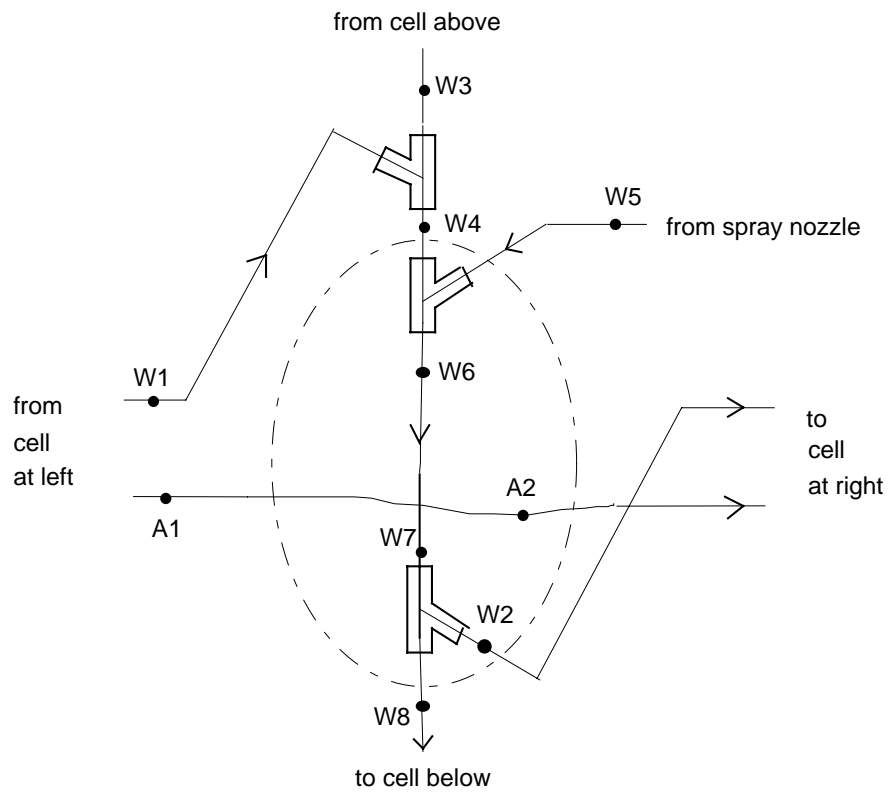
$$m_{v0} - m_{v1} = -(m_{w0} - m_{w1}) = K_d A_{aw} (g_{a1} - g_{sat}) \quad (3.103)$$

The matrix template is therefore

$$\begin{bmatrix} X & X & X & 0 \\ X & X & 0 & X \end{bmatrix} * \begin{bmatrix} A1 \\ W1 \\ A0 \\ W0 \end{bmatrix} = \begin{bmatrix} X \\ X \end{bmatrix} \quad (3.104)$$



(a) a simple cell model



(b) a cell model with consideration of droplet carry-over and presence of spray nozzle inside control volume

Figure 3.11 Cell Models in Air Washer

When a spray nozzle is present in the control volume, this can be viewed as a combination of two parts: a flow converger for the water streams plus the air-water interacting model described above. Similar argument applies when moist air or spray water enters the control volume from more than one adjacent cells or leaves to more than one adjacent cells, say because of the carrying over of water droplets that have entrained in the air stream or because of the complexity of the fluid flow in a 3-dimensional grid. These require the addition of flow convergers and flow diverger for the water streams, as illustrated in Figure 3.11(b). Here again shows a two-dimensional situation. The water droplet (liquid) carried in the moist air stream is taken as an individual fluid path. Two flow convergers are used for the mixing of the incoming water spray from the cell above with the water from the spray nozzle and with the water droplet from the cell at the left respectively. The flow diverger segregates out the water droplet to the cell at the right from the water spray travelling down to the cell below.

Up to now the analyses of mass and energy flow situations in a number of air conditioning plant equipment have been covered, the characteristic equations are developed, and the component matrix templates formulated. One clear observation in the process is that the matrix equations obtained so far are more or less similar. This is not surprising as the modes of heat and mass transfer in the system are finite. And further this suggests that each component model in fact can be built upon a selected combination of fundamental parts, each of which represents a particular mode of energy and mass transfer. This microscopic way of plant modelling will be explored in the next Chapter.

References

Braun, J.E., Klein, S.A. & Mitchell, J.W. 1989. "Effective Models for Cooling Towers and Cooling Coils." ASHRAE Transactions, Vol. 95, Part 2, pp.164-174.

Clark, D.R. 1985. HVACSIM+ Building Systems and Equipment Simulation Program Reference Manual. U.S. Department of Commerce, NBSIR 84-2996.

Clark, D.R., Hurley C.W. & Hill C.R. 1985. "Dynamic Models for HVAC System Components." ASHRAE Transactions, Vol. 91, Part 1B, pp.737-751.

Clarke, J.A. 1985. Energy Simulation in Building Design. Adam Hilger Ltd., Bristol and Boston.

Elmahdy, A.H. & Mitalas, G.P. 1977. "A Simple Model for Cooling and Dehumidifying Coils for Use in Calculating Energy Requirements for Buildings." ASHRAE Transactions, Vol. 83, Part 2, pp. 103-117.

Gartner J.R. & Harrison, H.L. 1963. "Frequency Response Transfer Functions for a Tube in Crossflow." ASHRAE Transactions, Vol. 69, pp.323-330.

Gartner, J.R. & Harrison, H.L. 1965 "Dynamic Characteristics of Water-to-air Crossflow Heat Exchangers." ASHRAE Transactions, Vol. 71, Part I, pp.212-224.

Gartner, J.R. & Daane, L.E. 1969 "Dynamic Response Relations for a Serpentine Crossflow Heat Exchanger with Water Velocity Disturbance." ASHRAE Transactions, Vol. 75, Part I, pp.53-68.

Goldstein, S.D. 1983. "A Mathematically Complete Analysis of Plate-fin Heat Exchangers." ASHRAE Transactions, Vol. 89, Part 2A, pp.447-470.

Hanby, V.I. & Clarke, J.A. 1988. "SERC Plant Component Model Catalogue." Final report, SERC Grant GR/D/07459, Co-ordination of HVAC Component Models, Glasgow, Scotland.

Holmes, M.J. 1982. "The Simulation of Heating and Cooling Coils." In proceedings of the System Simulation in Building International Conference, University of Liege, Belgium, December 1982, pp.245-282.

Holmes, M.J. 1988. "HVAC Component Specification: Heating and Cooling Coils." Energy Conservation in Buildings & Community Systems Programme, Annex X: System Simulation (S6), International Energy Agency.

Ip, K.C., Day B. & Richardson, D. 1989. "Fluid Flow and Heat Transfer in Pipework Systems: I Mathematical Model for Dynamic Modular Simulation." Building Services Engineering Research and Technology, Vol. 10, Part 4, pp. 143-149.

Klein, S.A. et al. 1990. TRNSYS, A Transient System Simulation Program. University of Wisconsin-Madison, Engineering Experiment Station Report 38-13, Version 13.1.

McCullagh, K.R., Green, G.H. & Shekar, S.C. 1969. "An Analysis of Chill Water Cooling Dehumidifying Coils Using Dynamic Relationships." ASHRAE Transactions, Vol.75, Part II, pp.200-209.

McLean, D.J. 1982. The Simulation of Solar Energy Systems. PhD Thesis, Department of Architecture and Building Science, University of Strathclyde, Scotland.

McNamara, R.T. & Harrison, H.L. 1967. "A Lumped Parameter Approach to Cross Flow Heat Exchanger Dynamics." ASHRAE Transactions, Vol.73, Part II.

McQuiston, F.C. 1981 "Finned Tube Heat Exchangers: State of the Art for the Air Side." ASHRAE Transactions, Vol. 87, Part 1, pp.1077-1083.

Ogata, K. 1992. System Dynamics. 2nd edit., Prentice-Hall, Inc.

Shekar, S.C. & Green, G.H. 1970. "Dynamic Study of a Chill Water Cooling and Dehumidifying Coil." ASHRAE Transactions, Vol. 76, Part II, pp.36-51.

Stoecker, W.F. 1975. Procedures for Simulating the Performance of Components and Systems for Energy Calculations. 3rd edit., compiled by the Task Group on Energy Requirements for Heating and Cooling of Buildings, ASHRAE.

Tamm, H. 1969. "Dynamic Response Relations for Multi-row Crossflow Heat Exchangers." ASHRAE Transactions, Vol.75, Part I, pp.69-80.

Tang, D. 1985. The Simulation of Wet Central Heating Systems. PhD Thesis, Department of Architecture and Building Science, University of Strathclyde, Scotland.

Tobias, J.R. 1973. "Simplified Transfer Function for Temperature Response of Fluids Flowing through Coils, Pipes or Ducts." ASHRAE Transactions, Vol. 79, Part 2, pp.19-22.

CHAPTER FOUR

THEORETICAL FRAMEWORK OF PRIMITIVE PART MODELLING

The simulation models of building and HVAC equipment are either too simple to be used in large scale simulations or too detailed and heavy to be used easily in reasonable coupling. For future modelling developments, a process where models remain at the mathematical equation level is the most appropriate for easy link. A reasonable level of computability has to be maintained. The state space (conservation) equations appear at the best compromise. In order to ensure the genericity, a strong physical meaning must be supplied. The definition of a physical state space and the corresponding rules of physical reduction offers all the required specifications on the parameters and model level adaptability. A first and obvious way to make modelling more efficient is to re-use basic existing pieces or component models: modularity of the modelling itself. This means that modelling have first to cut the physical component into some pieces, then to select the appropriate basic models in a library and finally to link the basic models to produce the desired global model. (Laret 1989)

The above accurately describes the motive of the work towards a generalized plant component database. The following introduces the mathematical concept of formulating component models from primitive parts, which is deemed to be the most generalized approach.

4.1 The Concept of Primitive Parts

Primitive parts are the most elementary sub-parts which are intended to model energy and fluid mass flow paths taking place in air-conditioning systems. Each primitive part is a small characteristic-equation-set which describes one particular aspect of thermofluid process using a minimum number of finite volumes, or 'nodes'. In essence, any basic air conditioning equipment can be modelled from some combinations of the primitive parts. A list of these sub-parts is shown in Table 4.1. Included in the list are twenty-seven 'objects' placed under 10 categories. A full description of the topology of the matrix representation of the primitive parts is given in Appendix B.

Table 4.1 List of Primitive Parts

1	Thermal conduction
1.1	solid to solid
1.2	with ambient solid
2	Surface convection
2.1	with moist air
2.2	with 2-phase fluid
2.3	with 1-phase fluid
2.4	with ambient
3.	Surface radiation
3.1	with local surface
3.2	with ambient surface
4.	Flow upon surface
4.1	for moist air; 3 nodes
4.2	for 2-phase fluid; 3 nodes
4.3	for 1-phase fluid; 3 nodes
4.4	for moist air; 2 nodes
4.5	for 1-phase fluid; 2 nodes
5	Flow divider & inducer
5.1	Flow diverger (for all fluid)
5.2	Flow multiplier (for all fluid)
5.3	Flow inducer (for all fluid)
6	Flow converger
6.1	for moist air
6.2	for 2-phase fluid
6.3	for 1-phase fluid
6.4	for leak-in moist air from outside
7	Flow upon water spray
7.1	for moist air
8	Fluid injection
8.1	water/steam to moist air
9	Fluid accumulator
9.1	for moist air
9.2	for liquid
10	Heat injection
10.1	to solid
10.2	to vapour-generating fluid
10.3	to moist air

Categories 1 to 3 describe respectively the three basic modes of heat transfer on and within any solid surfaces: thermal conduction, convection and radiation. Here totally eight different numbers of primitive parts are used to describe different thermal interactions of a solid node, depending on whether the state variables of an ambient air node, or a neighbouring surface node, or a solid node in direct contact, are unknowns to be solved in the solution process, or are known values (external excitations) throughout the simulation period. Category 4 describes the thermal behaviour of various types of fluid when flowing across a solid surface. The five primitive parts within this category are expected to have the widest application in air conditioning. Fluid types here include moist air and any pure fluid - be it a liquid or gas (single-phase), or a wet vapour (two-phase). There is no restriction to the physical shape, orientation, nature or dimensions of the surface - be it the interior surface of a ventilating fan casing or the exposed surface of a duct heater. While a 3-node primitive part for a single phase fluid or moist air stream flowing upon surface is used to describe the transport delay phenomenon, a 2-node representation is usual adequate for general applications. Categories 5 and 6 describe the occurrences of splitting, mixing or induction of fluid streams. The primitive parts here are basic objects for modelling tees, mixing box, and fan. The 'flow multiplier' primitive part is helpful to adjust the fluid flow rate in a specific ratio in order to simplify the component modelling task by narrowing down the modelling scope of the real piece, e.g. modelling only a half of the complete component in case of symmetry. It can also act as a filter, say in the case of modelling a steam trap which allows only liquid water to pass through but not steam vapour. Category 7 refers to the direct interaction of air and water streams, as in the case of air washer or cooling tower. Category 8 describes the injection of water or steam into a moist air stream as in the case of humidifiers. Category 9 covers the fluid accumulators like the expansion tank of a hydronic circuit, or the room air in an air-conditioned space. Category 10 covers the heat injection processes, like the operation of an electric heating element in an air duct or a water bath, etc.

In a software designed for modular simultaneous simulation, like the ESP-r system, a subprogram in association with each plant component model is basically a matrix coefficient generator. When the simulation is executed, the numerical values of the matrix coefficients are generated for the purpose of solving the state variables (temperature, first and second phase mass flows) of all the nodes during the iteration process of each time step (Hensen 1991). Under this software environment, each of these primitive parts can exist as a 'primitive part' subprogram in a library file. The function of each subprogram is to compute the numerical values of the coefficients of the corresponding primitive-part matrix template.

To construct a plant component model, a nodal discretisation scheme of the component is first to be fixed. An analysis of the energy and mass flow paths involved will give rise to the number and the types of primitive parts to be included. Coefficients of the matrix template of this plant component is then

matched to a 'mix' of the coefficients of the primitive-part matrix templates. To develop the corresponding plant component coefficient generator in the software, the involved primitive part subprograms will be called upon and on top of these of course, the other required utility subprograms for data input management, for calculating time-varying properties and empirical coefficients, and for checking the validity of the designer specified parameters prior to the actual simulation,etc.

This approach allows hierarchical decomposition or incremental component modelling - a 'compound' or 'meta' component can be built upon a combination of these 'single' plant components or other meta-components at a low level. To do this, before the meta component description is entered into the plant component database, the sub-components and their inter-connections must first be determined and the components at inlet and outlet has to be identified (Aasem 1993). In this way, the entire plant database will be a taxonomy of plant components built upon a finite number of primitive parts as the core and therefore, with a unified mathematical structure and a standardised hierarchy.

A chilled water cooling coil can be taken as an example. The coil model can be constructed through several stages. For instance, in the first place, a straight tube section of the coil can be modelled by using 4 nodes - a combination of the primitive-part numbers 4.3 'flow upon surface for single phase fluid; 3-nodes ' and 4.4 'flow upon surface for moist air; 2 nodes' - assuming that the thermal resistance of the tube wall is negligible. Then the cooling coil can be visualized as a network of these tube sections connected in the same configuration as the actual physical arrangements, i.e. single pass, serpentine or double serpentine arrangements - in the same way described in Chapter 3. If a counter-flow coil model is to be simplified by modelling only one counter-flow water circuit, the primitve part 5.2 'flow multiplier' can be added to both the air and the water sides to adjust the fluid flow rates accordingly. More extensive or complicated coil models can be constructed in a similar way, upto the modeller's discretion in the selection of the appropriate primitive parts in the analysis.

Such a plant component taxonomy concept (Chow 1993, 1995) provides an opportunity for the modeller a greater flexibility to tailor component models to suit specific simulation task. The following presents the mathematical background of this concept.

4.2 The Principle of Superposition

In the finite difference control volume conservation approach, the matrix equations of a plant system are transformed into a linear system of algebraic equations with the non-linear elements, if any, in the orginal equations either truncated or absorbed into the variable coefficients. A solution technique is then applied

to obtain the solution at any time increment. One important property of linear systems is the applicability of the 'principle of superposition' (Ogata 1992). This principle states that the response produced by simultaneous applications of two different forcing functions or inputs is the sum of the two individual responses. Consequently the response to several inputs can be calculated by dealing with one input at a time and then adding the results. If we think about this in terms of the interaction of thermal energy, the effect of the three modes of heat transfer (thermal conduction, convection and radiation) on a real object virtually obeys the superposition rule. A simple example is given below to illustrate this point and its importance on the concept of primitive parts modelling.

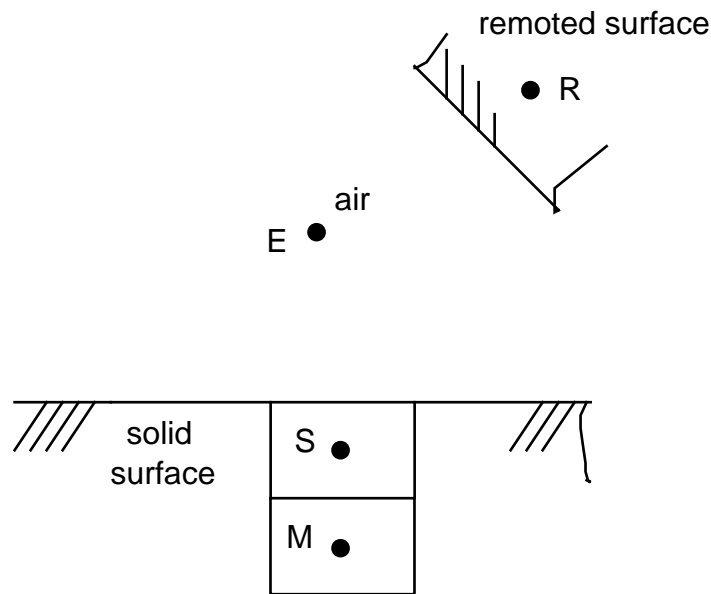


Figure 4.1 Discretization Scheme for Surface Node "S"

Consider a stationary solid surface which is in contact with moist air and is exposed to a remoted solid surface - all the three are at different temperatures initially. Figure 4.1 shows a model of the situation in which the node 'S' represents the solid surface which is our focus of interest. S is thermally interacting with the following 3 nodes in the discretization scheme:

Interacting Nodes	Means of Energy Exchange
M - neighbouring solid node	Thermal conduction
R - remoted solid surface node	Thermal radiation
E - ambient air node	Surface convection

In heat transfer, individual mode of energy exchange takes place as if the others were not present. When

they occur at the same time the mathematical rule of superposition can be applied in that the net sum of the energy transferred by individual process equals to the thermal energy stored in the node. The energy balance equation for the node S is therefore

$$(k_{ms}A_{ms}/x_{ms}) [\theta_m - \theta_s] + h_{es}A_{es} [\theta_e - \theta_s] + h_{rs}A_{rs} [\theta_r - \theta_s] = M_s C_s (d \theta_s / dt) \quad (4.1)$$

Or, when simplifying the coefficient expressions,

$$C_{ms}[\theta_m - \theta_s] + C_{es} [\theta_e - \theta_s] + C_{rs} [\theta_r - \theta_s] = M_s C_s (d \theta_s / dt) \quad (4.2)$$

in that,

$$C_{ms} = k_{ms} A_{ms} / x_{ms}$$

$$C_{es} = h_{es} A_{es}$$

$$C_{rs} = h_{rs} A_{rs}$$

Using the finite difference method, as explained in Chapter 3, by weighted-summation of the fully-implicit and fully explicit formulation with the ratio α to $(1-\alpha)$, the energy balance equation becomes

$$\begin{aligned} & [-\alpha(C_{ms} + C_{es} + C_{rs}) - M_s C_s / \delta t] \theta_s + \alpha C_{ms} \theta_m + \alpha C_{es} \theta_e + \alpha C_{rs} \theta_r \\ & = [(1-\alpha)(C_{ms}^* + C_{es}^* + C_{rs}^*) - M_s^* C_s^* / \delta t] \theta_s^* - (1-\alpha) C_{ms}^* \theta_m^* - (1-\alpha) C_{es}^* \theta_e^* - (1-\alpha) C_{rs}^* \theta_r^* \end{aligned} \quad (4.3)$$

It should be noted that in most of the practical applications, M_s^* is equal to M_s . The use of M_s^* in the equation represents the most generalized situation. Equation (4.3) can be put into the matrix form such that

$$[C(1) \ C(2) \ C(3) \ C(4)]^* \begin{bmatrix} \theta_s \\ \theta_m \\ \theta_r \\ \theta_e \end{bmatrix} = [C(5)] \quad (4.4)$$

where,

$$C(1) = -\alpha (C_{ms} + C_{es} + C_{rs}) - M_s \cdot C_s / \delta t$$

$$C(2) = \alpha C_{ms}$$

$$C(3) = \alpha C_{rs}$$

$$C(4) = \alpha C_{es}$$

$$C(5) = [(1-\alpha)(C_{ms}^* + C_{es}^* + C_{rs}^*) - M_s^* \cdot C_s^* / \delta t] \theta_s^* - (1-\alpha) C_{ms}^* \theta_m^* - (1-\alpha) C_{rs}^* \theta_r^* - (1-\alpha) C_{es}^* \theta_e^*$$

According to the method currently used in the ESP-r software, the mathematical expressions of the above five coefficients of the energy matrix equation (4.4) can be written to the appropriate component/sub-component coefficient generator sub-program. However, an alternative and more generalised way of describing the mathematical expressions of these coefficients in the component subprogram is by calling the primitive part subprograms from the library. In this case the following 3 primitive parts on the list of Appendix I are involved:

Part No.	Description	Nodes Involved
1.1	Thermal conduction: solid to solid	S, M
2.1	Surface convection: with moist air	S, E
3.1	Surface radiation: with local surface	S, R

As far as the node S is concerned, the relevant equations contributing from these parts, as transplanted from the primitive parts descriptions given in Appendix I, are:

Part No. 1.1: Thermal Conduction: solid to solid

$$[A(11,1) \ A(11,2)]^* \begin{bmatrix} \theta_s \\ \theta_m \end{bmatrix} = [B(11,1)] \quad (4.5)$$

where,

$$A(11,1) = -\alpha C_{ms} - M_s C_s / (N_i \delta t)$$

$$A(11,2) = \alpha C_{ms}$$

$$B(11,1) = [(1-\alpha)C_{ms}^* - M_s^* C_s^* / N_i \delta t] \theta_s^* - (1-\alpha)C_{ms}^* \theta_m^*$$

Part No. 2.1: Surface Convection: with moist air

$$[A(21,1) \ A(21,2)]^* \begin{bmatrix} \theta_s \\ \theta_e \end{bmatrix} = [B(21,1)] \quad (4.6)$$

where,

$$A(21,1) = -\alpha C_{es} - M_s C_s / (N_i \delta t)$$

$$A(21,2) = \alpha C_{es}$$

$$B(21,1) = [(1-\alpha)C_{es}^* - M_S^*C_S^*/Ni_S.\delta t] \theta_S^* - (1-\alpha)C_{es}^*\theta_e^*$$

Part No. 3.1: Surface Radiation: with local surface

$$[A(31,1) \ A(31,2)]^* \begin{bmatrix} \theta_s \\ \theta_r \end{bmatrix} = [B(31,1)]$$

(4.7)

where,

$$A(31,1) = -\alpha C_{RS} - M_S.C_S/(Ni_S.\delta t)$$

$$A(31,2) = \alpha C_{RS}$$

$$B(31,1) = [(1-\alpha)C_{RS}^* - M_S^*C_S^*/Ni_S.\delta t] \theta_S^* - (1-\alpha)C_{RS}^*\theta_r^*$$

One key parameter in the above expressions is Ni_S which is a connectivity term known as the 'primitive part connection index' (or the 'pp index' in short). This index indicates the number of primitive parts involved in describing the energy/mass flow paths linked to the node S. In this case, Ni_S is equal to 3.

The rule of superposition is then applied here in that each of the matrix coefficients is the sum of the corresponding coefficients coming from the primitive parts. Hence,

$$\begin{aligned} C(1) &= A(11,1) + A(21,1) + A(31,1) \\ &= [-\alpha C_{ms} - M_S C_S / (3\delta t)] + [-\alpha C_{es} - M_S C_S / (3\delta t)] + [-\alpha C_{RS} - M_S C_S / (3\delta t)] \\ &= -\alpha (C_{ms} + C_{es} + C_{RS}) - M_S C_S / \delta t \end{aligned}$$

$$C(2) = A(11,2) = \alpha C_{ms}$$

$$C(3) = A(31,2) = \alpha C_{RS}$$

$$C(4) = A(21,2) = \alpha C_{es}$$

$$\begin{aligned} C(5) &= B(11,1) + B(21,1) + B(31,1) \\ &= [(1-\alpha)C_{ms}^* - M_S^*C_S^*/(3.\delta t)] \theta_S^* - (1-\alpha)C_{ms}^*\theta_m^* \\ &\quad + [(1-\alpha)C_{es}^* - M_S^*C_S^*/(3.\delta t)] \theta_S^* - (1-\alpha)C_{es}^*\theta_e^* \\ &\quad + [(1-\alpha)C_{RS}^* - M_S^*C_S^*/(3.\delta t)] \theta_S^* - (1-\alpha)C_{RS}^*\theta_r^* \\ &= [(1-\alpha) (C_{ms}^* + C_{es}^* + C_{RS}^*) - M_S^*.C_S^*/\delta t] \theta_S^* \\ &\quad - (1-\alpha) C_{es}^* \theta_e^* - (1-\alpha) C_{RS}^* \theta_r^* - (1-\alpha) C_{ms}^* \theta_m^* \end{aligned}$$

The expressions are exactly the same as those derived from the first principle for the equation (4.4) mentioned above. It can be seen that the function of the pp index Ni is to maintain the heat capacitance of the node S as Ms.Cs whatever the number of primitive parts has been involved or added to the scenario.

It is not difficult to prove that the above addition of primitive parts also holds true for mass flow situation since no fluid mass flow is actually involved. The following expression for the node S will be resulted for both first and second phase mass flow:

$$[1 \ 0 \ 0 \ 0]^* \begin{bmatrix} m_s \\ m_m \\ m_r \\ m_e \end{bmatrix} = [0] \quad (4.8)$$

More practical examples of applying the primitive part concept to air conditioning equipment are given below.

4.3 Examples of Application

4.3.1 Insulated water pipe

The primitive part technique is applied to an insulated water pipe model. Taking the ambient air node as an external excitation, Section 3.2.2 shows that an insulated water pipe can be represented by a 4-node model with the matrix template as follows:

$$\begin{bmatrix} C(1) & C(2) & 0 & 0 & 0 \\ C(3) & C(4) & C(5) & 0 & 0 \\ 0 & C(6) & C(7) & C(8) & C(11) \\ 0 & 0 & C(9) & C(10) & 0 \end{bmatrix} * \begin{bmatrix} S1 \\ S2 \\ WM \\ W1 \\ W0 \end{bmatrix} = \begin{bmatrix} C(12) \\ C(13) \\ C(14) \\ C(15) \end{bmatrix} \quad (4.9)$$

This model can be fomulated by using 3 primitive parts namely:

- Part No. 1.1 Thermal conduction (solid to solid)
- Part No. 2.4 Surface convection (with ambient)
- Part No. 4.3 Flow upon surface (for 1-phase fluid)

The 15 coefficients of the matrix equation (4.9) for this pipe can then be given by the summation of primitive part coefficients as shown in Table 4.2.

Table 4.2 Development of Insulated Water Pipe Model
from Primitive Part Coefficients

PP 4.3		PP 1.1		PP 2.4	
Matrix Coefficients		Thermal conduction (solid to solid) S1,S2	Surface convection (with ambient)	Flow upon surface (for 1-phase fluid) S1,E	
S2-W1,W0					
C(1)	=	A(11,1)	+	A(24,1)	
C(2)	=	A(11,2)			
C(3)	=	A(11,3)			
C(4)	=	A(11,4)	+	A(43,1)	
C(5)	=		+	A(43,2)	
C(6)	=			A(43,4)	
C(7)	=			A(43,5)	
C(8)	=		+	A(43,6)	
C(9)	=			A(43,8)	
C(10)	=		+	A(43,9)	
C(11)	=			A(43,11)	
C(12)	=	B(11,1)	+	B(24,1)	
C(13)	=	B(11,2)	+	B(43,1)	
C(14)	=			B(43,2)	
C(15)	=			B(43,3)	

In the above formulation, the pp indices Ni are as follows:

Node	Ni
S1	2
S2	2
WM	1
W1	1

It can be shown that, following the similar steps as in Section 4.2, the coefficient expressions in terms of primitive parts given above holds true for all cases of energy and mass transfer.

4.3.2 Heat transfer tube

The other example applies the primitive part concept to the modelling of a heat transfer tube in Figure 3.4, whereby moist air flows across the outside surface of a metallic tube and water flows inside the tube. The tube body as a whole is at a uniform temperature θ_s . The component model of the tube will then consist of 4 nodes S, A1, WM and W1 and two connections A0 and W0.

There will be two energy flow paths: forced convection between the moist air stream and the tube body, as well as the forced convection between the water stream and the tube body. It has been shown from the first principle in Chapter 3 that the plant component matrix template is of the form

$$\begin{bmatrix} C(1) & C(2) & C(3) & 0 & 0 & 0 \\ C(4) & C(5) & 0 & 0 & C(11) & 0 \\ C(6) & 0 & C(7) & C(8) & 0 & C(12) \\ 0 & 0 & C(9) & C(10) & 0 & 0 \end{bmatrix} * \begin{bmatrix} S \\ A1 \\ WM \\ W1 \\ A0 \\ W0 \end{bmatrix} = \begin{bmatrix} C(13) \\ C(14) \\ C(15) \\ C(16) \end{bmatrix}$$

(4.10)

The above coefficients can be formulated using the primitive parts 4.3 and 4.4. The expression of the 16 coefficients of the matrix equation (4.10) in terms of primitive parts are shown in Table 4.3. This is true for both energy and mass flow (first and second phases) situations.

Table 4.3 Development of Heat Transfer Tube Model
from Primitive Part Coefficients

Matrix Coefficients		P/N 4.3 Flow upon surface: for single-phase fluid S-W1,W0		P/N 4.4 Flow upon surface for moist-air S-A1,A0
C(1)	=	A(43,1)	+	A(44,1)
C(2)	=			A(44,2)
C(3)	=	A(43,2)		
C(4)	=			A(44,3)
C(5)	=			A(44,4)
C(6)	=	A(43,4)		
C(7)	=	A(43,5)		
C(8)	=	A(43,6)		
C(9)	=	A(43,8)		
C(10)	=	A(43,9)		
C(11)	=			A(44,6)
C(12)	=	A(43,11)		
C(13)	=	B(43,1)	+	B(44,1)
C(14)	=			B(44,2)
C(15)	=	B(43,2)		
C(16)	=	B(43,3)		

In the above formulation, the values of the pp indices are as follows:

Node	Ni
S	2
A1	1
W1	1

The concept is more illustrative in the following example of modelling a humidifier where involves more complicated mass flow situation. More thorough derivation of the coefficients will be given.

4.3.3 Electrically Heated Pan Humidifier

Chapter 3 shows that a heated pan humidifier model (Figure 3.7) can be formed making use of 4 nodes (A1, V2, W3 and S4). This model can be built from the following 4 primitive parts:

Part No.	Descriptions	Nodes Involved
2.3	Surface convection: with single-phase fluid	W3, S4
9.2	Fluid accumulator: for liquid	W0, W2, (W1)
8.1	Fluid injection: water/steam to moist air	A0, V2, A1
10.2	Heat injection: to vapour generating fluid	V2, W3

It should be noted that the notation of the nodes assigned in this component is not exactly matching that quoted in the primitive parts. Node W2 of Part No. 9.2 in Appendix I (i.e. node W1 of this component) is not to be used in the model and hence is only a "dummy" node. To maintain the simplicity of the component model, there is no characteristic equation defined for a dummy node.

component matrix template

The matrix template of this humidifier model is of the following form:

$$\begin{bmatrix} C(1) & C(2) & 0 & 0 & 0 & C(9) \\ 0 & C(3) & C(4) & 0 & 0 & 0 \\ 0 & 0 & C(5) & C(6) & C(10) & 0 \\ 0 & 0 & C(7) & C(8) & 0 & 0 \end{bmatrix} * \begin{bmatrix} A1 \\ V2 \\ W3 \\ S4 \\ W5 \\ W0 \end{bmatrix} = \begin{bmatrix} C(11) \\ C(12) \\ C(13) \\ C(14) \end{bmatrix} \tag{4.11}$$

of which C(1), C(3), C(5) and C(8) are the coefficients for those nodes which the individual characteristic equations are specifically written about; C(11), C(12), C(13) and C(14) are the present-time & excitation coefficients. Identification of the coefficient types are important in order to match the template coefficients to the corresponding coefficients of the primitive parts. In this case their relationships are shown in Table 4.4.

Table 4.4 Development of Electrically Heated Pan Humidifier
from Primitive Part Coefficients

Coefficients	PP 2.3	PP 8.1	PP 9.3	PP 10.2
C(1) =		A(81,1)		
C(2) =		A(81,3)		
C(3) =				A(102,4)
C(4) =				A(102,3)
C(5) =	A(23,4)		+ A(92,1)	+ A(102,1)
C(6) =	A(23,3)			
C(7) =	A(23,2)			
C(8) =	A(23,1)			
C(9) =		A(81,2)		
C(10) =			A(92,5)	
C(11) =		B(81,1)		
C(12) =				B(102,2)
C(13) =	B(23,2)		+ B(92,1)	+ B(102,1)
C(14) =	B(23,1)			

The pp indices of the nodes are:

Node	Ni
A1	1
V2	1
W3	3
S4	1

Hence for energy flow,

$$C(1) = m_{a1}C_{pa1} + m_{v1}C_{pv1}$$

$$\begin{aligned}
C(2) &= - (m_{w2}C_{p_{w2}} + m_{v2}C_{p_{v2}}) \\
&= - m_{v2}C_{p_{v2}} \qquad \qquad \qquad \text{(since } m_{w2} = 0)
\end{aligned}$$

$$C(3) = 1$$

$$C(4) = -1$$

$$\begin{aligned}
C(5) &= - M_{w3}C_{p_{w3}}/(Ni_{w3} \cdot \delta t) - M_{w3}C_{p_{w3}}/(Ni_{w3} \cdot \delta t) + [- \alpha h_{sw}A_{sw} - M_{w3}C_{p_{w3}}/(Ni_{w3} \cdot \delta t)] \\
&= - \alpha h_{sw}A_{sw} - M_{w3}C_{p_{w3}}/\delta t
\end{aligned}$$

$$C(6) = \alpha h_{sw}A_{sw}$$

$$C(7) = \alpha h_{sw}A_{sw}$$

$$\begin{aligned}
C(8) &= - \alpha h_{sw}A_{sw} - M_{s4}C_{s4}/(Ni_{s4} \cdot \delta t) \\
&= - \alpha h_{sw}A_{sw} - M_{s4}C_{s4}/\delta t
\end{aligned}$$

$$C(9) = - (m_{a0}C_{p_{a0}} + m_{v0}C_{p_{v0}})$$

$$C(10) = \alpha m_{w0}C_{p_{w0}}$$

$$C(11) = - Hfg_1 m_{c1}$$

$$C(12) = 0$$

$$\begin{aligned}
C(13) &= -[M_{w3}^*C_{p_{w3}}^*/(Ni_{w3} \cdot \delta t)] \theta_{w3}^* - [\alpha m_{w3}Hfg_3 + (1-\alpha)m_{w3}^*Hfg_3^*] - [\alpha Q + (1-\alpha)Q^*] \\
&\quad - [M_{w3}^*C_{p_{w3}}^*/(Ni_{w3} \cdot \delta t)] \theta_{w3}^* + [(1-\alpha)m_{w1}^*C_{p_{w1}}^*\theta_{w1}^*] - (1-\alpha)m_{w0}^*C_{p_{w0}}^*\theta_{w0}^* \\
&\quad + [(1-\alpha)h_{sw}^*A_{sw} - M_{w3}^*C_{p_{w3}}^*/(Ni_{w3} \cdot \delta t)] \theta_{w3}^* - (1-\alpha)h_{sw}^*A_{sw}\theta_{s4}^* \\
&= [(1-\alpha)h_{sw}^*A_{sw} - (M_{w3}^*C_{p_{w3}}^*/\delta t)]\theta_{w2}^* - (1-\alpha)m_{w0}^*C_{p_{w0}}^*\theta_{w0}^* - (1-\alpha)h_{sw}^*A_{sw}\theta_{s4}^* \\
&\quad - [\alpha m_{w3}Hfg_3 + (1-\alpha)m_{w3}^*Hfg_3^*] - [\alpha Q + (1-\alpha)Q^*] \\
&\qquad \qquad \qquad \text{(since } m_{w1}, C_{p_{w1}} \text{ and } \theta_{w1} \text{ are undefined and therefore equal to zero)}
\end{aligned}$$

$$\begin{aligned}
C(14) &= [(1-\alpha)h_{sw}^*A_{sw} - (M_{s4}^*C_{s4}^*/Ni_{s4} \cdot \delta t)] \theta_{s4}^* - (1-\alpha)h_{sw}^*A_{sw}\theta_{w3}^* \\
&= [(1-\alpha)h_{sw}^*A_{sw} - (M_{s4}^*C_{s4}^*/\delta t)] \theta_{s4}^* - (1-\alpha)h_{sw}^*A_{sw}\theta_{w3}^*
\end{aligned}$$

For the first phase mass flow (dry air or liquid water),

$$\begin{aligned}
 C(1) &= 1/N_{i_{a1}} = 1 \\
 C(2) &= 0 \\
 C(3) &= 1/N_{i_{v2}} = 1 \\
 C(4) &= 0 \\
 C(5) &= 1/N_{i_{w3}} + 1/N_{i_{w3}} + 1/N_{i_{w3}} = 1 \\
 C(6) &= 0 \\
 C(7) &= 0 \\
 C(8) &= 1/N_{i_{s4}} = 1 \\
 C(9) &= -1 \\
 C(10) &= -1 \\
 C(11) &= 0 \\
 C(12) &= 0 \\
 C(13) &= -C_{vw} + 0 + 0 = -C_{vw} \\
 C(14) &= 0
 \end{aligned}$$

For the second phase mass flow (water vapour),

$$\begin{aligned}
 C(1) &= 1/N_{i_{a1}} = 1 \\
 C(2) &= 0 \\
 C(3) &= 1/N_{i_{v2}} = 1 \\
 C(4) &= 0 \\
 C(5) &= 1/N_{i_{w3}} + 1/N_{i_{w3}} + 1/N_{i_{w3}} = 1 \\
 C(6) &= 0 \\
 C(7) &= 0 \\
 C(8) &= 1/N_{i_{s4}} = 1 \\
 C(9) &= 0 \\
 C(10) &= -1/N_{i_{a1}} = -1 \\
 C(11) &= C_v \\
 C(12) &= C_{vw} \\
 C(13) &= 0 + 0 + 0 = 0 \\
 C(14) &= 0
 \end{aligned}$$

4.3.4 Fan with Submerged Motor

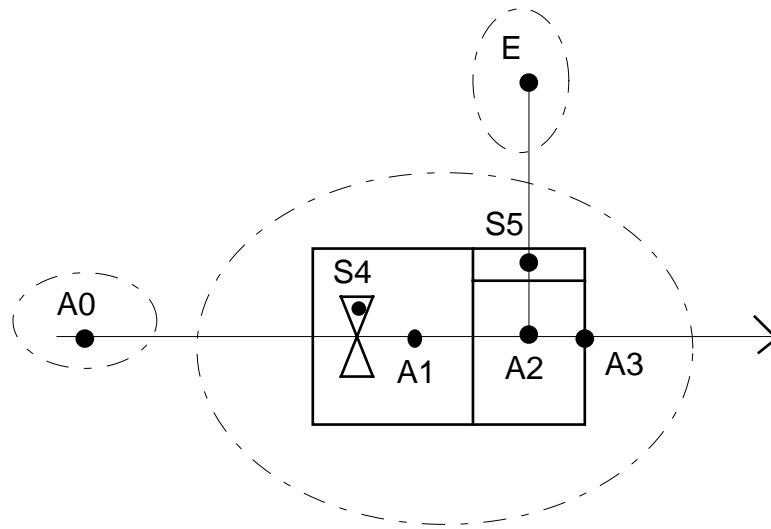


Figure 4.2 5-node Model of Fan with Submerged Motor

A type of primitive part, as identified by its number, can be used more than once in a plant component model. Figure 4.2 shows a discretization scheme of a plant component 'fan with a submerged motor'. The fan model is formed making use of 5 nodes (A1, A2, A3, S4 and S5), plus one connecting node A0 and one boundary node E. S4 and S5 are the two solid nodes representing the fan-motor body and the fan casing respectively. A1 is the air node in contact with the fan-motor body. A2 is the air node in contact with the fan casing. A3 is the air node at the fan exit. A0 represents the incoming air and E represents the ambient air node.

This model can be built from the following 5 primitive parts, of which Part No. 4.4 will be used twice and therefore identified separately by 4.4(1) and 4.4(2).

Part No.	Descriptions	Nodes Involved
2.4	Surface convection: with ambient	S5, E
4.4 (1)	Flow upon surface: for moist air (2 nodes)	A0, A1, S4
4.4 (2)	Flow upon surface: for moist air (2 nodes)	A1, A2, S5
5.3	Flow inducer (for all fluid)	A3
10.1	Heat injection: to solid	S4
10.3	Heat injection: to moist air	A1

component matrix template

The matrix template of this fan model is of the following form:

$$\begin{bmatrix} C(1) & 0 & C(2) & 0 & 0 & 0 \\ 0 & C(3) & 0 & C(4) & 0 & 0 \\ C(5) & 0 & C(6) & 0 & 0 & C(12) \\ 0 & C(7) & C(8) & C(9) & 0 & 0 \\ 0 & 0 & 0 & C(10) & C(11) & 0 \end{bmatrix} * \begin{bmatrix} S4 \\ S5 \\ A1 \\ A2 \\ A3 \\ A0 \end{bmatrix} = \begin{bmatrix} C(13) \\ C(14) \\ C(15) \\ C(16) \\ C(17) \end{bmatrix}$$

(4.12)

Table 4.5 Development of Fan Model from Primitive Part Coefficients

Coeff.	PP2.4	PP4.4(1)	PP4.4(2)	PP5.3	PP10.1	PP10.3
C(1)	=		A(44,1)		+ A(101,1)	
C(2)	=		A(44,2)			
C(3)	=	A(24,1)		+ A(44,1)		
C(4)	=			A(44,2)		
C(5)	=		A(44,3)			
C(6)	=		A(44,4)			
C(7)	=			A(44,3)		
C(8)	=			A(44,6)		
C(9)	=			A(44,4)		
C(10)	=			A(53,2)		
C(11)	=			A(53,1)		
C(12)	=	A(44,6)				
C(13)	=	B(44,1)			+ B(101,1)	
C(14)	=	B(24,1)		+ B(44,1)		
C(15)	=	B(44,2)				+ B(103,1)
C(16)	=		+ B(44,2)			
C(17)	=			B(53,1)		

The expressions of the matrix coefficients in terms of the primitive part coefficients are shown in Table 4.5.

The pp indices of the nodes are:

Node	Ni
A1	2
A2	1
A3	1
S4	2
S5	2

It should be noted that the air nodes A1, A2 and A3 of the fan model cannot be combined to form one single node, though physically this is possible in the discretization scheme. If they are combined, the matrix coefficients expressed in terms of the primitive part coefficients will be wrong and therefore an incorrect conservation equation will be introduced in the matrix template. Readers may wish to try this and observe the incorrect mass flow balance in dry air flow. Even combining only nodes A1 and A2 will introduce error such that the air flow rate at the node increases to two times of the actual value. The source of error is the sum of the two identical primitive part coefficient A(44,6) which gives a value of -2.0 rather the correct value of -1.0 for the mass flow coefficient of the connection A0.

Hence a basic rule in the primitive part approach is that a node of any fluid type should not be involved in two primitive parts which are belonging to the category 4 "flow upon surface", except when it appears as a connection in one of the two primitive parts.

Also in this ESP-r type of model, the air mass flow rate can be an input parameter (and therefore is constant in value throughout the simulation) or a variable which depends on the instantaneous operating point of the fan-duct system (and in this case the value is actually solved by the mass flow network solver based on the pressure-resistance relationship at each time-step).

The basic theory of primitive part modelling has been explained in this Chapter. The methodology is illustrated by applying the concept to model several practical air conditioning equipment. While this concept is developed based on the finite difference control volume conservation approach, it will be discussed in the next Chapter that this modelling approach is adaptable to a variety of simulation environments, in particular those more favourable for next generation simulation softwares.

References

Aasem, E.O. 1993. Practical Simulation of Building and Air-conditioning Systems in the Transient Domain. PhD Thesis, Energy Systems Division, Department of Mechanical Engineering, University of Strathclyde, Glasgow, U.K.

Chow, T.T. 1993. "A Plant Component Taxonomy for ESP-r Simulation Environment." In Proceedings of Building Simulation '93, International Conference of the International Building Performance Simulation Association, August, Adelaide, Australia, pp. 429-434.

Chow, T.T. 1995. "Generalization in Plant Component Modelling." In Proceedings of Building Simulation '95, International Conference of the International Building Performance Simulation Association, August, Madison, U.S.A., pp. 48-55.

Hensen, J.L.M. 1991. On the Thermal Interaction of Building Structure and Heating and Ventilating System. PhD Thesis, the FAGO Unit, Eindhoven University of Technology, Netherland.

Laret, L. 1989. "Building and HVAC Simulation: the Need of Well-suited Models." In Proceedings of Building Simulation '89, International Conference of the International Building Performance Simulation Association, June, Vancouver, Canada, pp.199-204.

Ogata, K. 1992. System Dynamics. 2nd edit., Prentice-Hall, Inc.

CHAPTER FIVE

SIMULATION ENVIRONMENTS AND PRIMITIVE PARTS

The working environments of the simulation softwares popularly in use today for instance TRNSYS, HVACSIM⁺, ESP-r, are described in this Chapter. Some of the plant component models in these named softwares will be later on used to validate the primitive part modelling approach. Furthermore, the way that the primitive parts and the plant components built upon them being added to the ESP-r software are explained. Possibility of applying the primitive part concept to other simulation environments including the Object-Oriented approach is also addressed.

5.1 TRNSYS

TRNSYS is a commercial program developed at the University of Wisconsin Madison. It was first made public in 1975. Both mainframe version and personal-computer version are available. This is a transient systems simulation program with a modular structure. A standard library of component models is provided. Users are also allowed to develop their own component models in TRNSYS. The level of detail of a simulation is determined by the components selected to describe the system. (Klein et al. 1990) In TRNSYS each component model can be taken as a 'black box' which requires some prescribed data inputs. Each black box simulates the functionality and internal operations of the representing component using the input data to generate the output data. The component models are basically algorithmic type. Component subroutines range from very complex differential equation descriptions to simple table look-ups. (Urban et al. 1991)

The use of the program begins with the identification of the physical components in a system. If the mathematical descriptions of all system components are checked available, an information flow diagram for the simulation can be constructed. An information flow diagram is a schematic representation of the flow of information into and out of each of the system components. In the diagram, each component is represented as a box. Each piece of information (or variable) required as a pre-requisite to understand the performance of a component is indicated by an arrow directed into the box. Each piece of information as

a solution of the equations describing the component performance is indicated by an arrow directed out of the box. In addition to the physical components, the execution of a simulation requires the insertion of components which are not a part of the physical system. These include the utility subroutines (e.g. data reader, psychrometric calculations, weather generator) and the output-producing devices (e.g. printer, plotter).

TRNSYS identifies the different kinds of components which appear in the information flow diagram by associating a TYPE number with each kind of component. The relation between a component and its TYPE number is determined by the name of the FORTRAN subroutine coded to model that component. Since a simulation may include more than one component of a particular kind, the TYPE number does not always uniquely identify a component in the information flow diagram. The position of each component in the information flow diagram is actually fixed by a unique but arbitrary user-assigned UNIT number. Four types of information flow may exist in the information flow diagram. A component may receive three types of information: INPUTS (those variables vary with time and mostly probably, they are the OUTPUT variables from another component in the system), PARAMETERS (those remains constant throughout the simulation) and TIME (this is handled internally by TRNSYS and normally need not concern the user; the time-step of a simulation is user-assigned). The information flowing from the component is its OUTPUTS.

An information flow diagram of a system may exhibit either recyclic or acyclic flow of information. Recyclic flow occurs whenever there is a path in the information flow diagram formed by the output arrows which leads from a component to one or more other components of the system and then back to the starting component. Acyclic flow occurs if the flow is not recyclic. Figure 5.1 shows an example of an information flow diagram with recycle. Represented in the diagram is a solar hot-water system with seven components. The OUTPUT variable (water flow rate) of the component 'Flow Collector' is controlled by the difference between temperatures θ_i and θ_o , where θ_o is an OUTPUT of the other component 'Solar Collector'. When recyclic flow occurs in a simulation, a numerical technique is needed to find the values of the OUTPUT variables which satisfy the equations of all of the components involved. TRNSYS is programmed to identify such problems should they exist, and if necessary, it uses successive substitution where iteration continues until all of the OUTPUT variables in the recyclic loop converge to within the convergence tolerance.

To model a TRNSYS component of a system, the user must be able to adequately describe the performance of the component mathematically by algebraic and/or differential equations, and identify the INPUTS, OUTPUTS, PARAMETERS, and DERIVATIVES (time dependent variables). For the reason of improving computational efficiency, many of these differential equations in the standard components are

either solved analytically or have been re-written as algebraic equations. Priority has been given to the analytical method, since the numerical method is found to require shorter timesteps and more computation for comparable accuracy and numerical stability. In addition, a choice amongst three numerical methods is offered to the user, namely, the modified Euler method, the original non-self-starting Heun method, and a fourth-order Adams method. The modified Euler method will be used by default.

To perform a simulation, a file known as the TRNSYS Deck is to be created by the user. Included in the deck are three types of control statements: simulation control statements, component control statements, and listing control statements. Simulation control statements direct the operation of the TRNSYS system and define simulation period and error tolerances. Component control statements define the components of the system and their interconnections. Listing control statements direct the output of the TRNSYS processor.

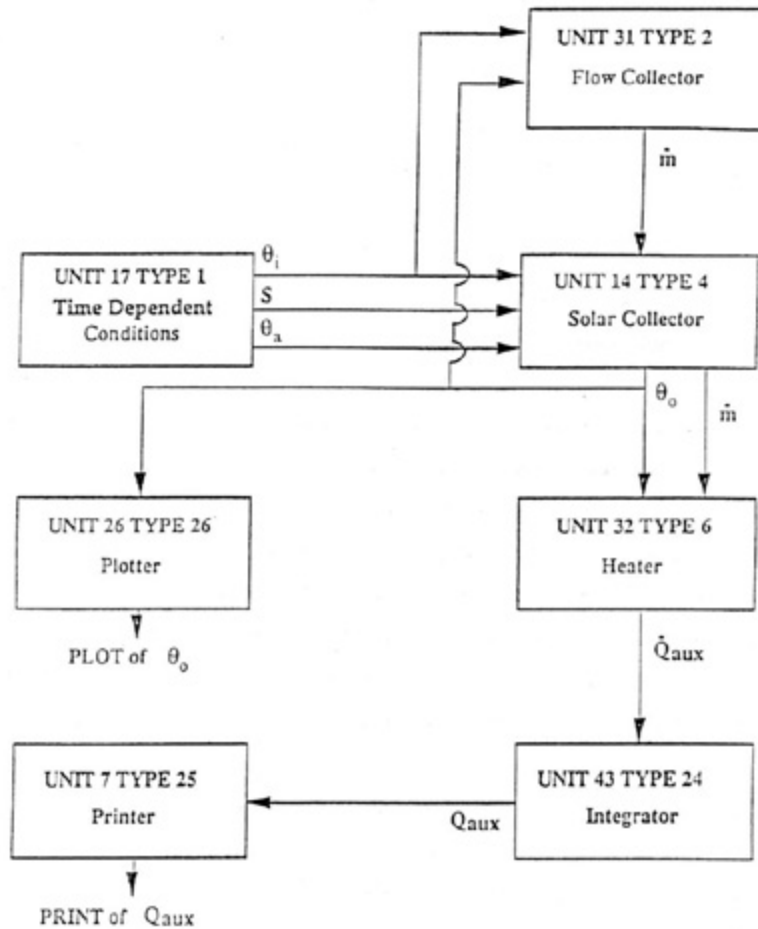


Figure 5.1 Information Flow Diagram with Recycle

5.2 HVACSIM⁺

HVACSIM⁺ is a non-proprietary computer simulation package developed at the National Bureau of Standards (NBS). It was designed to allow detailed simulation of building performance: the HVAC system and associated equipment control, the building shell, and their dynamic interactions. The architecture of HVACSIM⁺ is summarized in Figure 5.2. (Clark 1985, 1985a) The package consists of a main simulation program called MODSIM, a library of subroutines containing mathematical models of building energy system components, an interactive 'front end' program called HVACGEN (which is used to create a description of the system to be simulated), and a program called SLIMCON (which processes the output of HVACGEN and converts it into the form required by MODSIM). MODSIM, which stands for MODular SIMulation, by itself is a general-purpose simulation program, employing a hierarchical, modular approach to solve large sets of non-linear differential and algebraic equations. In principle, MODSIM could be used to simulate any system which can be represented as a set of discrete, interconnected components. Many ideas for the design of MODSIM were borrowed from TRNSYS. The program also uses a TYPE number and a user-assigned UNIT number to identify each component in the simulation. A model definition file informs MODSIM of the number of differential equations in each UNIT of the simulation. Provision has been made in the setup program, HVACGEN, to allow the number of differential equations in a given component to be determined by the values of one or more parameters. Thus different UNITS of a given TYPE may have different numbers of differential equations. The HVACGEN program allows any variables in the simulation to be designated time-dependent boundary variables.

MODSIM uses a simultaneous nonlinear equation-solving package called SNSQ to obtain a self-consistent solution at each time step. Since large scale simulations require simultaneous solution of a large number of algebraic and differential equations and this is prohibitively time-consuming, in MODSIM large sets of equations are partitioned into smaller subsets. Between the entire simulation and individual units, two intermediate levels of structure are defined: BLOCKS and SUPERBLOCKS. A block is simply a set of units, more or less arbitrarily defined by the user. The interconnections among the units in a block define a set of simultaneous equations which is to be solved by the equation solver SNSQ. The user can also view a block as a black box which takes a set of block inputs and produces a set of block outputs. The next level of structure is the superblock, which consists of a set of blocks. Blocks within a superblock are exactly analogous to units within a block. Connections among the blocks in a superblock define a set of simultaneous equations which is again solved by SNSQ. MODSIM then assumes that the couplings among superblocks are weak enough so that each superblock can be treated as an independent subsystem. No simultaneous equations are defined between superblocks. Instead, the equations are solved

sequentially. In this way, the convergence properties of the equation solver depend on the block/superblock structure. This fact limits the flexibility of simulation construction. Some care must be exercised in defining blocks to obtain good convergence properties, particularly when control loops are involved. In general, it is a good practice to have a control loop entirely contained in a single block.

During the course of a simulation, some of the state variables may reach steady state, i.e. cease to vary with time. Such a state variable, if being solved simultaneously, can be 'frozen' by removing it from the set of simultaneous equations. Afterwards, it is monitored so that it can be returned to the calculation (or 'unfrozen') if necessary. Similarly if all the simultaneous equations in a block are frozen, and all its block inputs are frozen, the block is marked inactive. Once a block is inactivated, it is no longer necessary to monitor the frozen state variables in the block. A block is marked active again as soon as one of its block inputs becomes unfrozen. This feature allows a saving of computation time.

The HVACSIM⁺ program allows any variable in the simulation to be designated as a reported variable. The time interval at which reported variable values are recorded in the output file can also be chosen. Different reporting intervals and reported variables may be used for each superblock.

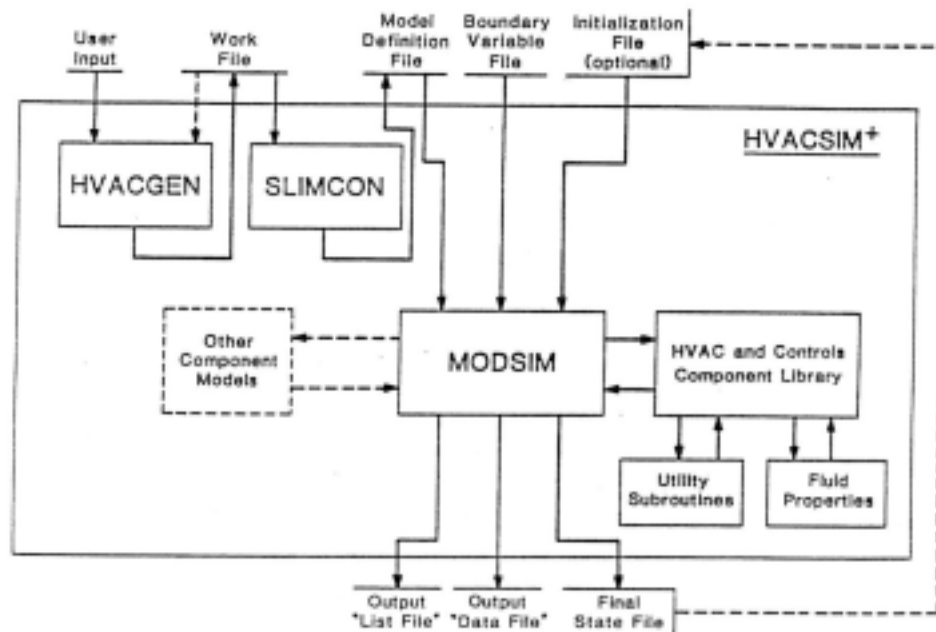


Figure 5.2 HVACSIM+ System Architecture

5.3 ESP-r

As mentioned earlier, the ESP-r software has been chosen as the testing platform of the primitive part theory. Given in this section is a brief description of the software starting from its development history.

The development of the ESP (Environmental Systems Performance) software was commenced in the University of Strathclyde in 1974. Evolutionary changes were taken place since the last two decades. From 1974 to 1977, Clarke (1977) developed the initial prototype as part of his doctoral research. From 1977 to 1982, the software was extensively re-worked from a single-zone model to allow simultaneous multi-zone processing. Between 1982 to 1984 plant and air flow modelling was added together with a move to the low cost Unix™ workstation technology and the installation of expert system primitives. By that time ESP was fully equipped to perform comprehensive energy and mass balance simulations for combined building and plant system when constrained to specified control action. It was then admitted as the European Reference Model for Passive Solar Architectural Design. With the objective of simulating the real world as rigorously as possible, the software is intended for a research orientated environment and the name ESP-r has been used since 1991 to reflect clearly the purpose. The structure of the ESP-r system is shown in Figure 5.3.

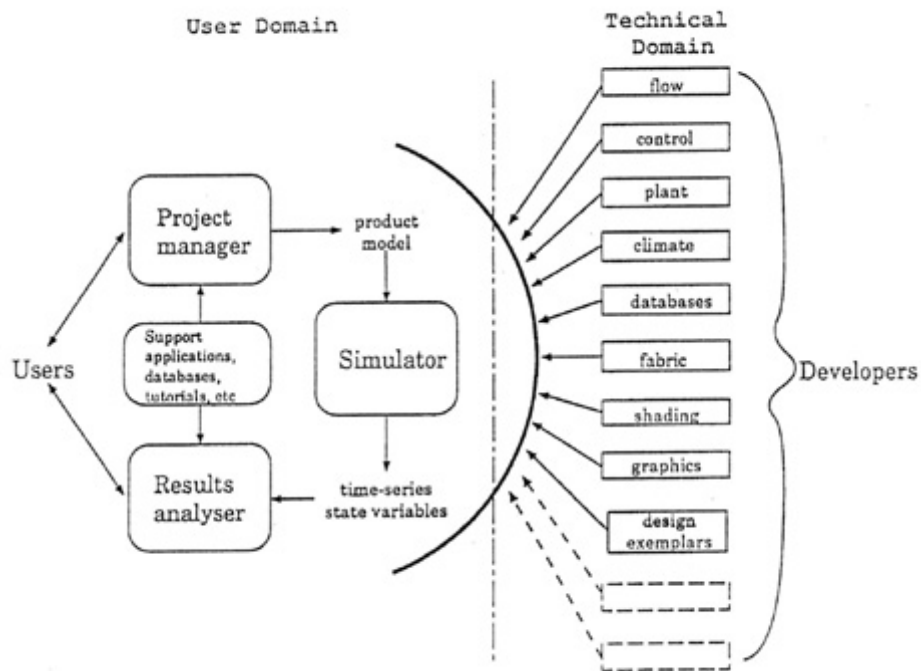


Figure 5.3 ESP-r System Structure

The ESP-r system has been made flexible in that separate simulation runs with building-only or plant-only mode is possible via respectively the BLD or PLT modules. These individual modules can be run together with the MFS module which computes the fluid mass flow quantities according to the pressure conditions at some prescribed physical locations. Alternatively an integrated building-plant-and-flow simulation run can be performed via the BPS module. Detailed descriptions of the ESP-r software structure and the simulation environment can be found in Hensen (1991), Aasem (1993) and ESRU (1995). The following descriptions concentrate on the plant simulation module PLT.

When coming to a plant performance evaluation exercise making use of PLT, the user has to convert his physical plant system into a simulation network making reference to the available components in the plant-database. Within ESP-r, the plant-database (i.e. component library) is a binary, random access file holding plant component descriptions to enable the establishment of the matrix type balance-equation representations. The available types of plant components allow the execution of basic air-conditioning and wet central heating systems simulation. These components can be simple single-node (algorithmic) type, or complex multi-node (numerical) type. The specification of physical components in a network follows a coded reference system similar to the UNIT and TYPE numbers used in TRNSYS and HVACSIM⁺. However, the 'link' concept has been applied in the software that the component are connected at the interface level with fluid type identified, rather than variable by variable as in the case of TRNSYS and HVACSIM⁺. The management module for the plant-database, known as PDB, allows the insertion of new plant components to the database. Such an insertion must go together with the addition of the component routines - the coefficient generators - to the PLT module of the source code and then recompiled. The main function of a coefficient generator subprogram are to find out the numerical values of the coefficients in the matrix type balance equations representing the plant component model, and to determine an appropriate solution scheme for that particular component. It generally consists of 4 sections. The first section updates the state variable values (temperature and mass flow rates) as computed from the plant (equation) solver in the previous iteration step or from the mass flow (equation) solver. The second section reads or computes the static, dynamic and control data (referred as the A-data, B-data and C-data) as well as other additional parameters in need to obtain the matrix coefficients. The third section checks the current component time-constant against the current simulation time step in order to fix a suitable numerical solution scheme by adjusting the implicit-explicit weighting factor (α) for that particular component. Lastly the fourth section calculates the matrix coefficients for passing over to the plant solver. The coefficient generators of the existing plant component library are distributed in three individual files: pcomp1.F, pcomp2.F and pcomp3.F, associated with the checking routines in the file pcomps.F. The function of the checking routines is to examine the user input file before execution to ensure that the types of specified components, their connections and controlled variables are legal in the

simulation environment.

Physical data of any existing plant component can be revised where necessary through the use of PDB, or alternatively stated in a user input file known as the system configuration file. Also specified in this file are the name of the plant-database in use, the plant component types and their inter-connections. Graphics has been incorporated in the latest version. It is allowable to define a plant network which comprises several sub-networks, for example one for a water flow circuit (like a wet central heating system), and the other for moist air flow (like a ventilation ductwork system). It is also allowed to specify the containment information which defines the immediate boundary condition of a plant component so that the component's parasitic heat loss or heat gain can be determined. The mass flow network is to be specified if mass flow simulation is required and otherwise, mass flow balance will be based on the user specified mass diversion ratios. Mass diversion ratio of a link between two plant components specifies the proportion of the total mass flow released from a sending node (of an upstream component) passes onto a particular receiving node (of the current component).

The system control information, where exists, is put into another user input file known as the 'configuration control file'. In the process of creating a new component model, those component variables subjected to control actions are to be clearly defined. So in the configuration control file, control loops can be assigned to these component variables (which will then be determined at real time) with respect to the specified sensor positions and active control laws (for instance on-off, proportional control etc.). In the absence of a control loop assignment to a plant component defined with a control variable, the user specified control variable quoted in the system configuration file will be used throughout the simulation period.

The simulation engine of PLT are those routines in the source file pmatrx.F. Before the time clock advances at the beginning of a simulation process, the plant database is first accessed and the needed data are extracted. At each time step, the setting up (i.e. computing the numerical values of the coefficients) of the three matrices of the energy/mass balance equations is done through a navigation to all required component coefficient generators. The required matrix type under processing is signalled by a process flag known as ISTATS. The three sets of plant matrix equations are solved one after the other, in the sequence of first phase mass flow (ISTAT=2), second phase mass flow (ISTAT=3), and energy flow (ISTAT=1). In this way the set of energy balance equations are linearized since the mass flow rates involved in the energy matrix coefficients can now be taken as known values within an iteration step. The reason for the sequence of solving mass flow before energy is that in general the dependency of energy balance on mass flow rates in the system is much stronger than the other way round and hence this will speed up the overall solution process. This effect however is less obvious in those multi-node models where direct-contact heat and mass transfer (say condensation on various tubings of a cooling coil) takes

place. In such a case, equally strong coupling between heat and water vapour transfer actually affects the interconnecting nodes.

The overall plant energy/mass flow matrices, which by nature come out to be sparse in topology, are solved by successive substitutions with a relaxation factor of 0.5. Each time after the mass and energy matrix equations have been solved in turn, it is checked whether further iteration is necessary by comparing the errors between the most up-to-date solution with the one obtained from the previous iteration (or from the previous time step in case of the first iteration). If either the absolute or relative errors of all state variables are within the user specified tolerance, the results for the future time-row of the current plant simulation time step are then stored as the present time-row values for the following plant time step. The program then proceeds with the next time increment. Otherwise iteration re-starts until an acceptable solution is reached or the maximum number of iteration has been exceeded in a time step.

Simulation results for plant can be analysed using either one of the following two methods. Firstly, the results can be viewed at simulation time using the state monitoring facility. This facility allows the user to monitor not only the plant component nodes state variables, but also zone variables such as air temperature and energy injection. Alternatively the ESP-r results recovery module can be used to extract the required information from a plant result file.

5.4 Primitive Parts Added to ESP-r

In order to test the validity of the primitive part theory introduced in Chapter 4, totally twenty-seven subprograms of the primitive parts have been installed in the PLT module of ESP-r. They are in a library file named pplib.F. Each primitive part forms an independent subprogram in the file. The function of each subprogram is to calculate the matrix coefficients of the primitive part and pass the numerical values to the component coefficient generator that calls upon this subprogram. In addition, the following three files are also created in PLT:

pcomp4.F	-for holding the new plant components created from primitive parts
pcomps1.F	- for holding the checking mechanism of the component models in pcomp4.F
ppsub.F	-for holding generic subprograms and functions to compute parameters or variables required by the above new files, e.g. moisture content of saturated air, heat transfer coefficients, array of fluid temperatures when transport delay is active, cascade time constant, additional thermal properties of fluid like steam etc.

The procedure of constructing a plant component from primitive parts and the subsequent installation in

ESP-r is described in Appendix C.

Table 5.1 A List of Plant Components Constructed from Primitive Parts

<u>Code</u>	<u>No. of nodes</u>	<u>Descriptions</u>
530	4 node	heat transfer tube with transport delay at water side
540	1 node	water/steam flow multiplier
550	1 node	air flow multiplier
560	5 node	fan with submerged motor
570	4 node	water pipe with transport delay
580	4 node	air duct with transport delay
600	4 node	duct electric heater
610	3 node	wet steam tube
620	4 node	steam boiler
630	2 node	steam panel radiator
640	1 node	steam/water flow converger
650	3 node	steam/water flow diverger
660	3 node	air flow diverger
680	1 node	air flow converger

Table 5.1 shows a list of the new plant component models in pcomp4.F constructed from primitive parts. Accompanying the component coefficient generators are the checking routines placed in pcomps1.F. Because checking the correct fluid type connections of the components is part of the function of the checking routines, flow divergers, convergers and multipliers of moist air and water/steam are created individually, though in principle the mathematical representation of the corresponding primitive parts are generically applying to all fluid types. In these multi-node components, cascade time constants are computed at each time step to determine whether the fully-implicit or Crank-Nicolson numerical scheme should be used. A brief description about the concept of cascade time constants of a multi-node component is given in Appendix D. If the cascade time constant defined for a plant component is greater than the simulation time step, the Crank-Nicolson scheme will be used. Otherwise, the fully-implicit scheme will follow. Minor adjustments to the other files are also required to make allowance for the change and additional storage of plant parameters, for performing simulation with 2-phase fluid flow, and for simulation with smaller time steps etc. To cope with these, the fluid types described by the 'first' and 'second' phase mass flows have been conceptually extended. The first phase fluids now refer to the dry air in the moist air stream as well as the liquid state of any pure fluid. The second phase fluids now refer to the water vapour in the moist air stream as well as the vapour state of any pure fluid. Descriptions, data and matrix topology of these 14 component models were inserted to the available plant database.

Simulation runs were then performed to test the validation of the primitive part theory. The results will be discussed in the next Chapter.

5.5 Primitive Parts in TRNSYS & HVACSIM⁺

The pre-selection of input-output variables in traditional component models like those of TRNSYS and HVACSIM⁺ leads to limitations in the actual use of the models. A reason for the pre-selection is obviously the ease of implementation. The black-box approach converts a large problem into a number of smaller problems, each of which can be more easily solved independently. While it has been demonstrated by actual installation that the primitive part concept applies well in the ESP-r system which is a typical modular simultaneous simulation environment, the concept actually can be extended to apply to other modelling environment like TRNSYS or HVACSIM⁺.

It is known that each component model in an input/output environment is described as an equation model along with a single input-output selection. In this sense, a component model in TRNSYS may also be represented by a set of finite difference control volume energy/mass balance equations (or a matrix equation as a whole), which when given the input parameters and variables, can be solved internally to generate the unknown state variables. An equation solver is required for the purpose and the energy and mass flow matrices can be solved in turn. In such a numerical-type component the matrix coefficients can be determined by calling upon a standard library of primitive parts. Subsequently, the numerical solutions of the output variables are passed to the downstream components. Each of the downstream components in the following TYPE routine call can also be solved internally making use of the same equation solver routine. Iterations will be involved in a recyclic flow scheme but the process will be exactly the same as if the components are of algorithmic type. Due to its numerical strategy, HVACSIM⁺ makes relatively few TYPE routine calls per unit of simulation time. In HVACSIM⁺ the sets of equations of a plant component built from the primitive parts can be solved either at the UNIT level or at the BLOCK level.

In the above arrangements the benefit of applying the primitive parts to allow flexible selection of energy and mass flow paths and to provide a coherent mathematical structure of component models still can be maintained. Nevertheless, the limitation is that the component models developed in this manner could not be interchanged among simulation environments because each environment employs its own semantics and syntax for model expression and interconnection. Without some form of standardization of component model definitions, the desired portability and hierarchy in model structure will be provided, at most, within modeling environments, but not between them.

A more desirable way of implementation will be to develop the primitive part concept in a library of standardized models which can be easily transported to any simulation environment. This can be achieved through the Neutral Model Format (NMF) and making use of automatic translation softwares. The view is explained below.

5.6. Primitive Parts in Neutral Model Format

The NMF was first proposed at the Building Simulation '89 conference in Vancouver, Canada (Sahlin & Sowell 1989). The basic objective is to provide a common format of model expression for a number of existing and emerging simulation environments. All of these environments are component-based. Hence, they are similar in that user defined mathematical models of components are expressed in separate modules that the user can interconnect as needed to define the system network. A typical component model for any of these simulation environments can be expressed as a system of ordinary differential and algebraic equations. The NMF draws on this similarity in order to define a standard source format from which models can be automatically or semi-automatically translated into the specific format of any environment. (Bring, Sahlin & Sowell 1992)

The NMF is "neutral" in the sense that models are expressed in a general manner, rather than in the format of any existing or planned environment. The standardized definition covers only the essential information needed to express a model unambiguously. This information is formalized in order to allow automatic translation to the format of a 'target' simulation environment. A workable translator will therefore comprises two portions. The first portion, called as interpreter, will be the same regardless of the target environment. The second portion, called the generator, is to generate the component models in the format of a particular environment. The interpreter knows the NMF syntax and library format, while the generator knows the syntax and format of the target environment.

Given such a format a number of benefits can be expected. Firstly, a single or several common model libraries can be formed, which will greatly enhance the usefulness of any individual environment. Secondly, informal model communication between users of different environments can be expected to increase and this would bring about higher model quality and usage. Finally, enhanced model and user mobility between environments will allow repeated environment comparisons and thereby provide more accurate information about relative environment performance.

The NMF is based on a few model structuring principles (Bring, Sahlin & Sowell 1992) viz:

- i) continuous models are expressed in terms of equations;
- ii) variables and interconnection links are typed;
- iii) models can inherit properties from ancestors;
- iv) large models must allow hierarchical decomposition;
- v) validation is integrated into the modelling process.

Continuous NMF models are described by a fully implicit differential-algebraic system of equations which

for the general case can be written as:

$$f(x, x', p, t) = 0 \quad (5.1)$$

where f is a vector function of the variable vector x , x' is its time derivative, p a parameter vector, and t the time. Instead of pre-selecting the input-output variables in the equations, the NMF asks for automatic input-output designation in which the equation models are kept separate from input-output selections until the components are actually connected together. This separation is made possible by declaring the equations explicitly. Nevertheless the inclusion of one possible input-output designation (one problem) for each NMF component model is required. There are two reasons for this: firstly, to ensure that the model is well posed for at least one problem, and secondly to make the automatic translation possible for those input-output oriented environments.

It is well aware that components developed via different environments will remain incompatible even when stored in a common library, unless there is a structured way to construct inter-component links. An important mechanism for increased model compatibility is so called the 'typing of interaction variables', i.e. the selection of a set of variables (e.g. dry air mass flow rate, temperature, pressure, humidity ratio etc.) which links through all components. This is handled by making available a number of groups of variable types to suit different levels of component model complexity. In the NMF, all variable types to be used in component models are declared globally. A new component model to be inserted in the NMF library has to stick to one of the already declared variable types.

The NMF originally has adopted a 'flat model' class concept, just like other conventional component based softwares. Later on in order to cope with the emerging object-oriented (OO) simulation environment, a single-inheritance mechanism has been developed. The basic idea is to let models of the same physical components, but with successively increasing level of complexity, inherit properties from less complicated ancestors. For example, a collector model with a link-type including the 3 variables: massflow, enthalpy and relative humidity, would inherit most of its properties from a massflow-enthalpy collector.

It is known that the heart of an NMF model is the EQUATIONS section. All the standard F77 floating point functions may be used here and equations may also refer to user defined functions. As for a ESP-r component model, the set of control volume energy/mass balance equations can be put under the EQUATIONS section for each ISTATS value (1, 2 and 3). The mapping of user provided parameters onto equation model parameters is to be done by algorithms which are stated under the heading PARAMETER PROCESSING. An example of a ESP-r plant component model put in the NMF format can be found in Aasem (1993). Aasem pointed out that the ESP-r system requires a plant component

model be discretised into the finite difference form; the disadvantage of this in NMF is that this will restrict the use of a model only to those environments which support model discretisation and therefore the advantage of having a common model format diminishes. For this reason, the translator should be made capable of converting the finite difference equations into the NMF equation format as in equation (5.1). Accordingly, the plant component models built from the primitive parts can be presented in the NMF form in the very similar way.

In the 'flat' model form of the NMF, a plant component model created by primitive parts can appear as an individual module in the common library. The primitive parts will be in subprograms installed separately as supporting routine, which will be invoked by the plant component modules by the appropriate call statements. The primitive part subroutines will be declared globally and can be called in the EQUATIONS sections of any component model in the library. They will be converted by the translator into a primitive part library in the target simulation environment in case the related component model is to be converted at the same time.

In the OO-extension of the NMF however, each primitive parts can exist as an object. They will be used to create simple component models or sub-parts which in turn will be used as parts of the composite or macro models. Indeed a promising future of the primitive part theory could be in the OO simulation environment in which hierarchical decomposition can be applied through a 'bottom-up' approach. This is described below making use of the product modelling as an illustration.

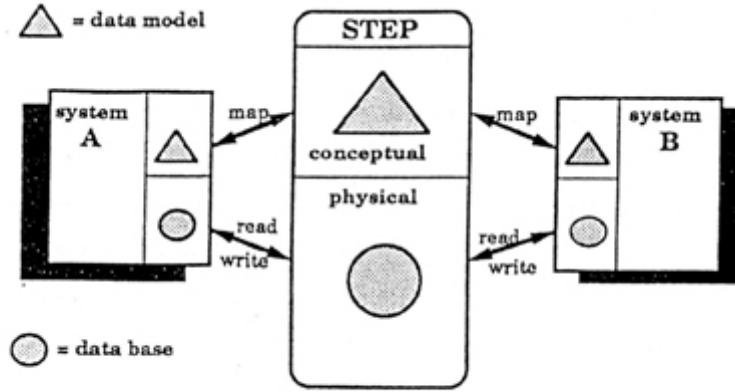
5.7 Product Modelling

A building project requires generating, updating and communicating an enormous amount of data. A comprehensive set of data about the design can be referred as the design object description. This description includes the topology and structure of the object, along with information that is relevant to specific tasks or participants in the design process, for instance data about costs, manufacturing, function, strength, color, tolerances, etc. Traditionally this description is stored and displayed in analog, segmented, and unstructured media. This incurs numerous problems due to the ambiguity, incompleteness, and inconsistency of the information being shared amongst the actors. Here actor is a generic name for anything or anybody playing a role or performing a task in the project. There is a strong consensus in the computer industry that the key to data/design integration is the definition of a complete data model for each product type that will satisfy all actors. A major effort in this direction is the formulation of the 'STEP' standard. STEP, the STandard for the Exchange of Product model data, has been developed for the electronic transfer of engineering information. It is concerned with establishing communication between

different software systems, and is independent of the hardware (Evans 1994; Griffin & Evans 1994). A complete data model generated in this sense is called a 'product model'. An integration based on the product models spans the entire life cycle of the product, i.e. throughout the various stages of design, construction, and operation. The research work has been started since 1983 under the initiative of the International Standards Organization (ISO). The exchange of multiple representations of the design object between computers is critical in an integrated environment since each domain, aspect, and particular simulation tool requires a different representation of the same design object. These different representations of the object are referred as the aspect models. The key to providing a standard that permits an exchange of data is the definition of a central and complete product model, which serves as a reference from which all aspect models can be derived. (Augenbroe & Winkelmann 1991)

The data model is specified in two layers: a conceptual layer (schema) and a physical layer (file or database). (Figure 5.4) The conceptual layer is the exchange reference; it serves as the basis for implementing the physical layer (the neutral format for the storage of data), making possible the actual exchange of the product model data. Recent advances in simulation, computer-aided design, intelligent systems, and information technology raise important expectations for future integrated intelligent building-design systems (IIBDS's). IIBDS's are design aids which cover all stages of building design, offering an intelligent user interface which will help the designer with decision making. Underlying this user interface will be a set of design tools for modelling and simulation which will be able to exchange data and information freely. These tools will cater for all of the design disciplines involved in a building project and will address the problem of managing the interaction of these practitioners. The construction of such systems is a substantial task and will involve research in the areas of Intelligent Front Ends, OO simulation tools and Knowledge engineering, in addition to the application of product modelling techniques to buildings. (Managhan et al. 1991) In Figure 5.4, systems A and B might be two different IIBDS's. If both systems were (independently) developed with the awareness of the emerging STEP standard, there is a fair chance that the exchange of object representations between the systems would be possible without much loss of information content. Obviously both systems would have to supply a STEP translator to make the actual data exchange work. In this way the two systems (addressing different design domains, for example) could be easily integrated.

During the design process, decisions are often made based on an evaluation of the design as it exists at a particular point in time. For example, a dynamic simulation of the building would be required to assess thermal performance as a function of the time-varying exterior weather conditions. In this case, the design system obviously needs to provide access to an appropriate BPE (building performance evaluation) simulation tool.



Figures 5.4 Data exchange between two systems using a product model standard

	Concerned with	Example : Design Object=Office
<i>Design Process</i>	Process Model, which defines: - U-value - operations on U-value	Operation on U-value: " Check heat loss". Heat loss involves calculating U-values of exterior walls.
<i>Design</i>	Design Object, which contains: - wall entities - U-value attributes	Find all components of exterior envelope. Calculate U-values. Calculate heat loss.
<i>Interface</i>	Simulation Request Simulation Result	Request ↑ Result ↓
<i>Simulation</i>	Operations on Discrete Model Aspect Model	BPE Tool
<i>Discrete Modelling</i>	Discrete Model	
<i>Physical Modelling</i>	Physical Model	Fourier's Law

Figure 5.5 Relation between simulation and design

When considering the integration problem between design and simulation, there are two basically different approaches in use by the designers: 'top-down' and 'bottom-up'. In the top-down approach, which is methodology oriented and typically used by architects, the questions asked are when and how to do what, based on what information etc. In the bottom-up approach, which is performance oriented and typically used by consulting engineers, the question is how a particular aspect or component of a building will perform. To be successful, an integration scheme must account for both approaches and provide an interface between them. Figure 5.5 shows the top-down migration of general design knowledge and the bottom-up migration of physical knowledge. The interface layer handles the 'client-supplier' relation by providing the translation of information in the two directions. In the present design practice, this interface operates mainly as a person-to-person communication via exchange of object descriptions (architect gives drawings to engineering consultant), formulation of a design-oriented request (which is cast by the consultant into a simulation input), and description of simulation output (to be translated into the design context by either the architect or the consultant). This type of person-to-person interface is generally cumbersome, time-consuming, and inefficient, and thus performs poorly in everyday practice. The general requirements of the interface are:

- i) for data transfer - the interface has to map design-oriented data to BPE-oriented input;
- ii) for knowledge transfer - the interface has to translate design requests into simulation instructions and translate simulation output into meaningful design rules.

For the top layers in Figure 5.5, better models for the design process is needed. These models will have to provide the purpose, context, and data for specific BPE requests. For the bottom layers, research on the integration of BPE tools and associated validation work are required. Also, additional research is needed to produce better simulation of physical process interactions. It is noted that primitive part modelling can assist in the latter. As each primitive part describes a specific mass and energy transfer phenomenon, its use is not restricted to construct plant component models but can be extended to construct building component models. As a matter of fact, a direct consequence of the primitive part theory is a move of the plant-side modelling approach towards the building-side modelling approach.

It has been pointed out in Chapter 1 that the monolithic, non-modular nature of current-generation BPE tools makes them extremely difficult to adapt to the future needs of designers. Model developers have been investigating new methods of structuring simulation programs. Out of this has emerged the idea of OO simulation environments in which models of arbitrary complexity can be built by linking together calculation objects. In the context of a system simulation tool, primitive parts and the plant component models built upon them are calculation objects at different levels, communicating with one another by messages. Distinction between physical building entities and abstract (equation) entities and how to treat

them in the product model is important in the future development work. (Bjork 1989) To ensure that a unique system configuration information is being shared amongst simulation/design tools, the system modelling function is to be carried out in the local HVAC aspect model. Building related input data will be captured from this aspect model which has direct communication with the central product model through a STEP translator. Other plant input data which are not available from the product model can be obtained through the simulation tool's own user interface. Simulation results will be stored in the local aspect model for further use in the design process. When the designer has reached a system design solution, a report about the chosen system configuration with details of its technical performance can be compiled automatically via the data in the aspect model and at the same time, some restructured design-oriented information will be transferred to the product model for the use of other actors. At any time afterwards, dependent drawings and documentation e.g. system schematic diagrams, commissioning procedures, maintenance schedule can be generated electronically.

In the process as far as the OO simulation environment is concerned, there will be the following features:

- i) a processor links calculation objects together to form simulation models;
- ii) the methods and data associated with an object are encapsulated; i.e. they are internal to the object and cannot, in general, be altered by other objects;
- iii) classes of objects can be defined, then instantiated to create particular instances of an object for use in a simulation model;
- iv) small objects can be assembled in a hierarchical fashion into larger objects (macro-objects or sub-components);
- v) objects and macro-objects can be stored in a library.

This new environment will provide several advantages over the traditional methods.

- i) A broad spectrum of component models can be assembled with a unified mathematical structure, ranging from simplified fewer-node models appropriate to early design, to detailed models appropriate to final design.
- ii) Objects can be reused at a later time for building other models.
- iii) Good graphical interfaces can be constructed for a corresponding hierarchical presentation of a model, where a user first get an overall view of the system and then can zoom down for successively increased levels of detail.
- iv) Energy and mass flow paths can easily be added to a model; incremental model validation can be possible; the internal calculation of an object can be modified without affecting the structure in the rest of the model. These features make models easy to upgrade and extend.
- v) Objects can be shared among different simulation environments if they are expressed in a standard form (i.e. objects in the NMF format), then translated for use in a particular

environment.

This new simulation environment could be imbedded in an IIBDS, so that application models tailored to the design questions as they emerge could be generated in real time, executed to provide answers, and then saved for later use or released at the end of the design session.

In this Chapter, the implementation of the primitive parts modelling approach in the ESP-r software has been discussed, together with the introduction of some other contemporary and emerging simulation environments and the feasibility of applying the primitive parts concept to each of these. The validity of this new approach making use of the ESP-r system as a testing platform will be evaluated in the next Chapter.

References

Aasem, E.O. 1993. Practical Simulation of Building and Air-conditioning Systems in the Transient Domain. PhD Thesis, Energy Systems Division, Department of Mechanical Engineering, University of Strathclyde, Glasgow, U.K.

Augenbroe, G. & Winkelmann, F. 1991. "Integration of Simulation into the Building Design Process." In Proceedings of Building Simulation '91 International Conference of the International Building Performance Simulation Association, August, Nice, pp.367-374.

Bjork, B. 1989. "Product Models of Buildings and Their Relevance to Building Simulation." In Proceedings of Building Simulation '89 International Conference of the International Building Performance Simulation Association, June, Vancouver, pp.193-198.

Bring, A., Sahlin, P. & Sowell, E. 1992. The Neutral Model Format for Building Simulation, Final Report. Department of Building Services Engineering, Royal Institute of Technology, Stockholm, Sweden.

Clark, D.R. 1985. HVACSIM⁺ Building Systems and Equipment Simulation Program Reference Manual. U.S. Department of Commerce, NBSIR 84-2996.

Clark, D.R. 1985. HVACSIM⁺ Building Systems and Equipment Simulation Program Users Guide. U.S. Department of Commerce, NBSIR 85-3243.

Clarke, J.A. 1977. Environmental Systems Performance. PhD Thesis, Department of Architecture and Building Science, University of Strathclyde, Glasgow, U.K.

ESRU. 1995. ESP-r: A Building Energy Simulation Environment. User Guide Version 8 Series, Manual U95/1, Energy Systems Research Unit, Department of Mechanical Engineering, University of Strathclyde, U.K.

Evans, F. 1994. "Why Are We So out of STEP?" Computing and Control Engineering Journal, Vol. 5, No. 3, pp.155-158.

Griffin, C.R. & Evans, F.J. 1994. "STEP Technology for Building Services Projects." Building Services Engineering Research and Technology, Vol. 15, No. 4, pp.205-210.

Hensen, J.L.M. 1991. On the Thermal Interaction of Building Structure and Heating and Ventilating Systems. PhD Thesis, Technische Universiteit, Eindhoven, Netherland.

Klein, S.A. et al. 1990. TRNSYS, A Transient System Simulation Program. University of Wisconsin-Madison, Engineering Experiment Station Report 38-13, Version 13.1.

Monaghan, P.F. 1991. "COMBINE: HVAC-Design Prototype Specification." In Proceedings of Building Simulation '91 International Conference of the International Building Performance Simulation Association, August, Nice, pp.393-401.

Sahlin, P. & Sowell, E.F. 1989. "A Neutral Format for Building Simulation Models." In Proceedings of Building Simulation '89 International Conference of the International Building Performance Simulation Association, June, Vancouver, pp.147-154.

Urban, R.E., Beckman, W.A. & Mitchell, J.W. 1991. "The Development and Support of Public Domain Simulation Software." In Proceedings of Building Simulation '91 International Conference of the International Building Performance Simulation Association, August, Nice, pp.669-671.

CHAPTER SIX

VALIDATION

"Several distinct steps must be followed by the model-developer in forming a simulation model. ... Many assumptions, approximations and compromises are inevitably made at each of these steps. Consequently an exact replication of reality should not be expected. Rather the numerical solutions produced by the model may be shown to be valid over some range and have some specified uncertainty within this range, and that this range is appropriate to the model's subsequent use. ... The aim of model validation is to establish the accuracy of the numerical solutions produced and the range over which the model is valid and appropriate to the domain of its intended use." (Irving 1988)

In this Chapter, validation has a more specific purpose - to verify the accuracy and workability of the primitive part modelling approach in air-conditioning plant components.

6.1 Model Validation Techniques

According to the research initiative at the Solar Energy Research Institute (SERI) in 1983 three complimentary approaches in performing validation have been identified: analytical verification, empirical validation and inter-model comparison (Judkoff 1988). This methodology has further been refined and extended by a UK collaborative research project from the efforts of four British research teams to include (Bowman & Lomas 1985; Jensen & Van de Perre 1991):

- i) theoretical examination of the theory behind the submodels and a thorough inspection of the source code,
- ii) analytical verification involving a comparison of predictions with exact analytical solutions,
- iii) inter-model comparison involving a comparison of the target program with several other programs,
- iv) parametric sensitivity analysis,
- v) empirical validation involving a comparison of predictions with measured data.

Similar but slightly different model validation approach has been raised by the Gaz de France simulationists (Jeandel, Palero & Laret 1991). They identified four types of validation techniques named as numerical, analytical, qualitative and experimental. Figure 6.1 gives a classification of the simulation

world which has been described in Chapter One, showing the action of each of these types of validation techniques. A brief explanation of the terms are given below.

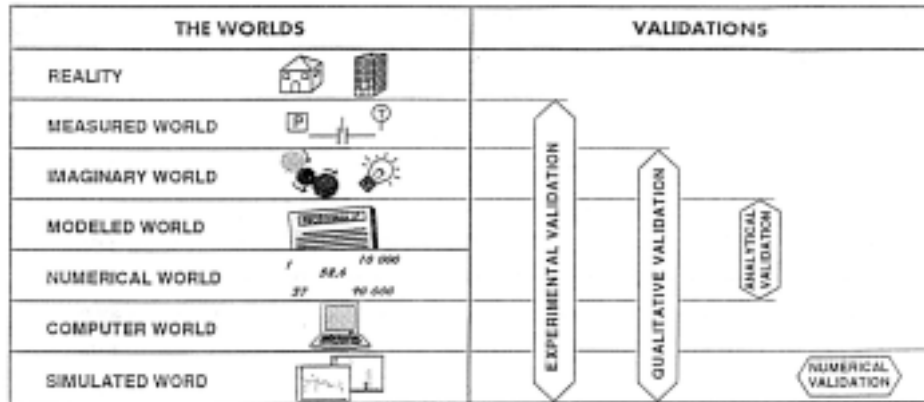


Figure 6.1 Simulation World and Validation Techniques

In analytical verification, the predictions of a model are compared with known exact solutions for simple test cases. Analytical tests may be used to measure the effect of discretization and roundoff errors on the algorithm and its boundary conditions. The response of simple systems to a step change or sinusoidal input is compared against a truncated series solution for the simple system.

Empirical validation involves the comparison of a model's predictions with the measured plant performance. This is one of the most powerful amongst the tools available because it provides a direct measure of truth of the simulation model against reality. Good experiment design and planning are required so that necessary data is available in terms of scanning interval, location and accuracy of sensors etc. (Jensen 1993).

In inter-model comparison, a component or system is modelled using different simulation programs and their predictions are compared. The method gives no indication about either the accuracy of a given model or the possible source of the observed differences; they simply indicate differences between models.

Numerical validation is the comparison of simulation results of a single model run on two different programs. This is used to compare 'simulation software' more than 'the model itself'.

Qualitative validation is the comparison of simulation results with the modeller's mental picture of reality. This is used to ensure that the modeller has really modelled what he intended to model and that the right phenomena have been taken into account.

6.2 Validation of Flow Conduit Model

A 4-node insulated water pipe model (Code 570) built from primitive parts, as described in Section 4.1 and Section 5.4, has been added to the ESP-r software. In this pipe model, the pipe wall is represented by 2 nodes each representing the inner and the outer solid layers. This is usually the case for a pipe with thermal insulation. For the use of this model to represent a bare pipe, one simple way to do so is to regard the two layers of the model as having the equal mass as well as the identical material properties. This was the way used in the validation exercises described underneath.

Three different types of validation tests: analytical comparison, inter-model comparison as well as experimental validation had been performed. The aim has been to test the application of the primitive part concept on a flow conduit model incorporating with a numerical transport delay subprogram. Simulation runs were performed firstly on a small computer program developed via Personal Computer (PC) and then later on the component model was developed in the ESP-r system.

6.2.1 Comparison with analytical solution

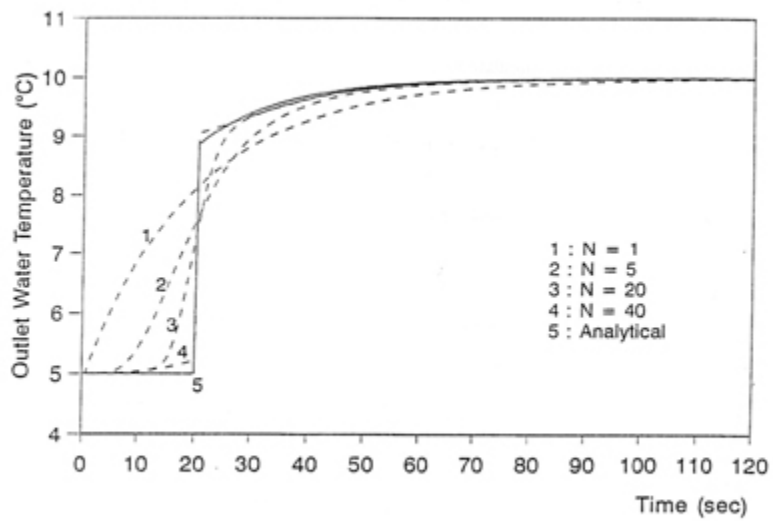
Technical data of a hypothetical but practical water pipe is shown in Table 6.1, in which the flow conditions of four separate simulation tests are also outlined. Figure 6.2(a) shows some time-domain simulation results of Test No. 1. This is a sensitivity test about the division of pipe length, i.e. the use of equation (3.13) in the transport delay calculations. With a steady flow velocity of 0.5 m/s, the transient response of the water outlet temperature as a result of a unit step change in inlet temperature from 5°C to 10°C was simulated. For a 10 m long pipe at this flow velocity, the transport lag is 20 seconds. The analytical solution worked out from equation (3.11) is used for comparison, in that in response to a step change of the inlet water temperature at $t = 0$ second, the outlet water temperature as a function of time was worked out to be

Table 6.1 Technical Data of Water Pipes in the Simulation Runs

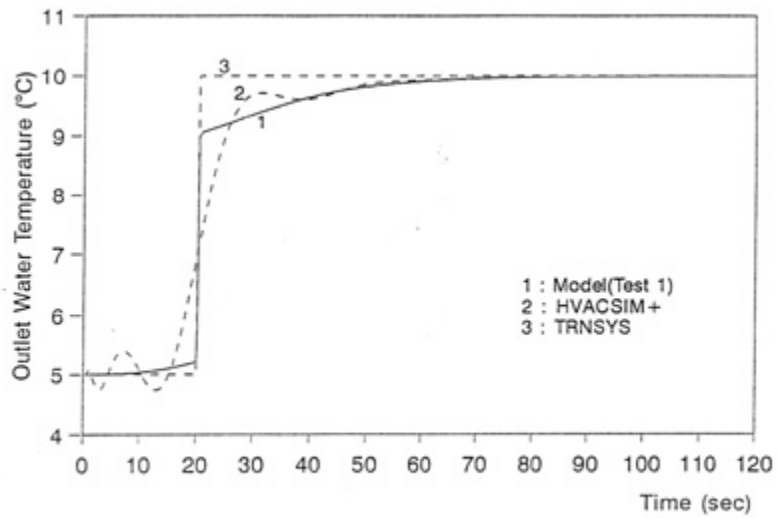
	Hypothetical Test Pipe		Laboratory Test Pipe	
Manufacturing Data				
D_i (m)	0.1		0.02	
Y (m)	10.0		3.0	
M_c (kg)	128.6		5.652	
C_c (J.kg. $^{\circ}$ C)	460		460	
A_o (m 2)	3.456		perfectly insulated	
Test Data				
Test No.	1	2	3	4
Domain	Time	Frequency	Time	Frequency
u (m/s)	0.5	0.5	0.5	0.5
h_o (W/m 2 . $^{\circ}$ C)	2.34	12.0	perfectly insulated	
θ_a ($^{\circ}$ C)	5.0	30.0	-	-
θ_f ($^{\circ}$ C)	5.0 to 10.0	5.0 - 10.0	14.2 to 23.2	16.0 - 23.0
Function	Unit Step	Sinusoidal	Exponential [#]	Sinusoidal
Note: # - experimental data used in the input file				

$$\theta_f(10,t) = 5.0 + 4.9975U(t - 20.012) - 1.1814U(t - 20.012)e^{-0.0678(t-20.012)} \quad (6.1)$$

The rationale of equation (3.13) of dividing the conduit into sections of length approaching δy , i.e. $N=Y/\delta y$ (with numerical truncation during simulation), is hereby justified when several sets of simulation results were obtained using the same time step of 0.5 second and with the section length as the only varying parameter. The family of curves in Figure 6.2(a) covers the extremes where the section length varies from Y (equal to 10 m; i.e. no transport delay; $N = 1$) down to δy (equal to 0.25 m; i.e. the distance travelled in a unit time step; $N = 40$). These were obtained by specifying the arbitrary value of N in the coefficient generator of this pipe model in the source file, before the transport delay subprogram was called. It can be seen from the results that without transport lag ($N=1$), the response is basically a first order system. With transport lag the response is second order - this is indicated by the 'S' shape of the response curve. As the section length approaches δy , the response curve shifts towards the analytical solution worked out from equation (6.1).



(a) Sensitivity Test



(b) Inter-model Comparison

Figure 6.2 Simulation Results of Test No. 1

6.2.2 Inter-model comparison

Component models of two popular simulation softwares TRNSYS and HVACSIM⁺ are used in the inter-model comparison exercises. Figure 6.2(b) compares the Test 1 result (N=40) with the solutions from the TRNSYS Component Type 31 'Pipe or Duct' and the HVACSIM⁺ Component Type 2 'Conduit (Duct or Pipe)', all based on the same technical data listed in Table 6.1. Also the same simulation time step of 0.5 second has been used. Slight oscillations can be observed on the HVACSIM⁺ curve. This indicates a side-effect of polynomial fit used in the HVACSIM⁺ transport delay model (Clark et al. 1985). In the case of the TRNSYS model (Type 31), the immediate jump to the final outlet temperature is a direct consequence of neglecting thermal capacitance of the conduit wall (Klein et al. 1990). The results from the primitive parts model 570 appear to be more superior.

Figures 6.3(a) and 6.3(b) show the frequency-domain comparisons by a Bode diagram (Ogata 1992) using the Test 2 results in Table 6.1. The analytical solutions were obtained from the equation (3.10) by substituting $j\omega$ for s and $y=10$ in that the equation becomes

$$H(10, j\omega) = e^{-20j\omega} e^{\left[-0.2702 \left(1 - \frac{0.9908}{1+12.7918j\omega} \right) \right]}$$

..... (6.2)

The logarithmic representation of the Bode plots allows the display of both the low- and high-frequency characteristics in one diagram. Expanding the low-frequency range by use of a logarithmic scale for the frequency is very advantageous since characteristics at low frequencies are most important in practical systems. The two Test 2 curves (amplitude-ratio and phase-shift) by primitive parts are found close to the analytical solutions throughout the frequency range as shown. As expected, both HVACSIM⁺ curves depart from the analytical solutions at high frequencies; this is again because of the limitation of the fifth-order polynomial fit. For phase-angle shift, the TRNSYS results match the analytical solution. For amplitude ratio, a deviation of the TRNSYS results can be observed. There could be two error sources for this deviation. Firstly, the Type 31 model, which neglects thermal capacitance of the pipe wall, is an over-simplification - in this simulation exercise at least. Secondly, there is a constraint in this model of limiting the maximum number of fluid segments to 25 and this is inadequate for very fine time step simulation. Overall speaking, the comparisons indicate that the pipe model constructed from primitive parts and incorporated with the numerical transport delay scheme can give more accurate predictions, in particular when there are rapid disturbances in the incoming water temperatures.

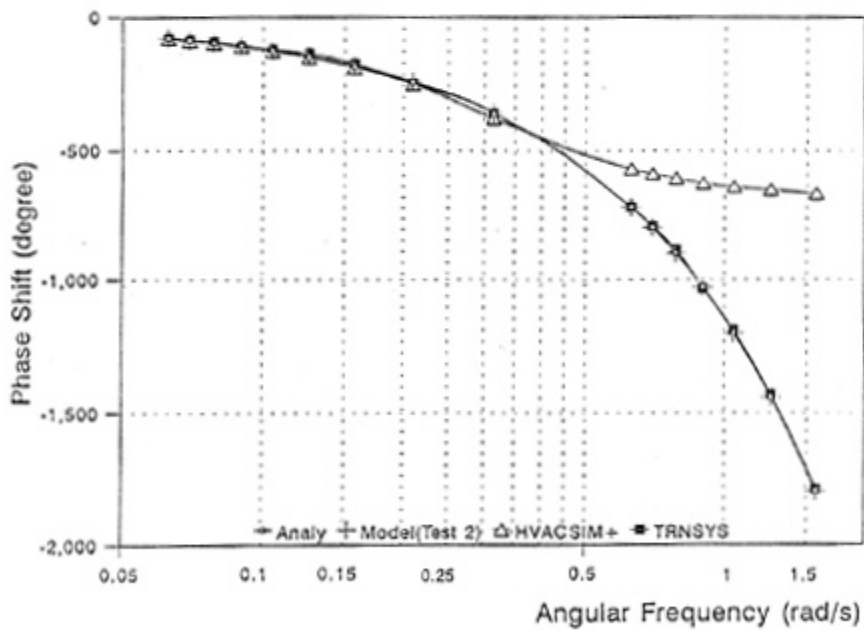
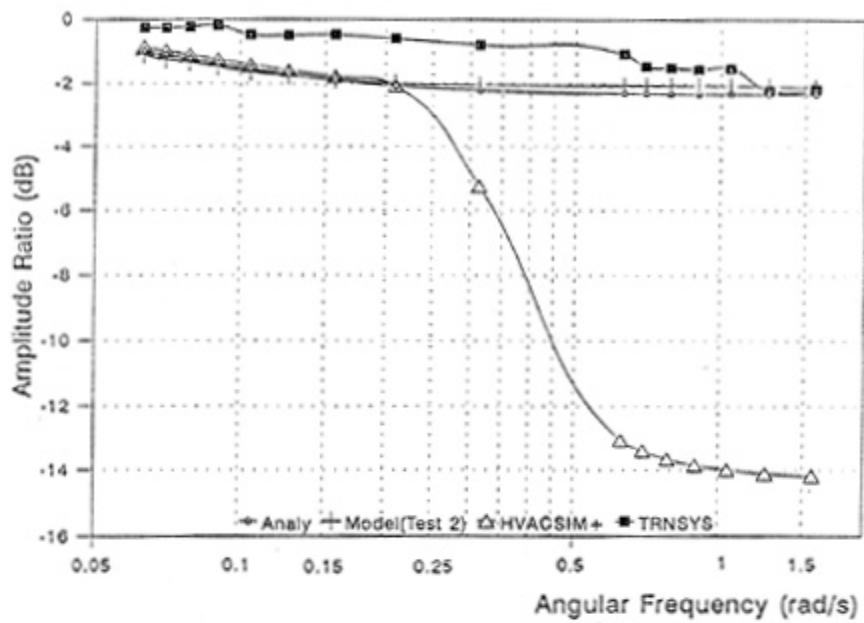


Figure 6.3 The Bode Diagram of Test No. 2 Results

6.2.3 Experimental validation

Experimental validations were carried out by comparing the primitive parts simulation results with the experimental results available from the laboratory work performed by the Mechanical Engineering Department of the University of Hong Kong. A brief description of the test rig and the test procedures are given below.

The general layout of the test rig is shown in Figure 6.4. Three well insulated galvanized iron test pipes each of diameter 15, 20 and 25 mm were installed. Water was delivered to each test pipe from two insulated water tanks via a centrifugal pump and interconnected pipework. The supply water temperature was controlled by a variable mix of water delivered from these two tanks via individual solenoid valves. Water stored in one of the tanks was kept at room temperature, and in the other at a lower temperature governed by a chilled water circuit. Water flow rate was adjusted via the manual valve and measured by either of the two "Platon" flowmeters of different measurement scales. Water temperatures at individual pipe inlet and outlet were measured by two K-type thermocouples which are at a separation of 3 metres. Time-series electronic temperature signals were stored in a data logger for future analysis.

In this data logger, an in-house computer program had been developed to control the on-off sequence of the solenoid valves, and hence vary the supply water temperature according to a pre-defined temperature profile. Three modes of test programs can be generated through this data logger: the step mode, the square wave mode, and the pseudo-random mode. Because of the thermal capacitance of, as well as the energy dissipated at, the equipment/instrument (i.e. pump, flowmeters etc.) between the two solenoid valves and the pipe inlet thermocouples, the temperature profile at the pipe inlet as recorded was not the same as the one pre-defined. For this reason, the step mode introduced an "exponential-like" temperature profile at both the pipe inlet and outlet, and in the case of the square wave mode, a "sinusoidal-like" pattern.

Figure 6.5 shows a set of measurements (curves 1 and 3) of the step mode based on the Test 3 data in Table 6.1. The experimental result indicates an exponential rise of temperature at the pipe outlet similar to the inlet curve but with a time lag. Time-variant inlet temperature data from the data logger was transformed to an input file and a computer simulation was then performed using the pipe model developed via PC. It can be seen from Figure 6.5 that the simulation results are close to the experimental result.

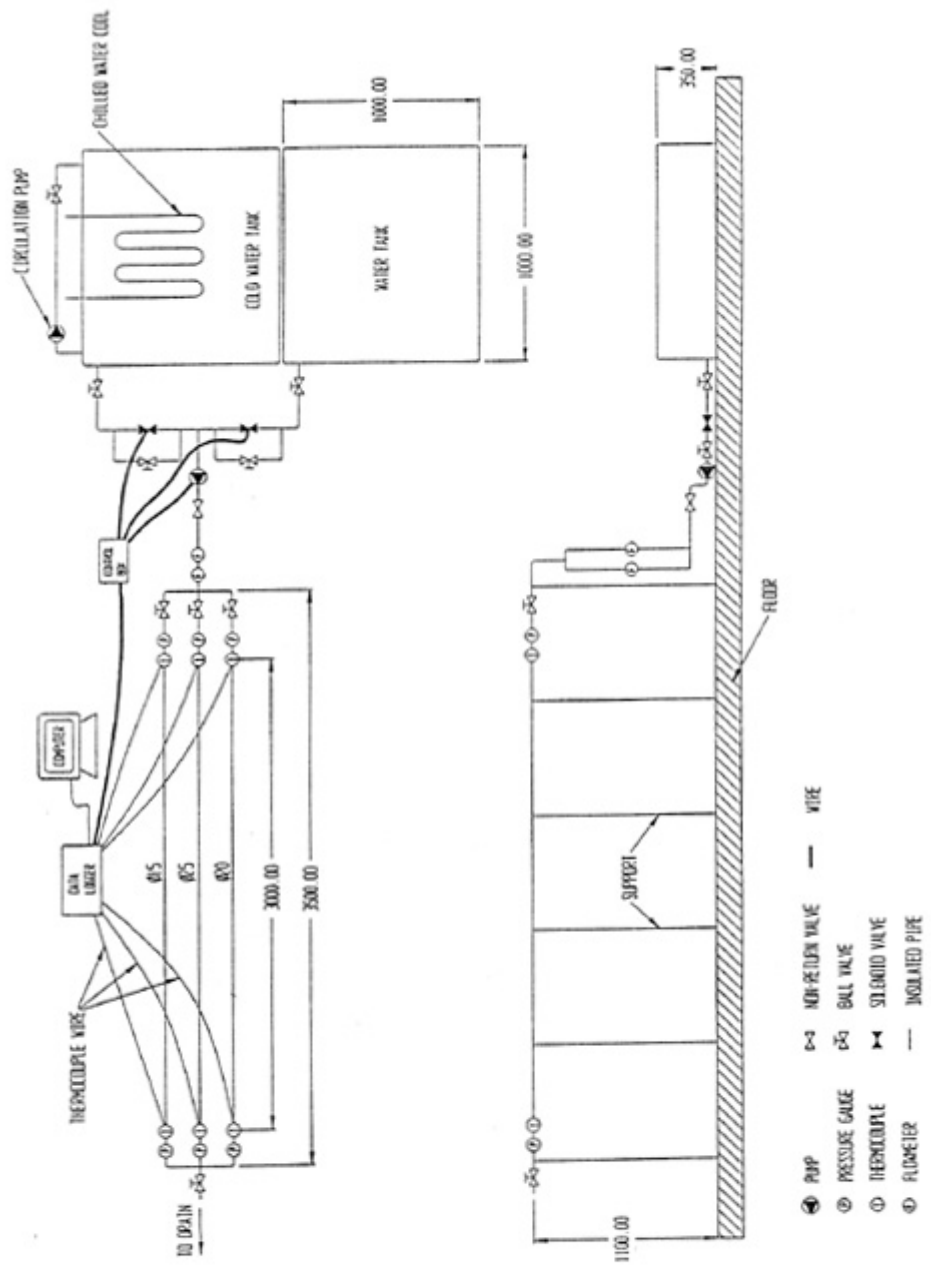


Figure 6.4 General Layout of Laboratory Test Rig

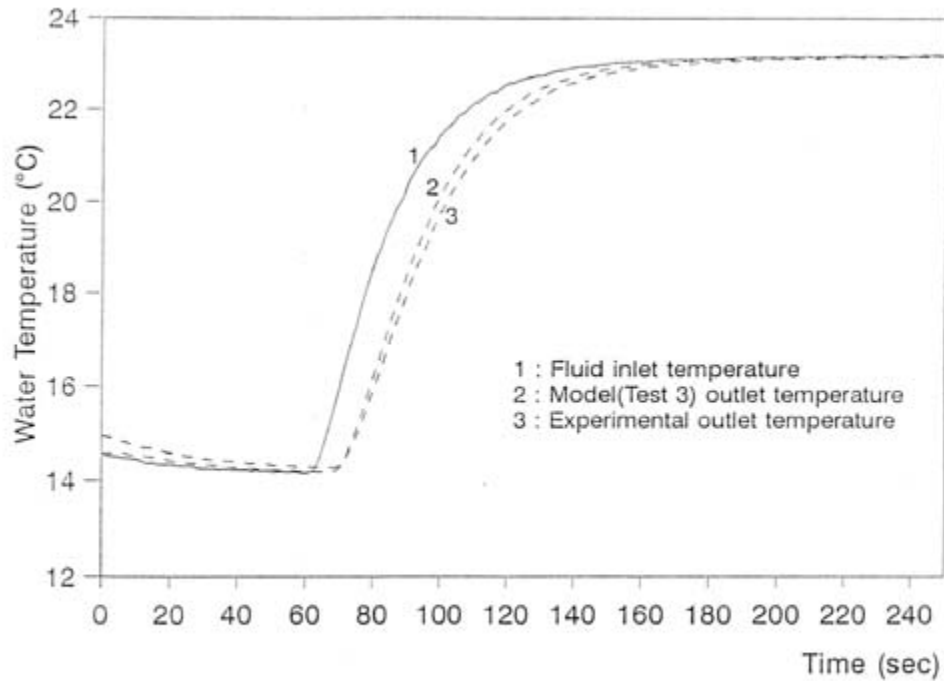


Figure 6.5 Experimental Validation in Time Domain

In the case of the square wave mode (Test 4), the comparison was done through frequency analysis based on the fact that the experimental data both at the inlet and outlet of the test pipe were approximately sinusoidal. The results in the form of a Bode diagram are shown in Figure 6.6. The simulation results are again close to the analytical solution. The amplitude-ratio of the experimental results is generally lower than the simulation results with an average error around 10% in real amplitude term. The results of phase angle shift nevertheless are found closely matched.

The above validation work, including a mix of analytical, inter-model and experimental comparisons, have verified the primitive part theory as applied to a flow conduit model, and also the accuracy and robustness of the new numerical transport delay model earlier introduced in Chapter 3. In the next section, the verification is extended to a cooling coil model where both heat and mass transfer take place at the same time.

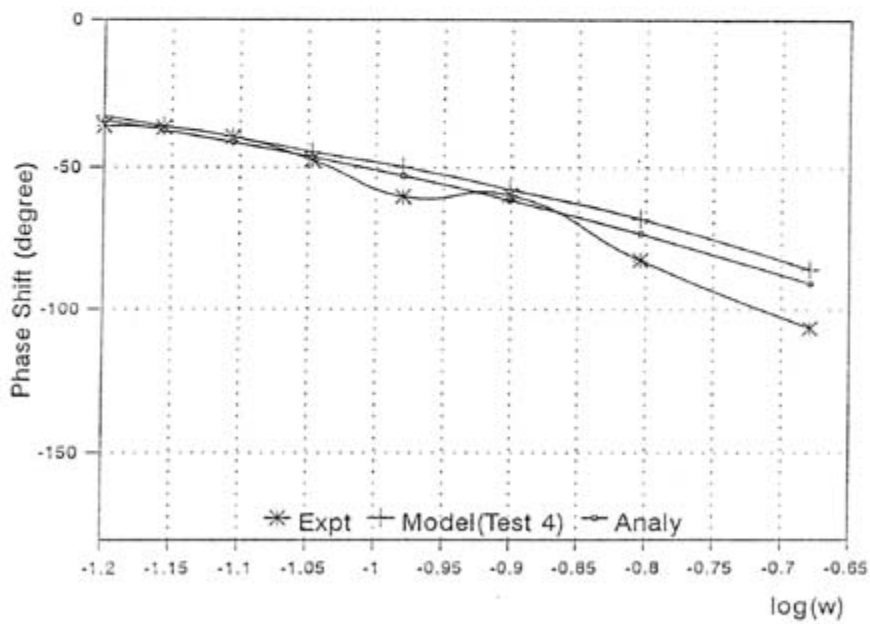
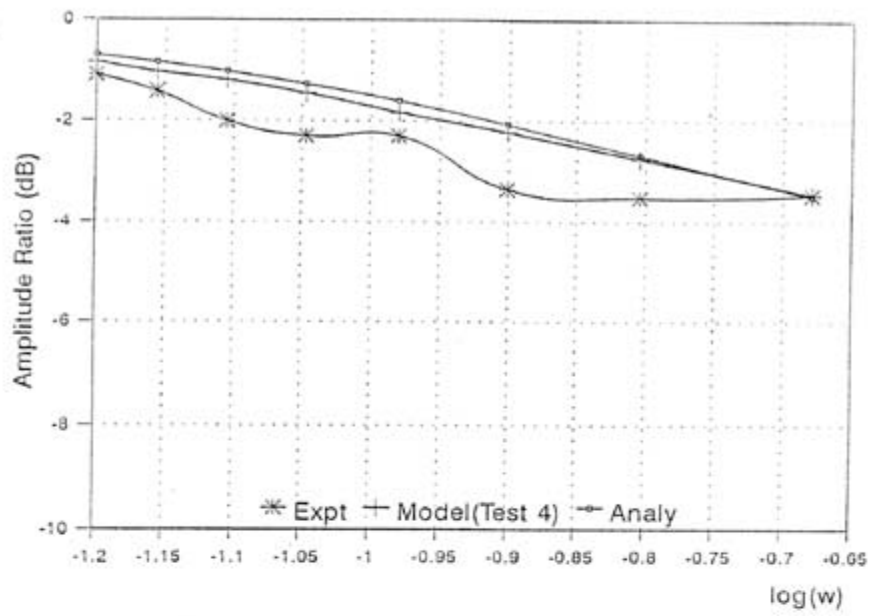


Figure 6.6 A Bode Diagram of the Test No. 4 Results

6.3 Validation of Cooling Coil Model

6.3.1 Inter-model comparison

A 4-node heat transfer tube component (for air-to-water heat exchange) was described in Section 4.3.2 and this component model (code 530) has been added to the ESP-r plant database. It has been shown that this component can be made use of to model a cooling coil explicitly. The validation tests carried out include both sensible cooling and latent cooling performance using realistic flow rates and temperature conditions. Coil data, as shown in Table 6.2, has been based on physical dimensions of a manufactured 4-row coil as well as the common thermal and material properties. In the ESP-r system configuration file, a 4-row counter-flow cooling coil with 36 passes was formulated by suitably connecting 4 heat transfer tubes in a counter-flow arrangement, and associated with 4 flow multipliers to adjust the air and water flow rates to those of a single circuit within the coil.

Based on these data sets simulation runs were executed on this coil model, hereafter called as the PP coil model, as well as three other well-established cooling coil models for comparisons. These three included the HVACSIM⁺ Type-12 which is based on the work of El-Mahdy and Mitala, ESP-r Code 400 which is based on the IEA bypass factor approach, and the TRNSYS Type-32 which is based on the Steocker empirical model developed in the 1970s. The results of the Type-32 model were from ESP-r since the model has been installed and validated in the ESP-r system by Aasem (1993). For the PP coil the dry surface air- and water-side heat transfer coefficients were the same as those in the ESP-r Type-400, and here described respectively by the equations (2.17) and (2.35). For wet surface, the equation (2.20) was used to relate the dry and wet surface heat transfer coefficients. The fin efficiency was determined by the equation (2.22). The simulation time step was 0.1 second.

6.3.2 Sensible cooling

A step change of chilled water flow rate was made for observation of the transient behaviour of the cooling coil. The coil inlet conditions were:

Table 6.2 Cooling Coil Physical Data

Configuration	counter-flow horizontal tubing with continuous flat plate fins	
Material of tube	copper	
Material of fin	aluminium	
No. of rows	4	
No. of tubes per row	36	
Tube array	rectangular	
<u>Basic parameters</u>		
Tube outside diameter		0.0127 m
Tube inside diameter		0.01185 m
Tube face spacing		0.033 m
Tube row spacing		0.033 m
Coil face width		1.03 m
Coil face height		1.20 m
Coil depth		0.132 m
Fin thickness		0.0002 m
Fin spacing		0.00225 m
No. of fins on face width		458
Density of tube		8900 kg/m ³
Density of fin		2700 kg/m ³
Specific heat of tube		0.385 kJ/kg.K
Specific heat of fin		0.880 kJ/kg.K
Thermal conductivity of tube		0.386 kW/m.K
Thermal conductivity of fins		0.204 kW/m.K
<u>Derived parameters</u>		
Total no. of tubes	144	
Fin height		0.01236 m
Equivalent circular fin diameter		0.03742 m
Hydraulic diameter of finned-tube		0.002738 m
Air side face area		1.2360 m ²
Air side free flow area		0.6928 m ²
Primary surface area		5.391 m ²
Secondary surface area		128.39 m ²
Total air side heat transfer area		133.8 m ²
Total water side heat transfer area		5.5217 m ²
Mass of encapsulated water		16.366 kg
Mass of tube		21.635 kg
Mass of fin		34.66 kg
Thermal capacitance (mass-capacitance) of coil		38.83 kJ/K
Thermal resistance of finned tube		0.00002761 m ² .K/W

Moist air inlet

temperature : 26.0 °C DB
moisture content : 0.007 kg/kg dry air
mass flow rate : 2.1 kg/s

Chilled water inlet

temperature : 12.0 °C
mass flow rate : from 1.5 kg/s step change to 0.6 kg/s

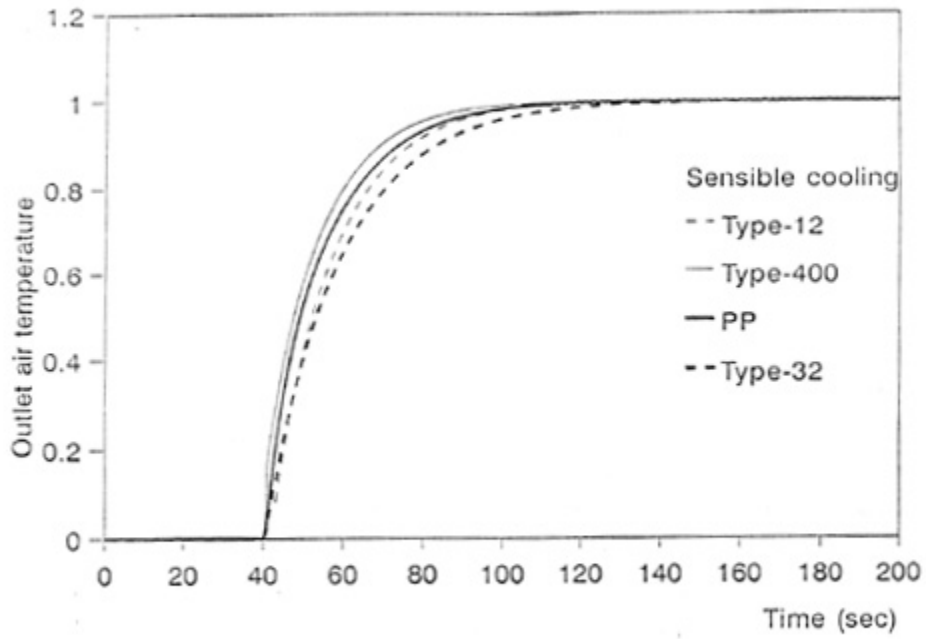
Surface effectiveness : 0.795

The coil outlet temperatures after the steady state had been reached were shown in Table 6.3. The stable simulation results of the PP model were obtained by re-adjusting the absolute allowable error of iteration to a small value and the relative error waived. It can be seen that the outlet temperatures of both air and water are close for PP, Type-12 and Type-400. The results from the empirical model Type-32 is relatively deviated.

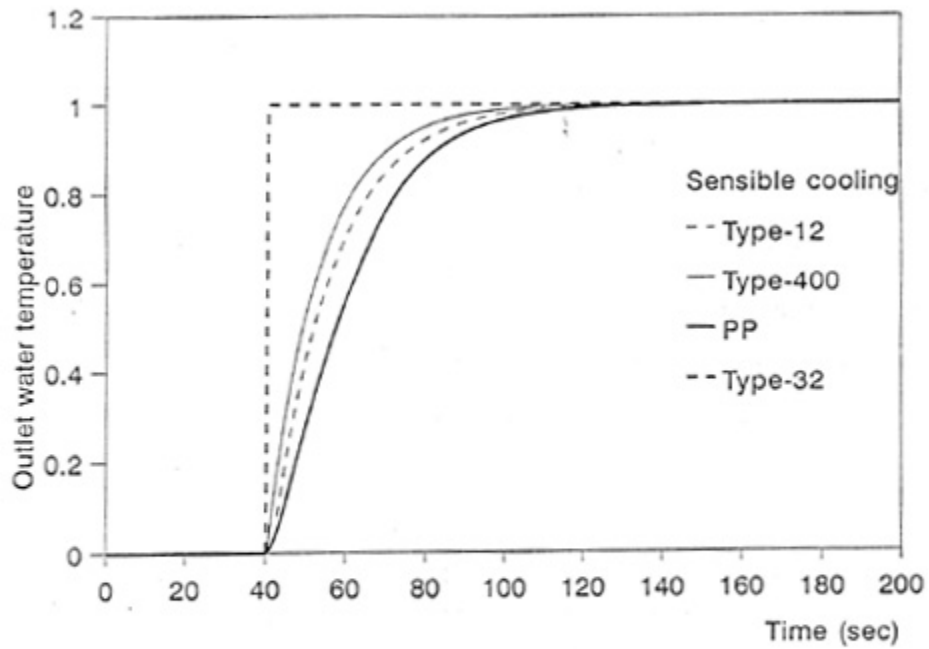
Table 6.3 Comparison of Steady State Results under Sensible Cooling

	PP	Type-12	Type-400	Type-32
Moist air outlet temperature (°C)				
before the step change	15.9	15.5	15.1	18.1
after the step change	18.3	18.0	17.9	19.3
Water outlet temperature (°C)				
before the step change:	15.1	15.6	15.7	14.7
after the step change	18.3	18.8	18.9	17.7

The dynamic responses of the outlet temperatures under the step change were determined and the normalized results are shown in Figure 6.7(a) and 6.7(b) for air and water respectively. In the case of air, all the curves are close. In the case water temperature the curves spread slightly wider. Type-32 shows a step change in outlet water temperature and this is because of an imperfect assumption used in the modelling algorithm and can be ignored.



(a) Outlet Air Temperature



(b) Outlet Water Temperature

Figure 6.7 Inter-model Comparisons of Dynamic Responses under Sensible Cooling

6.3.3 Latent cooling

Two test runs were performed: one with a step change in mass flow rate of the moist air stream and the other a step change in inlet water temperature.

change in air mass flow

The coil inlet conditions were as follows:

Moist air inlet

temperature : 24.0 °C DB
 moisture content : 0.012 kg/kg dry air
 mass flow rate : from 2.85 kg/s step change to 0.95 kg/s

Chilled water inlet

temperature : 11.0 °C
 mass flow rate : 0.9 kg/s

Fin efficiency : 0.737 before the step change
 0.826 after the step change

The coil outlet temperatures and moisture contents after the steady state had been reached were given in Table 6.4. More deviations in the steady state solutions can be observed as compared to the sensible cooling case. This indicates the complexity involved in modelling the moisture condensation process on cooling and dehumidifying coils which affects the accuracy in prediction through computer simulation.

Table 6.4 Comparison of Steady State Results under Latent Cooling with Changed Air Flow

	PP	Type-12	Type-400	Type-32
Moist air outlet temperature (°C)				
before the step change	17.7	18.8	16.0	16.0
after the step change	14.8	13.4	13.2	12.5
Air moisture content (kg/kg dry air)				
before the step change	0.0115	0.0110	0.0114	0.0114
after the step change	0.0096	0.0091	0.0095	0.0091
Water outlet temperature (°C)				
before the step change:	16.6	17.2	17.2	18.3
after the step change	14.7	15.0	13.8	15.8

change in water inlet temperature

The coil inlet conditions were as follows:

Moist air inlet

- temperature : 24.0 °C DB
- moisture content : 0.012 kg/kg dry air
- mass flow rate : 2.85 kg/s

Chilled water inlet

- temperature : from 12.0 °C step change to 8.0 °C
- mass flow rate : 0.9 kg/s

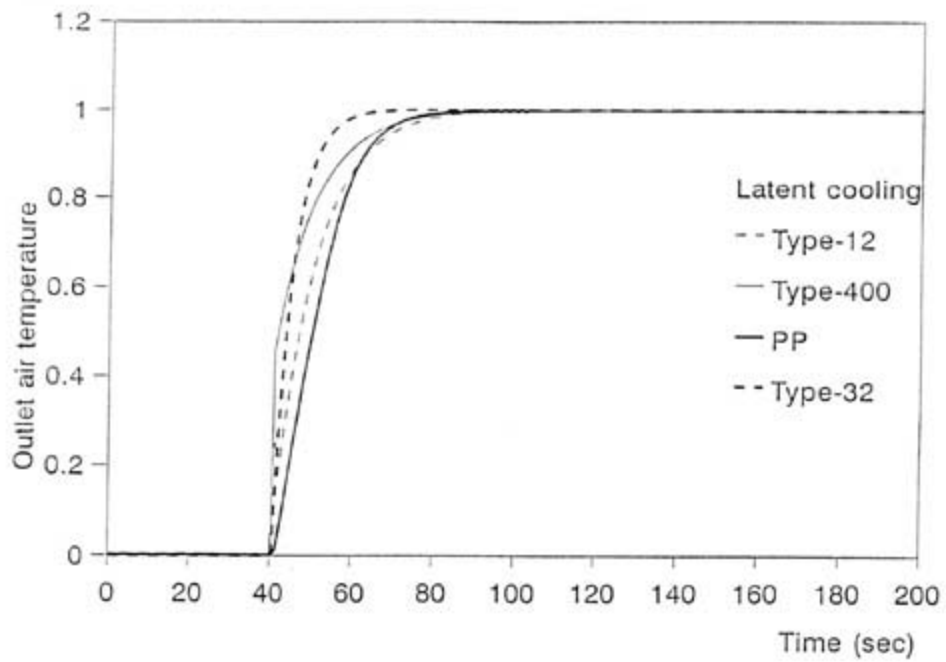
Fin efficiency : 0.745

The steady state solutions of the coil outlet temperature and moisture content are given in Table 6.5. The deviations in results amongst the 4 models are similar to the above case of change in air flow rate above.

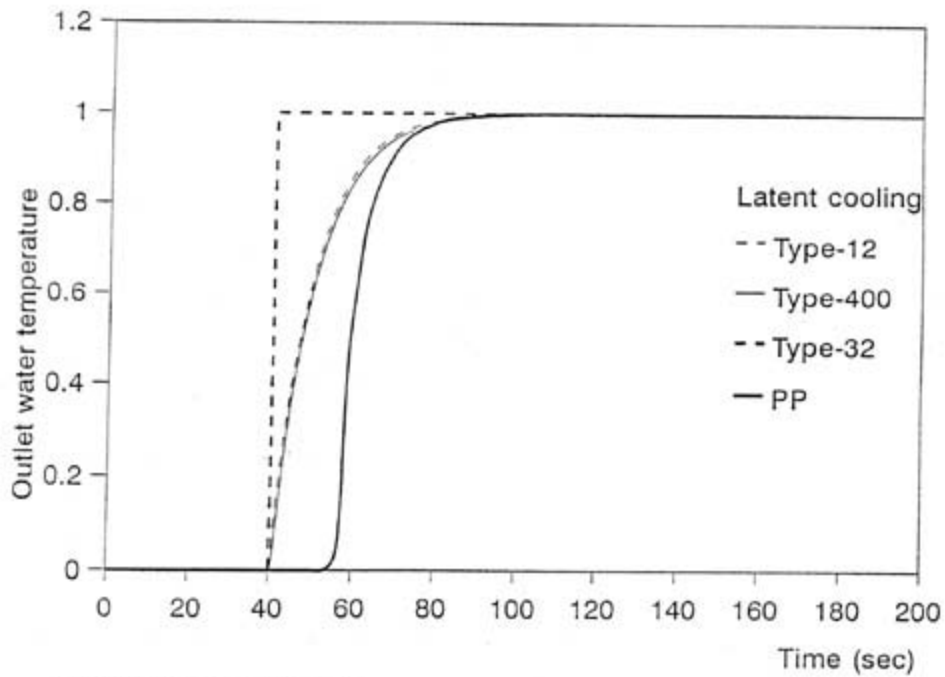
Table 6.5 Comparison of Steady State Results under Latent Cooling
with Changed Water Temperature

	PP	Type-12	Type-400	Type-32
Moist air outlet temperature (°C)				
before the step change	17.9	19.5	16.5	16.4
after the step change	16.9	17.2	14.4	14.9
Air moisture content (kg/kg dry air)				
before the step change	0.0117	0.0110	0.0118	0.0117
after the step change	0.0109	0.0102	0.0103	0.0106
Water outlet temperature (°C)				
before the step change:	17.1	17.5	17.8	18.4
after the step change	15.3	15.7	15.5	17.7

The dynamic responses of the outlet air and water temperatures under the step change were determined and the normalized results are shown in Figures 6.8(a) and 6.8(b). While the air temperature curves show similar response pattern, the PP water temperature curve gives a clear time lag but the others do not.



(a) Outlet Air Temperature



(b) Outlet Water Temperature

Figure 6.8 Inter-model Comparisons of Dynamic Responses under Latent Cooling

It is difficult to give concrete conclusions in inter-model comparisons about which model can produce the best results. One basic purpose of the validation exercise here is to demonstrate that the application of primitive parts on cooling coil modelling is workable. With this in mind then the degree of deviations for various individual cases among the 4 models does confirm the workability of the primitive part approach.

There is at least one aspect that the PP simulation result is much superior than the other three. In the dynamic response of outlet water temperature shown in Figure 6.8(b), it is the only model that gives accurately the second order response in outlet water temperature as observed by Shekar and Green (1970). The dead-lag of around 18 seconds originates from the flush time. It is known that in this simulation run, the water flow velocity in the coil tubings is steady and is given by

$$u_w = \frac{m_{wtub}}{\rho_w \frac{\pi}{4} D_i^2} = \frac{0.9/36}{1000 * \frac{\pi}{4} * 0.01185^2} = 0.2267 m/s \quad (6.3)$$

and the flush time is then given by

$$t_{flush} = \frac{circuit - length}{u_w} = \frac{4 * 1.03}{0.2267} = 18.2 sec \quad (6.4)$$

In an empirical coil model it has been so often that an artificial dead-lag and an artificial time constant (first order) are used to represent the dynamic response of the water circuit. In this PP model the results came naturally from a fundamental approach. Furthermore, since the water temperature response affects the air temperature response, then in Figure 6.8(a) it is more likely that the slower air temperature response predicted by the PP model is closer to the reality.

On the other hand, the PP model can always be improved by a more rigorous nodal scheme, or by using better heat transfer coefficients or mass diffusion coefficients once when they are identified. McQuiston (1994) pointed out the limitations in accuracy when applying the Lewis relationship. Improved theory on the air-side heat and mass transfer might come up in later years. It was noted that a change of either the air-side or water-side coefficient by 10% may vary the steady state outlet air and water temperature by 0.1 to 0.2 °C. For all these the primitive part modelling approach offers the mathematical structure and potential for future developments.

6.4 Validation of Fan-duct Components

A fan-duct system that serves a hypothetical industrial plant was made use of to validate the air-flow fan and air-duct component models constructed from primitive parts. Details of the fan and duct component models are given in Chapter 4. Figure 6.9 shows the model of the supply ventilation system that draws in outside air to the plant room at a constant volume flow rate. Duct diameter was chosen in accordance with the industrial design standard. The plant operates 24 hours a day and releases cyclic thermal energy from 10 to 20 kW with a 4-hour cycle. The load fluctuation was taken as sinusoidal. The analysis gave the daily variation in plant room air temperature on one particular day - the first of August based on the climatic data of Kew available in the ESP-r software.

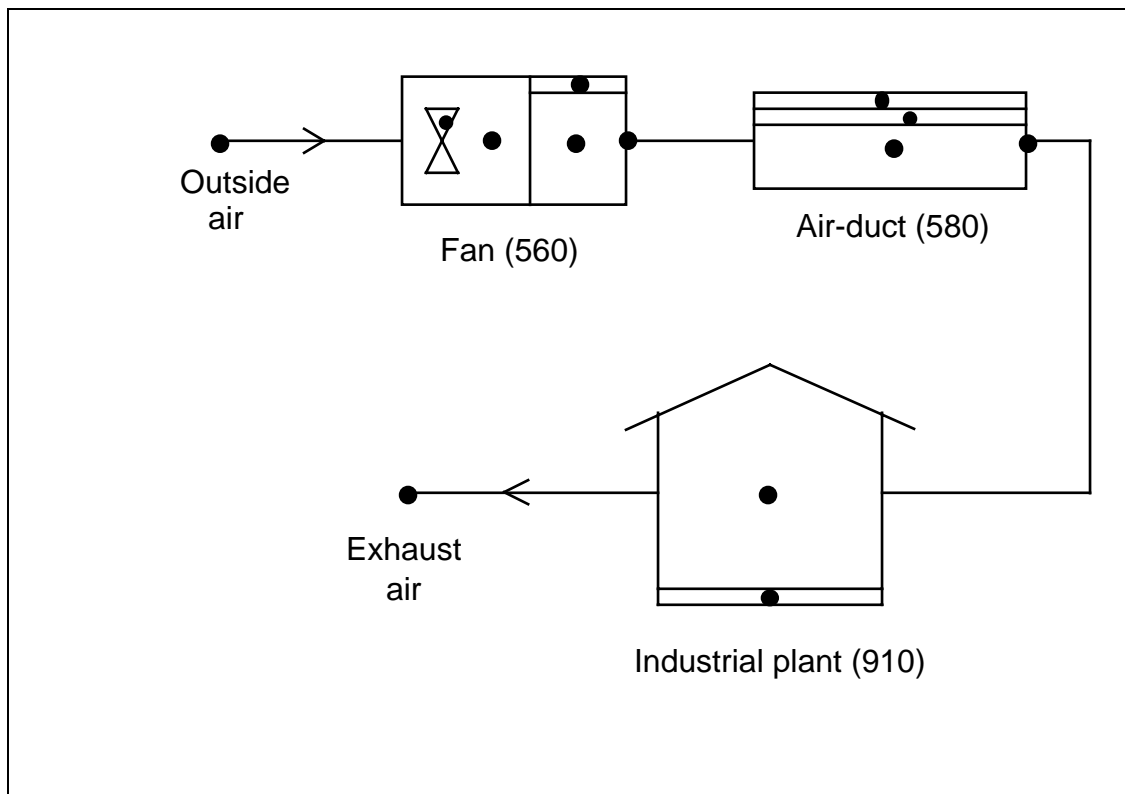


Figure 6.9 Supply Ventilation System Model

Input data are as follows:

fan

Fan component mass,	casing	= 12.0 kg
	motor	= 28.0 kg
Specific heat,	casing	= 465 J/kg.K
	motor	= 465 J/kg.K
Thermal resistance,	casing	= 0.01 m ² °C/W
Surface area,	motor	= 1.2 m ²
	casing interior	= 2.8 m ²
	casing outside	= 3.0 m ²
Rated absorbed power		= 165 W
Rated volume flow		= 0.825 m ³ /s
Air velocity,	casing interior, u _i	= 4 m/s
	casing outside, u _o	= 1 m/s
Efficiency at rated flow		= 0.7
Heat transfer coefficient,	casing interior	= 5.62 + 3.9u _o W/m ² .°C
	casing outside	= 5.62 + 3.9 u _i if u _i ≤ 5.0 m/s
		= 7.2 u _i ² if u _i > 5.0 m/s

metallic air-duct

Component mass		= 110 kg
Specific heat		= 465 J/kg.K
Thermal resistance of duct wall		= 0.6 x 10 ⁻⁵ m ² °C/W
Duct surface area,	interior	= 14.14 m ²
	outside	= 14.40 m ²
Duct diameter		= 0.3 m
Duct length		= 15 m

plant room

Component mass (wall/Furniture)		= 7.9 x 10 ⁵ kg
Enclosing wall, U-value		= 0.4 W/m ² °C
surface area		= 170 m ²
convective heat transfer coefficient, inside		= 7.5 W/m ² °C
	outside	= 25 W/m ² °C
Room volume		= 400 m ³

Infiltration: negligible

Two individual simulation runs were performed via ESP-r - one using the original fan and duct components (Code 30 and 60 respectively) and the other, the new fan and duct components built upon primitive parts (Code 560 and 580 respectively). The daily variation of plant room temperature and supply air temperature are shown in Figure 6.10. It can be seen that the results of the two simulation runs (with the same time step of 2 minutes) are almost identical. This confirms that when using longer time steps, as usually is the case in energy appraisal studies, the primitive part approach can be as good as the conventional approach.

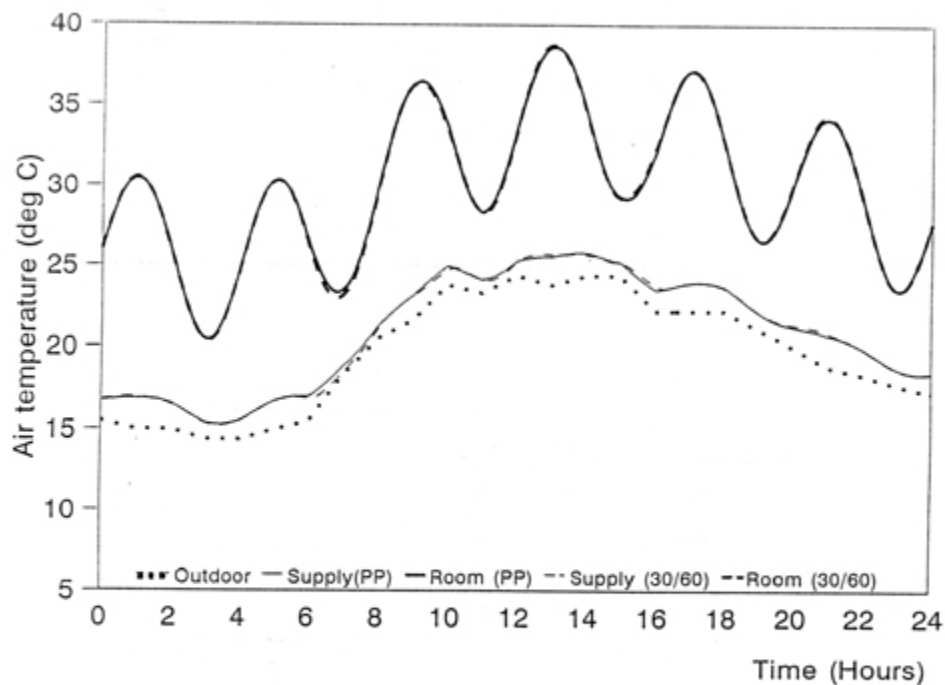


Figure 6.10 Comparison of Daily Temperature Variations

6.5 Validation of Air-conditioning System

A hypothetical CAV air-conditioning system had been made use of to verify the practicability of using the components built from primitive parts to simulate the performance of an air-conditioning system.

The configuration of the all-air type air-conditioning system under study is shown in Figure 6.11. In the Air Handling Unit the supply air fan delivers conditioned air to the room at a fixed flow rate. Supply air temperature varies with the change in chilled water flow at the cooling coil. Chilled water flow rate is controlled by a return signal from a thermostat which measures the room air temperature. Proportional control is used to maintain the room air temperature. Room relative humidity is not controlled. The room air is at positive pressure so that a small amount of the room air is leaking to the outside. Infiltration is basically negligible. By fixing the position of the air dampers at the entrance of the AHU, the return air mixes with the outdoor stream at a pre-setted ratio before sending back to the AHU.

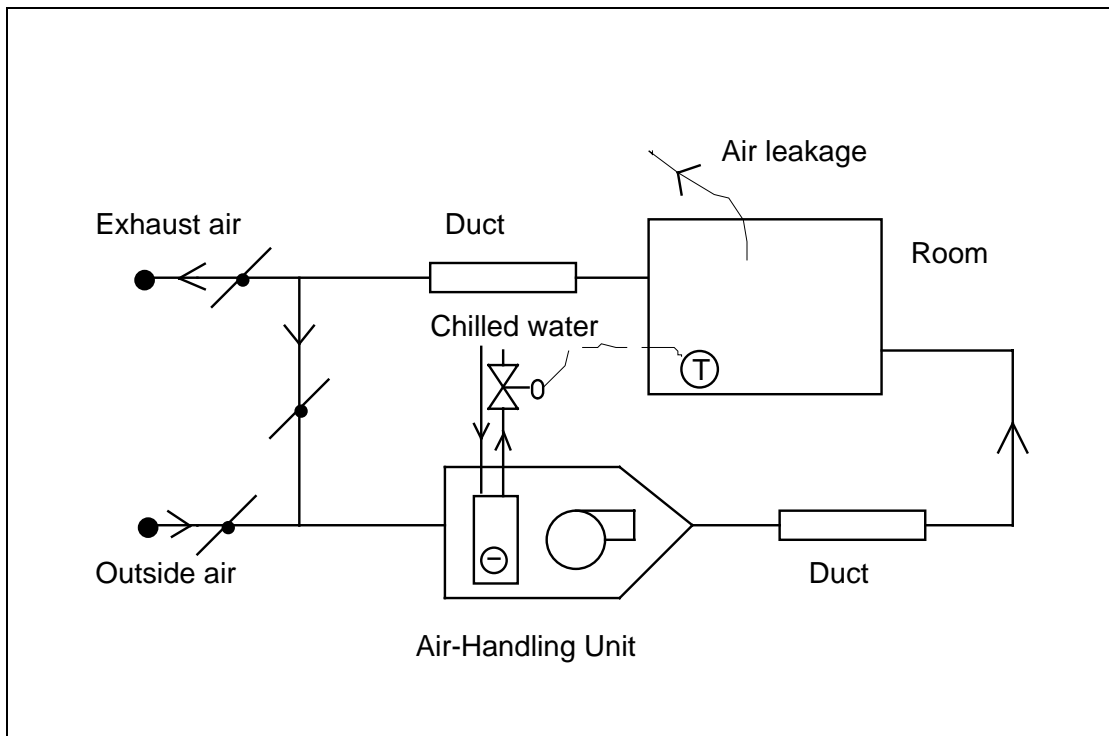
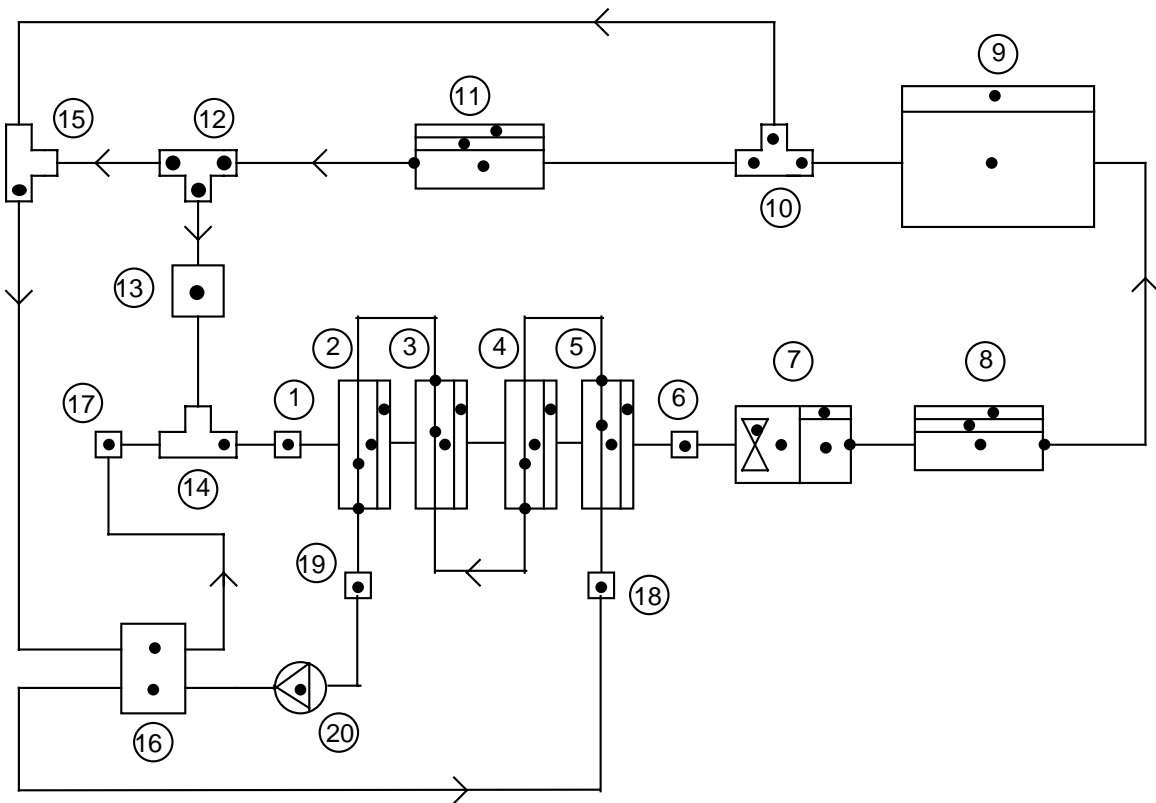


Figure 6.11 All-air Air-conditioning System



<u>Component Nos.</u>	<u>Descriptions</u>
1, 6	air flow multiplier (550)
2, 3, 4, 5	heat transfer tube (530)
7	fan (560)
8, 11	air duct (580)
9	imaginary building-like plant load (910)
10, 12	air flow diverger (660)
13, 17	air damper (70)
14, 15	air flow converger (680)
16	air & water temperature source (900)
18, 19	water/steam flow multiplier (540)
20	pump (240)

Figure 6.12 Simulation Network of the CAV System

Practical operating conditions and design data were used in the simulation. The air-conditioning space has been considered as a lecture theatre somewhere at the interior region of a large building. The internal loads (lighting, equipment, people etc.) dominate the space cooling load throughout the year. The room is served by an independent air-conditioning plant. The central plant is designed for a maximum cooling load of 30 kW.

Simulations were performed to analyse the change in room air temperature when the plant start-up at an initial room temperature of 30°C. The simulation network is shown in Figure 6.12. The results by the primitive part modelling approach have been compared with the predictions by the HVACSIM⁺ software.

The key plant data and boundary conditions are given below.

air-conditioned space

Sensible cooling load	= 0.0 kW,	before start-up
	= 16.8 kW,	after start-up
Room air temperature setting	= 24.0°C	
Proportional band	= ± 2.0°C	

supply fan

flow capacity	= 2.08 m ³ /s
operating efficiency	= 70%

air ducts

Both the supply duct and return duct are thermally insulated. The physical parameters are taken as identical.

Duct length	= 30 m
Duct diameter	= 0.6 m

cooling coil

The physical dimensions of the cooling coil is the same as the one specified in Section 6.3, except that the number of parallel circuit was changed from 36 to 24 to meet the design thermal load of the air-conditioned space.

Chilled water supply temperature	= 8.0°C
Chilled water flow rate	= 4.0 kg/s (maximum)
	= 0.05 kg/s (minimum)

air mass flow rates

fresh air rate = 0.706 kg/s
supply air rate = 2.5 kg/s
room exhaust air rate = 0.351 kg/s
return air rate = 2.149 kg/s

outside air conditions

dry bulb temperature = 30°C
moisture content = 0.020 kg/kg dry air

Comparing the two curves in Figure 6.13 it can be seen that the predictions about the dynamic system response are generally agreeable. In either case the initially slight rise of room temperature due to the plant inertia has been detected; the room temperature drops to 25°C at around 400 seconds and the final state lies within the controller throttling range.

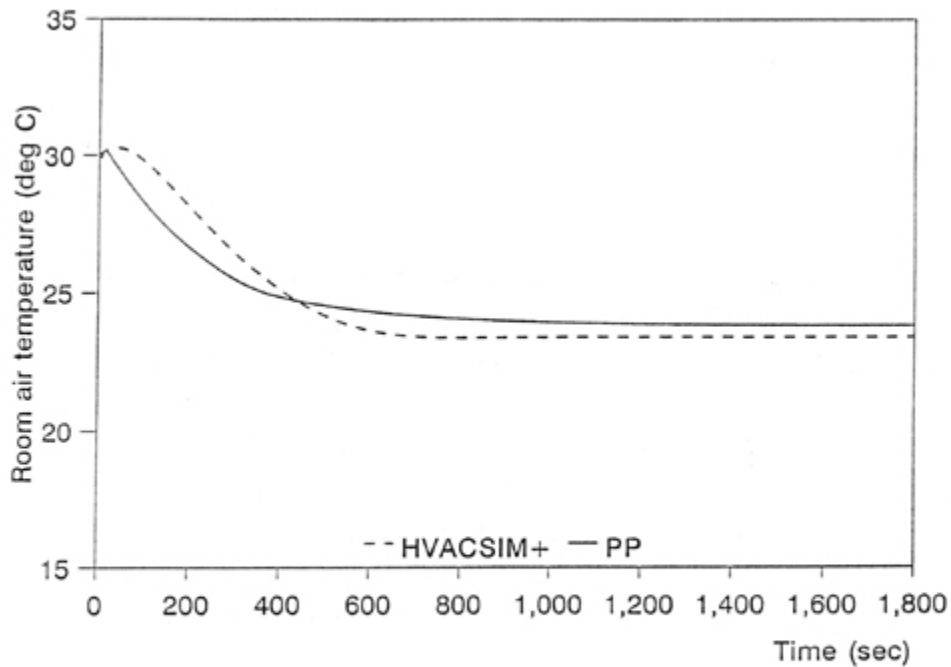


Figure 6.13 Comparison of Start-up Response of a CAV System

The primitive part modelling approach has been verified in this Chapter through different stages - from component level upto system level. The results show that this approach can be more accurate and flexible than other conventional plant simulation approaches. However, the expenses are very fine simulation time steps and simulation preparation/running costs; also sometimes there are problems with solution convergence. More discussions about the applications of this new concept will be explored in the next Chapter.

References

Aasem, E.O. 1993. Practical Simulation of Building and Air-conditioning Systems in the Transient Domain. PhD Thesis, Energy Systems Division, Department of Mechanical Engineering, University of Strathclyde, Glasgow, U.K.

Bowman, N.T. & Lomas, K.J. 1985. "Empirical Validation of Dynamic Thermal Computer Models of Buildings." Building Services Engineering Research & Technology, Vol.6, No.4, pp.153-162.

Clark, D.R., Hurley, C.W. & Hill, C.R. 1985. "Dynamic models for HVAC system components." ASHRAE Transactions, Vol. 91, Part 1B, pp.737-751.

Irving, A.D. 1988. "Validation of Dynamic Thermal Models." Energy and Buildings, Vol.10, No.3, pp.213-220.

Jeandel, A., Palero, I. & Laret, L. 1991. "An Approach to Thermal Modelling and Simulation of Buildings at Gaz de France." In Proceedings of Building Simulation '91, International Conference of the International Building Performance Simulation Association, August, Nice, France, pp.539-546.

Jensen, S.O. 1993. "Empirical Whole Model Validation Case Study: the PASSYS Reference Wall." In Proceedings of Building Simulation '93, International Conference of the International Building Performance Simulation Association, August, Adelaide, Australia, pp.335-341.

Jensen, S.O. & Van de Perre, R.C. 1991. "Tools for Whole Model Validation of Building Simulation Programs Experience from the EEC Concerted Action PASSYS." In Proceedings of Building Simulation '91, International Conference of the International Building Performance Simulation Association, August, Nice, France, pp.547-552.

Judkoff, R.D. 1988. "Validation of Building Energy Analysis Simulation Programs at the Solar Energy Research Institute." *Energy and Building*, Vol.10, No. 3, pp.221-239.

Klein, S.A., et al. 1990. TRNSYS, A Transient System Simulation Program. University of Wisconsin-Madison, Engineering Experiment Station Report 38-13, Version 13.1.

McQuiston, F.C. & Parker, J.D. 1994. *Heating, Ventilating, and Air Conditioning Analysis and Design*. 4th edit., John Wiley & Son, New York.

Ogata, K. 1992. *System Dynamics*. 2nd edit., Prentice-Hall, Inc.

Shekar, S.C. & Green, G.H. 1970. "Dynamic Study of a Chill Water Cooling and Dehumidifying Coil." *ASHRAE Transactions*, Vol. 76, Part II, pp.36-51.

CHAPTER SEVEN

APPLICATIONS

A number of application examples of using the primitive parts are described in this Chapter. Several advantages of this approach can be visualized, for instance, the flexibility of including energy and mass flow paths in the component model development process, the availability of thorough simulation data for performance appraisal at a microscopic level, the generality of the concept to model thermal components other than air conditioning equipment - in particular, those involve two-phase fluid flows. Perceived technical barriers at present and possible future developments of the work are also addressed.

7.1 Study of Effect of Radiant Energy in Duct Electric Heater

A duct electric heater is a sensible heating device that serves a moist air stream in conduit flow. For air conditioning purpose, it may be used as a 're-heater' in a CAV cooling system with humidity control or a 'heater' in the winter operating mode. On-off control of the electricity supply is used in most cases, though more sophisticated control techniques can be adopted without much difficulty. Because of the thermal capacitance of the heating element and the radiant exchange between the heating element and the duct heater casing, heating of the moist air stream continues even if the electricity supply has been temporarily cut off. In order to investigate the significance of the radiant energy exchange in the equipment performance, a 4-node duct heater model (Code 600) as in Figure 7.1(a) constructed from primitive parts was added to the ESP-r plant database.

The primitive parts involved in this model are:

Part No.	Descriptions	Nodes Involved
2.4	Surface convection with ambient	S3, E
3.1	Surface radiation with local surface	S1, S3
4.4	Flow upon moist air: 2 nodes	S1, A2, A0
4.4	Flow upon moist air: 2 nodes	S3, A4, A2
10.1	Heat injection to solid	S1

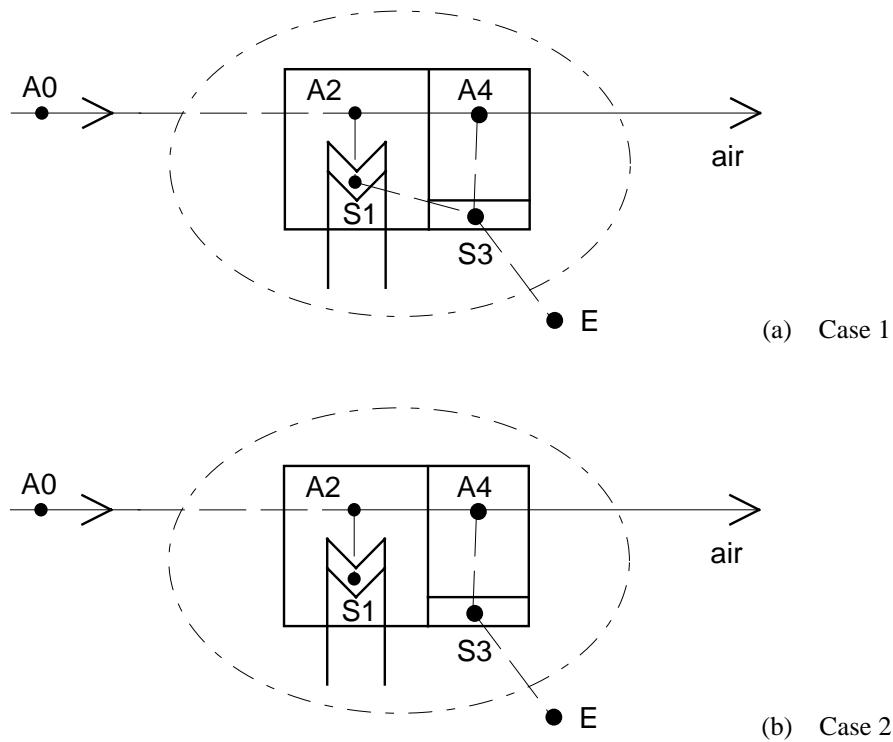


Figure 7.1 4-node Duct Heater Model by Primitive Parts

The primitive part No. 4.4 has been used twice in this model in that one is for the interaction between the moist air stream (Node A2) and the heating element surface (Node S1), and the other between the moist air stream (Node A4) and the duct heater casing surface (Node S3). The model structure assumes that all the radiant energy released from the heater element will be absorbed by the heater casing interior surface only, not the connecting duct surfaces either upstream or downstream. Node A0 represents the incoming air node and Node E the ambient air - a boundary node. The pp indices of S1, A2, S3, A4 are respectively 3, 2, 3, 1. Input data of the duct heater model for the simulation runs is given in Table 7.1.

A sensitivity test was carried out in that the radiant energy flow path between the heater element and the casing was included in Case 1, but then was excluded in Case 2. This means that the primitive part No. 3.1 was omitted in Case 2 when formulating the duct heater model. See Figure 7.1(b). The pp indices of S1, A2, S3 and A4 then become 2, 2, 2, 1 respectively.

Table 7.1 Input data of the duct heater model

Heater element total mass	=	3 kg
Metallic casing total mass	=	2 kg
Specific heat of metallic casing	=	465 J/kg. °C
Specific heat of heater element	=	420 J/kg. °C
Heater element heat transfer area	=	0.025 m ²
Casing interior surface area	=	1.0 m ²
Air flow cross-sectional area	=	0.28 m ²
Heater power	=	2.0 kW
Moist air flow rate	=	1.65 kg/s
Entering air temperature	=	13.24 °C
Outside surface hA module	=	3.5 W/ °C

Figures 7.2(a) and 7.2(b) show the simulation results when the heater was turned on for 1 hour and then turned off. The time variation of heater element temperature and heater casing temperature for both Cases 1 & 2 are shown in Figure 7.2(a), and air temperatures at heater inlet and outlet in Figure 7.2(b). It can be seen from both figures that the time constants of Case 2 are greater than Case 1, in view of the slower responses. When the heater is turned on, the heater element reaches a steady temperature of 561.6 °C in Case 1 within an hour. In Case 2 a temperature of 838.7 °C was recorded after an hour and the steady state has not been reached. The casing temperature in Case 1 rises to 50.6 °C after reaching the steady state, and the temperature rise for Case 2 is negligible. The results of Case 2 can be a serious mistake if the purpose of the study lies on 'heater metallurgy'.

In the prediction of air temperature rise, the dynamic response curves in Figure 7.2(b) are affected by the component time constants. Case 2 overestimates the steady-state outlet air temperature by more than 8% compared with Case 1. This is obviously a result of its failure to predict accurately the energy loss to the ambient air because of an elevated casing temperature. When the heater is turned off, it requires more than half an hour for the heater to lose its heating effect completely and again the two dynamic response curves show the difference in time constant.

The work above indicates that the Case 2 model is over-simplified and the radiant energy flow should not be ignored. It should be noted that to execute these two simulation runs the change over from Case 1 simulation to Case 2 simulation is very straight forward for this component model built from

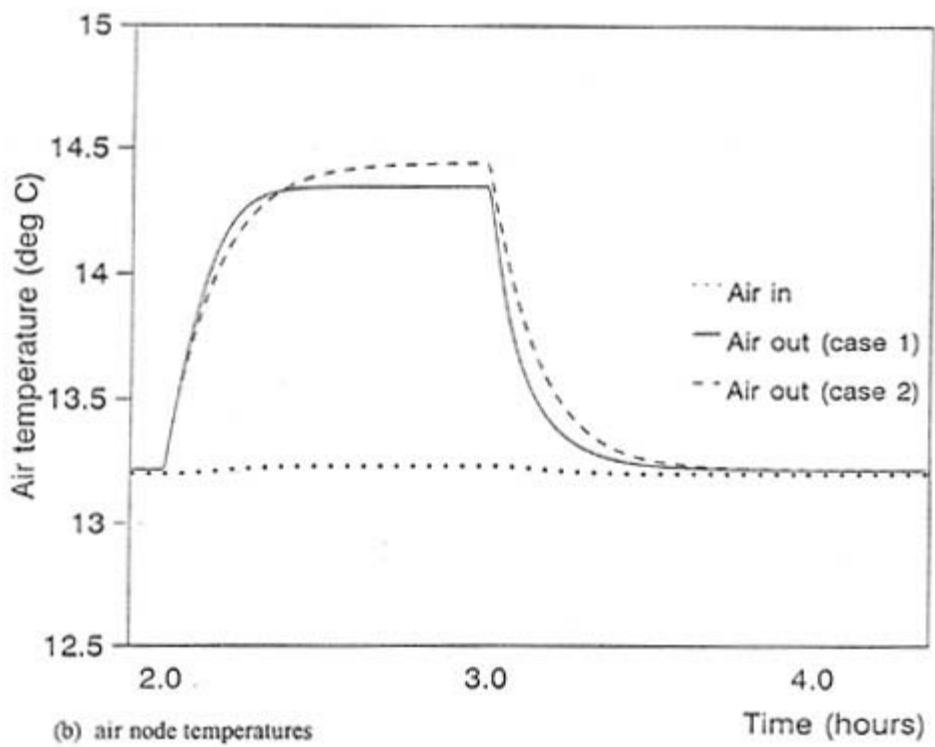
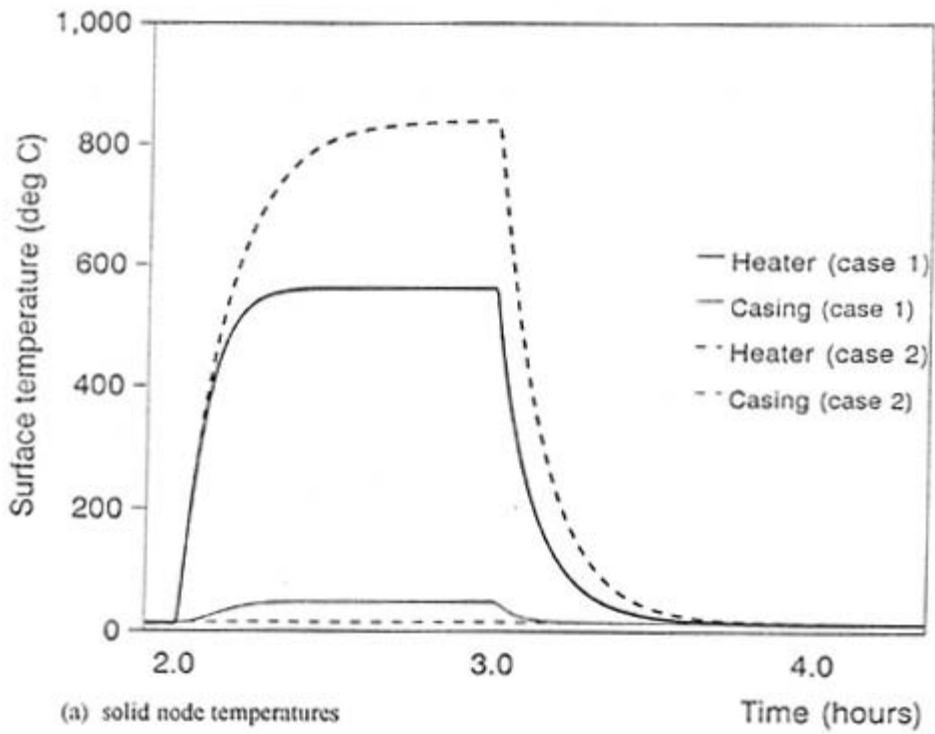


Figure 7.2 Performance Comparison of Duct Heater Model With & Without Considering Radiant Heat Transfer

primitive parts. In the source file the only required changes are, firstly, the disabling of the CALL statement of the PP3.1 subprogram in the duct heater component coefficient generator (which results in returning the zero value of the coefficients from PP3.1 during the simulation run) and then changes the pp index (Ni) of the two affected solid nodes from a value of 3 to 2 (which signals the deletion of one energy flow path in the solid mass computation). The affected plant component file pcomp4.F is then re-compiled and the same simulation process repeated. In achieving this sensitivity test the time of developing a new component coefficient generator or extensive modification of an existing component coefficient generator is not required. With experience the whole change-over process can be completed in a minute.

7.2 Microscopic Analysis of Cooling Coil Performance

The PP cooling coil model decomposed into heat transfer tubings as described in Chapter 4 can be made use of to study the performance of cooling coil in details. Consider the same 4-row counterflow cooling coil validated in Chapter 6, which now operates with a set of operating conditions given in Table 7.2.

Table 7.2 Operating Conditions of the Cooling Coil

The coil inlet conditions:	
Moist air inlet	
temperature	: 24.0 °C DB
moisture content	: 0.012 kg/kg dry air
mass flow rate	: 2.85 kg/s
Chilled water inlet	
temperature	: 8.0 °C
mass flow rate	: 0.9 kg/s

Suppose during site installation of this coil, the workman has connected the chilled water supply and return pipes incorrectly such that the inlet pipe was connected to the outlet header of the coil and the outlet pipe to the inlet header. The coil will then behaves in the manner of parallel flow rather than counter-flow.

(Figure 7.3) The effect of such an installation mistake can easily be examined via computer simulation by re-constructing the cooling coil model. The change from counter-flow to parallel-flow arrangement in the simulation process is simply an interchange of two connection descriptions in the system configuration file. Amendment to the source code is not required.

The coil outlet temperatures after the steady state had been reached are given in Table 7.3(a). The operating conditions at each row of the coil are also listed for comparisons in Table 7.3(b). The result data tells that for parallel flow the coil is totally wet; and for counter flow the coil is partially wet (the first row being dry). The condensation rates at individual rows can be recorded. The heat exchange rate is lower for the incorrect parallel-flow connection - a lower leaving chilled water temperature can be observed. This is the result of a reduction in the coil dehumidification capability - the moisture content of the leaving air is higher in the case of parallel flow than in the counter flow.

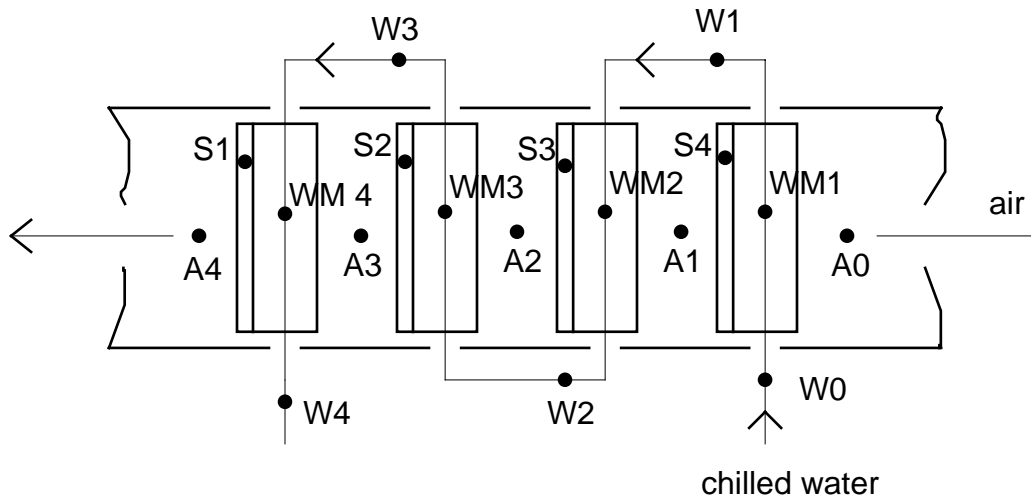


Figure 7.3 Cooling Coil in Parallel Flow Arrangement

Figure 7.4 shows the dynamic response of the mis-installation based on the data of step change in incoming chilled water temperature covered in Section 6.3.3, i.e. from 12 °C changed to 8 °C. It can be seen that the "S" shape (second order response) in the water temperature curve is more obvious in the parallel flow. This is because in the parallel flow arrangement, once the entering water temperature has changed, the heat transfer at all rows will be affected. As a matter of fact, transport delay at the air side is negligible.

Table 7.3(a) Cooling Coil Leaving Air & Water Conditions: Counter-flow Vs Parallel-flow

Outlet Conditions	Counter-flow	Parallel-flow
Air temperature (°C)	16.89	17.00
Air moisture content (kg/kg dry air)	0.01086	0.01131
Water outlet temperature (°C)	15.27	14.38

Table 7.3(b) Intra-coil Performance: Counter-flow Vs Parallel-flow

	Counter-flow	Parallel-flow
Temperature of leaving air at row number (°C):		
1	21.77	20.99
2	19.76	19.05
3	18.25	17.80
4	16.89	17.01
Temperature of metallic tube at row number (°C):		
1	18.21	16.03
2	16.53	15.84
3	15.58	15.74
4	14.34	15.68
Moisture condensation rate of each tube at row number (10^{-4} kg/s):		
1	0.	0.2333
2	0.0498	0.1576
3	0.3420	0.0988
4	0.5141	0.0594

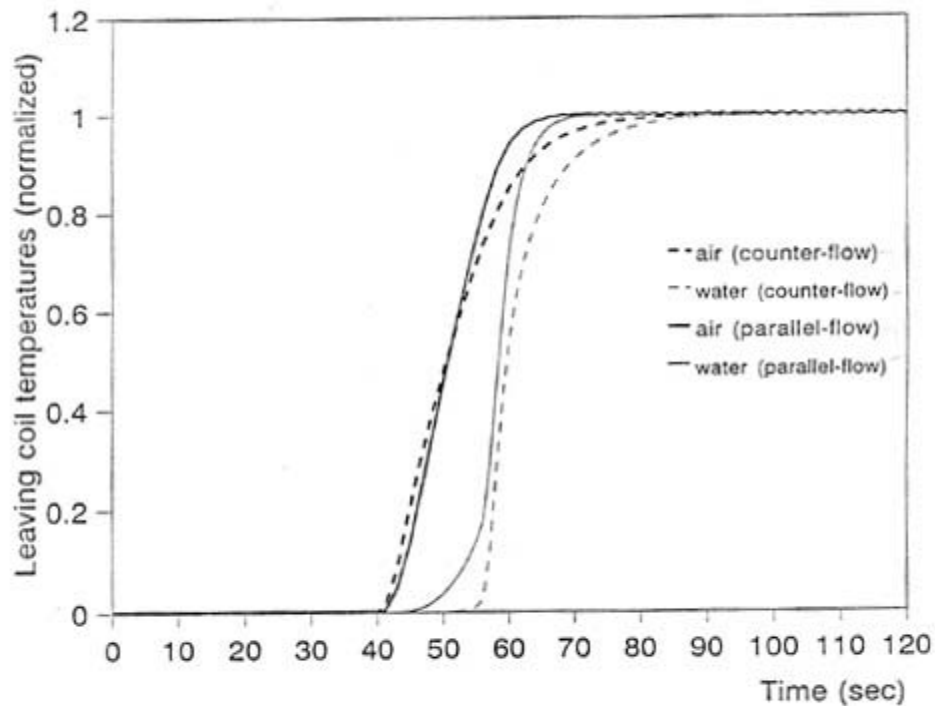


Figure 7.4 Dynamic Response: Parallel Flow Vs Counter Flow

7.3 Study of Varying Heat Flux Distribution on a Boiling Tube

Boiling tube is an elementary component in a water-tube fossil fuel steam boiler (El-Wakil 1985). Water flowing in the tubings are pressurized with heat flux adding to it along the tube wall. Outside the tube is a combustion chamber which is the heat energy source. As the water flows along the tube, it picks up heat energy and gradually converts from liquid water into saturated steam through a film boiling process. In some industrial boilers steam in tubes finally reach the superheated state. Heat flux along the tube is basically uniform but is affected by the stability of flame in the combustion chamber. This example demonstrates a simple investigation of the thermal effect on the water-side of the tube as a result of a change in heat flux distribution along the tube.

A hypothetical situation has been used for the analysis. A 20 mm diameter boiling tube-section of 10 m

long was considered. The working pressure was taken as 5 bars. Under a slow flow situation the pressure drop inside the tube is negligible. For simulation purpose the entire tube was decomposed into 10 numbers of sub-sections, each of length either 0.5 m or 1.5 m. This is indicated in Figure 7.5. Shorter sub-sections are used at the two ends in order to give more accurate predictions for those regions where changes in fluid temperature is likely to occur (i.e. in the regions likely occupied by liquid water or superheated steam). To represent each sub-section, a 3-node wet steam tube model (Code 610) has been created using the following two primitive parts (see Figure 7.6):

- 4.2 2-phase fluid upon surface
- 10.1 Heat injection to solid

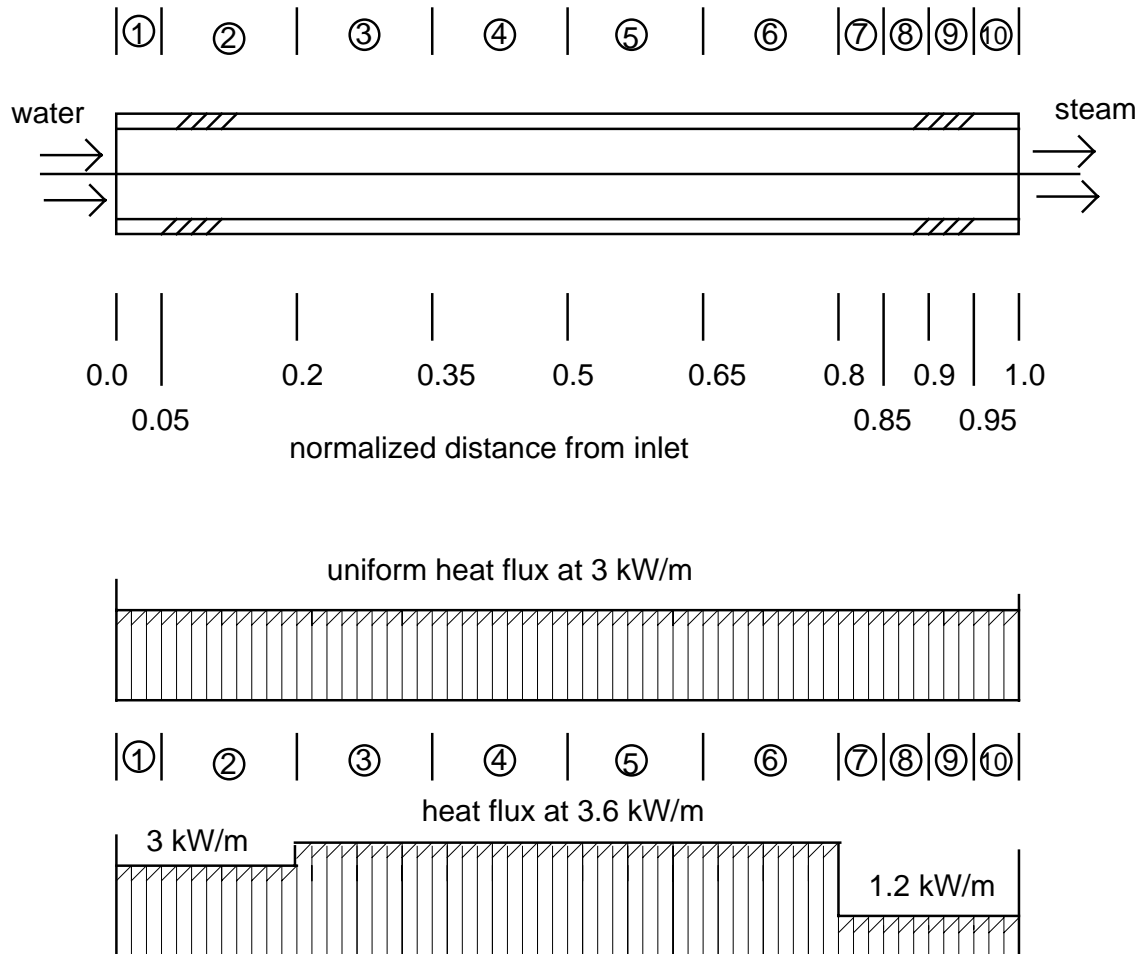


Figure 7.5 10 Meter Boiling Tube Divided into 10 Sections

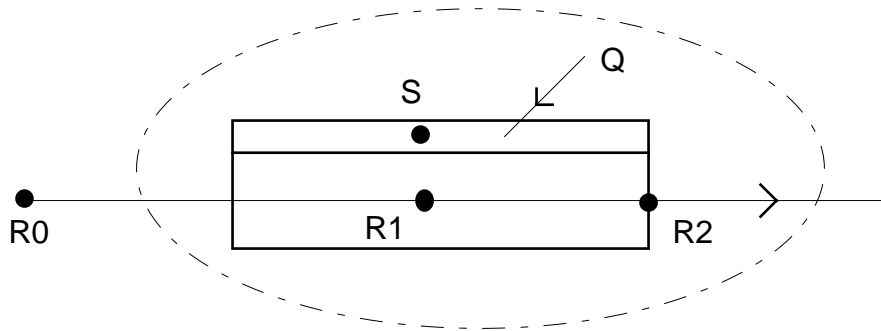


Figure 7.6 3-node Wet Steam Tube Model

For local boiling inside vertical tubes under forced convection, the heat transfer coefficient can be taken as (Holman 1989)

$$h_i = 2.54 \exp\left(\frac{P_{sat}}{1551}\right) (\theta_s - \theta_{rm})^3 \quad (7.1)$$

To speed up solution convergence during simulation run, a maximum limit has been imposed on value of h_i such that $h_i \leq 2 \times 10^5 \text{ W/m}^2 \cdot ^\circ\text{C}$.

Because the intention of this exercise was to demonstrate the use of the primitive part theory in two phase fluid flow, a detailed modelling of the burnt gas side of the heat exchange process (which otherwise includes a mix of radiant and convective heat exchange) was omitted. Instead, the heat energy from the fuel was considered as directly "injected" to the metallic tubing. The inside surface convective heat transfer coefficient is determined by a switching between equation (2.35) and equation (7.1), depending on whether the fluid is at liquid state or at vapour state at a particular time step. More accurate empirical coefficients can be used in more demanding exercises. Table 7.4 lists the parameters used in the simulation.

Table 7.4 Physical Parameters of the Boiling Tube and Steam Conditions

Mass of metallic tube	3.0 kg
Specific heat of metallic tube	692.6 W/kg.°C
Internal diameter of tube	20 mm
Tube length	10 m
Internal heat transfer surface area	0.1257 m ²
Mass flow rate of fluid	0.01275 kg/s
Fluid temperature at inlet	140°C
Fluid pressure	5 bar
Heat flux	3,000 W/m
Thermodynamic properties of water/steam at 5 bar:	
Saturated temperature	151.8°C
Latent heat of evaporation	2,109 W/kg
Specific heat of fluid at inlet	4,305 W/kg.°C
Specific heat of saturated liquid	4,316 W/kg.°C
Specific heat of saturated vapour	2,330 W/kg.°C

Table 7.5 Steady State Fluid Conditions along the Boiling Tube

Normalized Distance from Inlet	Fluid Temperature (°C)	Dryness Fraction
0.0	140.0	0.0
0.05	151.8	0.032
0.20	151.8	0.200
0.35	151.8	0.368
0.50	151.8	0.535
0.65	151.8	0.702
0.80	151.8	0.870
0.85	151.8	0.926
0.90	151.8	0.982
0.95	186.0	1.0
1.0	236.5	1.0

Table 7.5 shows the numerical results of the steady state fluid conditions along the boiling tube. Graphical results including the tube wall temperature distribution are given in Figure 7.7. It can be seen that the fluid in tube is mainly at the wet vapour state. Accordingly, the tube temperature is uniform along the length until the superheated region is reached. The steady state solution of the outlet steam temperature has been proved accurate by checking with manual calculations. The calculations are show below.

$$\begin{aligned} \text{Heat required to raise water temperature from 140 to 151.8}^\circ\text{C} \\ = 0.01275 * [(4,305 + 4,316) * 0.5] * (151.8 - 140) = 648.5 \text{ W.} \end{aligned}$$

$$\begin{aligned} \text{Heat required to convert saturated water to saturated steam} \\ = 0.01275 * 2,109 * 1,000 = 26,889.8 \text{ W.} \end{aligned}$$

$$\begin{aligned} \text{Heat required to raise saturated steam to superheated steam of 234.8}^\circ\text{C} \\ = 0.01275 * (2,930 - 2,749) * 1,000 = 2,307.7 \text{ W} \end{aligned}$$

where 2,930 and 2,749 in kJ/kg are respectively the specific enthalpy of superheated steam at 236.5°C and saturated steam at 5 bar respectively.

$$\text{Total heat required} = 648.5 + 26,889.8 + 2,307.7 = 29,846 \text{ W.}$$

$$\text{Actual heat input for simulation} = 3,000 * 10 = 30,000 \text{ W.}$$

The difference between the hand calculated heat input and the actual heat input used in the simulation is only 0.5%. This example is hence also a good validation exercise for the primitive part theory involving two phase fluid flow.

Figure 7.8 gives the steady state solution for a slightly non-uniform distribution of heat flux along the tube. Here a portion of the thermal energy is shifted from the outlet end sub-sections towards the central part sub-sections. The total heat injection rate remains unchanged. It can be observed from this figure that while the steam outlet temperature is relatively the same, the superheated steam region in the tube has been enlarged.

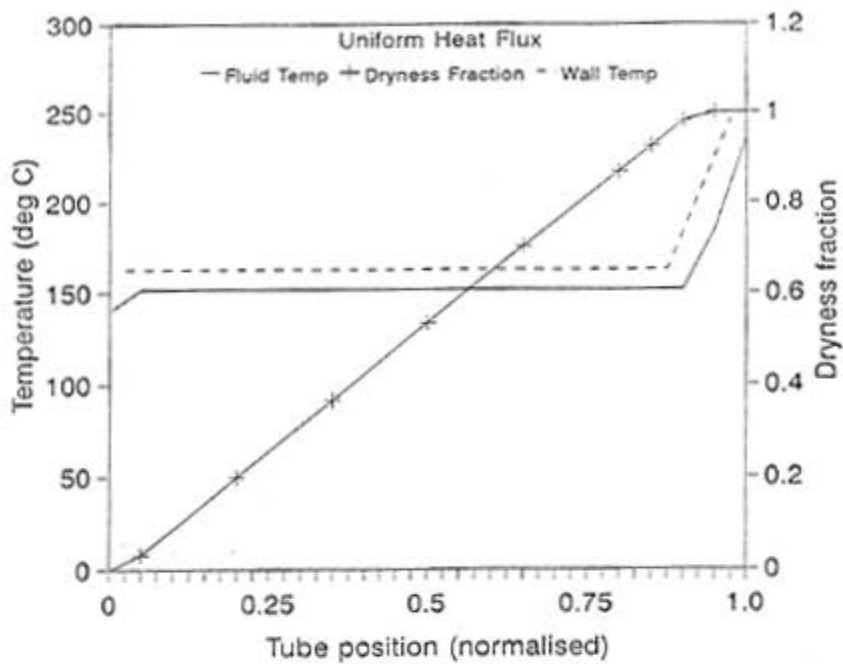


Figure 7.7 Axial Temperature Distribution under Uniform Heat Flux

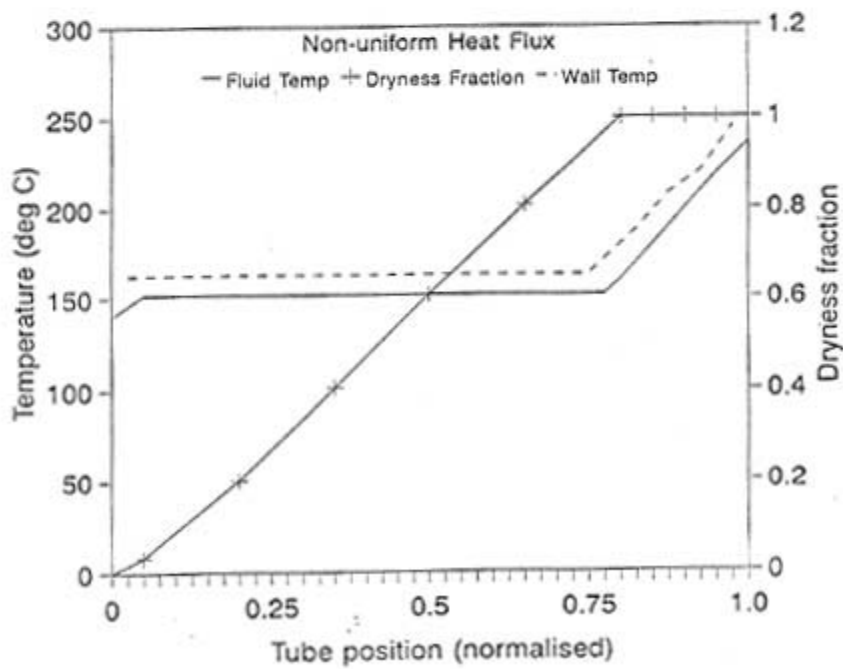


Figure 7.8 Axial Temperature Distribution under Slightly Non-uniform Heat Flux

Dynamic response

The dynamic responses of the steam temperature at the outlet and the tube wall temperature of the last sub-section (0.5 m long) to a sudden change of heat flux pattern (Figure 7.9) were simulated using a time step of 0.1 second. A drop in outlet steam temperature can be observed at the beginning of the change. This is because the tube temperature of the last section requires time to rise up to the steady state value when the fluid inside has changed from wet vapour state to superheated state.

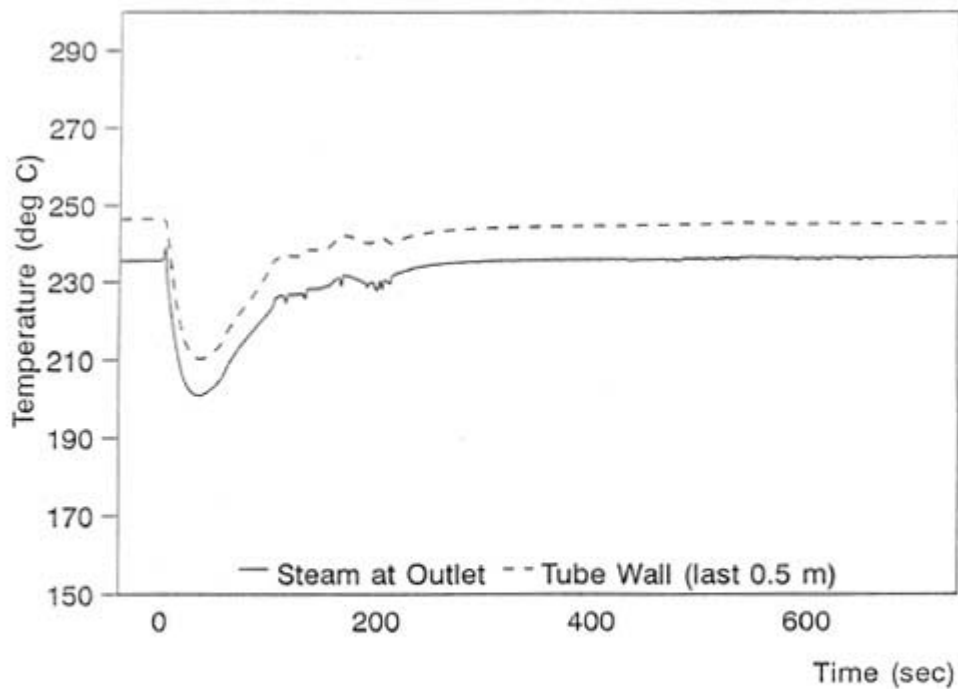


Figure 7.9 Transient Temperature Response of Boiling Tube under Changed Heat Flux Distribution

7.4 Steam Heating System Simulation

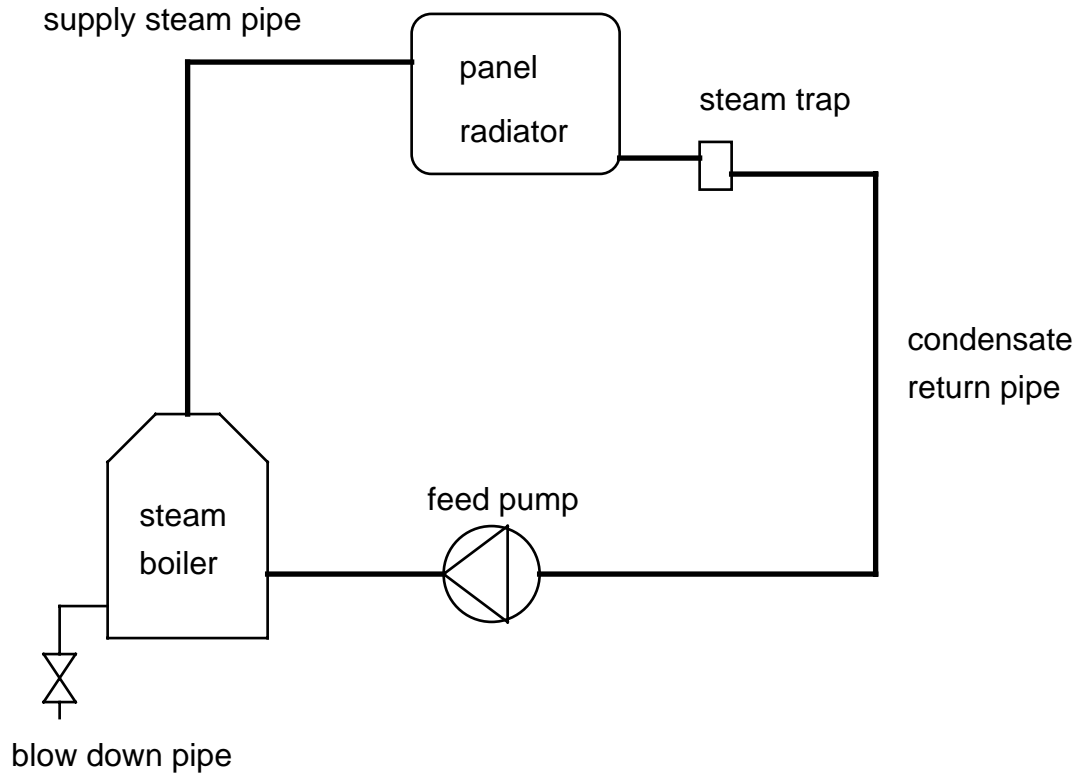


Figure 7.10 Steam Heating System

In this example, a simple steam space-heating system shown in Figure 7.10 is modelled (Bovay 1981). In the system, saturated steam is generated by the electric steam boiler at 5 bar (corresponding to a saturated steam temperature of 151.8 °C). The steam is conveyed to a space-heating radiator panel via thermally insulated steam piping. Thermal loss at the exposed pipe surface causes the formation of small amount of condensate in the supply steam flow. Heat released from the radiator panel surface to the room air results in substantial amount of steam condensation inside the radiator. Because of the relatively high metallic surface temperature the radiator is usually positioned at an elevated level beyond the reach of the occupants. The steam trap allows the drain-off of condensed steam from the radiator but not the steam vapour. Condensate in the return piping is sent back to the boiler via the feed pump. Any loss of steam in the

process is compensated by the make-up water stream to maintain a constant water level in the boiler. In order to limit the accumulation of impurities in the boiler chamber to a controllable level, the water inside the boiler will be drained off periodically according to a pre-set programme. Such a draining process is allowable even when the boiler is in service and the process is referred as "blow-down" (ABMA 1984).

This steam system is represented by a simulation network which consists of eight component models as shown in Figure 7.11. The supply steam pipe and the return condensate pipe are modelled by the wet steam tube model covered in Section 7.3.

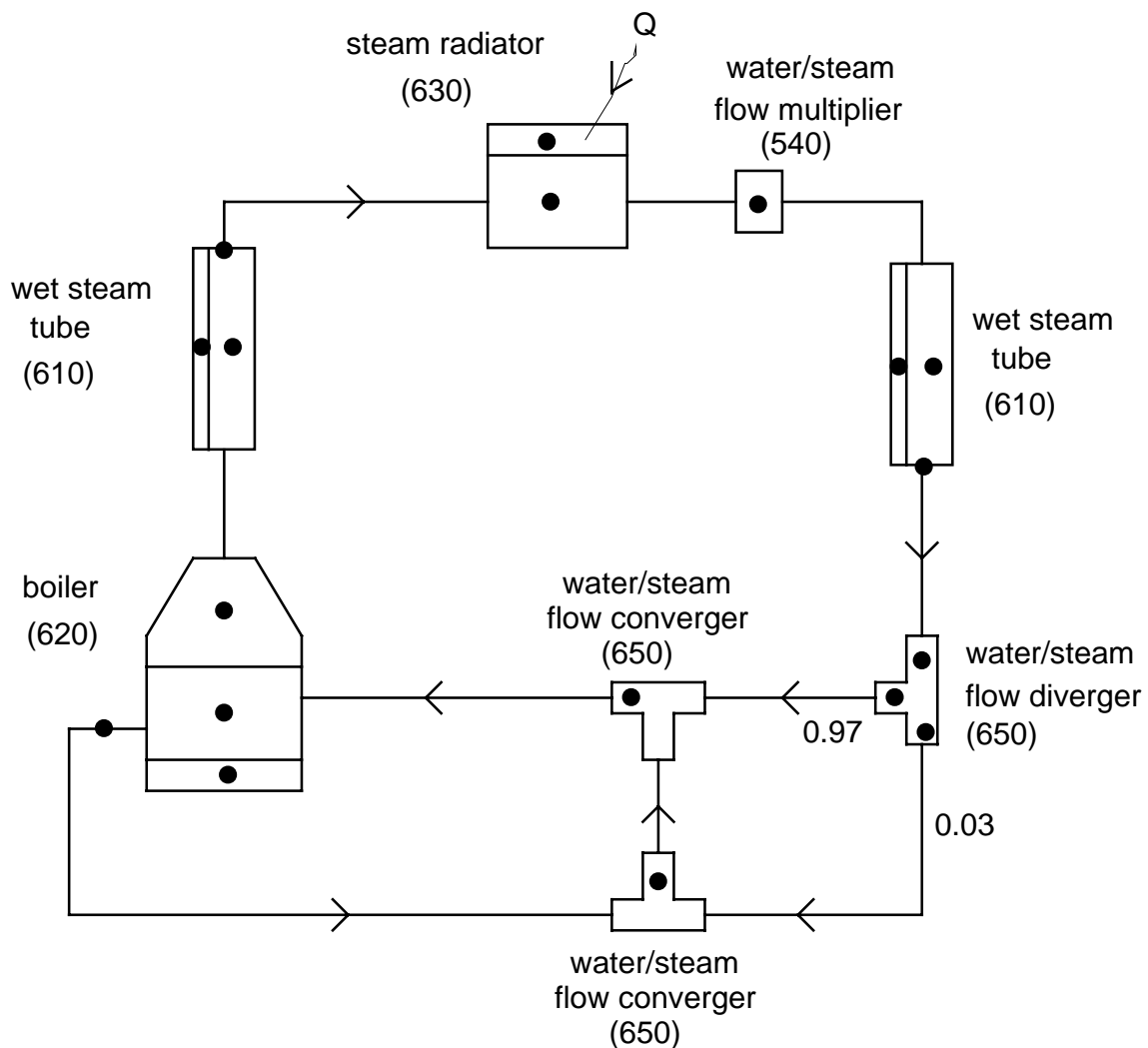


Figure 7.11 Simulation Network of Steam Heating System

Several new component models have been created. They are briefly described as follows:

Steam Boiler (Code 620)

The steam boiler is a 4-node model constructed from the following three primitive parts:

- PP2.3 Surface convection with single phase fluid
- PP9.3 Fluid accumulator for single phase fluid
- PP10.2 Heat injection to vapour-generating fluid

Node 1 represents the casing material.

Node 2 represents the water in chamber.

Node 3 represents the leaving steam.

Node 4 represents the leaving water (blow down).

The input data are:

- i) total mass of boiler chamber (excluding water/steam mixture) = 180 kg
- ii) specific heat of chamber (weighed average) = 700 J/kg.K
- iii) water holding capacity = 0.2 m³
- iv) wetted surface area of chamber = 1.0 m²
- v) working pressure = 5 bars
- vi) electric heater rated capacity = 40 kW

Steam Panel Radiator (Code 630)

The steam panel radiator is a 2-node model constructed from the following two primitive parts:

- PP4.2 Flow (2-phase fluid) upon surface
- PP10.1 Heat injection to solid

Node 1 represents the panel casing material.

Node 2 represents the wet steam inside the panel.

The leaving steam node in PP4.2 is not involved in this model and hence is a "dummy" node in this radiator component. The thermal load is taken as a negative heat source rejected directly at the panel casing and is a CDATE to facilitate a user-defined time-varying pattern.

The input data are:

- i) total mass of metallic panel (excluding steam/water mixture) = 30 kg
- ii) specific heat of panel (weighed average) = 700 J/kg.K
- iii) panel internal surface area = 5.0 m²
- iv) working pressure = 5 bars

Steam Trap (Water/Steam Flow Multiplier; Code 540)

The steam trap is modelled by a water/steam flow multiplier which is a 1-node model constructed from the primitive part 5.2: Flow multiplier for all fluid types.

In order to simulate the operation of the component that allows only liquid to pass through, the flow ratios are set as follows:

- i) out-to-in flow ratio for first phase mass flow = 1.0
- ii) out-to-in flow ratio for second phase mass flow = 0.0

Steam/Water Flow Converger (Code 650)

The steam/water flow converger is a 1-node model constructed from the primitive part PP6.3: flow converger for single phase fluid.

Two convergers have been used in the simulation network: one for the mix of the blow down stream and the "lost" steam stream and the other for the mix of the returned condensate stream and the make-up water stream. The make-up water temperature is set at 15 °C which has been taken as steady throughout the simulation period.

Steam/Water Flow Diverger (Code 640)

The steam/water flow diverger is a 3-node model constructed from the primitive part PP5.1: flow diverger for all fluid types.

Node 1 represents the fluid at the first outlet.

Node 2 represents the fluid at the second outlet.

Node 3 represents the fluid at the component inlet.

3% of the steam supply flow has been assumed loss in the steam/condensate flow process and therefore the feed water to the boiler is a mixture of 97% from the condensate return and 3% from the make-up water supply.

simulation run

Simulation run was performed with the thermal load at the radiator being fixed at 25 kW and the thermal losses at the steam supply pipe and the condensate return pipe at 90 W and 60 W respectively. After the steady state had been reached, a blow down operation then took place at a ramp input mode of increasing from 0.0 to 0.02 kg/s in an hour. A time-step of 10 seconds was used.

The results of the steady-state system performance, before the blow down operation, are listed in Table 7.6. With a ramp increase of the blow down rate at 0.02 kg/hour (started at 3.0 hours), Figure 7.12 shows the dynamic simulation results of changes in boiler electricity demands, boiler feed water flow rate, and feed water temperature. It can be seen that the boiler electricity demands increases linearly with the blow down rate. The extra electricity demand is for heating up the increased flow of make-up water from the ambient temperature of 15 °C to 151.8 °C. And accordingly, the mixed feed water temperature to the boiler decreases.

Table 7.6 Steady State Operation at 25 kW Thermal Load

Operating Conditions at the outlet of:	Fluid Temperature	Mass flow rates	
		Steam Vapour	Liquid Water
Boiler	152.36	0.011889	0.0
Steam supply pipe	151.80	0.011854	0.000353
Steam trap	151.80	0.0	0.011889
Condensate return pipe	150.63	0.0	0.011533
Boiler feed-water pipe	146.59	0.0	0.011889
Make-up water pipe	15.00	0.0	0.000357
Radiator metallic panel temperature= 148.09 °C			
Boiler electric power		= 25.36 kW	

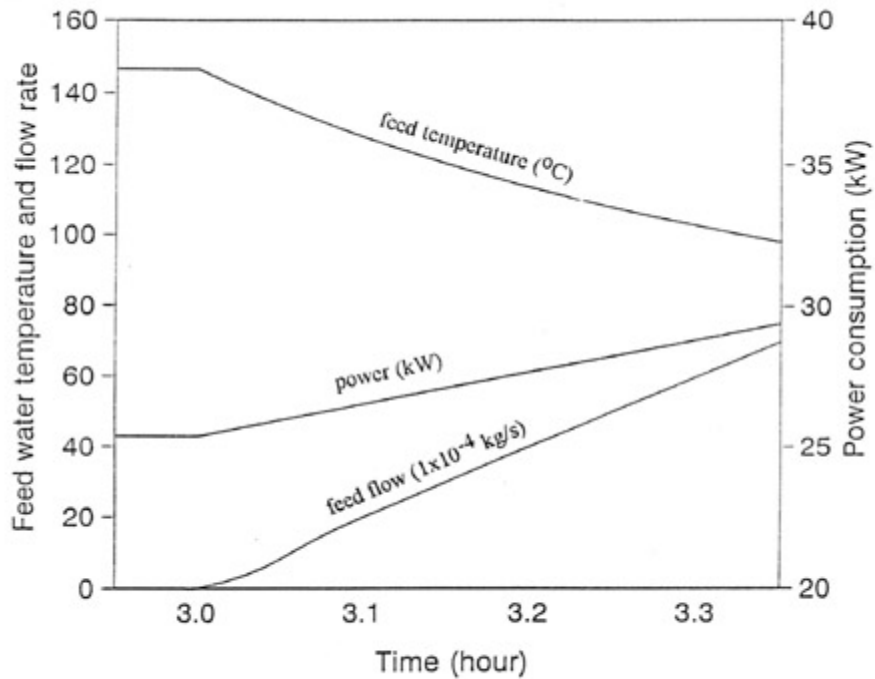


Figure 7.12 Dynamic Performance of Boiler in the Steam Heating System

7.5 Barriers & Future Work

7.5.1 Uncertainties in input data

One of the principal barriers to the use of this explicitly modelling approach is the problem of data preparation in the face of uncertainty. Plant models require a substantial amount of input data and obviously much of this is difficult to obtain. Empirical heat transfer coefficient is one particularly problematic. Two difficulties are quoted below. Firstly in the simulation exercises performed so far, most of the heat transfer coefficients locally applied to a primitive part are only proved globally correct for the component as a whole - for instance, equations (2.17) and (2.35) for the air- and water-side coefficients of a heat transfer coil now has been applied in the heat transfer tube model. McQuiston (1981) pointed out that actually the air-side coefficient of the coil is row dependent. Secondly, some coefficients are nowhere found in the literature, e.g. the heat transfer coefficients for the air in touch with the interior casing of a centrifugal fan, or over a flow-control damper. It is perhaps doubtful if these missing data will be made available in the near future.

Nevertheless, such a barrier should not be taken as a justification for a simplification of the physical laws,

so that a model can be developed and operates with a reduced data set. An alternative possibility, as suggested here, is to retain the best representation of the reality - an explicit simulation model with high integrity and hierarchy. And instead, to generate the complete data set from whatever information the designer can offer, or the best the model developer can predict, at any stage. In all cases, accuracy of the model has to be verified by a structured validation scheme. This attitude promotes developments towards state-of-the-art intelligent performance appraisal tools rather than simplified performance appraisal tools. The concept actually has been demonstrated workable through a variety of validation exercises already presented in Chapter 6.

7.5.2 Cost effectiveness

Another difficulty experienced from the work so far is that the tedious computational effort required by the plant models created from primitive parts makes this extensive modelling approach not favourable at this point in time. The solution process often becomes unstable when there are strong links between the energy and mass exchanges, for instance when wet surfaces exist on consecutive rows of a cooling coil and, in most cases of two-phase fluid flow. Very fine time step in terms of fractions of a second must be used in order to obtain reasonably stable solutions from these plant components. And, when these components become part of a large plant system, further reduction of time step is required. The rationale of adopting this approach is, perhaps, not attractive to the users based on the computer technology today. Yet, if one looks back to the evolutionary changes in computer technology in the past decades, one should be confident that with the further advancements in machine technology, the performance/cost ratio of this explicit approach will rise rapidly. Until then, the primitive part modelling concept will become widely applied. It could come to a situation, that the concept of variable time steps actually applies to the level of individual plant components or sub-components, rather than merely as a link for integrating building components and plant components in a single simulation run.

Coming back to the modelling task that the simulationists have to face today, there appears no reason why a mixed use of the single-/multi- node algorithmic type (component-based) models and the explicit multi-node models developed from primitive parts in the same plant network not a good compromise. The decision lies on the nature and objectives of the simulation task and so can be totally flexible to suit individual needs. Figure 7.13 shows an example of an integrated building-and-plant simulation run performed via the Project Manager of the ESP-r program. The reception zone of the building is equipped with a CAV air-conditioning system with proportional control. The air-conditioning equipment in the system are represented by explicit primitive-part component models,

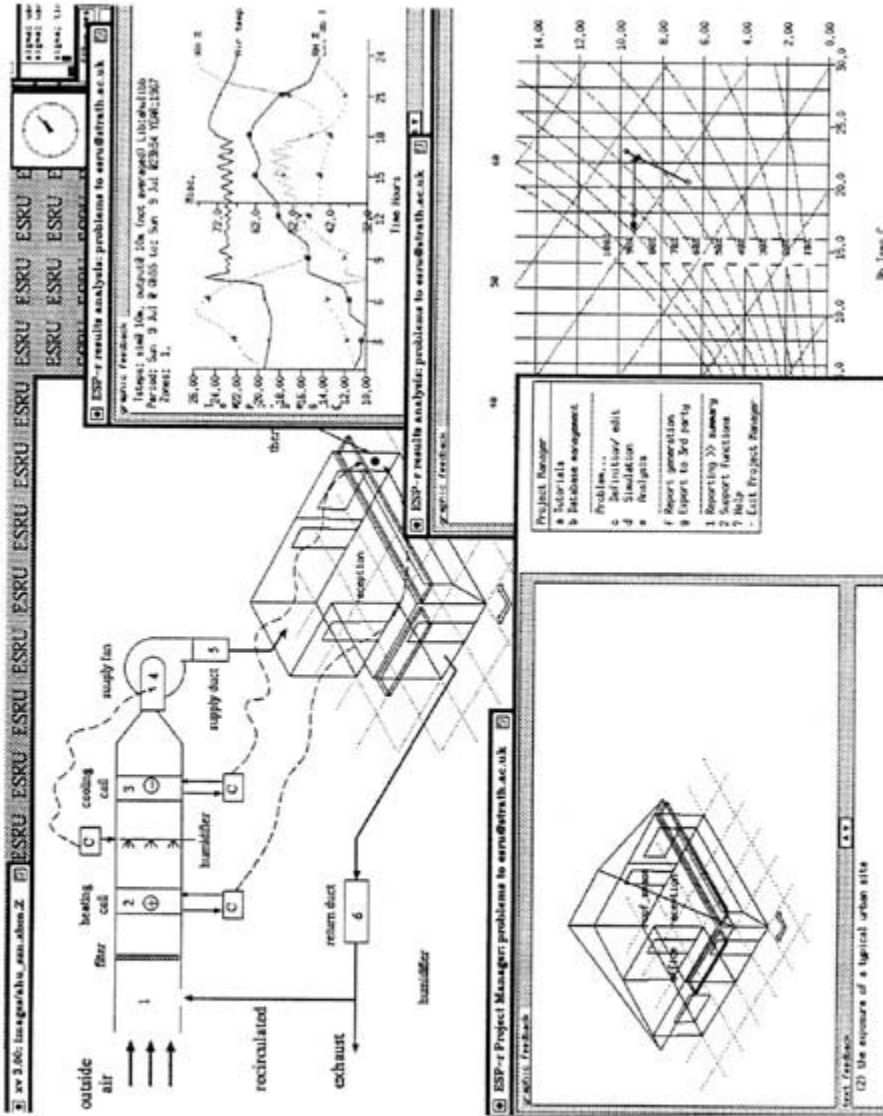


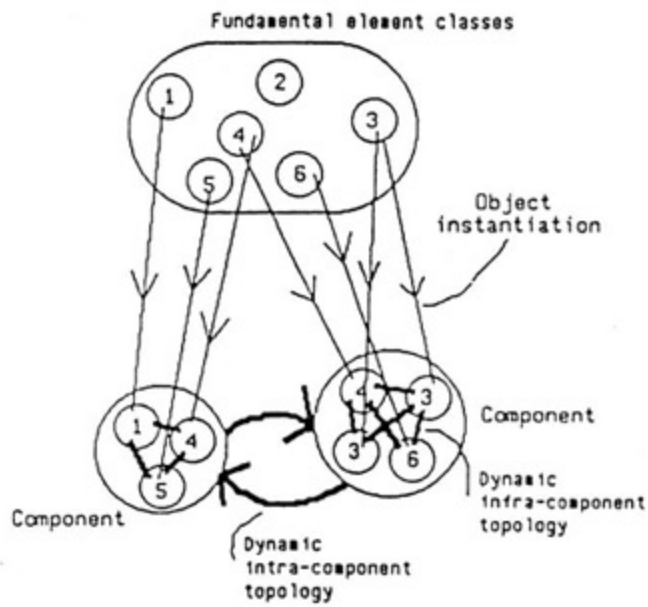
Figure 7.13 Mixed Use of Primitive Parts and Conventional Plant Components in Integrated Building-and-Plant Simulation

except for the cooling coil and the humidifier which are represented by single-node conventional components in the ESP-r plant database. Also shown in this figure are the simulation results on the ninth of July, based on the Kew climatic data. The graph at the top right corner shows the daily variation of the indoor and outdoor air temperature and relative humidity conditions. The psychrometric chart displays the moist air conditions at various system components at a particular simulation time step - at 3:00 pm in this case. The mixed use of components speeds up the simulation process but provides better resolution at selective components (say ducts, fan etc.) where desirable.

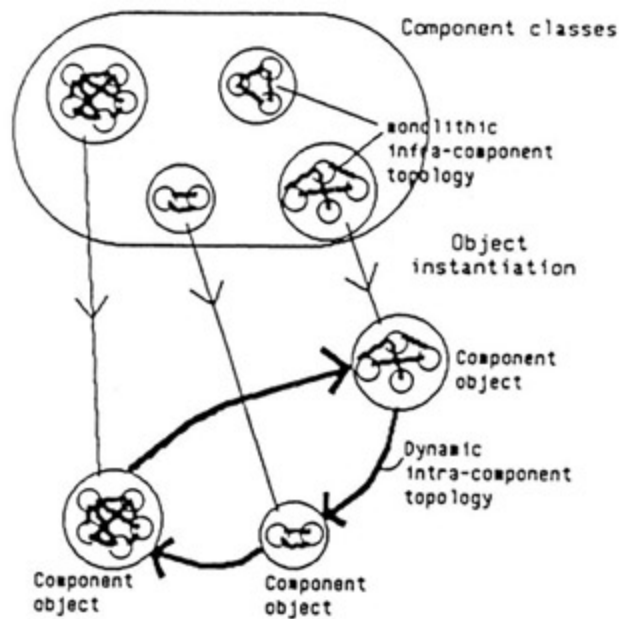
7.5.3 Automatic model construction

While the primitive part theory has been shown highly successful - in the sense of unifying the mathematical structure and simplifying the component modelling task - strictly speaking, the model building process here introduced, as outlined in Appendix C, should only be regarded as a preliminary product rather than a mature product. It has been pointed out in Chapter 5 that the theory should be linked to the Neutral Model Format developments in order to benefit a wider population in the field of system simulation. Another promising future of the work is perhaps with the object oriented simulation environment. The primitive parts, by nature, are elementary calculation objects from which a taxonomy of plant component objects can be defined. In this regards, one very important area remains to be solved is how to make the plant component creation process fully automatic, as opposed to the manual technique presented in the earlier Chapters.

From an object-oriented software structure point of view, there can be two approaches for plant representation: the atomic approach and the component based approach. This has been a research outcome of the UK EKS project (Tang & Clarke 1993). The component based approach treats each component as a topologically pre-defined equation structure and therefore the mathematical complexity is hidden away within each individual component. The system is responsible for the creation and maintenance of the dynamic inter-component topology. This approach has been adopted initially for the plant modelling process, with an aim to support the creation of state-of-the-art simulation models e.g. the sequential and the simultaneous architectures. In the atomic approach, the fundamental entities or atomic objects are used to construct any component in general. By doing so, it is not possible to apply instantiation control over the atomic entities as the structure of the components are radically different. This implies that, for a plant component taxonomy developed through this approach, the system should be able to handle two levels of arbitrary system topologies - firstly the intra-component topology which is created within the component, and secondly, the inter-component topology which is created dynamically at run-time. Figures 7.14 (a) & (b) make contrasts to the concepts of these two approaches.



(a) The atomic approach



(b) The component based approach

Figure 7.14 Atomic Vs Component-based Approach in Plant Modelling

If the atomic approach as suggested in UK EKS is a basic feature of the next generation simulation software, then the work on the primitive parts so far has not come to a concrete idea how this is to be implemented. The intelligent knowledge-base in the application of the primitive parts is obviously a good topic to be addressed in the next stage of development.

7.5.4 Extension of applications

The primitive part theory originates from the analysis of energy and mass flow paths in basic air conditioning equipment. Because of the generic nature of the primitive parts, they can be used to model components in any thermal systems.

Consider an internal partition of a building as an example. The wall can be modelled by a combination of primitive parts 1.1 (thermal conduction - solid to solid) and 2.1 (surface convection with moist air). Several primitive parts 1.1 should be used for explicit modelling of a composite or reasonably-thick wall, and part 2.3 (surface convection with ambient) should be used when the thermal condition of the air in contact become known and is therefore a boundary condition. For an external wall, part 10.1 (heat injection to solid) can be useful to represent the direct solar heat gain at the outer surface. The amount of heat gain in a time step must then be firstly quantified. Part 3.2 (surface radiation with local surface) can be applied to determine the radiation exchange among internal wall surfaces when the effect of this energy flow path becomes significant. Models of various degrees of detail can also be created to study the thermal bridges, the ground temperature effects etc. in the context of building simulation. The extension of the primitive part concept to the building components allows the integrated building-and-plant simulation be taken place within a unified mathematical framework.

The application examples introduced earlier in this Chapter show how the work applies in steam heating equipment models. Steam heating equipment has a wide range of applications, for instance in thermal power plants or in food processing plants. Hence the application of the primitive part theory can be extended to other industrial thermal processes. In doing so, the introduction of new primitive parts might be required for instance those dealing with chemical energy exchange or combustion, moisture diffusion, adsorption or absorption. An important future development of the present work is therefore to seek applications in a wide range of areas, including more specialized air conditioning systems and the related, for instance desiccant cooling (ASHRAE 1992), cool storage (ASHRAE 1987, 1989), solar technology (Kreider & Kreith 1982; SERI 1989), waste heat recovery such as the use of enthalpy wheels and heat pipe (SMACNA 1984), combined heat and power (Marecki 1988) and district heating (ASHRAE 1987a) etc. The result will be an enriched and consolidated primitive parts library. It is confident that only a very

finite number of new primitive parts has to be added in order to model almost any thermal systems.

Up to this point, the theory, methodology, validity and applications of a generalized plant modelling approach based on interacting energy and mass flow paths that exist in air conditioning systems have been covered. Barriers and future development work are also addressed. In the final Chapter that comes next, the work achieved so far will be summarized, together with an overview on the significance and implications of this new modelling concept.

References

ABMA. 1984. Boiler Water Requirements and Associated Steam Purity for Commercial Boilers. 1st edit., American Boiler Manufacturers Association, Virginia.

ASHRAE. 1987. Cool Storage. ASHRAE Technical Data Bulletin, Vol.3, No.1, American Society of Heating, Refrigerating and Air-Conditioning Engineers, Inc., Atlanta.

ASHRAE. 1987a. District Heating and Cooling. ASHRAE Technical Data Bulletin, Vol.3, No.5, American Society of Heating, Refrigerating and Air-Conditioning Engineers, Inc., Atlanta.

ASHRAE. 1989. Cool Storage Modelling and Design. ASHRAE Technical Data Bulletin, Vol.5, No.4, American Society of Heating, Refrigerating and Air-Conditioning Engineers, Inc., Atlanta.

ASHRAE. 1992. Desiccant Cooling and Dehumidification. American Society of Heating, Refrigerating and Air-Conditioning Engineers, Inc., Atlanta.

Bovay, H.E. 1981. Handbook of Mechanical and Electrical Systems for Buildings. McGraw-Hill, New York.

El-Wakil, M.M. 1985. Powerplant Technology. McGraw Hill, Singapore.

Holman, J.P. 1989. Heat Transfer. SI metric edit., McGraw-Hill, Singapore.

Kreider, J.F. & Kreith, F. 1982. Solar Heating and Cooling Active and Passive Design. 2nd edit., McGraw-Hill.

Marecki, J. 1988. Combined Heat and Power Generating Systems. Peter Peregrinus Ltd., London.

McQuiston, F.C. 1981. "Finned tube heat exchangers: state of the art for the air side." ASHRAE Transaction, Vol. 87, Part 1, pp.1077-1083.

SERI. 1988. Engineering Principles and Concepts for Active Solar Systems. Solar Energy Research Institute, Hemisphere Publishing Corporation, New York.

SMACNA. 1984. Energy Conservation Guidelines. Sheet Metal and Air Conditioning Contractors' National Association, Inc., U.S.A.

Tang, D. & Clarke, J.A. 1993. "Application of the Object Oriented Programming Paradigm to Building and Plant System Modelling." In Proceedings of Building Simulation '93, International Conference of the International Building Performance Simulation Association, August, Adelaide, Australia, pp.317-323.

CHAPTER EIGHT

SUMMARY AND CONCLUSIONS

In the human process of analysing the real world, a conversion of the real occurrences to a conceptual model within the reach of our mind and capability is unavoidable and that is in fact how knowledge has been developed in the history of mankind. It is not surprising in this process that we often come to conclusions which are theoretically sound and logical within the simplified framework but actually wrong because of an inappropriate extraction from the complex reality. Within the context of system simulation, the primitive part modelling approach here introduced is a step in the direction of imitating the reality within the constraints of continuous developments in computer technology, mathematics, fundamental theory of thermofluids, as well as the related engineering sciences. In essence, component modelling by primitive parts provides a unified mathematical structure which can retain the complexity of plant components in the real world, the convenience for the modellers to develop new models for various applications, and the potential for the models of to-day to be upgraded in pace with the state-of-the-art technology in the future.

8.1 Summary of Work Achieved

The following is a brief outline of the progression and achievements in this piece of work:

- i) A literature review has been given to the developments of the building and plant simulation in the past decades. The review showed that the developments had been driven by the community needs and evolutionary changes took place at different stages. The products of these had been the simulation softwares of different generations. Current development work in the field is a consequence of a major review in the mid 1980s searching for the ways ahead. There had been a strong wish of seeking integration of different studying fields in order to improve the simulation capability and accuracy. To achieve such a non-trivial task a flexible and sophisticated software structure and support is indispensable. An object oriented programming environment plus intelligent knowledge based user interface plus atomic/equation-based component models is possibly a solution for the simulation softwares of the coming generations. In the area of system simulation in particular, the need of a generalised plant database in the form of a taxonomy structure has been raised.

- ii) Based on the above review, three objectives have been set in this research study: firstly, to identify the energy and mass flow paths in real air conditioning systems so as to enhance development of plant component models from a comprehensive and fundamental approach; secondly, to give recommendation to a generalised plant database; and thirdly, to verify the work making use of the ESP-r system as the testing platform.

- iii) An analysis of the energy and mass flow paths in air conditioning systems was then carried out. It appears from the analysis that lots of the heat and mass transfer processes in real systems are either outside the intended psychrometric duties of the equipment themselves or too specific/intermittent in their occurrence and therefore, are often ignored in the component modelling process. A view has been put forward to develop a generalised plant database at the level allowing the inclusion, or exclusion, of some, or all of the energy and mass flow paths while their existence may be desirable or redundant for a particular simulation task. The concept of primitive part modelling was then evolved.

- iv) Theory review on plant component models in particular the heat transfer coils and fluid flow conduits gave insight to the modelling requirements. Subsequently a variety of air conditioning equipment have been explicitly modelled based on fundamental physical laws and the finite difference control volume conservation method. Extension of the method has been found a necessity when modelling the transport delay as well as the phase-change phenomena in fluid flows. A new numerical transport delay model has been proposed which is theoretically robust and more accurate than other models currently in use.

- v) Direct outcome of the modelling experience in point (iv) above has been the identification of 27 primitive parts, or atomic objects, each of which represents a distinct combined energy and mass transfer phenomenon. These primitive parts, when integrated through different combinations, can produce matrix templates representing component models of any air conditioning equipment. The rationale of primitive part modelling was explained through the superposition rule and several demonstrations of the methodology on typical air conditioning components were given. Matrix templates of the plant components obtained through the use of primitive parts were shown identical to those derived from a more conventional approach given in point (iv).

- vi) The possibility of extending this new modelling approach to other simulation environments was then reviewed. By appropriate modifications, the concept can apply to the more conventional sequential and simultaneous software environments like TRNSYS and HVACSIM+. However, a more positive

direction of development is the implementation in the neutral model format and the object oriented software structure, of which a link to the product modelling will be much promising.

vii) Validations of this new approach to plant modelling were then carried out making use of the PLT module of the ESP-r software as the testing platform. The 27 primitive parts have been added as a separate source file together with necessary changes and additions to the existing plant module. A number of new components built upon primitive parts have been added to the plant database. Three different validation approaches: analytical comparison, inter-model comparison and experimental validation were performed on various occasions. The results have verified that the plant components developed from primitive parts can be as accurate as, if not better than, the other modelling techniques popularly in use to-day.

viii) Several application examples which started from air conditioning equipment and extended to other thermal system (steam) components were presented to demonstrate the strength and flexibility of this new approach. The work has been fully justified in that at present these explicit multi-node models can be used flexibly in mix with other implicit fewer-node models to achieve a vast simulation objectives and in future, provides a unified mathematical structure to thermal system simulations at large. Possible future work has been suggested, of which the incorporation of automatic component generation will be most valuable to further simplify the modelling task of the simulationists and becomes an indispensable feature thinking about technology transfer to the majority of the building professionals as the final goal.

ix) From all of the above it can be seen that the objectives of this study raised at the early stage of the project has been fulfilled relatively in full.

8.2 The Significance

The idea of using primitive parts evolves in parallel with a number of new developments currently taking place in various countries in the 1990's, all in the direction of seeking a better simulation environment for the next generation softwares. There appears a clear direction of favouring an input-output free modular simultaneous simulation environment. In this way the use of the component models is broadened to override the hurdle of solving merely the pre-defined problems in the model-developers' mind.

The primitive part approach adopts the concept that the only way to analyse a real system as rigorously as possible is the provision of a mechanism that allows the inclusion of any energy or mass flow path which

interacts in the system in reality. Such a flow path can be steady, intermittent, or temporal - no matter in which form that can exist in reality. The concept comes from the simulation structure offered by ESP-r in that "for any energy flow path in the real world, there is a corresponding mathematical structure". Each primitive part is in essence an attempt to model a distinct thermal phenomenon that can appear in air conditioning systems. A component model built upon the primitive parts is therefore a fundamental model with explicit physical intents.

When attempting to build a model, a compromise must be made between the simplicity of the model and the accuracy of the results that affect a particular analytical task. It is important to note that the results obtained from computer simulation are valid only to the extent that the model approximates a given physical system. In determining a reasonably simplified model, we must decide carefully which physical variables and causal relationships are negligible and which are crucial to the accuracy of the model. Numerous trial-and-error procedures or sensitivity tests may have been involved in the decision-making process. The use of primitive parts helps to provide the flexibility and therefore simplify such a process. The conventional model-developing process, which starts from deriving either an algorithm or a set of algebraic-differential equations for a discretized nodal scheme, is replaced by a much simplified and structured process of identifying appropriate primitive parts, writing the matrix template, and then deriving matrix coefficients by arithmetic additions of primitive part coefficients.

Theoretically a component can be discretized into as many finite volumes or "nodes" as possible in the modelling process. During simulation, each node carry information about the thermal conditions at any time step, for instance temperatures, flow rates, thermal state of fluids etc. at a pre-defined sub-region of the component. In this sense, the simulation process of an explicitly modelled system can generate as many run-time thermal data as possible. This can help to provide answers to a wide range of problem definitions once spelt out by the users at the pre-simulation stage.

The primitive parts are the basic elements, or the "atomic" objects, upon which any plant sub-components, equipment or systems can be built upon. There is no reason why a building cannot be modelled in the same way. If this is the case, a plant system or a building-and-plant integrated simulation system can have a unified and integrated structure throughout. Following similar line of thought, if we are interest about the performance of an air-conditioning plant in an aircraft, an aircraft-and-plant integrated simulation model can also be developed in a unified framework without much difficulties. This provides a controlled complexity to the software architecture of an advanced simulation tool in the years to come.

A first and obvious way to make modelling more efficient is to re-use basic existing pieces or component models: modularity of the modelling itself. The use of primitive parts as a concept includes many good

features of the OO (object orientated) software environment. The component models as a result are highly modular and hierarchical. The flexible and unified simulation environment allows the re-use of computer code to a high extent, and make easy the model validation and software maintenance work. As a matter of fact, model validation is much easier to be done at the component or sub-component level than the whole system level. It is deemed when the sub-component models were validated extensively, the users will have more confidence about the reliability and validity of the meta-component models that have been built from the sub-parts. In an input-and-output free simulation environment, the same component models can be transformed to work in more than one software simulation platform. One simplest way to achieve this is to develop the generalized plant library in a neutral model format, which can then be added to any simulation environment through the use of translators. Therefore the research efforts or "good products" from different simulation communities can be readily shared whereas "unsatisfactory products" (like the existence of bugs in a computer model) can be readily located and rectified because of the enlarged circulation and usage. The work, when moving in the direction of product modelling, will benefit the integrated intelligent building-design systems in the long run.

As a summary, a number of advantages can be identified in using this generalised and explicit approach to component modelling. They are:

- i) input-ouput free and simultaneous modelling environment,
- ii) use of fundamental modelling approach,
- iii) flexible description of real systems with reasonable accuracy,
- iv) thorough information for results analysis,
- v) controlled complexity and integrity of source code,
- vi) modular and hierarchical OO features,
- vii) simplified software maintenance, development, and validation work,
- viii) facilitating joint research efforts.

8.3 Conclusions

In the human process of analysing the real world, a conversion of the real occurrences to a conceptual model within the reach of our mind and capability is unavoidable and that is in fact how knowledge has been developed in the history of mankind. It is not surprising in this process that we often come to conclusions which are theoretically sound and logical within the simplified framework but actually wrong because of an inappropriate extraction from the complex reality. Within the context of system simulation, the primitive part modelling approach here introduced is a step in the direction of imitating the reality

within the constraints of continuous developments in computer technology, mathematics, fundamental theory of thermofluids, as well as the related engineering sciences. In essence, component modelling by primitive parts provides a unified mathematical structure which can retain the complexity of plant components in the real world, the convenience for the modellers to develop new models for various applications, and the potential for the models of to-day to be upgraded in pace with the state-of-the-art technology in the future. Decomposing a plant component into primitive pieces that precisely describe a distinct combined energy and mass flow behaviour allows the representation of all real components by a minimum set of sub-parts in the plant database and yet the maximum flexibility upto the modeller's personal perception of the best way to perform a simulation task. The method has been proved workable through the validation exercises and justified through application examples. A highly modular and hierarchical structure of plant component taxonomy can be built and an intelligent knowledge base can be added in the times to come.

The conceptual framework of primitive part modelling, although developed via air conditioning system, is actually not system specific. It can be generalised to apply to any thermal systems within the context of building, or extended for use in any industrial or non-industrial processes. New primitive parts can always be added where necessary. Afterall, the Universe began with the processes of energy and mass exchanges long before the existence of building or plant. The work here hopefully can trigger new thoughts and generate new dimensions in the wide applications of comprehensive dynamic thermal simulation.

Appendix A

LIST OF SYMBOLS

English Letter Symbols

A	area, m ²
A	matrix coefficient, left hand side
B	matrix coefficient, right hand side
C	matrix coefficient
C	specific heat of solid, J/kg.K
C	thermal capacitance of solid, J/kg.K
C _f	correction factor, -
C _p	specific heat of fluid at constant pressure, J/kg.K
D	diameter, m
f	friction factor, -
F	view factor, -
g	moisture content, kg/kg dry air
G	mass velocity, kg/m ² .s
h	heat transfer coefficient, W/m ² .K
H	enthalpy, J/kg
H	height, m
j	j factor, -
k	thermal conductivity, W/m.K
K	thermal conductance, W/K
K _d	mass diffusion coefficient, kg/m ²
l	length, m
L	length, m
m	mass flow rate, kg/s
M	mass, kg
N	number of
N _i	primitive part connectivity index, -
Nu	Nusselt number
P	pressure, Pa
Pr	Prandtl number
Q	heat flux, W
r	radius, m
R	thermal resistance, m ² .K/W
Re	Reynolds number
RH	relative humidity, %
SHR	sensible heat ratio, -
St	Stanton number
t	time, s
u	velocity, m/s
U	overall heat transfer coefficient, W/m ² .K
v	volume flow rate, m ³ /s
V	volume, m ³
W	power, W
x	dryness fraction, -
x	spacing or thickness, m
X	matrix coefficient
y	distance or thickness, m
Y	length, m

Greek Letter Symbols

α	weighting factor
δ	small distance, m
ε	emissivity, -
ϕ	view angle, rad
η	efficiency or effectiveness, -
μ	dynamic viscosity, kg/m.s
ν	kinematic viscosity, m ² /s
θ	temperature, °C
Θ	absolute temperature, K
ρ	density, kg/m ³
λ	normalized distance, -
τ	time constant, s

Subscripts

a	air
c	condensation
c	conduit
d	direction
d	dry
dew	dew point
e	environment or ambient
f	face
f	fin
f	frost
f	saturated liquid
fg	latent exchange
g	saturated vapour
i	internal or inside
m	mean
m	metal
o	outside
p	prime
r	refrigerant
r	rated
s	solid or surface
s	saturated air
set	set point
TU	transfer unit
v	vapour
w	water or wet
x	cross-section or exposed

Superscript

*	present time value
---	--------------------

Appendix B

List of Primitive Parts

- 1 **Thermal conduction**
 - 1.1 solid to solid
 - 1.2 with ambient

- 2 **Surface convection**
 - 2.1 with moist air
 - 2.2 with 2-phase fluid
 - 2.3 with 1-phase fluid
 - 2.4 with ambient

3. **Surface radiation**
 - 3.1 with local surface
 - 3.2 with ambient surface

4. **Flow upon surface**
 - 4.1 for moist air; 3 nodes
 - 4.2 for 2-phase fluid; 3 nodes
 - 4.3 for 1-phase fluid; 3 nodes
 - 4.4 for moist air; 2 nodes
 - 4.5 for 1-phase fluid; 2 nodes

- 5 **Flow divider & inducer**
 - 5.1 Flow diverger (for all fluid)
 - 5.2 Flow multiplier (for all fluid)
 - 5.3 Flow inducer (for all fluid)

- 6 **Flow converger**
 - 6.1 for moist air
 - 6.2 for 2-phase fluid
 - 6.3 for 1-phase fluid
 - 6.4 for leak-in moist air from outside

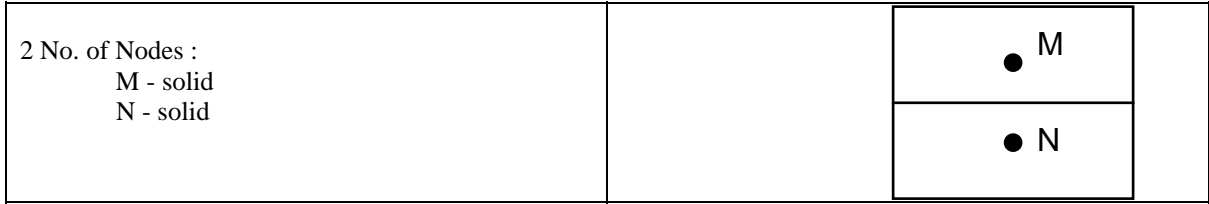
- 7 **Flow upon water spray**
 - 7.1 for moist air

- 8 **Fluid injection**
 - 8.1 water/steam to moist air

- 9 **Fluid accumulator**
 - 9.1 for moist air
 - 9.2 for liquid

- 10 **Heat injection**
 - 10.1 to solid
 - 10.2 to vapour-generating fluid
 - 10.3 to moist air

Part No. 1.1 Thermal Conduction (solid to solid)



Energy flow matrix :

$$\begin{bmatrix} A(11,1) & A(11,2) \\ A(11,3) & A(11,4) \end{bmatrix} * \begin{bmatrix} \theta_m \\ \theta_n \end{bmatrix} = \begin{bmatrix} B(11,1) \\ B(11,2) \end{bmatrix}$$

where,

$$A(11,1) = -\alpha C_{mn} - M_m C_m / (N i_m \delta t)$$

$$A(11,2) = \alpha C_{mn}$$

$$A(11,3) = \alpha C_{mn}$$

$$A(11,4) = -\alpha C_{mn} - M_n C_n / (N i_n \delta t)$$

$$B(11,1) = [(1-\alpha) C_{mn}^* - M_m^* C_m^* / (N i_m \delta t)] \theta_m^* - (1-\alpha) C_{mn}^* \theta_n^*$$

$$B(11,2) = [(1-\alpha) C_{mn}^* - M_n^* C_n^* / (N i_n \delta t)] \theta_n^* - (1-\alpha) C_{mn}^* \theta_m^*$$

where C_{mn} = reciprocal of thermal resistance between M and N

Mass flow matrix (for both first and second phase mass balance):

$$A(11,1) = 1/N i_m$$

$$A(11,2) = 0$$

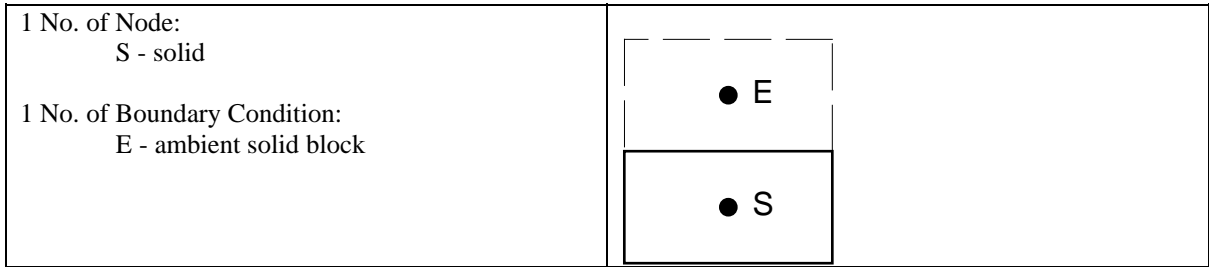
$$A(11,3) = 0$$

$$A(11,4) = 1/N i_n$$

$$B(11,1) = 0$$

$$B(11,2) = 0$$

Part No. 1.2 Thermal Conduction (with ambient solid block)



Energy flow matrix :

$$[A(12,1)] * [\theta_s] = [B(12,1)]$$

where,

$$A(12,1) = -\alpha C_{ES} - M_S \cdot C_S / (N_{iS} \cdot \delta t)$$

$$B(12,1) = [(1 - \alpha) C_{ES}^* - M_S^* C_S^* / (N_{iS} \delta t)] \theta_s^* - [\alpha C_{ES} \theta_e + (1 - \alpha) C_{ES}^* \theta_e^*]$$

where C_{ES} = reciprocal of thermal resistance between S and E

Mass flow matrice

for first phase(liquid):

$$A(12,1) = 1/N_{iS}$$

$$B(12,1) = 0$$

For second phase (vapour):

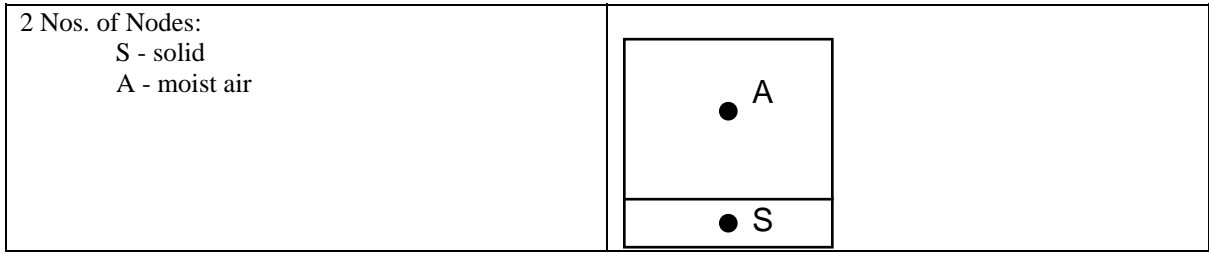
$$A(12,1) = 1/N_{iS}$$

$$B(12,1) = 0$$

Notes:

The thermal state of the ambient solid block is taken as not controllable by the heat exchange with the solid node S; θ_e thus becomes an external excitation and its values during the simulation period is user specified.

Part No. 2.1 Surface Convection (with moist air)



Energy flow matrix

$$\begin{bmatrix} A(21,1) & A(21,2) \\ A(21,3) & A(21,4) \end{bmatrix} * \begin{bmatrix} \theta_s \\ \theta_a \end{bmatrix} = \begin{bmatrix} B(21,1) \\ B(21,2) \end{bmatrix}$$

where,

$$A(21,1) = -\alpha C_{as} - M_s \cdot C_s / (Ni_s \cdot \delta t)$$

$$A(21,2) = \alpha C_{as}$$

$$A(21,3) = \alpha C_{as}$$

$$A(21,4) = -\alpha C_{as} - M_a \cdot C_{pma} / (Ni_a \cdot \delta t)$$

$$B(21,1) = [(1-\alpha) C_{as}^* - M_s^* C_s^* / (Ni_s \delta t)] \theta_s^* - (1-\alpha) C_{as}^* \theta_a^* + [\alpha C_{av} + (1-\alpha) C_{av}^*]$$

$$B(21,2) = [(1-\alpha) C_{as}^* - M_a^* C_{pma}^* / (Ni_a \delta t)] \theta_a^* - (1-\alpha) C_{as} \theta_s^*$$

Note :

$$C_{as} = h_{as} A_{as}$$

$$C_{pma} = C_{pa} + g_a C_{pv}$$

$$C_{av} = Hf g_a m_v$$

Mass flow matrix

for first phase(dry air):

$$A(21,1) = 1/Ni_s$$

$$A(21,2) = 0$$

$$A(21,3) = 0$$

$$A(21,4) = 1/Ni_a$$

$$B(21,1) = 0$$

$$B(21,2) = 0$$

For second phase (water vapour):

$$A(21,1) = 1/Ni_s$$

$$A(21,2) = 0$$

$$A(21,3) = 0$$

$$A(21,4) = 1/Ni_a$$

$$B(21,1) = 0$$

$$B(21,2) = -Cc$$

where,

$$Cc = 0 \quad \text{for dry surface i.e. when } \theta_s > \theta_{a,dew} \text{ \& } M_w = 0$$

$$= K_d A_{as} (g_a - g_s) \quad \text{for wet surface i.e. } M_w > 0$$

where M_w is the amount of condensate on the surface.
 g_s is the saturated moist content at θ_s

Notes:

1. If M_v is the total mass of water vapour in the control volume of moist air, then

$$M_v = M_v^* + m_v \cdot \delta t$$

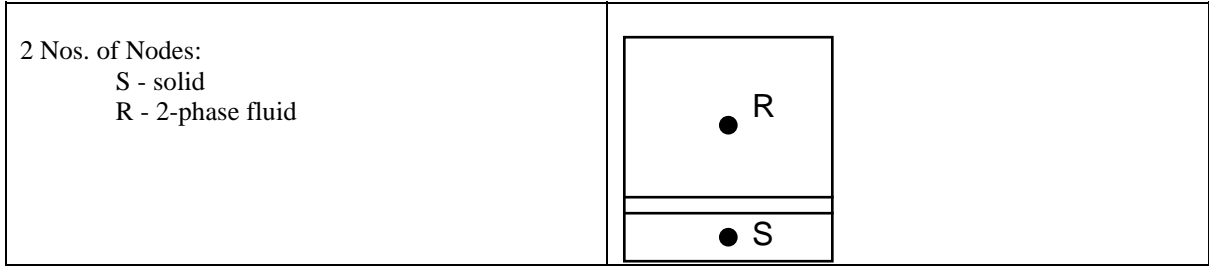
$$M_w = M_w^* - m_v \cdot \delta t$$

2. If $M_w < 0$ as calculated from the equation above then

$$M_w = 0$$

$$m_v = M_w^*$$

Part No. 2.2 Surface Convection (with 2-phase fluid)



Energy flow matrix

$$\begin{bmatrix} A(22,1) & A(22,2) \\ A(22,3) & A(22,4) \end{bmatrix} * \begin{bmatrix} \theta_s \\ \theta_r \end{bmatrix} = \begin{bmatrix} B(22,1) \\ B(22,2) \end{bmatrix}$$

where,

$$A(22,1) = -\alpha C_{RS} - M_s C_s / (N_i s \delta t)$$

$$A(22,2) = \alpha C_{RS}$$

$$A(22,3) = 0$$

$$A(22,4) = 1$$

$$B(22,1) = [(1-\alpha) C_{RS}^* - M_s^* C_s^* / (N_i s \delta t)] \theta_s^* - (1-\alpha) C_{RS}^* \theta_r^* + [\alpha C_{wv} + (1-\alpha) C_{wv}^*]$$

$$B(22,2) = \theta_{sat}$$

where,

$$\begin{aligned} C_{RS} &= h_{RS} A_{RS} \\ C_{wv} &= H f g_r C_c \\ C_c &= h_{RS} A_{RS} (\theta_r - \theta_s) / h f g_r \end{aligned}$$

Mass flow matrix

for first phase(liquid):

$$A(22,1) = 1/N_i s$$

$$A(22,2) = 0$$

$$A(22,3) = 0$$

$$A(22,4) = 1/N_i r$$

$$B(22,1) = 0$$

$$B(22,2) = Cc$$

For second phase (vapour):

$$A(22,1) = 1/Ni_s$$

$$A(22,2) = 0$$

$$A(22,3) = 0$$

$$A(22,4) = 1/Ni_r$$

$$B(22,1) = 0$$

$$B(22,2) = -Cc$$

Notes:

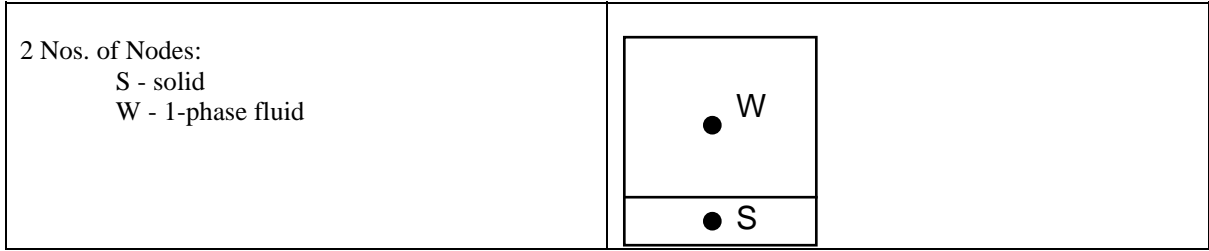
- $$M_v = M_v^* - Cc \cdot \delta t$$
$$M_w = M_w^* + Cc \cdot \delta t$$
$$M_r = M_w + M_v$$
$$M_r C_{p_r} = M_w C_{p_w} + M_v C_{p_v}$$

- If $M_w < 0$ as calculated from the equation above then
$$M_w = 0$$
$$m_v = M_r$$
or if $M_v < 0$ as calculated from the equation above then

$$M_v = 0$$
$$m_w = M_r$$

- If either $M_v = 0$ or $M_w = 0$, switch to PN 2.3 surface convection (with single phase fluid).

Part No. 2.3 Surface Convection (with 1-phase fluid)



Energy flow matrix

$$\begin{bmatrix} A(23,1) & A(23,2) \\ A(23,3) & A(23,4) \end{bmatrix} * \begin{bmatrix} \theta_s \\ \theta_w \end{bmatrix} = \begin{bmatrix} B(23,1) \\ B(23,2) \end{bmatrix}$$

where,

$$A(23,1) = -\alpha C_{SW} - M_S \cdot C_S / (Ni_S \cdot \delta t)$$

$$A(23,2) = \alpha C_{SR}$$

$$A(23,3) = \alpha C_{SW}$$

$$A(23,4) = -\alpha C_{SW} - M_W \cdot Cp_W / (Ni_W \cdot \delta t)$$

$$B(23,1) = [(1-\alpha) C_{SW}^* - M_S^* C_S^* / (Ni_S \delta t)] \theta_s^* - (1-\alpha) C_{SW}^* \theta_w^*$$

$$B(23,2) = [(1-\alpha) C_{SW}^* - M_W^* Cp_W^* / (Ni_W \delta t)] \theta_w^* - (1-\alpha) C_{SW}^* \theta_s^*$$

where,

$$C_{SW} = h_{SW} A_{SW}$$

Mass flow matrix

for first phase(liquid):

$$A(23,1) = 1/Ni_S$$

$$A(23,2) = 0$$

$$A(23,3) = 0$$

$$A(23,4) = 1/Ni_w$$

$$B(23,1) = 0$$

$$B(23,2) = 0$$

For second phase (vapour):

$$A(23,1) = 1/Ni_s$$

$$A(23,2) = 0$$

$$A(23,3) = 0$$

$$A(23,4) = 1/Ni_w$$

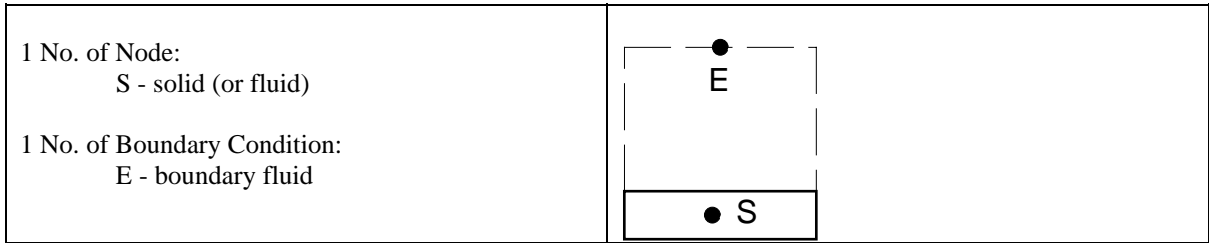
$$B(23,1) = 0$$

$$B(23,2) = 0$$

Notes:

1. If θ_w reaches boiling point, switch to PN 2.2 surface convection (with 2-phase fluid).

Part No. 2.4 Surface Convection (with ambient)



Energy flow matrix :

$$[A(24,1)] * [\theta_s] = [B(24,1)]$$

where,

$$A(24,1) = -\alpha C_{es} - M_s \cdot C_s / (N_i \delta t)$$

$$B(24,1) = [(1-\alpha) C_{es}^* - M_s^* C_s^* / (N_i \delta t)] \theta_s^* - [\alpha C_{es} \theta_e + (1-\alpha) C_{es}^* \theta_e^*]$$

and, $C_{es} = h_{es} A_{es}$ for solid
 $= U_{es} A_{es}$ for fluid

Mass flow matrix

for first phase(liquid):

$$A(24,1) = 1/N_i$$

$$B(24,1) = 0$$

For second phase (vapour):

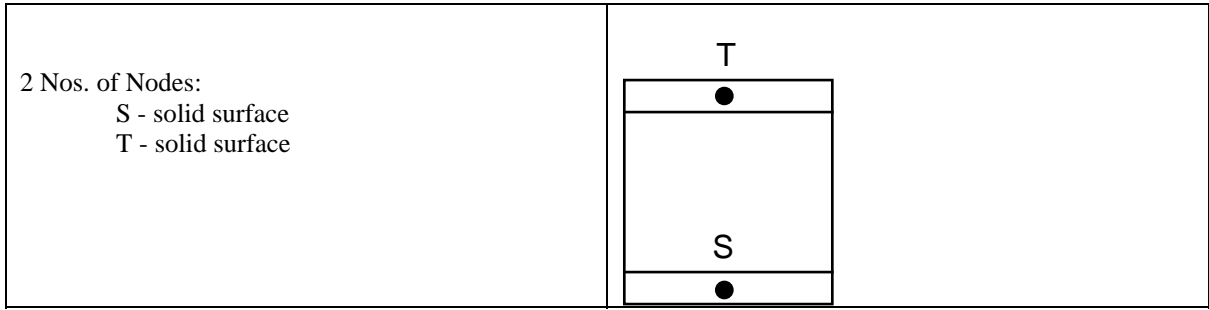
$$A(24,1) = 1/N_i$$

$$B(24,1) = 0$$

Notes:

1. The thermal state of the boundary fluid in bulk is taken as not controllable by the heat exchange with the surface; θ_e thus becomes an external excitation and its values during the simulation period is user specified.
2. Possibility of mass exchange (e.g. condensation) on the surface is not considered.

Part No. 3.1 Surface Radiation (with local surface)



Energy flow matrix

$$\begin{bmatrix} A(31,1) & A(31,2) \\ A(31,3) & A(31,4) \end{bmatrix} * \begin{bmatrix} \theta_s \\ \theta_t \end{bmatrix} = \begin{bmatrix} B(31,1) \\ B(31,2) \end{bmatrix}$$

where,

$$A(31,1) = -\alpha C_{st} - M_s \cdot C_s / (Ni_s \cdot \delta t)$$

$$A(31,2) = \alpha C_{st}$$

$$A(31,3) = \alpha C_{st}$$

$$A(31,4) = -\alpha C_{st} - M_t \cdot C_t / (Ni_t \cdot \delta t)$$

$$B(31,1) = [(1-\alpha) C_{st}^* - M_s^* C_s^* / (Ni_s \delta t)] \theta_s^* - (1-\alpha) C_{st}^* \theta_t^*$$

$$B(31,2) = [(1-\alpha) C_{st}^* - M_t^* C_t^* / (Ni_t \delta t)] \theta_t^* - (1-\alpha) C_{st}^* \theta_s^*$$

where,

$$C_{st} = h_{st} A_{st} = h_{ts} A_{ts}$$

Mass flow matrice

for first phase(liquid):

$$A(31,1) = 1/Ni_s$$

$$A(31,2) = 0$$

$$A(31,3) = 0$$

$$A(31,4) = 1/Ni_t$$

$$B(31,1) = 0$$

$$B(31,2) = 0$$

For second phase (vapour):

$$A(31,1) = 1/Ni_s$$

$$A(31,2) = 0$$

$$A(31,3) = 0$$

$$A(31,4) = 1/Ni_t$$

$$B(31,1) = 0$$

$$B(31,2) = 0$$

Notes:

1. The values of the radiative heat transfer coefficients h_{st} & h_{ts} are expressed in terms of the present-time surface temperatures because of the nature of the Stefan's law, in that for black body radiation,

$$h_{st} = F_{s-t} \sigma f(\Theta_s^*, \Theta_t^*)$$

$$h_{ts} = F_{t-s} \sigma f(\Theta_s^*, \Theta_t^*)$$

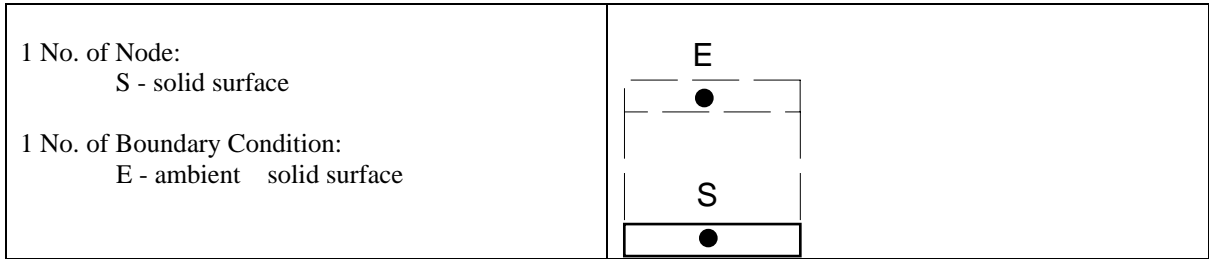
where, F - view factor
 σ - Boltman's constant

$$f(\Theta_s^*, \Theta_t^*) = [(\Theta_s^*)^3 + (\Theta_s^*)^2 \cdot \Theta_t^* + \Theta_s^* \cdot (\Theta_t^*)^2 + (\Theta_t^*)^3]$$

2. The Theorem of Reciprocity states that

$$F_{s-t} A_s = F_{t-s} A_t$$

Part No. 3.2 Surface Radiation (with ambient surface)



Energy flow matrix :

$$[A(32,1)] * [\theta_s] = [B(32,1)]$$

where,

$$A(32,1) = -\alpha C_{es} - M_s \cdot C_s / (N_{i_s} \cdot \delta t)$$

$$B(32,1) = [(1-\alpha) C_{es}^* - M_s^* C_s^* / (N_{i_s} \delta t)] \theta_s^* - [\alpha C_{es} \theta_e + (1-\alpha) C_{es}^* \theta_e^*]$$

$$\text{and, } C_{es} = h_{es} A_s$$

Mass flow matrix

for first phase(liquid):

$$A(32,1) = 1/N_{i_s}$$

$$B(32,1) = 0$$

For second phase (vapour):

$$A(32,1) = 1/N_{i_s}$$

$$B(32,1) = 0$$

Notes:

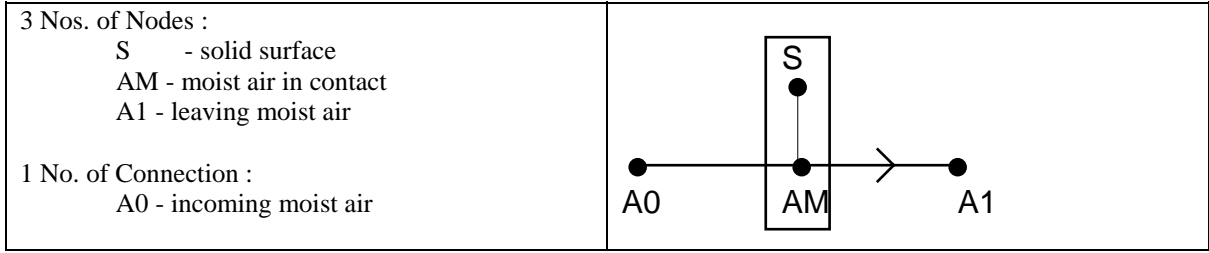
1. The thermal state of the ambient surface is taken as not controllable by the heat exchange with the surface S; θ_e thus becomes an external excitation and its values during the simulation period is user specified.
2. The values of the radiative heat transfer coefficient h_{es} are expressed in terms of the present-time surface temperatures because of the nature of the Stefan's law, in that for black body radiation,

$$h_{es} = F_{e-s} \sigma f(\Theta_s^*, \Theta_e^*)$$

where, F - view factor
 σ - Boltman's constant

$$f(\Theta_s^*, \Theta_e^*) = [(\Theta_s^*)^3 + (\Theta_s^*)^2 \cdot \Theta_e^* + \Theta_s^* \cdot (\Theta_e^*)^2 + (\Theta_e^*)^3]$$

Part No. 4.1 Flow upon surface (for moist air; 3 nodes)



Energy flow matrix :

$$\begin{bmatrix} A(41,1) & A(41,2) & 0 & 0 \\ A(41,4) & A(41,5) & A(41,6) & A(41,11) \\ 0 & A(41,8) & A(41,9) & 0 \end{bmatrix} * \begin{bmatrix} \theta_s \\ \theta_{am} \\ \theta_{a1} \\ \theta_{a0} \end{bmatrix} = \begin{bmatrix} B(41,1) \\ B(41,2) \\ B(41,3) \end{bmatrix}$$

where,

self-coupled & cross-coupled coefficients:

$$A(41,1) = -\alpha C_{as} - (M_s C_s / Ni_s \cdot \delta t)$$

$$A(41,2) = \alpha C_{as}$$

$$A(41,4) = \alpha C_{as}$$

$$A(41,5) = -\alpha C_{as} - M_a C_{pma} / Ni_{a1} \cdot \delta t$$

$$A(41,6) = -\alpha C_{a1}$$

$$A(41,8) = -1$$

$$A(41,9) = 1$$

$$A(41,11) = \alpha C_{a0}$$

$$A(41,12) = 0$$

present-time & excitation coefficients:

$$B(41,1) = [(1 - \alpha) C_{as}^* - M_s^* C_s^* / (Ni_s \delta t)] \theta_s^* - (1 - \alpha) C_{as}^* \theta_{a1}^* + [\alpha C_{av} + (1 - \alpha) C_{av}^*]$$

$$B(41,2) = [(1 - \alpha) C_{as}^* - M_a^* C_{pma}^* / (Ni_{a1} \delta t)] \theta_{am}^* - (1 - \alpha) C_{as}^* \theta_s^* - (1 - \alpha) C_{a0}^* \theta_{a0}^*$$

$$- (1-\alpha) C_{a1} * \theta_{a1} *$$

$$B(41,3) = 0$$

where,

$$\begin{aligned} M_a &= \text{mass of dry air in the control volume of moist air} \\ C_{pma} &= \text{specific heat of moist air at } \theta_{am} = C_{pam} + g_{am} C_{pvm} \\ C_{a0} &= m_{a0} C_{pa0} + m_{v0} C_{pv0} \\ C_{a1} &= m_{a1} C_{pa1} + m_{v1} C_{pv1} \\ C_{as} &= h_{as} A_{as} \\ C_{av} &= - h_{fg} (m_{v0} - m_{v1}) = - h_{fg} C_c \end{aligned}$$

$$\text{For dry surface, } m_{v1} = m_{v0} \quad \text{so } C_{av} = 0$$

In case the DELAY flag is ON, the following coefficients will be revised as

$$A(41,4) = 0$$

$$A(41,5) = 1$$

$$A(41,6) = 0$$

$$A(41,4) = 0$$

$$A(41,8) = 0$$

$$A(41,11) = 0$$

$$B(41,2) = \text{DELAY}(\theta_{am})$$

$$B(41,3) = \text{DELAY}(\theta_{a1})$$

Mass flow matrixe :

for first phase (dry air):

$$A(41,1) = 1/Ni_s$$

$$A(41,2) = 0$$

$$A(41,4) = 0$$

$$A(41,5) = 1/Ni_{am}$$

$$A(41,6) = 0$$

$$A(41,8) = -1$$

$$A(41,9) = 1$$

$$A(41,11) = -1$$

$$B(41,1) = 0$$

$$B(41,2) = 0$$

$$B(41,3) = 0$$

for second phase (water vapour):

$$A(41,1) = 1/Ni_s$$

$$A(41,2) = 0$$

$$A(41,4) = 0$$

$$A(41,5) = 1/Ni_{am}$$

$$A(41,6) = 0$$

$$A(41,8) = -1$$

$$A(41,9) = 1$$

$$A(41,11) = -1$$

$$B(41,1) = 0$$

$$B(41,2) = -Cc$$

$$B(41,3) = 0$$

where,

$$Cc = \begin{cases} 0 & \text{for dry surface i.e. when } \theta_s > \theta_{a0dew} \text{ \& } M_w = 0 \\ K_d A_{as} (g_{am} - g_s) & \text{for wet surface i.e. } M_w > 0 \end{cases}$$

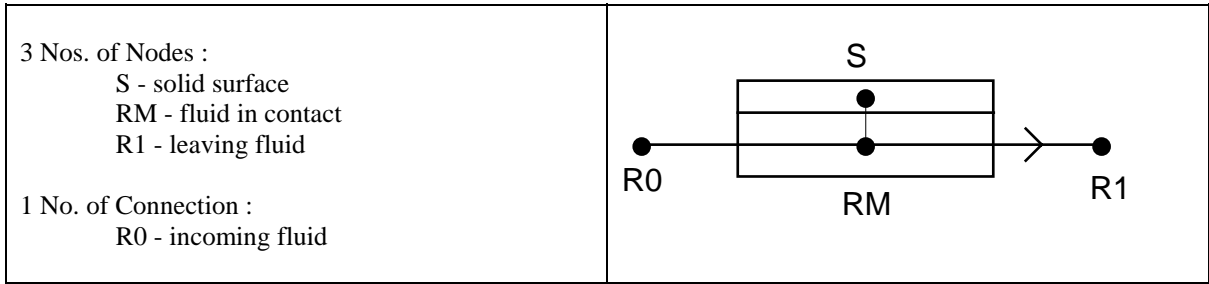
where M_w is the amount of condensate on the surface;
 g_s is the saturated moist content at θ_s .

Notes:

For the equation: $M_w = M_w^* + Cc \cdot \delta t$

- i) If $M_w < 0$, then $M_w = 0$ and $Cc = -M_w^*$
- ii) If $M_w > M_{max}$ where M_{max} specifies the maximum condensate holding capacity on the surface S, then $M_w = M_{max}$.

Part No. 4.2 Flow upon surface (for 2-phase fluid)



Energy flow matrix :

$$\begin{bmatrix} A(42,1) & A(42,2) & 0 & 0 \\ A(42,4) & A(42,5) & A(42,6) & A(42,11) \\ 0 & A(42,8) & A(42,9) & 0 \end{bmatrix} * \begin{bmatrix} \theta_s \\ \theta_{rm} \\ \theta_{r1} \\ \theta_{r0} \end{bmatrix} = \begin{bmatrix} B(42,1) \\ B(42,2) \\ B(42,3) \end{bmatrix}$$

where,

i) when $\theta_{rm} = \theta_{sat}$

self-coupled and cross-coupled coefficients:

$$\begin{aligned} A(42,1) &= -\alpha C_{RS} - (M_S C_S / Ni_S \cdot \delta t) \\ A(42,2) &= 0 \\ A(42,4) &= 0 \\ A(42,5) &= 1 \\ A(42,6) &= 0 \\ A(42,8) &= 0 \\ A(42,9) &= 1 \\ A(42,11) &= 0 \end{aligned}$$

present-time & excitation coefficients:

$$\begin{aligned} B(42,1) &= [(1-\alpha) C_{RS}^* - M_S^* C_S^* / (Ni_S \cdot \delta t)] \theta_s^* - (1-\alpha) C_{RS}^* \theta_{rm}^* - \alpha C_{RS}^* \theta_{sat} \\ B(42,2) &= \theta_{sat} \\ B(42,3) &= \theta_{rl} \end{aligned}$$

where θ_{rl} is at the value of the previous iteration or of the previous time step

ii) If θ_{rm} not equal to θ_{sat} for a particular time step, then

self-coupled coefficients:

$$A(42,1) = -\alpha C_{rs} - M_s C_s / (N_{is} \cdot \delta t)$$

$$A(42,2) = \alpha C_{rs}$$

$$A(42,4) = \alpha C_{rs}$$

$$A(42,5) = -\alpha C_{rs} - M_w C_{pwm} / (N_{irm} \cdot \delta t)$$

$$A(42,6) = -\alpha C_{r1}$$

$$A(42,8) = -1$$

$$A(42,9) = 1$$

$$A(42,11) = -\alpha C_{r0}$$

present-time & excitation coefficients:

$$B(42,1) = [(1-\alpha) C_{rs}^* - M_s^* C_s^* / (N_{is} \cdot \delta t)] \theta_s^* - (1-\alpha) C_{rs}^* \theta_{rm}^* - \alpha C_{rs}^* \theta_{sat}$$

$$B(42,2) = -(1-\alpha) C_{rs}^* \theta_s^* + [(1-\alpha) C_{rs}^* - M_w^* C_{pwm}^* / (N_{irm} \cdot \delta t)] \theta_{rm}^* + (1-\alpha) C_{r1}^* \theta_{r1}^* - (1-\alpha) C_{r0}^* \theta_{r0}^*$$

$$B(42,3) = 0$$

where,

$$C_{rs} = h_{rs} A_{rs}$$

$$M_w = M_{wt} (1-x_{r1})$$

Note :

r	- 2-phase fluid	
v	- vapour	
w	- liquid	
wt	- fluid entirely at liquid state	
x_{ri}	- dryness fraction	$= m_{vi} / m_{ri}$ where $i = 0, 1$

Mass flow matrix:

for first phase (liquid):

$$\begin{aligned}
A(42,1) &= 1/Ni_s \\
A(42,2) &= 0 \\
A(42,4) &= 0 \\
A(42,5) &= 1/Ni_{rm} \\
A(42,6) &= 0 \\
A(42,8) &= -1 \\
A(42,9) &= 1 \\
A(42,11) &= -1 \\
B(42,1) &= 0 \\
B(42,2) &= m_c \\
B(42,3) &= 0
\end{aligned}$$

for second phase (vapour):

$$\begin{aligned}
A(42,1) &= 1/Ni_s \\
A(42,2) &= 0 \\
A(42,4) &= 0 \\
A(42,5) &= 1/Ni_{rm} \\
A(42,6) &= 0 \\
A(42,8) &= -1 \\
A(42,9) &= 1 \\
A(42,11) &= -1 \\
B(42,1) &= 0 \\
B(42,2) &= -m_c \\
B(42,3) &= 0
\end{aligned}$$

where m_c = condensation rate $= m_{w1} - m_{w0} = m_{v0} - m_{v1}$

Notes :

1. No accumulation of fluid mass in the component is generally assumed (i.e. incompressible flow)

and therefore $m_{r0} = m_{rm} = m_{r1}$).

2. Q_s represents the heat transfer rate from solid surface to fluid at 2-phase flow,
 $Q_s = h_{rs} A_{rs} (\theta_s - \theta_{sat})$

If $Q_s > 0$, fluid is heated, or
 $Q_s < 0$, fluid is cooled.

3. Under 2-phase flow fluid temperatures θ_{rm} & θ_{r1} are determined at the same time when the 1st & 2nd mass balances are solved; the following 3 individual cases are considered separately:

Case A $m_{w0} \neq 0$ & $m_{v0} \neq 0$ - 2-phase flow at inlet
 Case B $m_{w0} > 0$ & $m_{v0} = 0$ - sub-cooled liquid at inlet
 Case C $m_{w0} = 0$ & $m_{v0} > 0$ - superheated vapour at inlet

4. For Case A, $\theta_{r0} = \theta_{rm} = \theta_{sat}$; m_c & θ_{r1} can be determined through the following procedure:

Firstly let $m_e = Q_s / H_{fg}$

- i) If $0 < m_e < m_{w0}$ or $0 > m_e > -m_{v0}$, then 2-phase fluid flow at outlet
 $m_c = -m_e$
 $\theta_{r1} = \theta_{sat}$

- ii) If $m_e \leq -m_{v0}$ (condensing process), then sub-cooled liquid flow at outlet
 $m_c = m_{v0}$

$$\theta_{r1} = \theta_{sat} + \frac{Q_s + H_{fg} m_{v0}}{m_{r0} C_{p_{wm}}}$$

- iii) If $m_e \geq m_{w0}$ (evaporating process), then superheated vapour flow at outlet
 $m_c = -m_{w0}$

$$\theta_{out} = \theta_{sat} + \frac{Q_s - H_{fg} m_{w0}}{m_{r0} C_{p_{vm}}} - \frac{M_w^* H_{fg}}{\delta t m_{r0} C_{p_{vm}}}$$

$\theta_{r1} =$ the smaller value comparing θ_{sat} & θ_{out}

5. For Case B,

- i) If $\theta_{r0} < \theta_{sat}$ & $\theta_{r1} < \theta_{sat}$, then subcooled liquid always ($\theta_{rm} \neq \theta_{sat}$) and
 $m_c = 0$

- ii) If $\theta_{r0} < \theta_{sat}$ & $\theta_{rm} \geq \theta_{sat}$ at an iteration step, then evaporation started from subcooled liquid;

set $\theta_{rm} = \theta_{sat}$

let

$$m_e = \frac{Q_s - m_{w0} C_{p_{w0}} (\theta_{sat} - \theta_{r0})}{H_{fg}}$$

If $m_e \leq m_{w0}$, then $m_c = -m_e$ (wet vapour at outlet) & $\theta_{r1} = \theta_{sat}$

If $m_e > m_{w0}$, then $m_c = -m_{w0}$ (superheated vapour at outlet)

$$\theta_{out} = \theta_{sat} + \frac{H_{fg} (m_e - m_{w0})}{m_{r0} C_{p_{vm}}} - \frac{M_w^* H_{fg}}{\delta t m_{r0} C_{p_{r0}}}$$

θ_{r1} = the smaller value comparing θ_{sat} & θ_{out}

6. For Case C,

i) If $\theta_{r0} > \theta_{sat}$ & $\theta_{r1} > \theta_{sat}$, then superheated vapour always ($\theta_{rm} \neq \theta_{sat}$) and $m_c = 0$

ii) If $\theta_{r0} > \theta_{sat}$ & $\theta_{rm} \leq \theta_{sat}$ at an iteration step, then condensation started from superheated vapour;

set $\theta_{rm} = \theta_{sat}$

let

$$m_e = \frac{Q_s + m_{v0} C_{p_{v0}} (\theta_{r0} - \theta_{sat})}{H_{fg}}$$

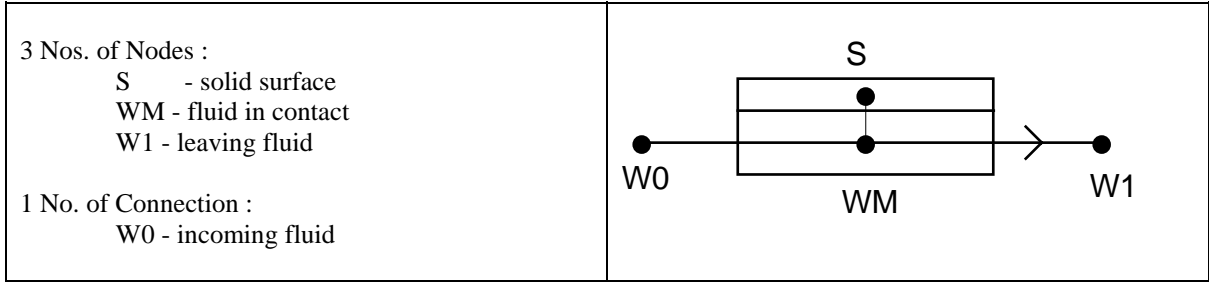
If $m_e \geq -m_{v0}$, then $m_c = -m_e$ (wet vapour at outlet)

$$\theta_{r1} = \theta_{sat}$$

If $m_e < -m_{v0}$, then $m_c = m_{v0}$ (subcooled liquid at outlet)

$$\theta_{r1} = \theta_{sat} + \frac{H_{fg} (m_e + m_{v0})}{m_{r0} C_{p_{wm}}}$$

Part No. 4.3 Flow upon surface (for single-phase fluid; 3 nodes)



Energy flow matrix :

$$\begin{bmatrix} A(43,1) & A(43,2) & 0 & 0 \\ A(43,4) & A(43,5) & A(43,6) & A(43,11) \\ 0 & A(43,8) & A(43,9) & 0 \end{bmatrix} * \begin{bmatrix} \theta_s \\ \theta_{wm} \\ \theta_{w1} \\ \theta_{w0} \end{bmatrix} = \begin{bmatrix} B(43,1) \\ B(43,2) \\ B(43,3) \end{bmatrix}$$

where,

self-coupled & cross-coupled coefficients:

$$A(43,1) = -\alpha C_{sw} - (M_s C_s / Ni_s \cdot \delta t)$$

$$A(43,2) = \alpha C_{sw}$$

$$A(43,4) = \alpha C_{sw}$$

$$A(43,5) = -\alpha C_{sw} - M_w C_{pw} / Ni_{w1} \cdot \delta t$$

$$A(43,6) = -\alpha C_{w1}$$

$$A(43,8) = -1$$

$$A(43,9) = 1$$

$$A(43,11) = \alpha C_{w0}$$

present-time & excitation coefficients:

$$B(43,1) = [(1 - \alpha) C_{sw}^* - M_s^* C_s^* / (Ni_s \delta t)] \theta_s^* - (1 - \alpha) C_{sw}^* \theta_{wm}^*$$

$$B(43,2) = - (1 - \alpha) C_{sw}^* \theta_s^* + [(1 - \alpha) C_{sw}^* - M_w^* C_{pw}^* / (Ni_{wm} \delta t)] \theta_{wm}^*$$

$$- (1-\alpha) C_{w1}^* \theta_{w1}^* - (1-\alpha) C_{w0}^* \theta_{w0}^*$$

$$B(43,3) = 0$$

where,

M_w	=	mass of fluid in the control volume
C_{pwm}	=	specific heat of fluid θ_{wm}
C_{w0}	=	$m_{w0} C_{pw0}$
C_{w1}	=	$m_{w1} C_{pw1}$
C_{sw}	=	$h_{sw} A_{sw}$

In case the DELAY flag is ON, the following coefficients will be revised as:

$$A(43,4) = 0$$

$$A(43,5) = 1$$

$$A(43,6) = 0$$

$$A(43,8) = 0$$

$$A(43,11) = 0$$

$$B(43,2) = \text{DELAY}(\theta_{wm})$$

$$B(43,3) = \text{DELAY}(\theta_{w1})$$

Mass flow matrice :

for first phase (dry air):

$$A(43,1) = 1/Ni_s$$

$$A(43,2) = 0$$

$$A(43,4) = 0$$

$$A(43,5) = 1/Ni_{wm}$$

$$A(43,6) = 0$$

$$A(43,8) = - 1$$

$$A(43,9) = 1$$

$$A(43,11) = - 1$$

$$B(43,1) = 0$$

$$B(43,2) = 0$$

$$B(43,3) = 0$$

for second phase (water vapour):

$$A(43,1) = 1/Ni_s$$

$$A(43,2) = 0$$

$$A(43,4) = 0$$

$$A(43,5) = 1/Ni_{am}$$

$$A(43,6) = 0$$

$$A(43,8) = 0$$

$$A(43,9) = 1$$

$$A(43,11) = 0$$

$$B(43,1) = 0$$

$$B(43,2) = 0$$

$$B(43,3) = 0$$

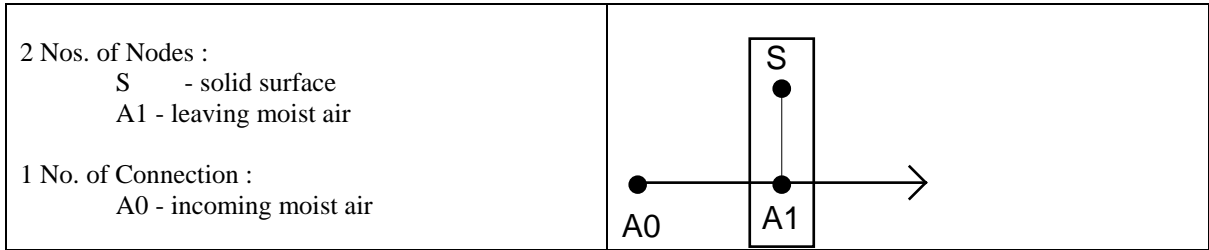
Notes:

For vapour i.e. steam or refrigerant gas, if $\theta_{w1} < \theta_{w_{sat}}$,

or for liquid, if $\theta_{w1} > \theta_{w_{sat}}$,

then set $\theta_{w1} = \theta_{w_{sat}}$ and switch to Part No. 4.2.

Part No. 4.4 Flow upon surface (for moist air; 2 nodes)



Energy flow matrix :

$$\begin{bmatrix} A(44,1) & A(44,2) & 0 \\ A(44,3) & A(44,4) & A(44,6) \end{bmatrix} * \begin{bmatrix} \theta_s \\ \theta_{a1} \\ \theta_{a0} \end{bmatrix} = \begin{bmatrix} B(44,1) \\ B(44,2) \end{bmatrix}$$

where,

self-coupled coefficients:

$$A(44,1) = -\alpha C_{as} - M_s C_s / (N_{i_s} \delta t)$$

$$A(44,2) = \alpha C_{as}$$

$$A(44,3) = \alpha C_{as}$$

$$A(44,4) = -\alpha (C_{a1} + C_{as}) - (M_a C_{pma} / N_{i_{a1}} \delta t)$$

cross-coupled coefficients:

$$A(44,6) = \alpha C_{a0}$$

present-time & excitation coefficients:

$$B(44,1) = [(1 - \alpha) C_{as}^* - M_s^* C_s^* / (N_{i_s} \delta t)] \theta_s^* - (1 - \alpha) C_{as}^* \theta_{a1}^* + [\alpha C_{av} + (1 - \alpha) C_{av}^*]$$

$$B(44,2) = [(1 - \alpha) (C_{a1}^* + C_{as}^*) - M_a^* C_{pma}^* / (N_{i_{a1}} \delta t)] \theta_{a1}^* - (1 - \alpha) C_{as}^* \theta_s^* - (1 - \alpha) C_{a0}^* \theta_{a0}^*$$

where,

- M_a - mass of dry air in the control volume of moist air
- C_{pma} = specific heat of moist air at θ_{a1} = $C_{pa1} + g_{a1} C_{pv1}$
- C_{a0} = $m_{a0} C_{pa0} + m_{v0} C_{pv0}$
- C_{a1} = $m_{a1} C_{pa1} + m_{v1} C_{pv1}$
- C_{as} = $h_{as} A_{as}$
- C_{av} = $-h_{fg} (m_{v0} - m_{v1})$ = $-h_{fg} C_c$

For dry surface, $m_{v1} = m_{v0}$ so $C_{av} = 0$

Mass flow matrix :

for first phase (dry air):

$$A(44,1) = 1/Ni_s$$

$$A(44,2) = 0$$

$$A(44,3) = 0$$

$$A(44,4) = 1/Ni_{a1}$$

$$A(44,6) = -1$$

$$B(44,1) = 0$$

$$B(44,2) = 0$$

for second phase (water vapour):

$$A(44,1) = 1/Ni_s$$

$$A(44,2) = 0$$

$$A(44,3) = 0$$

$$A(44,4) = 1/Ni_{a1}$$

$$A(44,6) = -1$$

$$B(44,1) = 0$$

$$B(44,2) = -C_c$$

where,

$$C_c = 0 \quad \text{for dry surface i.e. when } \theta_s > \theta_{a0\text{dew}} \text{ \& } M_w = 0$$

$$= K_d A_{as} (g_{a1} - g_s) \quad \text{for wet surface i.e. } M_w > 0$$

where M_w is the amount of condensate on the surface.
 g_s is the saturated moist content at θ_s

Notes:

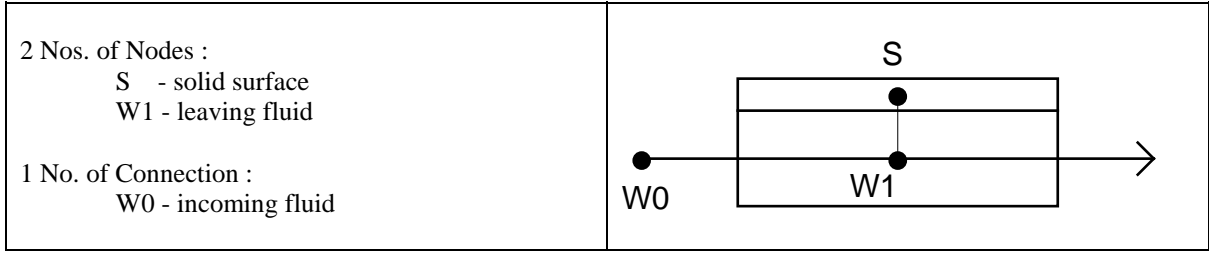
1. For the equation: $M_w = M_w^* + C_c \cdot \delta t$

i) If $M_w < 0$, then $M_w = 0$ and $C_c = -M_w^*$

ii) If $M_w > M_{\text{max}}$ where M_{max} specifies the maximum condensate holding capacity on the surface S, then

$$M_w = M_{\text{max}}$$

Part No. 4.5 Flow upon surface (for single-phase fluid; 2 nodes)



Energy flow matrix :

$$\begin{bmatrix} A(45,1) & A(45,2) & 0 \\ A(45,3) & A(45,4) & A(45,6) \end{bmatrix} * \begin{bmatrix} \theta_s \\ \theta_{w1} \\ \theta_{w0} \end{bmatrix} = \begin{bmatrix} B(45,1) \\ B(45,2) \end{bmatrix}$$

where,

self-coupled coefficients:

$$A(45,1) = -\alpha C_{sw} - (M_s C_s / Ni_s \cdot \delta t)$$

$$A(45,2) = \alpha C_{sw}$$

$$A(45,3) = \alpha C_{sw}$$

$$A(45,4) = -\alpha(C_{w1} + C_{sw}) - (M_w C_{pw1} / Ni_{w1} \cdot \delta t)$$

cross-coupled coefficients:

$$A(45,6) = \alpha C_{w0}$$

present-time & excitation coefficients:

$$B(45,1) = [(1-\alpha) C_{sw}^* - M_s^* C_s^* / Ni_s^* \delta t] \theta_s^* - (1-\alpha) C_{sw}^* \theta_{w1}^*$$

$$B(45,2) = [(1-\alpha)(C_{w1}^* + C_{sw}^*) - M_w^* C_{pw1}^* / (Ni_{w1} \delta t)] \theta_{w1}^* - (1-\alpha) C_{sw}^* \theta_s^* - (1-\alpha) C_{w0}^* \theta_{w0}^*$$

Mass flow matrixe :

for first phase (liquid):

$$A(45,1) = 1/Ni_s$$

$$A(45,2) = 0$$

$$A(45,3) = 0$$

$$A(45,4) = 1/Ni_{a1}$$

$$A(45,6) = -1$$

$$B(45,1) = 0$$

$$B(45,2) = 0$$

for second phase (water vapour):

$$A(45,1) = 1/Ni_s$$

$$A(45,2) = 0$$

$$A(45,3) = 0$$

$$A(45,4) = 1/Ni_{a1}$$

$$A(45,6) = 0$$

$$B(45,1) = 0$$

$$B(45,2) = 0$$

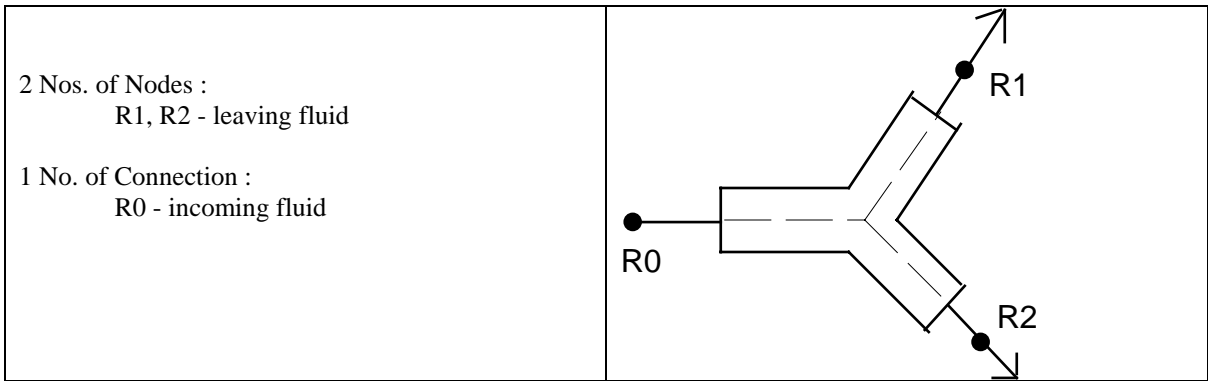
Note :

For vapour i.e. steam or refrigerant gas, if $\theta w_1 < \theta w_{sat}$,

or for liquid, if $\theta w_1 > \theta w_{sat}$,

then set $\theta w_1 = \theta w_{sat}$

Part No. 5.1 Flow diverger (for all fluid types)



Energy flow matrix :

$$\begin{bmatrix} A(51,1) & 0 & A(51,5) \\ A(51,3) & A(51,4) & A(51,6) \end{bmatrix} * \begin{bmatrix} \theta_{r1} \\ \theta_{r2} \\ \theta_{r0} \end{bmatrix} = \begin{bmatrix} B(51,1) \\ B(51,2) \end{bmatrix}$$

where,

$$A(51,1) = 1$$

$$A(51,3) = 0$$

$$A(51,4) = 1$$

$$A(51,5) = -1$$

$$A(51,6) = -1$$

$$B(51,1) = 0$$

$$B(51,2) = 0$$

Mass flow matrix:

for both first & second phase:

$$A(51,1) = 1$$

$$A(51,3) = 1$$

$$A(51,4) = 1$$

$$A(51,5) = -K$$

$$A(51,6) = -1$$

$$B(51,1) = 0$$

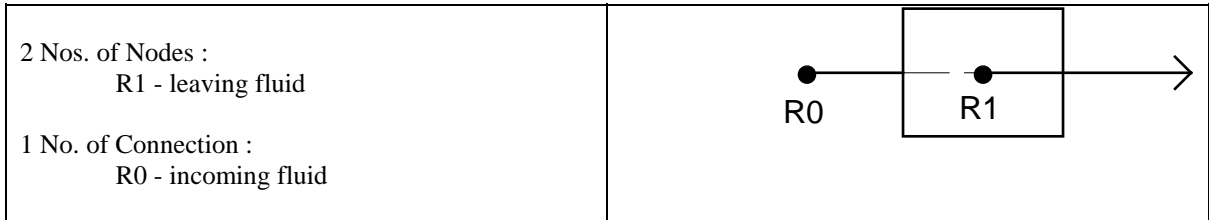
$$B(51,2) = 0$$

$$\text{where } K = m_{a1}/m_{a0} \quad \text{or} \quad = m_{v1}/m_{v0} \quad \text{or} \quad = m_{w1}/m_{w0}$$

Note:

The value of K can be either specified by the user or determined by the mass flow network solver.

Part No. 5.2 Flow multiplier (for all fluid types)



Energy flow matrix :

$$[A(52,1) \quad A(52,2)] * \begin{bmatrix} \theta_{r1} \\ \theta_{r0} \end{bmatrix} = [B(52,1)]$$

$$A(52,1) = 1$$

$$A(52,2) = -1$$

$$B(52,1) = 0$$

Mass flow matrice:

for both first & second phase :

$$A(52,1) = 1$$

$$A(52,2) = -K$$

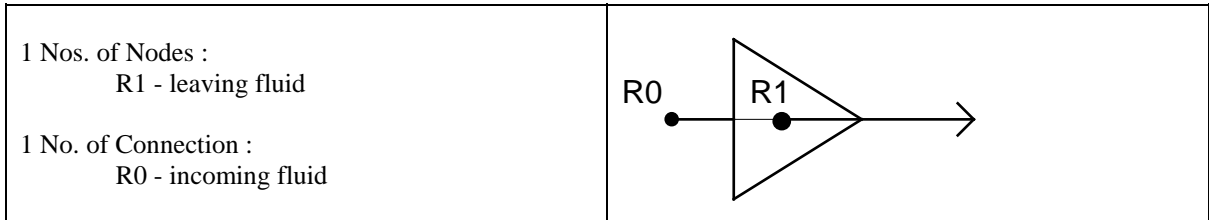
$$B(52,1) = 0$$

$$\text{where } K = m_{w1}/m_{w0} \quad \text{or} \quad = m_{a1}/m_{a0} \quad \text{or} \quad = m_{v1}/m_{v0}$$

Note:

The value of K can be either specified by the user or determined by the mass flow network solver.

Part No. 5.3 Flow inducer (for all fluid types)



Energy flow matrix :

$$[A(53,1) \quad A(53,2)] * \begin{bmatrix} \theta_{r1} \\ \theta_{r0} \end{bmatrix} = [B(53,1)]$$

where,

$$A(53,1) = 1$$

$$A(53,2) = -1$$

$$B(53,1) = 0$$

Mass flow matrice:

first phase (liquid):

$$A(53,1) = 1$$

$$A(53,2) = 0$$

$$B(53,1) = k_1 m_i$$

seoncd phase (vapour):

$$A(53,1) = 1$$

$$A(53,2) = 0$$

$$B(53,1) = k_2 m_i$$

Note:

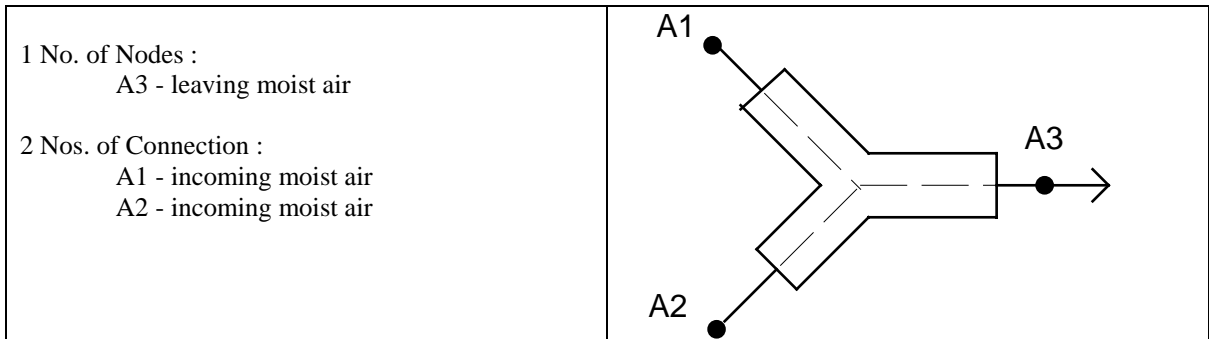
- i) m_i is the induced mass flow rate.
- ii) The values of k_1 & k_2 are fluid-type dependant:

	moist air	liquid	wet vapour	dry vapour
k_1	1	1	1-x	0
k_2	ξ_{a0}	0	x	1

where $\xi_{a0} = m_{v0}/m_{a0}$

$x = m_{v0}/(m_{w0} + m_{v0})$

Part No. 6.1 Flow converger (for moist air)



Energy flow matrix :

$$[A(61,1) \quad A(61,2) \quad A(61,3)] * \begin{bmatrix} \theta_{a3} \\ \theta_{a2} \\ \theta_{a1} \end{bmatrix} = [0]$$

where,

$$A(61,1) = C_{a3}$$

$$A(61,2) = -C_{a2}$$

$$A(61,3) = -C_{a1}$$

$$\text{and } C_{ai} = m_{ai} C_{p_{ai}} + m_{vi} C_{p_{vi}} \quad \text{for } i = 1,2,3$$

Mass flow matrix:

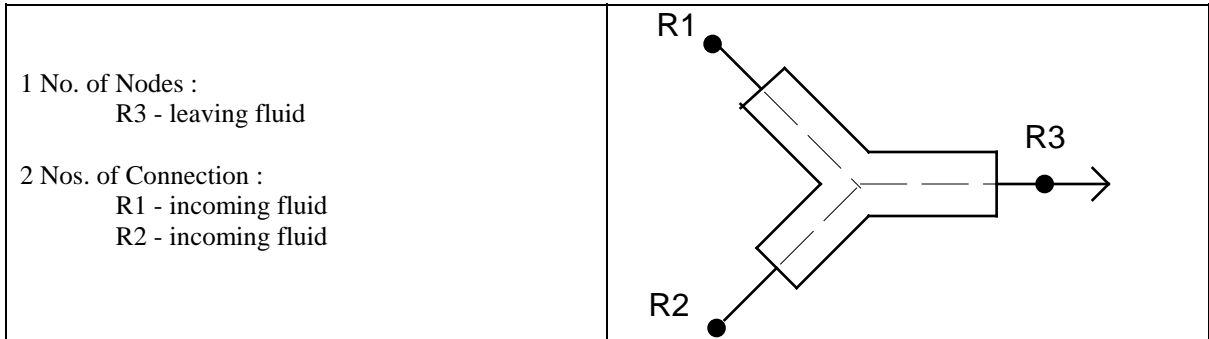
for both first & second phase:

$$A(61,1) = 1$$

$$A(61,2) = -1$$

$$A(61,3) = -1$$

Part No. 6.2 Flow converger (for 2-phase fluid)



Energy flow matrix :

$$[A(62,1) \quad 0 \quad 0]^* \begin{bmatrix} \theta_{r3} \\ \theta_{r2} \\ \theta_{r1} \end{bmatrix} = [B(62,1)]$$

where,

$$A(62,1) = 1$$

$$B(62,1) = C_t$$

Notes:

1. Apply for cases where 2 fluid streams in liquid, wet vapour or dry vapour forms are mixed. Fluid streams can be at different temperatures before mixing.
2. Working pressure P_{r3} (with saturated temperature θ_{sat}) is assumed to be the same for the two streams before mixing and remains unchanged throughout the converging process i.e. friction loss has not been included; H_{fr} and H_{gr} can then be obtained using P_{r3} as the saturation pressure.

3. H_{r3} can be obtained by the following equation:

$$H_{r3} = [(m_{w1} \cdot C_{pW} + m_{v1} \cdot C_{pV}) \theta_{r1} + (m_{w2} \cdot C_{pW} + m_{v2} \cdot C_{pV}) \theta_{r2}] / (m_{r1} + m_{r2})$$

where, $m_{ri} = m_{wi} + m_{vi}$ for $i = 1, 2, \text{ or } 3$

4. The following three cases determine the values of x_{r3} , m_{v3} and m_{w3} :

- i) If $\theta_{r3} = \theta_{sat}$ (i.e. $H_{fr} < H_{r3} < H_{gr}$), then $C_t = \theta_{sat}$

$$x_{r3} = (H_{r3} - H_{fr}) / H_{fg}$$

$$\begin{aligned} C_w &= m_{w3} = m_{r3}(1-x_{r3}) \\ C_v &= m_{v3} = m_{r3} x_{r3} \end{aligned}$$

ii) If $H_{r3} < H_f$, then $C_t = \theta_{sat} - (H_{fr} - H_{r3})/C_{pw}$

$$\begin{aligned} x_{r3} &= 0 \\ C_w &= m_{w3} = m_{r3} \\ C_v &= m_{v3} = 0 \end{aligned}$$

iii) If $H_{r3} > H_g$, then $C_t = \theta_{sat} + (H_{r3} - H_{gr})/C_{pv}$

$$\begin{aligned} x_{r3} &= 1 \\ C_w &= m_{w3} = 0 \\ C_v &= m_{v3} = m_{r3} \end{aligned}$$

Mass flow matrix:

first phase (liquid):

$$A(62,1) = 1$$

$$B(62,1) = C_w$$

where $C_w = m_{v1} + m_{v2} - m_{v3}$
 $= m_{r1} x_{r1} + m_{r2} x_{r2} - (m_{r1} + m_{r2})(1-x_{r3})$

second phase (vapour):

$$A(62,1) = 1$$

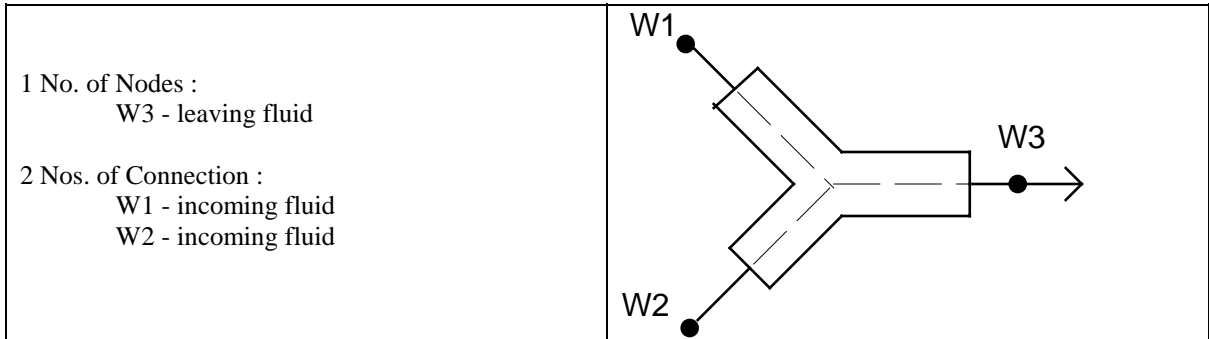
$$B(62,1) = C_v$$

where $C_v = m_{r3} \cdot x_{r3}^*$

Notes:

1. x_{r3}^* can be obtained firstly from the previous time step or later on from the previous iteration step.
2. If either $m_{v1} = m_{v2} = 0$ or $m_{w1} = m_{w2} = 0$, switch to PN6.3 : Flow converger (for 1-phase fluid).

Part No. 6.3 Flow converger (for single-phase fluid)



Energy flow matrix :

$$[A(63,1) \quad A(63,2) \quad A(63,3)]^* \begin{bmatrix} \theta_{r3} \\ \theta_{r2} \\ \theta_{r1} \end{bmatrix} = [0]$$

where,

$$A(63,1) = (m_{w1} + m_{w2}) C_{pw3} + (m_{v1} + m_{v2}) C_{pv3}$$

$$A(63,2) = - m_{w2} C_{pw2} - m_{v2} C_{pv2}$$

$$A(63,3) = - m_{w1} C_{pw1} - m_{v1} C_{pv1}$$

Mass flow matrice:

for both first (liquid) & second (dry vapour) phase :

$$A(63,1) = 1$$

$$A(63,2) = - 1$$

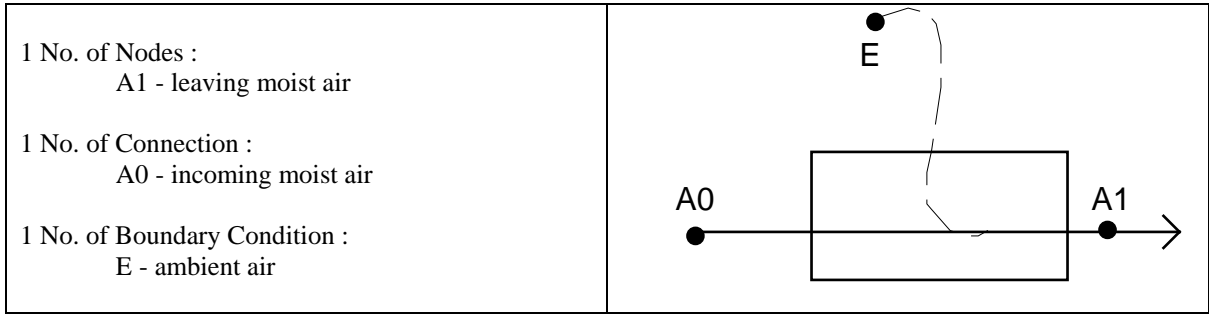
$$A(63,3) = - 1$$

Note:

In this primitive part, either $m_{w1} = m_{w2} = 0$ or $m_{v1} = m_{v2} = 0$

If this is not the case, switch to PN6.2 : Flow converger (for 2-phase fluid).

Part No. 6.4 Flow converger (for leak-in moist air from outside)



Energy flow matrix :

$$[A(64,1) \quad A(64,2)] * \begin{bmatrix} \theta_{a1} \\ \theta_{a0} \end{bmatrix} = [B(64,1)]$$

where,

$$A(64,1) = m_{a1} C_{p_{a1}} + m_{v1} C_{p_{v1}}$$

$$A(64,2) = m_{a0} C_{p_{a0}} + m_{v0} C_{p_{v0}}$$

$$B(64,1) = (m_{ae} C_{p_{ae}} + m_{ve} C_{p_{ve}}) \theta_e$$

Mass flow matrix:

first phase (dry air):

$$A(64,1) = 1$$

$$A(64,2) = -1$$

$$B(64,1) = m_{ae}$$

second phase (water vapour):

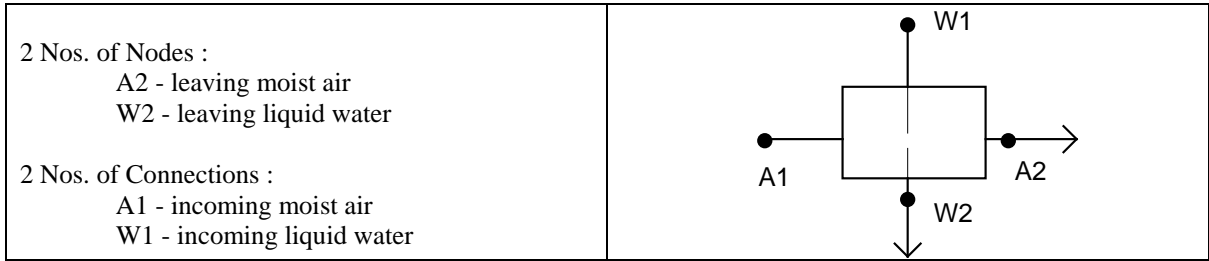
$$A(64,1) = 1$$

$$A(64,2) = 1$$

$$B(64,1) = m_{ve}$$

Note: This primitive part applies to the situation when the moist air from an ambient, of which the detail is not to be modelled, leaks into an moist air stream of negative pressure; one typical application is the leakage of moist air from the outside into a suction air-duct through the duct seams.

Part No. 7.1 Flow upon water spray (for moist air)



Energy flow matrix :

$$\begin{bmatrix} A(71,1) & A(71,2) & A(71,5) & A(71,6) \\ A(71,3) & A(71,4) & A(71,7) & A(71,8) \end{bmatrix} * \begin{bmatrix} \theta_{a2} \\ \theta_{w2} \\ \theta_{a1} \\ \theta_{w1} \end{bmatrix} = \begin{bmatrix} B(71,1) \\ B(71,2) \end{bmatrix}$$

where,

$$A(71,1) = -\alpha(C_{a2} + C_{aw}) - (M_a C_{pa2} / Ni_{a2} \cdot \delta t)$$

$$A(71,2) = \alpha C_{aw}$$

$$A(71,3) = \alpha C_{aw}$$

$$A(71,4) = -\alpha(C_{w2} + C_{aw}) - (M_w C_{pw2} / Ni_{w2} \cdot \delta t)$$

$$A(71,5) = \alpha(C_{a1} - C_{aw})$$

$$A(71,6) = \alpha C_{aw}$$

$$A(71,7) = \alpha C_{aw}$$

$$A(71,8) = \alpha(C_{w1} - C_{aw})$$

$$B(71,1) = [(1 - \alpha)(C_{a2}^* + C_{aw}^*) - (M_a^* C_{pa2}^* / Ni_{a2} \cdot \delta t)] \theta_{a2}^* - (1 - \alpha) C_{aw}^* \theta_{w2}^* - (1 - \alpha)(C_{a1}^* - C_{aw}^*) \theta_{a1}^* - (1 - \alpha) C_{aw}^* \theta_{w1}^* + \alpha C_{av} + (1 - \alpha) C_{av}^*$$

$$B(71,2) = - (1 - \alpha) C_{aw}^* \theta_{a2}^* + [(1 - \alpha)(C_{w2}^* + C_{aw}^*) - (M_w^* C_{pw2}^* / Ni_{w2} \cdot \delta t)] \theta_{w2}^* - (1 - \alpha) C_{aw}^* \theta_{a1}^* - (1 - \alpha)(C_{w1}^* - C_{aw}^*) \theta_{w1}^*$$

where,

$$C_{ai} = m_{ai} C_{pai} + m_{vi} C_{pvi} \quad \text{for } i = 1, 2$$

$$C_{wi} = m_{wi} C_{pwi}$$

$$C_{aw} = 0.5 h_{aw} A_{aw}$$

$$C_{av} = - H_{fg} (m_{v1} - m_{v2})$$

Mass flow matrixe :

for first phase (dry air or liquid water),

$$A(71,1) = 1/Ni_{a2}$$

$$A(71,2) = 0$$

$$A(71,3) = 0$$

$$A(71,4) = 1/Ni_{w2}$$

$$A(71,5) = -1$$

$$A(71,6) = 0$$

$$A(71,7) = 0$$

$$A(71,8) = -1$$

$$B(71,1) = 0$$

$$B(71,2) = C_{21}$$

for second phase (water vapour),

$$A(71,1) = 1/Ni_{a2}$$

$$A(71,2) = 0$$

$$A(71,3) = 1$$

$$A(71,4) = 1/Ni_{w2}$$

$$A(71,5) = -1$$

$$A(71,6) = 0$$

$$A(71,7) = -1$$

$$A(71,8) = -1$$

$$B(71,1) = -C_{21}$$

$$B(71,2) = 0$$

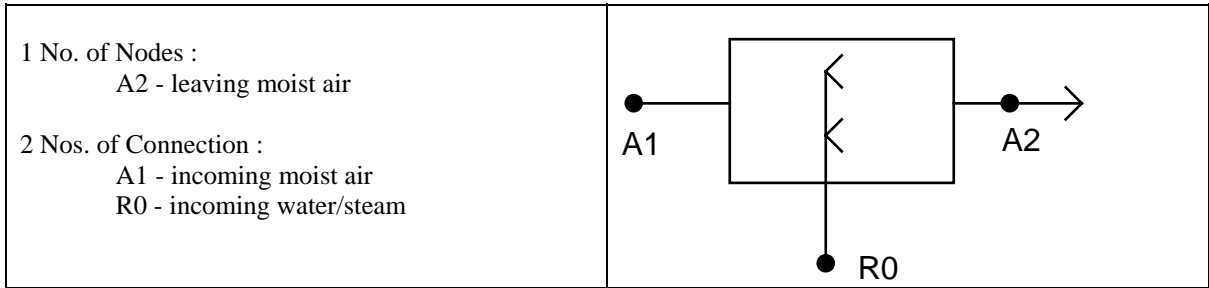
$$\text{where } C_{21} = K_d A_{aw} (g_a - g_w) = m_{v1} - m_{v2} = m_{w2} - m_{w1}$$

$$g_a = (g_{a1} + g_{a2}) / 2 = 0.5 (m_{v1}/m_{a1} + m_{v2}/m_{a2})$$

$$g_w = 0.62198 P_{ws} / (P_{a1} - P_{ws}) \quad \& \quad P_{ws} = f(\theta_{w1})$$

Note: If i) $g_a > g_w$, dehumidification takes place;
 ii) $g_a < g_w$, humidification takes place.

Part No. 8.1 Fluid Injection (water/steam to moist air)



Energy flow matrix :

$$[A(81,1) \quad A(81,2) \quad A(81,3)]^* \begin{bmatrix} \theta_{a2} \\ \theta_{a1} \\ \theta_{r0} \end{bmatrix} = [B(81,1)]$$

where,

$$A(81,1) = C_{a2}$$

$$A(81,2) = -C_{a1}$$

$$A(81,3) = -C_{r0}$$

$$B(81,1) = H_{fg} m_c$$

$$\text{and } \begin{matrix} C_{ai} \\ C_{r0} \end{matrix} = \begin{matrix} m_{ai} C_{pai} + m_{vi} C_{pvi} \\ m_{w0} C_{pw0} + m_{v0} C_{pv0} \end{matrix} \quad \text{for } i = 1,2$$

Note :

a	- air
r	- 2-phase fluid
v	- vapour (water)
w	- liquid (water)
c	- condensate

Mass flow matrix:

first phase (dry air):

$$A(81,1) = 1/N_{i_{a2}}$$

$$A(81,2) = -1$$

$$A(81,3) = 0$$

$$B(81,1) = 0$$

second phase (water vapour):

$$A(81,1) = 1/N_{i_{a2}}$$

$$A(81,2) = 0$$

$$A(81,3) = 0$$

$$B(81,1) = C_v$$

Notes :

1. Working pressure P_{a2} (with saturated temperature θ_{sat}) is assumed to be the same (approx. atmospheric pressure) for the two streams before mixing and remains unchanged throughout the process.

2. Water droplets carried downstream is not allowed; excessive steam will condense out of the air stream; amount of condensate = m_c .

3. Get $g_{a2} = m_{v2}/m_{a2} = (m_{v1} + m_{r0})/m_{a1}$
and from θ_{a2} get g_{a2sat} .

If A2 is not saturated (indicated by $g_{a2} < g_{a2sat}$), then

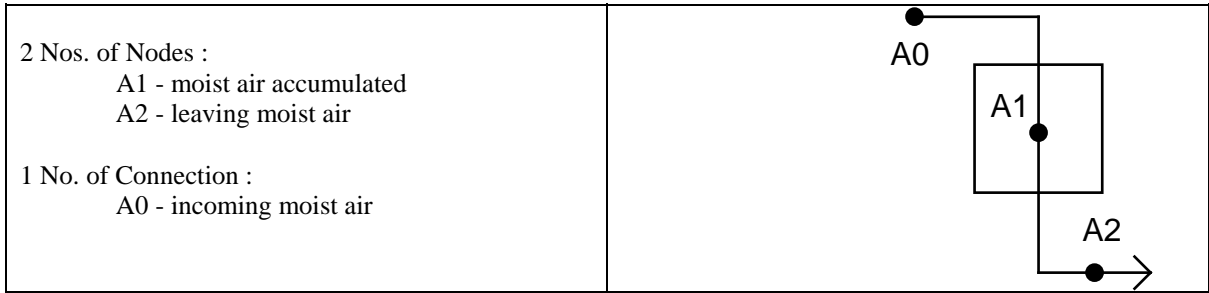
$$\begin{aligned} m_c &= 0 \\ C_v &= m_{a1} g_{a2} \end{aligned}$$

If A2 is saturated, then

$$\begin{aligned} m_c &= m_{v0} + m_{v1} - m_{a2} \cdot g_{a2sat} \\ C_v &= m_{a2} \cdot g_{a2sat} \end{aligned}$$

4. If $m_{v0} + m_{v1} < m_{a2} \cdot g_{a2sat}$, then $m_c = 0$.

Part No. 9.1 Fluid Accumulator (for moist air)



Energy flow matrix :

$$\begin{bmatrix} A(91,1) & A(91,2) & A(91,5) \\ A(91,3) & A(91,4) & 0 \end{bmatrix} * \begin{bmatrix} \theta_{a1} \\ \theta_{a2} \\ \theta_{a0} \end{bmatrix} = \begin{bmatrix} B(91,1) \\ B(91,2) \end{bmatrix}$$

where,

self-coupled & cross-coupled coefficients:

$$A(91,1) = - (M_{a1}C_{pa1} + M_{v1}C_{pv1}) / (N_{ia1} \cdot \delta t)$$

$$A(91,2) = - \alpha (m_{a2} \cdot C_{pa2} + m_{v2} \cdot C_{pv2})$$

$$A(91,3) = -1$$

$$A(91,4) = 1$$

$$A(91,5) = \alpha (m_{a0} \cdot C_{pa0} + m_{v0} \cdot C_{pv0})$$

present-time & excitation coefficients:

$$B(91,1) = - [(M_{a1}^* C_{pa1}^* + M_{v1}^* C_{pv1}^*) / N_{ia1} \cdot \delta t] \theta_{a1}^* + (1-\alpha) C_{a2}^* \theta_{a2}^* - (1-\alpha) C_{a0}^* \theta_{a0}^*$$

$$B(91,2) = 0$$

Mass flow matrice:

first phase (dry air):

$$A(91,1) = 1 / N_{ia1}$$

$$\begin{aligned}
A(91,2) &= 0 \\
A(91,3) &= 0 \\
A(91,4) &= 1/Ni_{a2} \\
A(91,5) &= -1 \\
B(91,1) &= 0 \\
B(91,2) &= C_{m2}
\end{aligned}$$

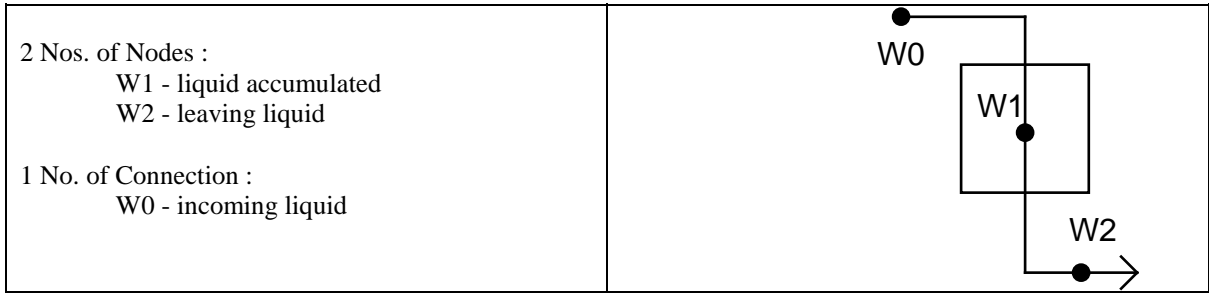
second phase (water vapour):

$$\begin{aligned}
A(91,1) &= 1/Ni_{a1} \\
A(91,2) &= 0 \\
A(91,3) &= 0 \\
A(91,4) &= 1/Ni_{a2} \\
A(91,5) &= -1 \\
B(91,1) &= 0 \\
B(91,2) &= g_{a1}.C_{m2}
\end{aligned}$$

Notes:

1. m_{a1} & m_{a0} are to be either specified by the user or determined by mass flow network solver.
2. $M_{a1} = M_{a1}^* + m_{a1} \cdot \delta t$
 $M_{v1} = M_{v1}^* + m_{v1} \cdot \delta t$

Part No. 9.2 Fluid Accumulator (for liquid)



Energy flow matrix :

$$\begin{bmatrix} A(92,1) & A(92,2) & A(92,5) \\ A(92,3) & A(92,4) & 0 \end{bmatrix} * \begin{bmatrix} \theta_{w1} \\ \theta_{w2} \\ \theta_{w0} \end{bmatrix} = \begin{bmatrix} B(92,1) \\ B(92,2) \end{bmatrix}$$

where,

self- and cross-coupled coefficients:

$$A(92,1) = - M_{w1} C_{pw1} / N_{iw1} \cdot \delta t$$

$$A(92,2) = - \alpha C_{w2}$$

$$A(92,3) = -1$$

$$A(92,4) = 1$$

$$A(92,5) = \alpha C_{w0}$$

present-time & excitation coefficients:

$$B(92,1) = - [M_{w1}^* C_{pw1}^* / N_{iw1} \cdot \delta t] \theta_{w1}^* + (1-\alpha) C_{w2}^* \theta_{w2}^* - (1-\alpha) C_{w0}^* \theta_{w0}^*$$

$$B(92,2) = 0$$

where $C_{wi} = m_{wi} C_{pwi}$ $i = 0,1,2$

Mass flow matrice :

first-phase (liquid) balance:

$$A(92,1) = 1/N_{i_w1}$$

$$A(92,2) = 1$$

$$A(92,3) = 0$$

$$A(92,4) = 1/N_{i_w2}$$

$$A(92,5) = -1$$

$$B(92,1) = 0$$

$$B(92,2) = C_{m2}$$

where C_{m2} is user specified.

second-phase (vapour) balance: not defined hence,

$$A(92,1) = 1/N_{i_w1}$$

$$A(92,2) = 1$$

$$A(92,3) = 0$$

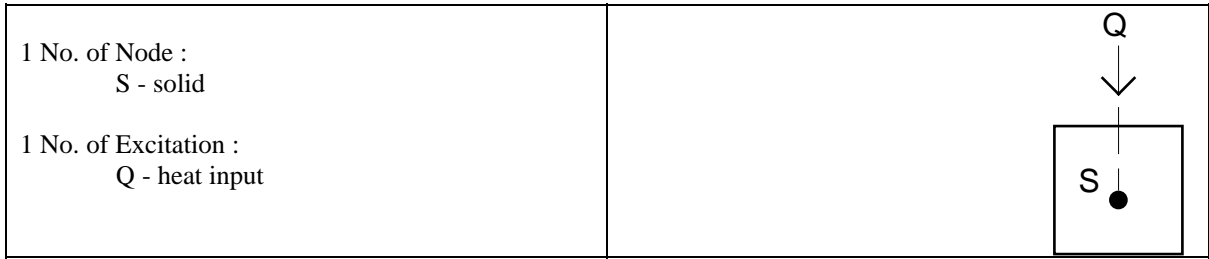
$$A(92,4) = 1/N_{i_w2}$$

$$A(92,5) = 0$$

$$B(92,1) = 0$$

$$B(92,2) = 0$$

Part No. 10.1 Heat Injection (to solid)



$$[A(101,1)] * [\theta_s] = [B(101,1)]$$

Energy flow matrix :

where,

$$A(101,1) = - M_s \cdot C_s / (N_i_s \cdot \delta t)$$

$$B(101,1) = - [M_s^* C_s^* / (N_i_s \cdot \delta t)] \theta_s^* - [\alpha Q + (1-\alpha)Q^*]$$

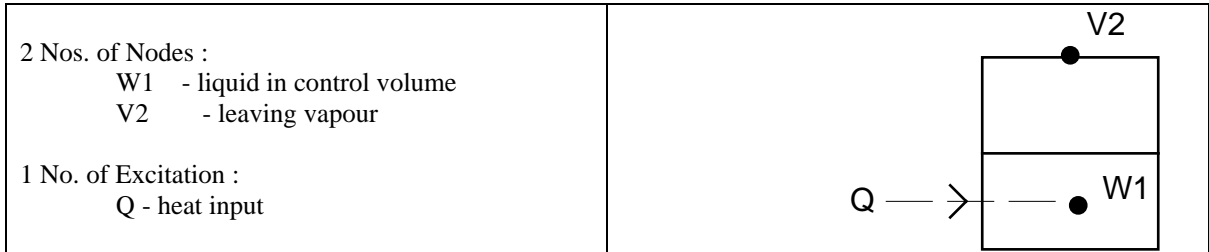
Mass Flow matrixe :

for both first & second phase: N.A.

$$A(101,1) = 1/N_i_s$$

$$B(101,1) = 0$$

Part No. 10.2 Heat Injection (to vapour-generating fluid)



Energy flow matrix :

$$\begin{bmatrix} A(102,1) & 0 \\ A(102,3) & A(102,4) \end{bmatrix} * \begin{bmatrix} \theta_{w1} \\ \theta_{v2} \end{bmatrix} = \begin{bmatrix} B(102,1) \\ B(102,2) \end{bmatrix}$$

where,

$$A(102,1) = -M_{w1} \cdot C_{pw1} / (Ni_{w1} \cdot \delta t)$$

$$A(102,3) = -1$$

$$A(102,4) = 1$$

$$B(102,1) = -[M_{w1}^* C_{pw1}^* / (Ni_{w1} \cdot \delta t)] \theta_{w1}^* + [\alpha m_{v2} H_{fg} + (1-\alpha) m_{v2}^* H_{fg}^*] - [\alpha Q + (1-\alpha) Q^*]$$

$$B(102,2) = 0$$

Notes :

1. If $\theta_{w1} > \theta_{w1} \text{ boiling}$, then $\theta_{w1} = \theta_{w1} \text{ boiling}$
2. $M_{w1} = M_{w1}^* + m_{w1} \cdot \delta t = M_{w1}^* - m_{v2} \cdot \delta t$
3. If $\theta_{w1} < \theta_{w1} \text{ boiling}$, then $C_{vw} = 0$

Mass flow matrixe :

first-phase (dry air or liquid water):

$$A(102,1) = 1/Ni_{w1}$$

$$A(102,3) = 0$$

$$A(102,4) = 1/Ni_{v2}$$

$$B(102,1) = -C_{vw}$$

$$B(102,2) = 0$$

second-phase (water vapour):

$$A(102,1) = 1/N_{iw1}$$

$$A(102,3) = 0$$

$$A(102,4) = 1/N_{iv2}$$

$$B(102,1) = 0$$

$$B(102,2) = C_{vw}$$

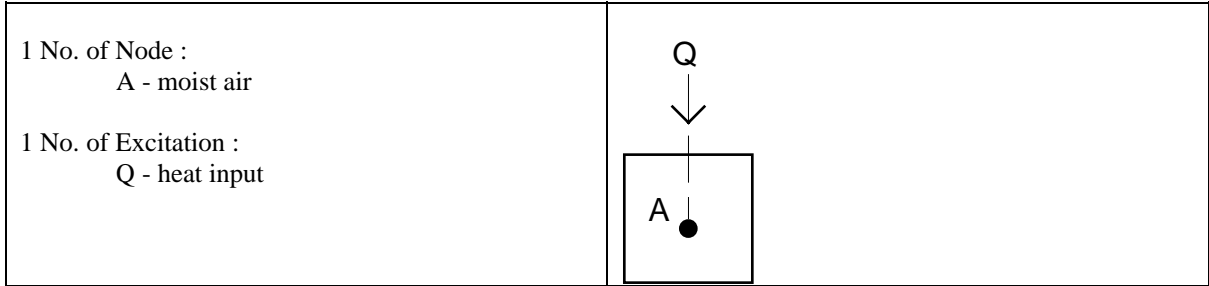
Notes :

1. If $\theta_{w1} < \theta_{w1\text{boiling}}$, then

C_{vw}	$= K_d A_{vw} (g_{ws} - g_v)$	for moist air (e.g. humidifier)
	$= 0$	for pure steam/water circuit (e.g. boiler)

where g_{ws} - saturated vapour pressure at θ_{w1}
 g_v - water vapour pressure at θ_{w1}
2. If $\theta_{w1} = \theta_{w1\text{boiling}}$, then $C_{vw} = [\alpha Q + (1-\alpha) Q^*] / H_{fg}$

Part No. 10.3 Heat Injection (to moist air)



Energy flow matrix :

$$[A(103,1)] * [\theta_a] = [B(103,1)]$$

where,

$$A(103,1) = - [\alpha C_a + (1-\alpha)C_a^*] / (Ni_a \cdot \delta t)$$

$$B(103,1) = - [\alpha C_a + (1-\alpha)C_a^*] \theta_s^* / (Ni_a \cdot \delta t) - [\alpha Q + (1-\alpha)Q^*] - [\alpha H_{fg} m_c + (1-\alpha)H_{fg}^* m_c^*]$$

where,

$$m_c^* = \text{condensation rate} = (M_v^* - M_v) / \delta t$$

$$C_a = M_a C_{p_a} + M_v C_{p_v}$$

Note: Check $g_a = M_v / M_a$ against g_{asat} at each time step;
if $g_a > g_{asat}$ then $M_v = M_a \cdot g_{asat}$

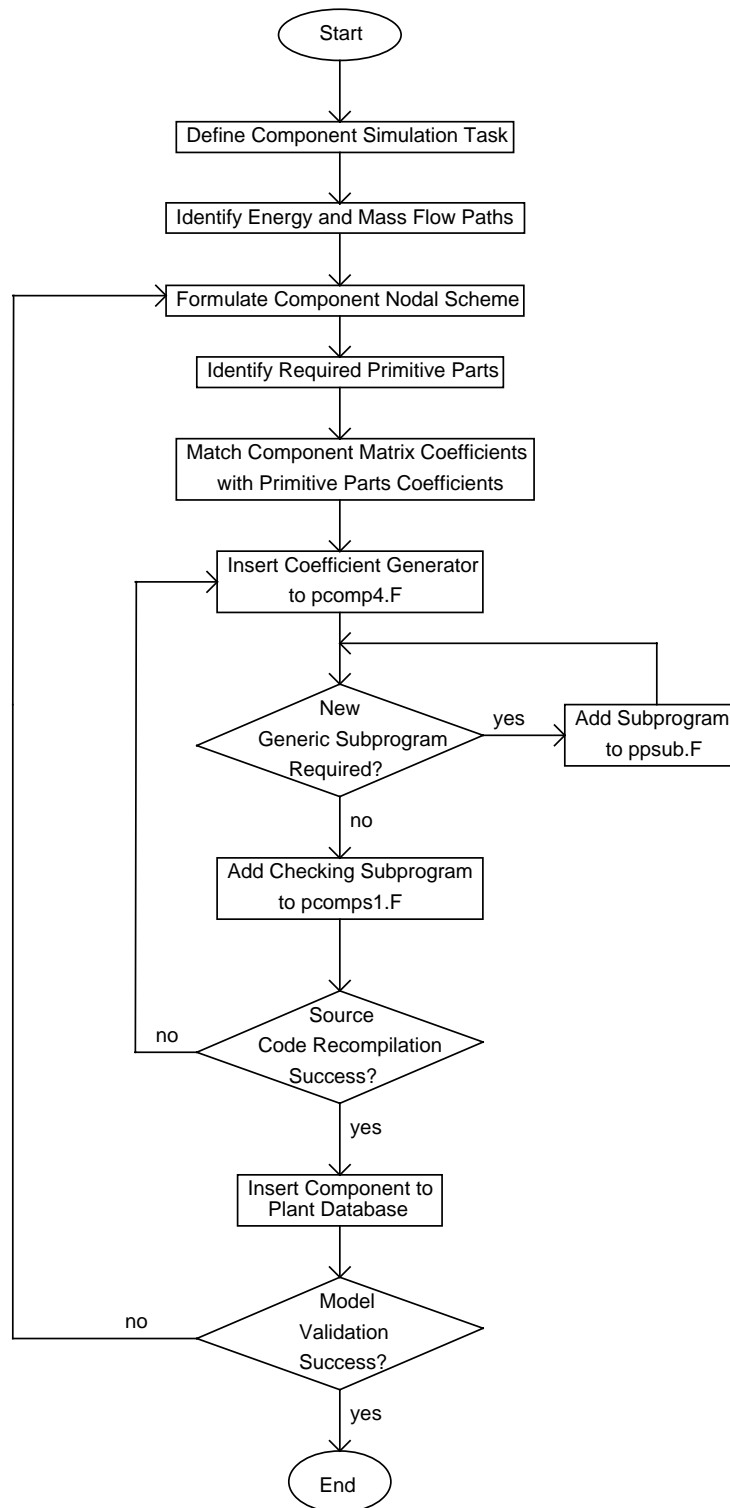
Mass Flow matrix :

for both first & second phase: N.A.

$$A(101,1) = 1 / Ni_a$$

$$B(101,1) = 0$$

Appendix C Procedure of Building a ESP-r Plant Component from Primitive Parts



The flow chart as shown gives an indicative description of the key steps in the component modelling process. The decision on the plant component discretization (nodal) scheme, as well as the number or types of primitive parts involved, solely depends on the objectives of the underlying simulation task. The optimization lies between the required resolution and accuracy at one end and the simulation speed and costs at the other. However, as explained in Section 4.3.4, it must be cautious that a flowing fluid node (for instance when using those primitive parts in category 4 "flow upon surface") should not be interacting with more than one solid surface node.

Once the matrix template of the plant component has been fixed, it is required to match each matrix coefficient of the component to the primitive part coefficients. A matrix coefficient, when matched with more than one primitive part coefficient, is having a numerical value equal to the sum of the corresponding primitive part coefficients.

The insertion of a new plant component built from primitive parts into the ESP-r system is more or less the same as the way inserting the existing plant components. The main difference is that in the new coefficient generator, rather than expressing the matrix coefficients directly in terms of the mathematical expressions as derived from the characteristic equations, the required primitive part subroutines are firstly called and then the matrix coefficients are expressed in terms of the primitive part coefficients. Because of the coherence in the structure of the "PP" plant components compared to the other existing plant components in the source code, both the existing and the new PP plant components can be installed in the same plant database plantc.db1, and can be used interchangeably to describe any plant network.

Appendix D The Concept of Cascade Time-constant

1. Characteristics of Time-Constant

One of the frequently occurring processes in thermal systems is a response where the rate of change of a variable is proportional to the difference between the magnitude of a driving force and the value of the variable. Such a process can be characterized by a "time constant".

Consider a solid node in contact with a fluid such as air. The change of solid temperature θ_s in response to the change in air temperature θ_a can be given by the following energy balance equation:

$$M_s C_s \frac{d\theta_s}{dt} = h_{as} A_{as} (\theta_a - \theta_s) \quad (C1)$$

Or after re-arranging,

$$\frac{M_s C_s}{h_{as} A_{as}} \frac{d\theta_s}{dt} = \theta_a - \theta_s \quad (C2)$$

The (MC/hA) group has the units of time and is the "time constant" τ for the process. In response to a step increase of magnitude of θ_a , it can be shown that the temperature of the solid - starting with θ_{s0} - will change according to the following time function:

$$\theta_s - \theta_{s0} = \Delta_s (1 - e^{-t/\tau}) \quad (C3)$$

where Δ_s is the ultimate rise in solid temperature.

τ has the geometric significance such that

$$\tau = 0.632 \Delta_s \quad (C4)$$

2. Cascaded Time-Constant

Suppose the above solid has two surfaces such that the other surface is in contact with another fluid, for instance water. This is a common situation for instance in the case of air-to-water heat exchanger. The energy balance equation for the solid in this case is

$$M_s C_s \frac{d\theta_s}{dt} = h_{as} A_{as} (\theta_a - \theta_s) + h_{sw} A_{sw} (\theta_w - \theta_s)$$

(C5)

The response of change in water temperature to a step change in air temperature will be a cascaded one and is given by

$$\frac{\theta_w - \theta_{w0}}{\Delta_w} = 1 - \frac{\tau_1}{\tau_1 - \tau_2} e^{-t/\tau_1} - \frac{\tau_2}{\tau_2 - \tau_1} e^{-t/\tau_2}$$

(C6)

where, $\tau_1 = M_s C_s / h_{as} A_{as}$ and $\tau_2 = M_s C_s / h_{sw} A_{sw}$.

This is a second order response and has the following characteristics:

- (i) As one τ becomes very short relative to the other, e.g. $\tau_1 \ll \tau_2$, then

$$\theta_w - \theta_{w0} = \Delta_w (1 - e^{-t/\tau_2})$$

(C7)

- (ii) When $\tau_1 = \tau_2 = \tau$, the equation becomes

$$\frac{\theta_w - \theta_{w0}}{\Delta_w} = 1 - e^{-t/\tau} - \frac{t e^{-t/\tau}}{\tau}$$

(C8)

In order to calculate the cascade time constant from known values of τ_1 and τ_2 , if we put

$$1 - e^{-t/\tau} = 1 - \frac{\tau_1}{\tau_1 - \tau_2} e^{-t/\tau_1} - \frac{\tau_2}{\tau_2 - \tau_1} e^{-t/\tau_2}$$

(C9)

and when $t = \tau$, we can write

$$f(\tau) = \frac{\tau_1}{\tau_1 - \tau_2} e^{-\tau/\tau_1} - \frac{\tau_2}{\tau_2 - \tau_1} e^{-\tau/\tau_2} - e^{-1} = 0$$

(C10)

τ , or here we call as τ_s where s represents the "solid" node, can then be solved by a numerical method such as the Newton-Raphson method.

3. Multi-node Component

In the case when the water and air streams flow with the mass flow rates of m_w and m_a respectively, the time constants of the water and the air nodes can be expressed in the similar ways:

$$\begin{aligned} \tau_{w1} &= M_w C_{p_w} / (h_{sw} A_{sw}) & \text{and} & & \tau_{a1} &= M_a C_{p_a} / (h_{as} A_{as}); \\ \tau_{w2} &= M_w C_{p_w} / (m_w C_{p_w}) & \text{and} & & \tau_{a2} &= M_a C_{p_a} / (m_a C_{p_a}). \end{aligned} \quad (C11)$$

The time constant τ_c of a multi-node "heat exchanger" model is thus not a simple expression. It varies for different situations and for different emphasis, for instance in the following two cases:

- (i) The response of air temperature to the change in water temperature

The time constant can be found firstly by getting the cascade value of τ_w from τ_{w1} and τ_{w2} , and then getting the cascade value τ_c from τ_s and τ_w .

- (ii) The response of water temperature to the change in air temperature

The time constant can be found firstly by getting the cascade value of τ_a from τ_{a1} and τ_{a2} , and then getting the cascade value τ_c from τ_s and τ_a .